

CARMENES input catalogue of M dwarfs

IX. Multiplicity from close spectroscopic binaries to ultra-wide systems

C. Cifuentes¹, J. A. Caballero¹, J. González-Payo^{2,3}, P. J. Amado⁴, V. J. S. Béjar^{5,6}, A. J. Burgasser⁷, M. Cortés-Contreras², N. Lodieu^{5,6}, D. Montes², A. Quirrenbach⁸, A. Reiners⁹, I. Ribas^{10,11}, J. Sanz-Forcada¹, W. Seifert⁸, and M. R. Zapatero Osorio¹

¹ Centro de Astrobiología, CSIC-INTA, Camino Bajo del Castillo s/n, Campus European Space Astronomy Centre, 28692 Villanueva de la Cañada, Madrid, Spain, e-mail: ccifuentes@cab.inta-csic.es

² Departamento de Física de la Tierra y Astrofísica & IPARCOS-UCM (Instituto de Física de Partículas y del Cosmos de la UCM), Facultad de Ciencias Físicas, Universidad Complutense de Madrid, 28040 Madrid, Spain

³ UNIE Universidad, Departamento de Ciencia y Tecnología, Arapiles 14, 28015 Madrid

⁴ Instituto de Astrofísica de Andalucía (CSIC), Glorieta de la Astronomía s/n, 18008 Granada, Spain

⁵ Instituto de Astrofísica de Canarias, Vía Láctea s/n, 38205 San Cristóbal de La Laguna, Tenerife, Spain

⁶ Departamento de Astrofísica, Universidad de La Laguna, Astrofísico Francisco Sánchez s/n, 38206 La Laguna, Tenerife, Spain

⁷ Department of Astronomy and Astrophysics, University of California, San Diego, 9500 Gilman Drive, La Jolla, CA 92093, USA

⁸ Landessternwarte, Zentrum für Astronomie der Universität Heidelberg, Königstuhl 12, 69117 Heidelberg, Germany

⁹ Institut für Astrophysik und Geophysik, Georg-August-Universität-Göttingen, Friedrich-Hund-Platz 1, 37077 Göttingen, Germany

¹⁰ Institut de Ciències de l'Espai (CSIC-IEEC), Can Magrans s/n, Campus UAB, 08193 Bellaterra, Barcelona, Spain

¹¹ Institut d'Estudis Espacials de Catalunya (IEEC), 08034 Barcelona, Spain

Received 8 October 2024 / Accepted 28 November 2024

ABSTRACT

Context. Multiplicity studies greatly benefit from focusing on M dwarfs because they are often paired in a variety of configurations with both stellar and substellar objects, including exoplanets.

Aims. We aim to address the observed multiplicity of M dwarfs by conducting a systematic analysis using the latest available astrophotometric data.

Methods. For every star in a sample of 2214 M dwarfs from the CARMENES catalogue, we investigated the existence of resolved and unresolved physical companions in the literature and in all-sky surveys, especially in *Gaia* DR3 data products. We covered a very wide range of separations, from known spectroscopic binaries in tight arrangements (~ 0.01 au) to remarkably separated ultra-wide pairs ($\sim 10^5$ au).

Results. We identified 835 M dwarfs in 720 multiple systems, predominantly binaries. Thus, we propose 327 new binary candidates based on *Gaia* data. If these candidates are finally confirmed, we expect the multiplicity fraction of M dwarfs to be $40.3_{-2.0}^{+2.1}\%$. When only considering the systems already identified, the multiplicity fraction is reduced to $27.8_{-1.8}^{+1.9}\%$. This result is in line with most of the values published in the literature. We also identified M-dwarf multiple systems with FGK, white dwarf, ultra-cool dwarf, and exoplanet companions, as well as those in young stellar kinematic groups. We studied their physical separations, orbital periods, binding energies, and mass ratios.

Conclusions. We argue that based on reliable astrometric data and spectroscopic investigations from the literature (even when considering detection biases), the multiplicity fraction of M dwarfs could still be significantly underestimated. This calls for further high-resolution follow-up studies to validate these findings.

Key words. astronomical data bases – virtual observatory tools – stars: late-type – stars: binaries

1. Introduction

Stellar multiplicity is a natural consequence of the stellar formation process (Chabrier 2003; Goodwin et al. 2007; Bate 2012; Tokovinin 2018, also see Duchêne & Kraus 2013 and Offner et al. 2023 for reviews). The frequency of multiple systems is known to increase with the primary stellar mass (Lada 2006; Parker & Meyer 2014; Offner et al. 2023). The observational evidence shows that multiplicity is greater than 80 % for OBA-type stars (Kouwenhoven et al. 2007; Mason et al. 2009; Chini et al. 2012), around 50 % for solar-type stars (Abt & Levy 1976; Duquennoy & Mayor 1991; Raghavan et al. 2010), and 10–30 % for very low-mass stars and brown dwarfs (Burgasser et al. 2003,

2007; Bouy et al. 2003; Joergens 2008; Fontanive et al. 2018). In the case of M dwarfs, several studies in the last three decades have pointed to a multiplicity of 20–30 % (e.g. Janson et al. 2012; Ward-Duong et al. 2015; Cortés-Contreras et al. 2017; Winters et al. 2019a; Clark et al. 2024).

If all stars are indeed born together with their siblings in groups, it is natural to question how single stars came to be. Many of them may not have remained together as they evolved, while a significant fraction could also remain undetected. The dynamical interplay between the components turns into a competition for attaining stable orbits (Elliott et al. 2014; Sadavoy & Stahler 2017, but see King et al. 2012). It comes as no surprise that young stars are usually found to be part of multiple systems

(e.g. Leinert et al. 1993; Reipurth & Zinnecker 1993; Kouwenhoven et al. 2007; Shan et al. 2017). The lifetimes of young systems are too short for them to have settled down into stable configurations (we refer e.g. to the simulations carried out by Allison & Goodwin 2011). For them, it is often unclear whether a given group of stars can be treated as a young trapezia-like architecture, a small stellar kinematic group, or a mature mini-cluster (Mamajek et al. 2010; Tokovinin 2022; González-Payo et al. 2023).

Systems that contain more than two components are, in principle, unstable (Harrington 1972; Goodwin & Kroupa 2005). However, the dynamical evolution is able to produce a hierarchical arrangement of binaries within binaries or nested orbits, which leads to stability (Evans 1968; Bonnell et al. 2003; Tokovinin 2014; Powell et al. 2023). In their seminal work, Poveda et al. (1967) numerically simulated the formation of runaway stars in few-body clusters, where the high kinetic energy of the runaways is balanced by the binding energy of the binaries formed during close interactions. The loss of angular momentum during the shrinkage of the closest pair is transferred to the third component, which can result in an ejection from the original compact arrangement, a process that unfolds during the first tens to hundreds of millions of years¹ (Delgado-Donate et al. 2003; Tokovinin et al. 2006; Moeckel & Bate 2010; Kouwenhoven et al. 2010, and especially Reipurth & Mikkola 2012). A consequence of the momentum transfer is that a large fraction of close binaries are part of hierarchical triple systems (e.g. Czavalinga et al. 2023), a fact that different investigations noted some time ago (e.g. Mazeh 1990; Bate et al. 2003; Tokovinin et al. 2006; Pribulla & Rucinski 2006; Basri & Reiners 2006; Caballero 2007; Kouwenhoven et al. 2010; Rappaport et al. 2013, and see some examples by Cifuentes et al. 2021). This means that in many instances of wide binaries, one of the components is (or will be) further resolved as a very compact binary itself. The Proxima- α Cen AB triple system constitutes the nearest example of this kind. Luckily, from a mathematical perspective, these configurations can be treated dynamically as two-body problems (e.g. Evans 1968). However, the formation of close binaries in triple systems has also been linked to the Kozai-Lidov mechanism (Kozai 1962; Lidov 1962), but this has been challenged by the discovery of many wide tertiaries with isotropic orientations and low eccentricities that are inconsistent with the mechanism's predictions (Hwang 2023).

While an upper limit for binary separation is not formally established, wide binary systems, particularly those exceeding 0.1–0.2 pc, are extremely fragile and can be easily disrupted by the Galactic field (Weinberg et al. 1987; Caballero 2009; Tokovinin 2017; González-Payo et al. 2023). Increasingly refined data from surveys such as Hipparcos (Perryman et al. 1997), Tycho-2 (Høg et al. 2000), and its successor *Gaia* (*Gaia* Collaboration et al. 2016) have shown that stellar systems with very large orbital separations (of up to 1 pc or greater) do exist (Caballero 2010; Shaya & Olling 2011; Oh et al. 2017; Andrews et al. 2017). The conclusion of these analyses is that there is no strict cut-off in the semimajor axis (a) of wide binary systems, as previously theoretically predicted by Wasserman & Weinberg (1987); rather, a cut-off in binding energy is more likely ($\min |U_g^*| \approx 10^{33}$ J; Caballero 2010). Proxima Centauri serves as an example of a star that remains bound to its system despite having a value of a roughly similar to the Hill radius of α Cen-

tauri AB (Matthews & Gilmore 1993; Wertheimer & Laughlin 2006; Reipurth & Mikkola 2012; Kervella et al. 2017).

Momentum transfer is not the only mechanism to account for the large separations of the widest binary systems. Considering two modes of binary breakup, namely, core splitting and stellar ejection, Sadavoy & Stahler (2017) predicted that the majority of wide binaries break apart, but with some systems becoming tighter within several million astronomical units (au). Goodwin & Kroupa (2005) noted that these ejections in hierarchical systems would also produce a significant population of close binaries that are typically only detectable using advanced techniques. Some binaries are so closely packed that they are disguised as single objects by direct imaging. While very close binaries are undetectable by direct imaging, they can be recognised in the Doppler shift of the spectral lines (spectroscopic binaries), in the periodic eclipsing of their light (eclipsing binaries), or in the measurable change in their motion (astrometric binaries). There are also compact unresolved triples with hierarchical orbits (Mazeh et al. 2001; Baroch et al. 2021, even existing within a space of only a few au; see Moharana et al. 2024). The lack of detailed observations regarding many individual stars carries an important observational bias, leaving some very close pairs unrecognised as such. Kroupa et al. (1991) found that previous studies had underestimated the number of low-mass stars and proposed that assuming independent component masses for binary systems reconciles discrepancies between different luminosity function samples. Piskunov & Mal'Kov (1991) noted that the impact of photometrically unresolved binaries on the luminosity function depends on the mass ratio, $q = M_2/M_1$, and is strongest when both components have similar masses.

Stars in multiple systems offer the precious opportunity to directly measure fundamental parameters, such as masses, radii, or both (e.g. Popper 1980; Mathieu et al. 2000; Zapatero Osorio et al. 2004; Torres et al. 2010; Schweitzer et al. 2019). However, close companions are capable of influencing every stage of the stellar evolution. Stars that have a common origin must have the same age and chemical composition. Therefore, wide binaries are assumed to be coeval (Hartigan et al. 1994; White & Ghez 2001; Jørgensen & Lindegren 2005; Stassun et al. 2006; Makarov et al. 2008; Kraus & Hillenbrand 2009), as well as co-chemical (Gizis 1997; Gray et al. 2001; Desidera et al. 2004, 2006; Kraus & Hillenbrand 2009; Hawkins et al. 2020). Sufficiently resolved pairs can be useful to prove this assumption and serve as pieces in the puzzle of the Galactic formation. Fitting these pieces together and reassembling the original configuration is the goal of Galactic archaeology studies, which benefits from wide pair systems (Andrews et al. 2019; Hawkins et al. 2020). Important applications of wide binaries are the calibration of metallicities of M dwarfs (e.g. Bonfils et al. 2005; Bean et al. 2006; Lépine et al. 2007; Rojas-Ayala et al. 2010; Montes et al. 2018; Marfil et al. 2021), age-metallicity relation (e.g. Rebassa-Mansergas et al. 2016; Zhang et al. 2024), age-magnetic activity relation (e.g. Garcés et al. 2011; Chanamé & Ramírez 2012; Kiman et al. 2021), and even investigations into the dark matter in the Milky Way (e.g. Yoo et al. 2004; Chanamé & Gould 2004). The statistics regarding the frequency of multiple systems, their primary-companion mass ratios and their physical separations can also set meaningful constraints for models of stellar formation and evolution. For instance, they can help determine whether a primordial population composed exclusively of multiples is as likely as predicted (Hartigan et al. 1994; White & Ghez 2001; Parker et al. 2009; Reggiani & Meyer 2011; Clark et al. 2012; Leigh & Geller 2013; Reipurth et al. 2014; Parker & Meyer 2014).

¹ Throughout the manuscript we use the symbol ‘a’ for annulus (Julian year) instead of ‘yr’. We refer to <http://exoterra.eu/annulus.html> for further details.

Table 1: Multiplicity fraction for M dwarfs calculated in this work and published in the literature.

| Reference | Spectral range ^a | Sample size | d_{lim}^b [pc] | s^c [au] | MF [%] | MF+ [%] | Methodology ^d |
|--------------------------------|-----------------------------|-------------|-------------------------|-----------------|----------------------|----------------------|--------------------------|
| This work | M0–M9 | 2214 | ~10–33 | $\lesssim 10^5$ | $27.8^{+1.9}_{-1.8}$ | $40.3^{+2.1}_{-2.0}$ | Meta (Sect. 3) |
| | M0.0–M4.5 | 2038 | ~24–33 | $\lesssim 10^5$ | $28.2^{+2.0}_{-1.9}$ | $40.5^{+2.1}_{-2.1}$ | |
| | M5.0–M9.5 | 176 | ~10–24 | $\lesssim 10^5$ | $22.7^{+6.7}_{-5.6}$ | $38.1^{+7.4}_{-6.8}$ | |
| Clark et al. (2024) | M0–M9 | 1125 | 15 | ... | 23.5 ± 2.0 | | SI, Meta |
| Susemehl & Meyer (2022) | M | 1550 | 15 | $\lesssim 10^4$ | 22.9 ± 2.8 | | Meta |
| Reylé et al. (2021) | M | 249 | 10 | ... | | 22.9^e | Meta |
| Winters et al. (2019a) | M | 1120 | 25 | $\lesssim 10^4$ | 26.8 ± 1.4 | | WI |
| Cortés-Contreras et al. (2017) | M0–M5 | 425 | 14 (86 %) | ~1.4–65.6 | 19.5 ± 2.3^f | | LI |
| Ward-Duong et al. (2015) | K7–M6 | 245 | 15 | ~3–10 000 | 23.5 ± 3.2 | | AO, WI |
| Jódar et al. (2013) | K5–M4 | 451 | 25 | $\lesssim 80$ | $20.3^{+6.9}_{-5.2}$ | | LI |
| Janson et al. (2012) | M0–M5 | 761 | 52 | ~3–227 | 27 ± 3 | | LI |
| Bergfors et al. (2010) | M0–M6 | 108 | 52 | ~3–180 | 32 ± 6 | | LI |
| Law et al. (2008) | M4.5–M6.0 | 108 | $\lesssim 20$ | $\lesssim 80$ | $13.6^{+6.5}_{-4.0}$ | | LI |
| Reid et al. (1997) | K2–M6 | 106 | 8 | $\lesssim 1800$ | 32 | | SI, WI, RV |
| Leinert et al. (1997) | M0–M6 | 34 | 5 | ~1–100 | 26 ± 9 | | SI |
| Simons et al. (1996) | M | 66 | 8 | ~100–1400 | 40 | | SI, WI, RV |
| Fischer & Marcy (1992) | M | 62 | 20 | $\lesssim 10^4$ | 42 ± 9 | | SI, WI |
| Henry (1991) | M | 74 | 8 | ... | 31.3% | | SI |
| Henry & McCarthy (1990) | M | 27 | 5.2 | $\lesssim 1000$ | 38 ± 9 | | SI |

Notes. ^(a) ‘M’ should be read as ‘all the M dwarfs within the volume limited by d_{lim} ’, when no specific limitation on the spectral classification of the sample is given. ^(b) The volume-complete samples limited by these distances are motivated in Sect. 2. ^(c) Not every star in the sample has been studied in the literature with the same level of detail. In Sect. 4.1 we distinguish between three possible categories depending on the resolution, from those only known (at most) *Gaia* to those studied in a higher detail. ^(d) Methods referred to data acquisition. SI: Speckle interferometry; LI: Lucky imaging; WI: Wide-field imaging; AO: Adaptive optics; RV: Radial-velocity; Meta: Literature meta-analysis. ^(e) Reylé et al. (2021) identified at least 94 multiple systems with M dwarfs in their 10-parsec sample, which covered a wide parameter space in mass ratios, magnitude differences, angular separations, inclinations, and orientations. They calculate a MF for all the range of masses of $27.4 \pm 2.3 \%$. While the authors did not provide a specific MF for M-dwarfs for direct comparison, we derived from their results (52 multiple M dwarfs out of 249 in total) a specific value, given the meticulous completeness of their study (see especially their Fig. 2). For this we employed the data of their first update (Reylé et al. 2022). ^(f) The authors indicated that the percentage may increase to at least 36 % by including the pairs at $\rho < 0.2$ arcsec and $\rho > 5$ arcsec.

Studies of stellar multiplicity take on particular significance for M dwarfs because they potentially rely on a vast sample of study. The nearest stars represent a valuable sample for multiplicity studies because they allow accurate photometric and astrometric measurements. Their multiplicity characteristics carry the imprints of the formation and evolution of our Galaxy. Although intrinsically small and faint ($M \lesssim 0.62 M_{\odot}$, $L \lesssim 0.076 L_{\odot}$, Cifuentes et al. 2020, and references therein), M dwarfs make up the majority of the stars in the Galaxy (Henry et al. 1994, 2006; Reid et al. 2004; Bochanski et al. 2010; Winters et al. 2015; Reylé et al. 2021; Golovin et al. 2023; Kirkpatrick et al. 2024). M dwarfs have also gained importance in the last two decades because of the search for Earth-like planets, especially in their habitable zone (Scalo et al. 2007; Kopparapu et al. 2013), either with space missions for transit surveys (CoRoT, Auvergne et al. 2009, Kepler, Borucki et al. 2010, TESS, Ricker et al. 2014) or with the radial-velocity (RV) method (Bonfils et al. 2013; Fouqué et al. 2018; Reiners et al. 2018a; Ribas et al. 2023). Among the notable high-resolution ground-based spectrographs that undertake RV searches is the Calar Alto high-Resolution search for M dwarfs

with Exoearths with Near-infrared and optical Échelle Spectrographs² (CARMENES, Quirrenbach et al. 2014).

Table 1 displays the multiplicity fraction (MF) of M dwarfs, namely, the proportion of these stars that are the most massive components of a multiple system (Sect. 4.1), along with the values reported in the literature by different authors during the past three decades, including the present work. We indicate (when possible) the relevant constraints of the studies: spectral range, sample size, completeness volume, search separations, and methodology. Not all the portions of the spectral range of M dwarfs have been studied equally well regarding their multiplicity. Also, the detection limits (again Sect. 4.1) are not consistent between studies, leading to different proportions of undetected binaries in very compact arrangements. While it has not been included in the list due to greater difficulty in comparison, we mention other systematic efforts in multiplicity investigations, such as the pioneering infrared imaging of 55 low-mass binaries by Skrutskie et al. (1989) or the *Hubble* Space Telescope snapshot high-resolution images of 225 stars by Dieterich et al. (2012).

² <https://carmenes.caha.es>

Table 2: Summary of the tables appended to this work.

| Table | Description |
|------------|---|
| Table A.1 | Full sample |
| Table A.2 | Bona fide binaries with astrometric anomalies |
| Table A.3 | New stellar multiple systems proposed |
| Table A.4 | Spectroscopic binaries, triples, and quadruples |
| Table A.5 | Eclipsing binaries |
| Table A.6 | Description of the full sample table |
| Table A.7 | Binaries with separations larger than 10^4 au |
| Table A.8 | M dwarfs + FGK stars |
| Table A.9 | M dwarfs + white dwarfs |
| Table A.10 | M dwarfs + ultra-cool dwarfs |
| Table A.11 | M dwarfs + planets |
| Table A.12 | Bibliographic references and abbreviations |

Notes. For simplification purposes, we generally abbreviate the name of the objects designated with long catalogue identifiers: Gaia DR3 as G3, Gaia DR2 as G2, and 2MASS as 2M.

Many of the publications in Table 1 predate *Gaia*, but some of them made predictions on *Gaia*'s impact on M-dwarf multiplicity. For instance, [Winters et al. \(2019a\)](#) foresaw that *Gaia*'s astrometric measurements over five years would enable the detection of low-mass binaries that remained undetected, providing a more complete picture of the nearby M dwarf population.

This is the ninth paper of the series of publications on the CARMENES input catalogue of M dwarfs. CARMENES aims to look for Earth-like planets around the closest, brightest, late-type stars with the radial velocities technique. In this work, we present an updated and systematic study of the multiplicity across all spatial separations in the brightness-spectral type-limited CARMENES input catalogue. The sample under study is a collection of more than two thousand M dwarfs as described in Sect. 2. Our study exploits the fruitful *Gaia* mission (up to the third data release, DR3, [Gaia Collaboration et al. 2023b](#)) to provide an updated revision of the multiplicity of M dwarfs, accounting for the impact of unresolved binaries on the MF. Since many definitions in this investigation are based on the resolution of the system components by the *Gaia* mission, in our analysis (in Sect. 3) we distinguish between systems with resolved and unresolved components in DR3. Section 4 is centred on results and discussion, which includes the description of the identified systems and their fundamental parameters. In particular, we differentiate between the canonical MF (Sect. 4.1) and the expected multiplicity fraction, MF+, which accounts for potential unresolved systems that could boost MF by more than 10 %. The conclusions are summarised in Sect. 5. Finally, the appendix compiles and organises useful data produced in this work. Table 2 offers twelve tables with a variety of content. In particular, Table A.1 includes an abridged version of the full dataset compiled and produced in this work.

2. Sample

The CARMENES project selected 350 M dwarfs as the targets for the main survey, whereby a total of 750 useful nights were reserved as guaranteed time observations, from 1 January 2016 to 31 December 2020. The observations of the guaranteed time observations sample continue within the CARMENES Legacy+ programme, which aims for 50 measurements for all suitable targets and is expected to run at least until the end of

2025. The raw data, calibrated spectra, and high-level data products were made publicly available as the CARMENES Data Release 1 ([Ribas et al. 2023](#)). The continuous update of the catalogue has introduced additional M dwarfs to the original sample, mostly objects of interest (TOI) identified by the Transiting Exoplanet Survey Satellite programme (*TESS*; [Ricker et al. 2014](#)). RV follow-up has confirmed many of these transiting exoplanets (e.g. [González-Álvarez et al. 2023b](#); [Goffo et al. 2024](#); [Kuzuhara et al. 2024](#); [Dai et al. 2024](#), just to mention a few recent ones). The left panel of Fig. 1 illustrates the distribution of M dwarfs in our sample according to spectral subtype. The latest-type star is an M9.5 dwarf, Scholz's star ([Karman³ J07200–087](#)).

The full sample of our study is dubbed Carmencita, the input catalogue for the CARMENES project ([Alonso-Floriano et al. 2015b](#); [Caballero et al. 2016](#)). Carmencita contains a total of 2214 M dwarfs, from M0.0 V to M9.5 V, including the targets for the main survey. The stars were intentionally chosen independently of their multiplicity, age, or metallicity. Only one Carmencita object classified as K7V (HD 97101) remains in the RV-monitored sample, as it is the bound companion of an M2 V star (HD 97101B). All these stars satisfy simple selection criteria based on their spectral types, their visibility from the Calar Alto Observatory in Southern Spain ($\delta \gtrsim -23$ deg), and on their apparent brightness in the *J*-band magnitude, between 4.2 mag and 11.5 mag (this range of magnitudes also depends on spectral type, as detailed by [Alonso-Floriano et al. 2015b](#)). The stars in our sample are located at distances ranging between 1.82 pc (Barnard's star) and 166.1 pc (Haro 6-36), with the majority of them in our immediate vicinity, with a median distance of 22.0 pc.

Magnitude-limited samples may be unintentionally overpopulated by intrinsically bright unresolved stellar systems due to the Malmquist bias (see [Duquennoy & Mayor 1991](#), and references therein). In particular, these samples may over-represent spectroscopic binaries because two stars are brighter than one. Since Carmencita started to be built well ahead of the *Gaia* launch, it is not a volume-limited sample. Furthermore, by construction it is not a magnitude-limited sample (the faintest M0.0–0.5 V stars are several magnitudes brighter in *J* than the brightest late-type M dwarfs). Therefore, we calculated a ‘completeness distance’, d_{com} , that depends on the spectral type. We used the definition of absolute magnitude in the *J* band, $M_J - J = 5 - 5 \log d_{\text{com}}$, where $J = J(\text{SpT})$ from the construction of Carmencita (Table 1 from [Alonso-Floriano et al. 2015b](#)), and $M_J = M_J(\text{SpT})$ from an empirical relation (Table 7 in [Cifuentes et al. 2020](#)). Therefore, $d_{\text{com}}(\text{SpT})$ is the radius of the sphere that contains all known M dwarfs with an equal or earlier spectral type. As a result, Carmencita contains all M dwarfs with spectral types M4.5 V or earlier up to 30 pc, and all M dwarfs with spectral types M9.5 V or earlier up to 10 pc. The latter finding was double-checked against the 10 pc sample study by [Reylé et al. \(2021\)](#). The right panel of Fig. 1 aims to illustrate this fact. Of course, this completeness is contingent on the additional condition that the stars must be visible in the northern hemisphere.

3. Analysis

3.1. Search for resolved systems

For each star in our M-dwarf sample, we started by searching for resolved physical companions in two steps. First, we re-

³ The Karman nomenclature is Jhhmm±ddm(N/S/E/W) with J2000 equatorial coordinates. We skip the Karman prefix from now on.

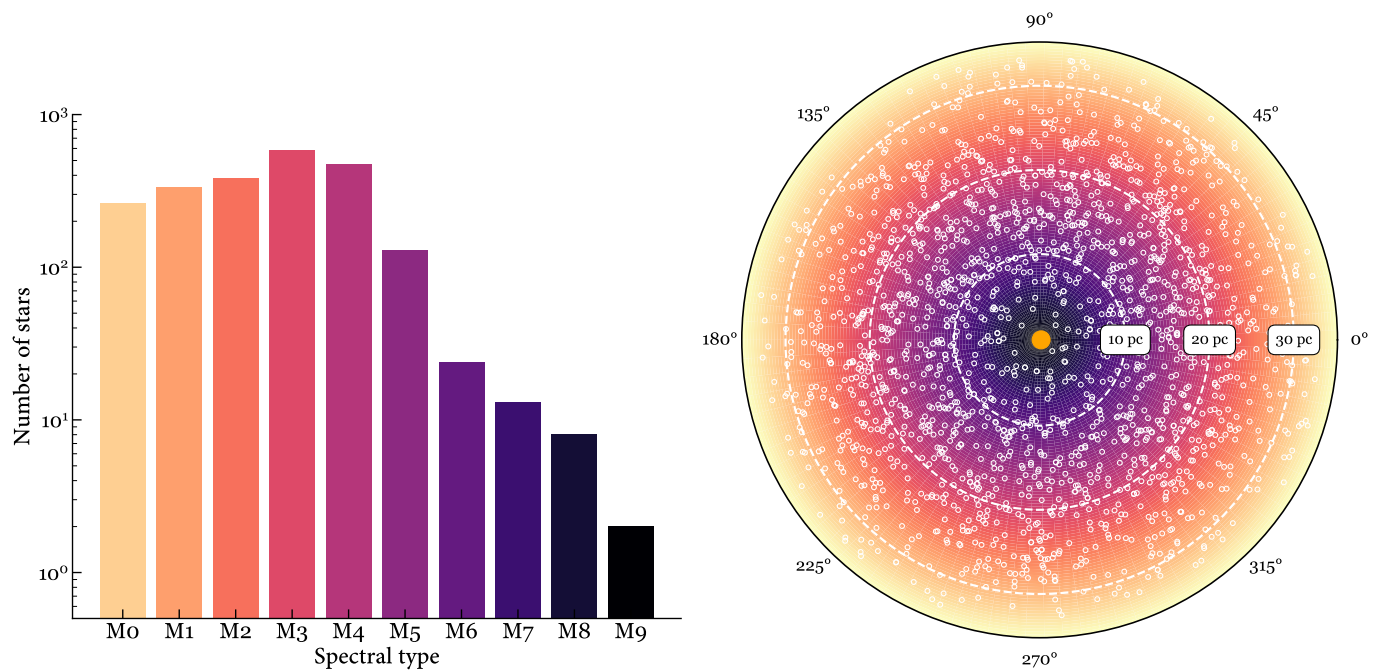


Fig. 1: Distribution of spectral types of the stars in the sample (left) and illustration of the completeness distance of Carmencita (right). The latter panel shows the distance and right ascension α of the Carmencita stars in the solar neighbourhood and colour-codes the spectral subtype as a function of the distance to which our sample is complete. The dashed lines depict 10-parsec increments of the distances.

viewed the Washington Double Star catalogue⁴ (WDS; Mason et al. 2001), and then we performed a dedicated, blind search employing the most updated astrometric information available from *Gaia* (i.e. DR3). In this context, a resolved physical companion (of a given star) is defined as an individual source in an astrometric catalogue such as *Gaia* with proper motions and trigonometric parallax that are compatible with physical binding with the primary.

As a preliminary step, we got equatorial coordinates at the 2016.0 *Gaia* epoch and apparent magnitudes in G for 100 % of our sample using the *Gaia* Archive⁵. Next, we ensured that each of our objects had a complete astrometric description. The full, five-parameter solution from *Gaia* DR3 (position, proper motion, and parallax: α , δ , $\mu_\alpha \cos \delta$, μ_δ , ϖ) is available for 93.0 % of the 2214 M dwarfs. Among them, 61.2 % also have barycentric radial velocity, V_r , from the second or third data releases of *Gaia*; we prefer the latter in case of availability in both. For the sources for which *Gaia* does not provide some of these data, we searched in the literature for published measurements (e.g. Gliese & Jahreiß 1991; van Leeuwen 2007; Faherty et al. 2012; Dittmann et al. 2014; Finch & Zacharias 2016). Of the remaining 4.9 % of stars without full *Gaia* solution, we compiled proper motions and parallaxes from other sources for all except for 34 (see below).

We performed a cross-match of our *Gaia* stars with WDS utilising the Tool for OPerations on Catalogues And Tables (TOPCAT; Taylor 2005). The WDS is the principal database for astrometric double and multiple star information, collecting 156 861 systems to submission date. For many of them, it compiles precise astrometric history and orbital description, making it a valuable resource for our study. In the WDS catalogue we found 411 systems that contain at least one M dwarf from

our sample. For them, we retrieved the last measured epoch (*sep2*), the corresponding position angle (*pa2*), and separation in the ‘precise’ format (i.e. non-rounded values), and incorporated them in the final table. We took into account that our M dwarfs could be either the WDS primary or a companion. At this stage we added one star and eight T-type dwarfs in multiple systems that are not tabulated by *Gaia* because of their brightness (Capella) or their faintness (e.g. GJ 570D, Ross 458C), respectively.

After identifying the resolved pairs already documented by WDS, we also looked for common proper motion and parallax companions within the *Gaia* data. We performed a blind search using the DR3 by dividing the search in two ranges of separations. First, for the closest systems, we used the automatic positional cross-match tool in TOPCAT, X-match, limiting to a search radius of 5 arcsec and setting the ‘find’ option to ‘all’. With this configuration we made sure to keep every source found in the vicinity of our sources, regardless of its apparent magnitude, parallax distance, or proper motion, even when some of this information was not available. Second, we conducted a much wider, separation-limited search using the Astronomical Data Query Language (ADQL) form in the *Gaia* Archive. We limited the search to a physical separation of 10^5 au (~ 0.5 pc), which translates to projected separations of 20 000–2000 arcsec for stars located at distances of 5–50 pc. As mentioned in Sect. 1, there is no consensus regarding an upper limit in wide binary separation. Therefore, we set a safe upper limit of 10^5 au to ensure that actual bound systems with remarkable separations were not missed in the process, but keeping in mind that projected separations are always less than or equal to the true separations (see e.g. Wertheimer & Laughlin 2006). In this search we looked for resolved sources with full five-parameter astrometric solutions compatible with physical binding to our source. To begin with, we automatically kept all the sources with separations $\rho >$

⁴ <http://www.astro.gsu.edu/wds/>

⁵ <https://gea.esac.esa.int/archive/>

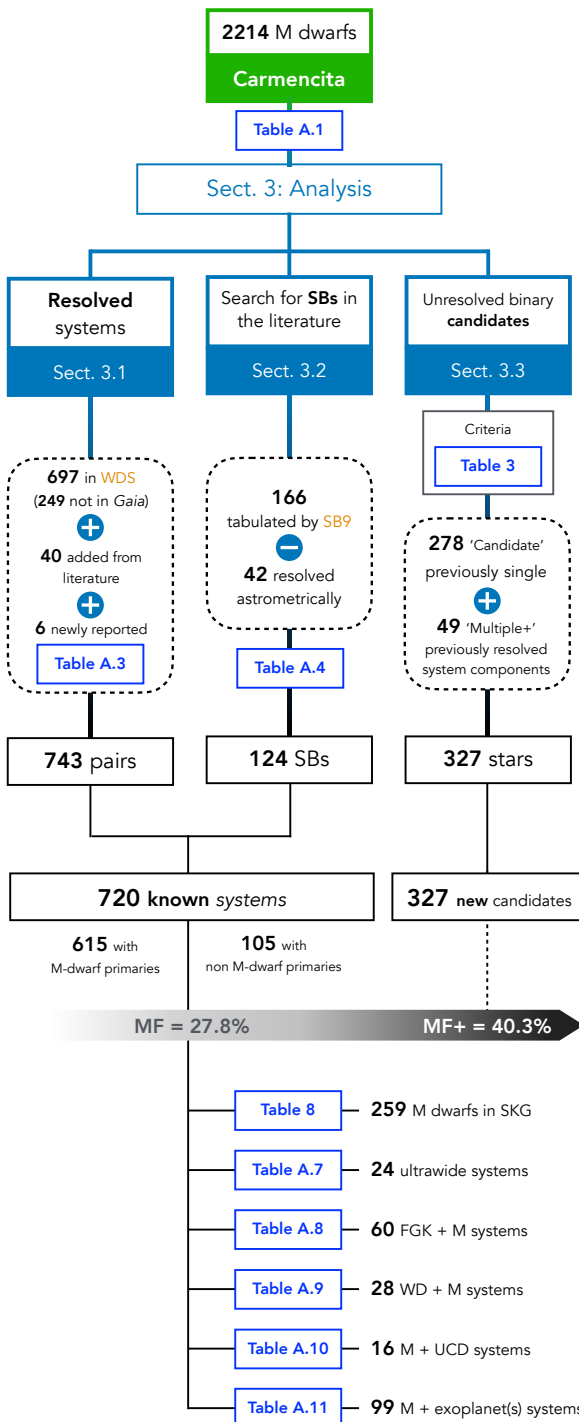


Fig. 2: Schematic summary of our analysis (Section 3).

5 arcsec exhibiting a conservative difference in their parallactic distances of 10 % with respect to our star, namely, distance ratio:

$$\Delta d = \left| \frac{d_1 - d_2}{d_1} \right| < 0.10. \quad (1)$$

For these sources, we computed two additional metrics to ensure that they are approximately co-moving. These are the μ ratio and the proper motion position angle difference, ΔPA , defined by Montes et al. (2018) and used afterwards by Cifuentes et al. (2021) and González-Payo et al. (2023):

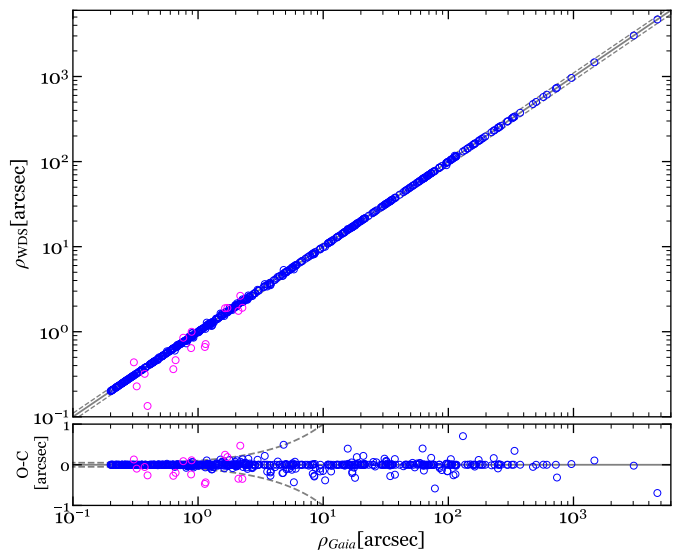


Fig. 3: Comparison of projected separations tabulated by the WDS and measured by us using *Gaia* astrometry. The solid and dashed grey lines represent the 1:1 relation, and the differences in 10 %. The magenta circles are stars beyond this limit. The error bars are rather small for almost all cases due to the high precision of *Gaia*'s astrometry and they have therefore been omitted.

$$\mu \text{ ratio} = \left(\frac{(\mu_{\alpha 1} \cos \delta_1 - \mu_{\alpha 2} \cos \delta_2)^2 + (\mu_{\delta 1} - \mu_{\delta 2})^2}{(\mu_{\alpha 1} \cos \delta_1)^2 + (\mu_{\delta 1})^2} \right)^{1/2} < 0.15, \quad (2)$$

$$\Delta PA = |PA_1 - PA_2| < 15 \text{ deg}. \quad (3)$$

This search recovered all 568 pairs known in WDS that *Gaia* is able to resolve (4.3.1). In Fig. 3 we compare the values of angular separations tabulated by the WDS with those computed by us using the *Gaia* astrometry. There are only 15 pairs of stars (shown in magenta) with separation differences larger than 10 % between WDS and our measurements. They correspond to well-documented binaries with very small projected separations ($\rho \lesssim 2$ arcsec) that exhibit significant orbital motion over relatively short timescales (of a few years; e.g. BL Cet + UV Cet, Wolf 424 AB, or AT Mic AB – the three of them located at less than 10 pc from the Sun). The observed scatter of the 1:1 relation justify a posteriori our 10 % distance ratio criterion. This scatter is due to a mixture of systematic effects on parallax, such as colour-dependent effects, under-estimated uncertainties of faint sources, or impact of unresolved binarity.

Figure 4 shows a comparative analysis of the proper motions (ΔPA vs μ ratio; top panel) and distances (companion's d vs primary's d ; bottom panel) of the identified pairs. The majority of our pairs comply with the criteria for physical association (shown in blue), although there are 78 sources (shown in red and amber) that exhibit anomalies in their relative positional angles, proper motions, or distances. Our individual examination of these sources allowed us to propose the most likely reasons for these outliers, and to keep all of them as very interesting instances of binarity, as summarised in Table A.2. Most of these outliers exhibit proper motion and parallax anomalies (Kervella

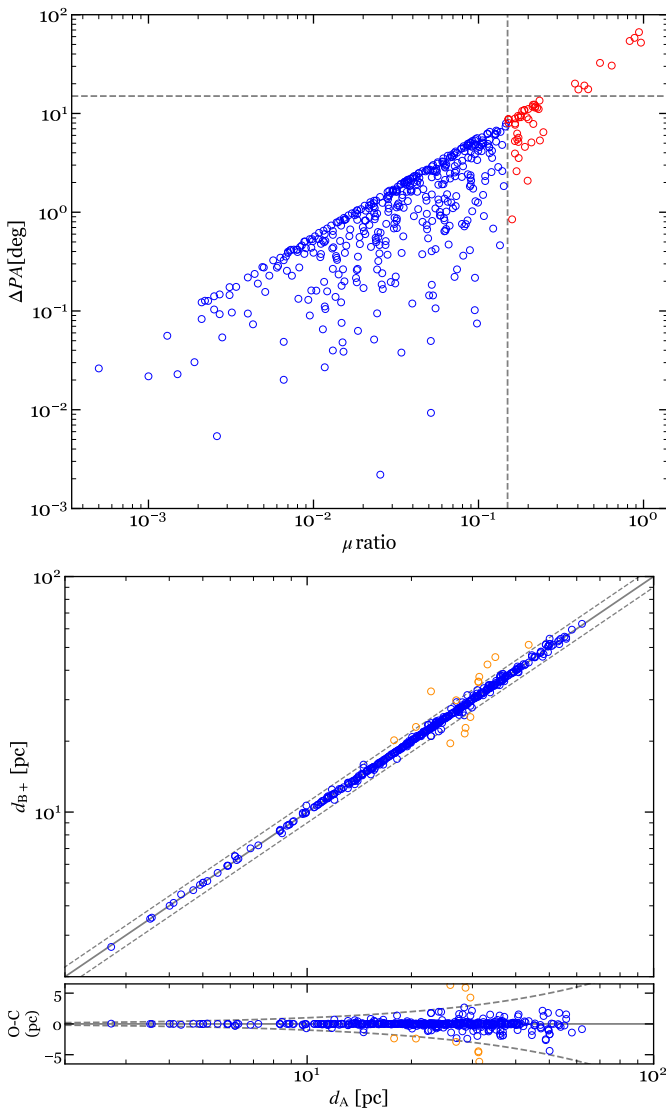


Fig. 4: Comparative analysis of the proper motions and distances of the identified pairs. *Top:* ΔPA vs μ ratio diagram, where the dashed grey lines set the upper limits of our criteria for physical association (Eqs. 2 and 3). The red open circles are pairs that do not comply, or do so partially, with those criteria, respectively. *Bottom:* Comparison of distances of the companions (denoted ‘B+’) and their corresponding primaries (‘A’). The amber circles are pairs that do not comply with our criterion (Eq. 1). Our Carmencita M dwarf may be the primary (i.e. the most massive) or a companion in the system.

et al. 2019; Brandt 2021) due to the closeness of the components. Their orbital periods are for this reason relatively short, of a few tens of years or less (Sect. 4.3.3). The systems containing some of these pairs are valuable because their dynamical masses could be determined in the near future.

In addition, there are 34 systems in which distances and proper motions are missing for one of the components, and so Δd , μ ratio, and ΔPA are unknown. For these, our criteria for physical associations are not fully conclusive, but they do all correspond to well-characterised close binaries listed by WDS, which we retained in our analysis nevertheless.

Even though for most of the cases, the criteria presented here are effective for determining whether a pair of components in a

system is physical or optical (unbound), there are some caveats. False positives (or chance alignments) can be found in wide pairs (Sect. 4.3.1 offers a deeper analysis), while false negatives, attributed to imprecise astrometry, are more commonly found in very close pairs. The nominal operations of *Gaia* up to DR3, spanning 1028 days, may not provide sufficient coverage, leading to ill-defined proper motions in those cases for which orbital periods notably exceed this timespan. Thus, these may reflect the instantaneous tangential path, including orbital motion, meaning that some bound systems might not qualify as binary. Given the small probability of finding a source at a similar distance within a small search radius, the benefit of finding a close companion justifies the effort of checking individually all the potential pairs by accessing to images and catalogues. For this particular inspection we used the Aladin interactive sky atlas (Bonnarel et al. 2000) and the SIMBAD database (Wenger et al. 2000). With Aladin we carefully examined every source at a separation $\rho < 5$ arcsec from our targets, discarding those with an astrometric description that identified them as background objects.

Most of the systems discovered in our *Gaia* blind search are tabulated by the WDS, as illustrated by Fig. 3. From a total of 720 systems found in our sample, 697 are tabulated in the WDS, of which 249 are not resolved by *Gaia*. Many of them are very close sub-arcsecond binaries detected with adaptive optics, lucky imaging, or speckle interferometry (Sect. 4.3.1), but there is also room for resolved ultra-cool dwarfs that are fainter than the *Gaia* magnitude limit (Sect. 4.4.3).

Despite the continued efforts by the WDS team at the United States Naval Observatory to keep this catalogue updated, there can still be missing pairs that appear in the literature. To address this gap, we also cross-matched our stars with the Robo-AO surveys (with $d \lesssim 30$ pc) of Lamman et al. (2020) and Salama et al. (2022), the *Gaia* catalogue of nearby stars (GCNS, *Gaia* Collaboration et al. 2021b), the million binaries from *Gaia* EDR3 of El-Badry et al. (2021), the 10-parsec sample of Reylé et al. (2021), the full-sky 20-pc census of Kirkpatrick et al. (2024), and the ultra-cool dwarf companion catalogue by Baig et al. (2024). Some of these compilations (mostly El-Badry et al. 2021 and *Gaia* Collaboration et al. 2021b) tabulated bound systems that are not yet tabulated in the WDS, but were also identified by us. For completeness, we also cross-matched the remaining systems with the Washington Double Star Supplemental Catalog⁶, which besides compiles the input from those and other large faint multiplicity surveys such as those by Dhital et al. (2015), Oh et al. (2017), Tian et al. (2020), or Hartman & Lépine (2020). Their findings are duly credited in the ‘Discoverer’ column across the various tables in this work.

While most pairs found in our custom *Gaia* search are known, either from WDS or the recent searches mentioned before, we report six physically bound systems for the first time. All but two are considered to be single stars; the exceptions are the triple systems HD 230017 in the Carina moving group (Sect. 4.5) and GJ 3261, which were thought to be close binaries. We show the six new systems in Table A.3. Apart from *Gaia* DR3 astrometric solutions (α , δ , ϖ , μ_{total}), for each pair, we tabulated their angular separations (ρ) and position angles (θ).

3.2. Search for known spectroscopic binaries

After determining the systems in our sample that are astrophotometrically resolved by *Gaia*, and those tabulated by WDS

⁶ <http://www.astro.gsu.edu/wds/Supplement/wdss.html>

and other recent catalogues, we carefully reviewed the literature for references to unresolved systems, namely spectroscopic binaries⁷ (SBs). For a comprehensive list of SBs, the main source of reference used in this work was the 9th Catalogue of Spectroscopic Binary Orbits (SB9, Pourbaix et al. 2004). In this catalogue, we found 166 spectroscopic multiples among the stars in our sample and their companions for which a spectroscopic investigation has been conducted (we refer to Sect. 4.1 for an explanation of the detection limits of the Carmencita stars and their physical companions). Among them, we found 42 cases in which the components have also been astrometrically resolved and compiled in the WDS. By checking the reported orbital periods and magnitude differences we ensured that both measurements refer in fact to the same pair. For these cases we removed the spectroscopic binary designation (Aab) and classified them as close resolved, AB or (AB). In case of doubt, we preferred to stay conservative and avoided losing a potential triple system (thought to be simply double) in a compact configuration. For instance, the physical pair GJ 3481 and GJ 3482 (COU 91), where the latter is further resolved as a spectroscopic binary ($a < 0.66$ au according to Shkolnik et al. 2010) and as an astrometric visual pair with the FastCam lucky imager ($\rho \approx 0.94$ arcsec or $s \sim 16.7$ au according to Cortés-Contreras et al. 2017), might potentially constitute a hierarchical quadruple. Another example is GJ 3522 (LHS 6158), a 7.6-day double-lined spectroscopic binary (Reid & Gizis 1997; Tokovinin 2018), with a third component in a 5.7-year period (Hartkopf et al. 2012) revealed using adaptive optics (Delfosse et al. 1999a), with spectral classification assumed roughly similar to the primary's (M3.5 V, Kirkpatrick et al. 2012) and constituting one of the nearest ($d = 6.7$ pc) hierarchical triples. A total of 124 spectroscopic systems found in our sample and are listed in Table A.4, including their published orbital periods, P_{orb} , semimajor axes, a , and mass ratios, $q = M_B/M_A$, together with their references. Values estimated from mass-luminosity relations, or directly from spectral typing, are not collected. None of the 123 SBs have been spatially resolved to date.

The cases in which the orbital plane of a binary system aligns with our line of sight are rare. Eclipsing binaries (EBs) are a unique category and serve as a valuable opportunity for determining empirical masses and radii (Huang & Struve 1956; Popper 1980; Andersen 1991). EBs enable the measurement of dynamical masses, especially in detached double-lined SBs, and provide accurate radius measurements with precision around 1–2% (Ribas 2003; Torres et al. 2010; Schweitzer et al. 2019). These parameters have the advantage of not relying on models, so they can serve to evaluate the accuracy of theoretical predictions. Shan et al. (2015) demonstrated an elevated occurrence of eclipsing binaries among detached M-dwarf SBs with orbital periods of 1–90 d, exceeding previous RV-based inferences. Stellar activity levels, particularly in young, magnetically active, or fast-rotating tidally-locked eclipsing binaries, can also introduce biases, leading to observed inflated radii (Caballero et al. 2010; Jackson et al. 2018; Kesseli et al. 2018; Parsons et al. 2018). All-sky surveys such as *Kepler* and TESS have made possible the identification of eclipsing binaries by the thousands (Kirk et al. 2016; Prša et al. 2022). In our sample there are five known eclipsing binaries, which are listed along with their masses and radii in Table A.5. Additionally, the objects GJ 3547 (J09193+620), GJ 3461 (J07418+050), and GJ 3793 (J13348+201) are sug-

gestive of eclipsing events from the study of TESS light curves (Skrzypinski 2021). The first two are double-lined spectroscopic binaries (in one case also featured in the variability catalogue of Eyer et al. 2023), while the third is a single star but flagged by us as a likely unresolved binary ('candidate'; see Sect. 3.3).

3.3. Search for new binary candidates using Gaia

Next, we exploited the wealth of *Gaia* data in order to identify binary candidates that have not been identified in previous work. This analysis also extended to companions of known multiple systems found in the previous sections, which added complexity to a number of these systems.

The spatial resolution of *Gaia* was limited to 0.4–0.5 arcsec in the second data release (DR2, Gaia Collaboration et al. 2018), and slightly improved in the early third data release (EDR3, Gaia Collaboration et al. 2021a). In particular, Fabricius et al. (2021) showed that EDR3 achieves completeness for separations larger than 1.5–2.0 arcsec, with a severe incompleteness below 0.7 arcsec. Objects closer than this limit can be identified with *Gaia*, but this identification depends on the magnitude difference, current angular separation, and orientation along the dominating scan directions (e.g. Gaia Collaboration et al. 2021b). *Gaia* EDR3 data can be affected by spurious signals linked to the time-dependent scan angle of the instrument, leading to false periodic signals in photometry and astrometry. Using numerical simulations, Holl et al. (2023) explored how these biases occur and provided statistics to identify and filter affected sources. They found that these signals often originate from unresolved binaries or other close optical pairs with fixed orientations and separations of less than 0.5 arcsec (including binaries with orbital periods of several years). Therefore, *Gaia* EDR3 is capable of resolving visual double stars, but unable to resolve the closest pairs, with $\rho \lesssim 0.13$ arcsec, although upcoming releases are expected to enhance these resolution capabilities (de Bruijne et al. 2015). Still, *Gaia* has been proven highly valuable to date in the detection of binary stars (see El-Badry 2024).

The third data release, DR3, maintains the same astrometric data as EDR3, but it includes a rich set of new data products that we exploited in this work. For instance, *Gaia* DR3 is the first release that provides an analysis of the RV time-series. By the time of this release, every source was observed with the Radial Velocity Spectrometer an average of ~ 70 times, varying from ~ 30 to ~ 240 , depending on the sky coordinates.

Gaia DR3 comes with numerous statistical parameters to assess the reliability of the astrometric data. We summarise in Table 3 some of these quality indicators or combinations of them, which serve to flag stars with astrometric issues. They have been proven to be sensitive to the presence of potential unresolved companions (e.g. Fabricius et al. 2021; Katz et al. 2023; Pourbaix et al. 2022; Penoyre et al. 2022a; Shahaf et al. 2023; Van der Swaelmen et al. 2023). A detailed description of them can be found in the *Gaia* DR3 documentation⁸. The usage of these parameters is explained next (Sects. 3.3.1–3.3.4), as well as complementary methods of assessing unresolved multiplicity exploiting the *Gaia* products, which overlap with the criteria of Table 3 (Sects. 3.3.5–3.3.6). Figures 5 and 6 illustrate the different unresolved multiplicity criteria.

⁷ It is customary to use the broad term ‘spectroscopic binary’ to also refer to triples or even quadruples spectroscopically detected, despite the specific implication of two components in the term.

Table 3: Criteria for the detection of unresolved sources based on *Gaia* DR3 statistical indicators.

| Criterion | Selection | Remarks |
|-----------|---|---|
| 1 | <code>RUWE > 2</code> | Goodness of fit between the observed astrometric data and a single-star model. |
| 2 | <code>ipd_gof_harmonic_amplitude > 0.1 & RUWE > 1.4</code> | Flag for spurious solutions of resolved doubles, not correctly handled in the <i>Gaia</i> EDR3 astrometric processing (Fabricius et al. 2021). |
| 3 | <code>ipd_frac_multi_peak > 30</code> | Fraction of windows for which the algorithm has identified a double peak (or double transit), meaning that the detection may be a visually resolved double star (e.g. Tokovinin 2023; Holl et al. 2023; Medan & Lépine 2023). |
| 4 | <code>rv_chisq_pvalue < 0.01 & rv_renormalised_gof > 4 & rv_nb_transits ≥ 10</code> | Measure of variability in RV among all the <i>Gaia</i> measurement epochs (Katz et al. 2023). |
| 5 | <code>radial_velocity_error ≥ 10 km s⁻¹</code> | Same as above. For the bright stars ($G \lesssim 13$ mag) it is the uncertainty on the median of the epoch radial velocities, to which a constant shift of 0.11 km s^{-1} was added to take into account a calibration floor. |
| 6 | <code>duplicated_source = 1</code> | Flag for the existence of a duplicated source during data processing, which may indicate observational, cross-matching, or processing problems, or stellar multiplicity, and probable astrometric or photometric problems in all cases. This metric works in support to the others, rather than being a standalone indicator on itself. |
| 7 | <code>non_single_star</code> | Flag for a possible non-constant behaviour using binary orbit models. Three bits indicate whether it has been identified as astrometric (bit 1 is set to one), spectroscopic (bit 2 is set to one), or eclipsing (bit 3 is set to one) binary, respectively (Pourbaix et al. 2022). |

3.3.1. RUWE (Criteria 1 and 2)

Perhaps the most widely used metric in Table 3 is the renormalised unit weight error (RUWE), which evaluates the behaviour of the centre of light. Belokurov et al. (2020) showed that the amplitude of the centroid perturbation correlates with the physical separation between companions and scales with the binary period and mass ratio. Unresolved binaries with periods similar to or longer than the *Gaia* timespan (which increases with each subsequent release) can show elevated RUWE due to orbital motion affecting the astrometric fit (see Penoyre et al. 2022a for a detailed discussion). Castro-Ginard et al. (2024) suggested that the majority of binary systems in our Galaxy will remain undetected because the wobble of the centre of mass around the photocentre is largely masked by the astrometric noise from *Gaia*, leading to a RUWE value below the detection threshold (we refer to their Fig. 1 for an illustration). However, the median distance of our M-dwarf stars is 22.0 pc, which locates them in our immediate vicinity and allows to detect that wobble in many cases. Penoyre et al. (2020) noted that assuming an object as a single point mass in astrometry can bias measurements due to unresolved binaries. They also concluded that orbital motion with period near one year can mimic parallax, distorting distance estimates. Additionally, distant objects (further than 100 pc) can show disproportionate values of RUWE (Baig et al. 2024), which has been mitigated by an additional renormalisation, namely local unit weight error (LUWE, Penoyre et al. 2022b), with well-

behaved single stars having a value close to 1.0. Still, RUWE remains a powerful and simple metric, especially when complemented with other indicators. Instead of the generally adopted value of 1.4 (e.g. Arenou et al. 2018; Lingam & Loeb 2018; Cifuentes et al. 2020), or even the position-dependent range of values from 1.15 to 1.37 developed by Castro-Ginard et al. (2024, their Fig. 3), in our analysis we set a conservative minimum of $\text{RUWE} > 2.0$, which leaves behind $\sim 80\%$ of the sample.

3.3.2. ipd metrics (Criteria 2 and 3)

The broad applications of many of the ipd metrics in the targeting of binary stars has been recognised, for instance, by Vrijmoet et al. (2020), who applied them to two decades of astrometric data from the RECONS program along with *Gaia* DR2 observations. Clark et al. (2022) demonstrated that *Gaia* was unable to resolve a great portion (58.9 %) of the close companions that they detected using speckle imaging, which motivates the need for additional high-resolution imaging (~ 40 mas). They investigated the usefulness of the metrics RUWE along with the parameter `ipd_frac_multi_peak` for assessing the likelihood of an unseen stellar companion (IPD stands for ‘image parameter determination’). For instance, Baig et al. (2024) built the ultra-cool dwarf companion catalogue exploring the likelihood of hidden binarity using LUWE and IPD.

Likewise, Golovin et al. (2023) identified sources with spurious astrometric solutions in their Fifth Catalogue of Nearby Stars (CNS5) by applying a simple cut on the

⁸ <https://gea.esac.esa.int/archive/documentation/GDR3>

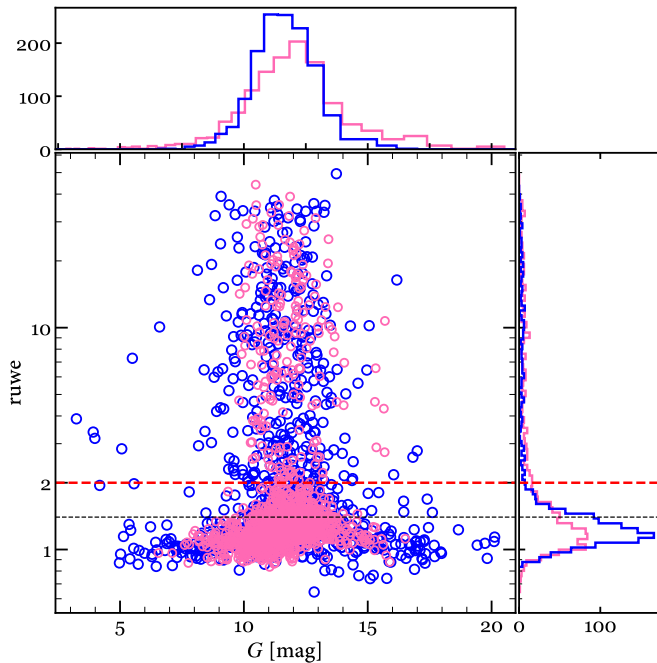


Fig. 5: RUWE as a function of G magnitude for single stars (pink open circles) and stars in multiple systems (open blue circles). The histograms follow the same colour coding. RUWE = 2.0 (thick red dashed line), used in this work, leaves behind $\sim 80\%$ of the sample and is more conservative than the traditionally used RUWE = 1.4 (thin black dashed line).

`ipd_gof_harmonic_amplitude` (see their Eq. 2). We did not include this criterion among ours, but we nevertheless applied it to every star and companion in our sample for which a measure of the parallax is available from *Gaia* DR3 (but excluding DR2). We found that only nine objects show spurious solution using this cut, with eight of them being known binaries, and one being single, but categorised as ‘Candidate’ via several other criteria in Table 3.

3.3.3. Variability in RV (Criteria 4 and 5)

The standard deviation of RV at several epochs (i.e. $\sigma(V_r) = \epsilon_{RV}$) is a powerful method of identifying (spectroscopic) binary systems. Furthermore, it allows to discriminate true orbital acceleration due to multiplicity from the acceleration due to an effect of perspective.

Among the stars with the largest $\sigma(V_r)$ measured in *Gaia* DR3, greater than 10 km s^{-1} , we selected the brightest ones to study their close multiplicity using medium-resolution spectra. We are carrying several observation campaigns with the high-resolution Fibre-fed Echelle Spectrograph (FIES) mounted on the 2.56 m Nordic Optical Telescope (NOT), in the medium-resolution mode ($R = 46\,000$), as well as with the High-Efficiency and high-Resolution Mercator Échelle Spectrograph (HERMES) at the 1.2 m Mercator telescope. From this ongoing program, we confirm the multiple nature of several of these candidates. Although the detailed results will be published in a forthcoming article, the preliminary results from those observations confirmed that our limit of 10 km s^{-1} is very robust.

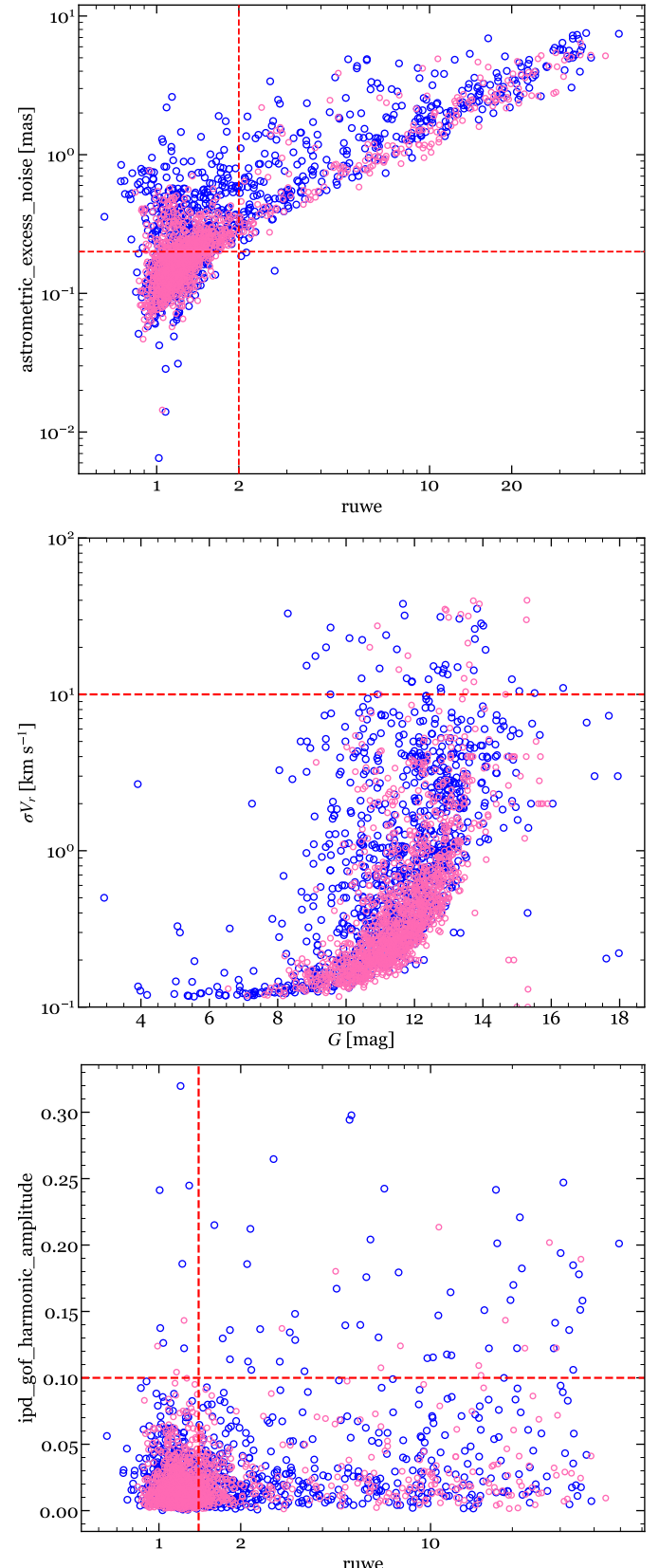


Fig. 6: *Gaia* DR3 statistical indicators of very close multiplicity. Top: $\text{astrometric_excess_noise} (\epsilon)$ vs RUWE. Middle: $\sigma(V_r)$ vs G . Bottom: `ipd_gof_harmonic_amplitude` vs RUWE. In all panels, pink and blue open circles are for stars that were considered single and part of multiple systems, respectively, and the red thick dashed lines indicate the corresponding close binary selection criterion in Table 3.

3.3.4. Lacking or poor data (Criteria 6 and 7)

Sources in DR3 apparently unaffected by the proximity of other objects, but showing excessive uncertainties in parallaxes and proper motions nonetheless, or lacking entries in these fields altogether, could actually be close binary candidates. For example, [Gaia Collaboration et al. \(2021b\)](#) noted that spurious astrometric solutions can be due, among a number of reasons, to the presence of more than one object in the astrometric window (close double systems, either real or in projection) or to binary orbital motion that is not accounted for. The odds for a chance alignment are much lower than for a physical connection, although these odds increase at wider separations and fainter magnitudes (e.g. [El-Badry et al. 2021](#); [Chulkov & Malkov 2022](#)). Chance alignments are more likely to occur in regions of high surface density of sources such as open clusters and near the galactic plane ([Gaia Collaboration et al. 2021b](#)). While DR3 benefits from a larger number of observation epochs with respect to previous releases, some very close binaries not resolved in DR2 were handled as single objects, with blended photometry and occasional spurious astrometric solutions ([Arenou et al. 2018](#); [Ziegler et al. 2018](#)). The `duplicated_source` flag is usually of help for those sources that also exhibit poor astrometric quality or lack some data (mainly proper motions and parallaxes). This flag is set to ‘1’ in those instances where the detection system on board *Gaia* generates multiple detections for the same source, which results in different data sets for the same target. The final DR3 catalogue retained only the solution with the best astrometric quality and flagged it as a `duplicated_source`, while the poorer ones were discarded.

3.3.5. Non-single star tables by *Gaia* DPAC

Among the built-in data products in *Gaia* DR3 by the Data Processing and Analysis Consortium (DPAC), the ‘non-single stars’ tables ([Pourbaix et al. 2022](#)) enable the identification of unresolved astrometric, spectroscopic, and eclipsing binaries ([Gaia Collaboration et al. 2023a](#)). Despite their name, these tables are unrelated to the `non_single_star` flag, which is primarily a modelling quality flag and not an identifier of multiplicity. These solutions are distributed in four tables: `nss_two_body_orbit` when the full orbital motion is known, `nss_acceleration_astro` and `nss_non_linear_spectro` when a trend is known, and `nss_vim_f1` for photometrically variable unresolved binaries. More details on the processing scheme, its validation, and the various types of reached solutions can be found in Chapter 7 of the *Gaia* DR3 documentation.

3.3.6. Astrometric excess noise

In addition to RUWE, another measure of *Gaia*’s astrometric goodness-of-fit is the `astrometric_excess_noise` (ϵ). It quantifies the disagreement between the observations of a source and the best-fitting standard astrometric model. Both are sensitive to the photocentric motions of unresolved objects, such as astrometric binaries, which are not revealed by the IPD statistics, and therefore complement the latter in binary detection ([Lindegren et al. 2021](#)). For well-behaved sources, ϵ should be zero, but since it accommodates excess noise originating from both the source and the instrument attitude, non-zero values are inevitable ([Lindegren et al. 2012](#)). For instance, in DR1 nearly all sources show significant excess noise ($\epsilon \sim 0.5$ mas), but only unusually large values ($\epsilon \gtrsim 1\text{--}2$ mas) are indicative of astrometric binarity or other issues ([Lindegren et al. 2016](#)). In DR2

roughly 20 % of the sources between $G = 12$ mag and 20 mag have excess noise ([Lindegren et al. 2018](#)). In EDR3, [Lindegren et al. \(2021\)](#) observed an improved homogeneity of ϵ despite increased noise in crowded regions. Nevertheless, ϵ can be regarded as insignificant (i.e. effectively zero) if the significance, `astrometric_excess_noise_sig` (D), is less than 2 mas.

The RUWE includes a scaling factor to compensate for calibration errors that correlate with colour and magnitude, but ϵ does not. For example, [Gandhi et al. \(2022\)](#) used astrometric excess noise to search for candidate X-ray binaries, selecting sources with $\epsilon \geq 0.01$ mas, $D \geq 2$ mas, `visibility_periods_used` > 10 , and G between 13 mag and 20 mag. They found that systematic effects, such as attitude errors, partially resolved double stars, and source variability, can be sources of contamination, especially when $\epsilon < 1$ mas, making interpretation more difficult.

In the stars of our sample, we found a linear correlation between the excess ϵ and its significance D , meaning that larger values of ϵ are generally associated to larger values of D . In particular, all the instances with notable ϵ happen to be known binaries in close configurations. Therefore, we found ϵ and D to be redundant and equivalent to RUWE, and stuck to the latter, as detailed in Sect. 3.3.1.

3.3.7. Photometric variability

Measuring the stellar brightness over time can reveal the presence of binaries that are otherwise indistinguishable in static images. *Gaia* DR3 provides a variability analysis of many objects using data from the 34 months. The variability processing and analysis was based mostly on time series of field-of-view transit (integrated) photometry in the calibrated G , G_{BP} , and G_{RP} bands, with additional input data, such as RV time series. We refer to [Eyer et al. 2017](#) for a more complete description of the models and methods. In *Gaia* DR3, `phot_variable_flag` tags with ‘VARIABLE’ those sources identified and processed as variable from the photometric data. The variables `GrVFlag`, `BPrVFlag`, and `RPrVFlag` accompanying the photometric measurements indicate the photometry rejected by variability processing ([Eyer et al. 2023](#)). Even so, 346 stars in our sample are identified as variables by *Gaia* DR3.

Figure 7 shows the photometric time series (or light curves) in the three *Gaia* passbands for three selected cases: a single star, a known binary, and a binary candidate. When an object crosses the focal plane of *Gaia* (see Fig. 4 of [Gaia Collaboration et al. 2016](#)), its flux is measured nearly simultaneously in the three passbands, but the G -band photometry is more precise and has a better spatial resolution ([Eyer et al. 2017](#), additionally, the object is typically detected by nine CCDs in the green photometer, which is larger than the red and the blue). Stellar variability of intrinsic nature (i.e. not due to the presence of a companion) is apparent in the three passbands simultaneously and with a common pattern. However, there are *Gaia* sources with relatively flat G_{BP} and G_{RP} light curves, but much scattered G light curves. Sometimes they even display a double G light curve separated by up to 0.7 mag; these sources are actually close binary systems unresolved in G_{BP} and G_{RP} but resolved or partially resolved, depending mostly on the scan angle, in G ([Vinagre Maqueda 2023](#); [Maíz Apellániz et al. 2023](#); [González-Payo et al. 2024](#); T. Prusti, priv. comm.). In the three examples of Fig. 7, only the G light curves of the known binary (LP 15–315, JNN 266) and our new candidate binary (RX J0507.2+3731B, $\rho \approx 0.48$ arcsec) display a “double-sequence” pattern.

Figure 8 compares the standard deviation, σ , between two *Gaia* passbands. It distinguishes between multiple systems and

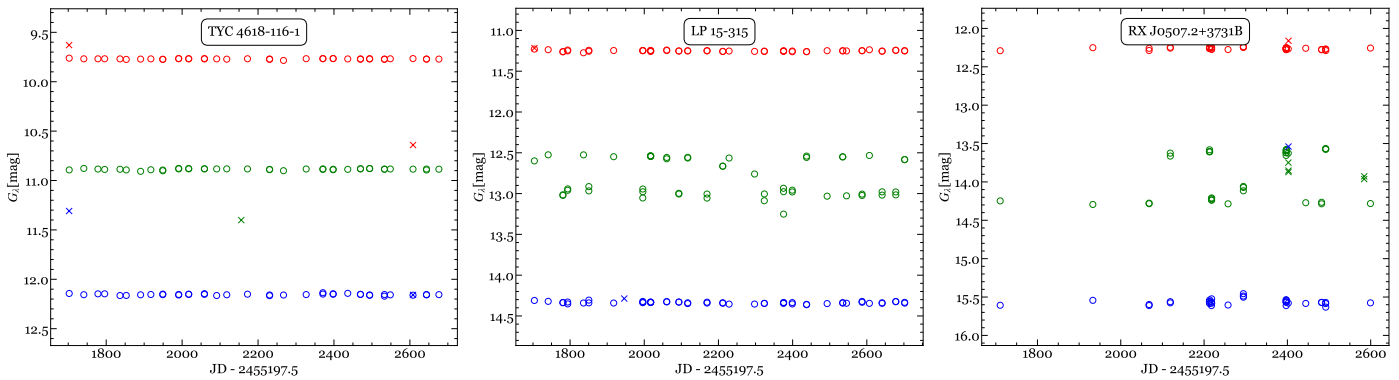


Fig. 7: Light curves corresponding to the *Gaia* passbands G_{RP} (red), G (green), and G_{BP} (blue) for three cases: a single star (*left*), a known close ($\rho = 0.1\text{--}0.2$ arcsec) binary system (JNN 266, [Janson et al. 2014b](#); *middle*), and a newly reported close ($\rho \approx 0.48$ arcsec) binary system (*right*). Isolated outliers (represented by crosses) are photometric errors, not consistent with flares, automatically rejected by variability processing. The remaining light curves for the unresolved binary candidates with double-sequence patterns are displayed in Fig. A.1.

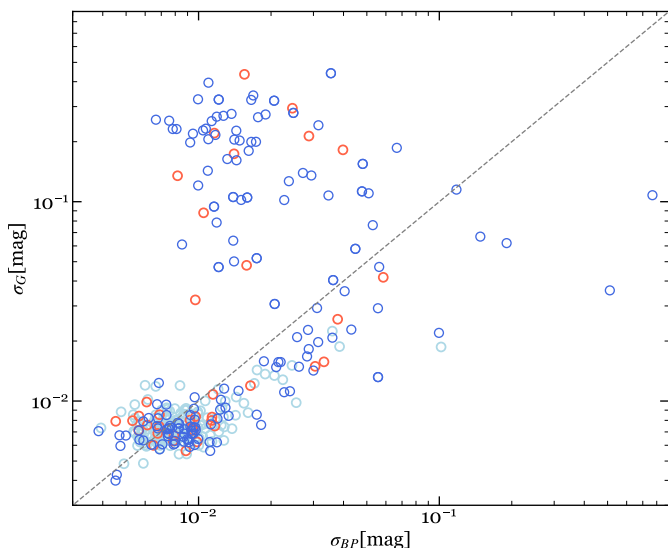


Fig. 8: Comparison of the standard deviations of G_{BP} against that of G for single stars (light blue), stars in multiple systems (blue), and new unresolved binary candidates (red). The dashed line represent a 1:1 relation. The similar plot for G_{RP} is omitted for simplicity.

single stars, and among these, the ones that are new unresolved binary candidates. Except for a few intrinsically variable young stars, single stars systematically show low standard deviations in the three passbands. All the sources with significant deviations are either confirmed binaries or close binary candidates. All the known binaries and new unresolved binary candidates in the agglomeration in top left corner show the G double-sequence pattern that is not detected in the G_{BP} (and G_{RP}) light curves.

3.3.8. Selection of candidates

We used all the seven criteria of Table 3 to identify new candidate binaries among the M dwarfs of our sample and their *Gaia* companions (2634 stars, white dwarfs, and ultra-cool dwarfs in total). We found that 327 of them meet one or more of the criteria. Of them, 278 were thought to be singles and 49 formed part of multiple systems with known companions but are sepa-

rated enough to exert a negligible influence. When the identified unresolved binary candidate is part of a know multiple system, we flagged them as ‘Multiple+’ in the full version of Table A.1. If the candidate is a single star without known companions, we flagged them as ‘Candidate’.

Figures 5 and 6 illustrate the correlation of four selected statistics of *Gaia*: `ipd_gof_harmonic_amplitude`, `ruwe`, `radial_velocity_error` (criteria 1, 2, and 5 in Table 3), and `astrometric_excess_noise`. Stars in multiple systems may only have wide companions and, therefore, experience insignificant (if any) change in `ruwe` or σ_{V_r} . Single stars are generally more scarce as we approach to the limits set by the criteria.

We also looked for matches of our sample (and their resolved companions) within non-single star tables provided by *Gaia*, and found 49, 6, 1, 0, and 2 coincidences in the tables enumerated in Sect. 3.3.5, respectively. These coincidences translate into 55 individual stars proposed as unresolved pairs by the *Gaia* processing scheme. Of them, 24 are known pairs with very close-in orbits, and 31 are bona fide single stars, or in a few cases component in very wide pairs, presumably unaffected by their distant companion. The 2 eclipsing binaries are the known systems of Castor C ([Joy & Sanford 1926](#); [Gizis et al. 2002](#)) and GJ 3547 ([Shkolnik et al. 2010](#); [Reiners et al. 2012](#)). The former belongs to the sextuplet system α Gem, one of the most complex configurations in our sample.

Additionally, we matched our list of candidates with those identified in the GCNS by [Penoyre et al. \(2022b\)](#). This yielded 227 objects with both RUWE and LUWE values pointing to possible binarity. All of them are also tagged by us as candidates, except in those cases where close (or very close) multiplicity is already known. Additionally, we cross-matched the table `vari_eclipsing_binary` ([Mowlavi et al. 2023](#); [Eyer et al. 2023](#)), which was the first *Gaia* catalogue of eclipsing binaries from the study of variability. No new EB candidates were found as a result.

4. Results and discussion

4.1. Multiplicity fraction

In the present work, we adopted the traditional definition for stellar multiplicity, requiring that the M dwarf is the primary (i.e. the most massive) component of its system. This means that M

dwarfs as companions to A-type stars⁹, FGK stars (Sect. 4.4.1) and white dwarfs (Sect. 4.4.2) do not count towards multiplicity statistics. In order to quantify the observed multiplicity frequency or multiplicity fraction (MF) of M dwarfs, we followed the convenient notation of Batten (1973), who denoted as f_n the fraction of primaries that have n companions:

$$\text{MF} = \frac{\sum_{n=1}^{\infty} f_n}{\sum_{n=0}^{\infty} f_n} = \frac{B + T + Q + \dots}{S + B + T + Q + \dots}, \quad (4)$$

where S, B, T, Q represent the number of single, binary, triple, and quadruple systems, respectively. In our sample of 2214 M dwarfs, 834 (37.7 %) belong to a multiple system, and from these almost three out of four (73.8 % or 615) are the primaries of their systems, which implies a multiplicity fraction of $\text{MF} = 27.8^{+1.9}_{-1.8}\%$, where the uncertainties correspond to the 95 % confidence interval using the Wilson formula (Wilson 1927). The remaining 1377 (62.2 % of the total) stars did not have suspected companions at any separation until now, with the exception of exoplanet hosts (Table A.11). However, 278 of them (plus 49 wide components among those in multiple systems) are proposed as new unresolved binary candidates in this work. These values imply that the multiplicity fraction of M dwarfs (from M0.0 V to M9.5 V) could be increased by 12.5 %, potentially reaching $\text{MF}+ = 40.3^{+2.1}_{-2.0}\%$, which is higher than the values typically found for M dwarfs. Our canonical MF is in agreement with the values reported in the literature, especially in those cases where a sizeable sample was studied. However, our expected MF+ notably exceeds previous estimations, with the exceptions of the early studies of Henry & McCarthy (1990), Fischer & Marcy (1992), and Simons et al. (1996).

For a proper comparison with Table 1, besides in the full M-dwarf spectral range, we also calculated the MF in the ranges from M0.0 to M4.5 V and from M5.0 V to M9.5 V. The former is volume-complete up to a distance of $d_{\text{com}} = 30$ pc, while the latter is only up to 10 pc (Sect. 2). Besides, given the uncertainties due to the smaller sample size at the lowest masses, we cannot confirm that the MF+ decreases with decreasing primary mass. While $\text{MF}+ = 40.5^{+2.1}_{-2.1}\%$ in the M0.0–4.5 V spectral type range, it is $38.1^{+7.4}_{-6.8}\%$ in the M5.0–M9.5 V range.

Likewise, the companion star fraction (CSF)¹⁰ is the ratio of the total number of companions to the total number of stars in the sample:

$$\text{CSF} = \frac{\sum_{i=1}^{\infty} (n - 1)f_n}{\sum_{i=0}^{\infty} f_n} = \frac{B + 2T + 3Q + \dots}{S + B + T + Q + \dots}. \quad (5)$$

The CSF is a measure of the average number of companions per system, and can be larger than one. In our sample, M dwarfs have a $\text{CSF} = 0.332^{+0.020}_{-0.019}$ ($\text{CSF}+ = 0.462^{+0.038}_{-0.079}$ if the new candidates are included). These values imply that roughly one in three M dwarfs have at least one (less massive) stellar or brown-dwarf companion (one in two M dwarfs if the new candidates are confirmed).

Regarding the configurations of the multiple systems with M dwarfs as primaries, binary arrangements embody the majority

of architectures (83.1 %), followed by triple systems (14.3 %), quadruples (2.1 %), and quintuples (0.3 %). V1311 Ori is either a marginally stable hierarchy or a disintegrating mini-cluster (Tokovinin 2022) and it is the only sextuple system with an M-dwarf primary (J05320–030) in our sample.

The multiplicity fractions provided above (MF, MF+, CSF, and CSF+) are intended to offer results that can be compared with previous investigations. However, one of the main concerns when claiming multiplicity fractions is selection bias. In other words, we need to understand the limitations of the observations available, and also factoring in the potential for undetected companions. Here, the ‘detection limits’ define the minimum separations at which one can be confident about the absence of companions (above a certain mass). This definition ensures that the probability of missing a bound companion above that limit is minimal. These limits are primarily based on the spatial resolution of the applied observational techniques, and the contrast limit between the primary star and potential companions. Following this idea, we assigned one of the following categories to each M dwarf of our sample, including their confirmed companions:

- Category 1: Stars observed with extreme precision spectrographs, with ten or more spectra in the CARMENES survey or monitored by other programmes (Ribas et al. 2023, and their Table 4). Some of them may have also been observed with high-resolution imagers (AO, LI), the *Hubble Space Telescope*, or even interferometric instruments (e.g. Caballero et al. 2022).
- Category 2: Stars observed with high-resolution imagers or those having less than ten high-resolution spectra.
- Category 3: Stars with only *Gaia* DR3 data.

Categories 1–3 refer to the maximum precision (in decreasing order) with which each star stands in our study. Among the 2214 M dwarfs in our sample of study, 447 are category 1, 408 are category 2, and 1359 are category 3 (included in Table A.1). We computed the MF, MF+, CSF, and CSF+ values, ultimately concluding that the expected (MF+, CSF+) fractions are larger than the canonical ones (MF, CSF) in all cases, but only significantly for category 3 stars. That is to say, *Gaia* DR3 is not enough for imposing restrictive detection limits to close multiplicity. Therefore more high-resolution spatial and spectral monitoring of stars from the ground are needed. Furthermore, it is more difficult to detect faint companions at further distance. Thus, the binary fraction measured with the whole sample may also be biased. We could have measured the binary fractions in more complete subsamples by limiting ourselves to shorter distances. However, since Carmencita was defined in the pre-*Gaia* era, it is better to get rid of this bias by repeating the analysis in well-defined volume-limited samples, such as those of Reyé et al. (2021, 2022, at 10 pc), Kirkpatrick et al. (2024, at 20 pc), and Gaia Collaboration et al. (2021b, at 100 pc). This new analysis is part of forthcoming work (e.g. González-Payo et al., in prep.).

4.2. Astrophysical parameters

The main stellar parameters that we inferred were luminosities (\mathcal{L}), radii (\mathcal{R}), and masses (\mathcal{M}). The radii and masses can be directly measured but only for a limited number of stars, which usually belong to multiple systems. Element abundances and surface gravities can be studied from high-resolution spectroscopy, which is not always available. Nevertheless, broadband

⁹ The three A-type stars with M-dwarfs companions are: Castor, HD 140232, and HD 29391.

¹⁰ In order to avoid confusion, we retain here the term ‘star’ even when the companion object may be substellar or a stellar remnant.

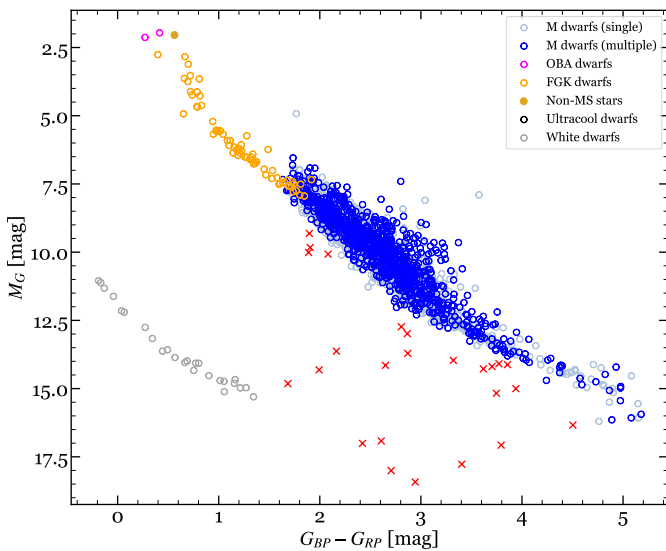


Fig. 9: Absolute magnitude M_G against $G_{BP} - G_{RP}$ colour for all the stars in our sample and their resolved companions with full photometry available in *Gaia* DR3. Red crosses correspond to components of multiple systems that are very close, very faint, or both, resulting in compromised photometry. Very bright stars (e.g. Capella or Castor) are necessarily excluded for lacking *Gaia* photometric measurements. Very compact systems, not resolved by *Gaia* (Sect. 3.2), and resolved young stars (Sect. 4.5) lie above the main sequence.

multi-wavelength photometric data have almost always been measured for relatively bright, nearby stars. With these data, the spectral energy distribution (SED) can be built and fitted to theoretical models. These fits provide a good estimation of the bolometric flux, which results in the luminosities and effective temperatures (T_{eff}), provided that the distance to the star is known (Cifuentes et al. 2020). Parallaxes were available in *Gaia* DR3, obviating the usage of photometric distances, subject to much larger uncertainties.

For each star in our sample and their resolved companions, first we compiled up to ten different magnitudes from the optical blue to the mid-infrared: three from *Gaia* (G_{BP} , G , G_{RP}), three from the Two Micron All Sky Survey (2MASS, Skrutskie et al. 2006 – J , H , K_s), and four from the Wide-field Infrared Survey Explorer All-Sky Data Release (AllWISE, Cutri et al. 2014 – W_1 , W_2 , W_3 , W_4). Our attempt to automatically include these catalogues by using the `best_neighbour` automatic cross-match from the *Gaia* Archive turned out to be unsuccessful. Instead, we performed this search manually to ensure a correct discrimination of the components of the systems as Cifuentes et al. (2020). This approach is of crucial importance in this work, because the description of each system fundamentally relies on whether 2MASS and *Gaia* are able to resolve the system or not.

At least one spectral classification is available in the literature for all but 15 of our 2214 M dwarfs. For these 15 M dwarfs and for 227 companions of M dwarfs, we photometrically estimated the spectral type using Table 7 from Cifuentes et al. (2020) for late-K and M dwarfs (242 cases), or the public table derived from Pecaut & Mamajek (2013)¹¹ for stars other than M dwarfs

Table 4: Coefficients for the polynomial fits of G -band absolute magnitudes to masses and radii.

| Parameter | \mathcal{M} | \mathcal{R} |
|-----------|-----------------------|------------------------|
| a | 2.124 ± 0.040 | 2.0585 ± 0.0026 |
| b | -0.2503 ± 0.0075 | -0.24208 ± 0.00012 |
| c | 0.00741 ± 0.00035 | 0.00728 ± 0.00012 |

Notes. The polynomial fit takes the form $Y = a + bX + cX^2$, where $Y = M_G$ (in mag) and X can be either \mathcal{M} (in \mathcal{M}_\odot) or \mathcal{R} (in \mathcal{R}_\odot).

(three ultra-cool dwarfs and five solar-type stars; see Sects. 4.4.1 and 4.4.3). None of these 242 stars have available spectra in the LAMOST DR9 database (Zhao et al. 2012).

One object is classified as a white dwarf, as discussed in Sect. 4.4.2. If both M_G and M_J were missing, we took advantage of the magnitude difference reported by the WDS, given that the spectral type of the primary is known and assuming that the two stars are at equal distance. There are six stars with spectral types ranging from G5 V to K7 V as displayed by SIMBAD, but without an assigned bibliographic reference. Finally, we reclassified all ‘K6 V’ and ‘K8 V’ stars as K7 V, as this is widely accepted in the literature (Morgan & Keenan 1973; Kirkpatrick et al. 1991; Alonso-Floriano et al. 2015b; Maíz Apellániz et al. 2024).

The faintest components of both very close and wide pairs have had their photometry compromised, and this has negatively impacted their photometrically derived parameters. For the closest ones, the photometry is affected by the brighter nearby source; for the wide ones, it is not feasible to obtain a good measure of the flux from *Gaia*’s blue filter, G_{BP} .

Using the compiled photometry and distances only, we constructed the empirical SEDs and fitted them to synthetic models. For the fitting, we used the Virtual Observatory Spectral energy distribution Analyzer (VOSA; Bayo et al. 2008) and the grid of BT-Settl CIFIST theoretical spectra (Baraffe et al. 1998; Allard et al. 2012), as Cifuentes et al. (2020). Because these models reproduce the stellar photospheres, we did not include magnitudes from passbands with $\lambda_{\text{eff}} \lesssim 420$ nm (i.e. u and bluer) because they are mostly of chromospheric origin. VOSA calculates the flux and provides T_{eff} and \mathcal{L} for a given metallicity, which we set to solar ([Fe/H] = 0.0 dex). We performed this process exclusively for the objects whose photometric measurements are not compromised by the presence of a companion that is very close, very bright, or both. As Cifuentes et al. (2020), we imposed that the flux of the secondary does not exceed 1% that of the primary, this is, $\Delta G = |G_A - G_B| > 5$ mag. Therefore, we excluded known spectroscopic binaries and resolved, but very close binaries. In particular, we did not determine \mathcal{L} and T_{eff} for binaries not resolved by both *Gaia* and 2MASS.

From \mathcal{L} we derived \mathcal{R} using the Stefan-Boltzmann law, $\mathcal{L} = 4\pi\mathcal{R}^2\sigma T_{\text{eff}}^4$, where σ is the Stefan-Boltzmann constant. M-dwarf \mathcal{M} are empirically related to \mathcal{R} via Eq. 6 of Schweitzer et al. (2019). This relation was derived from the study of detached, double-lined, double-eclipsing, main sequence M-dwarf binaries from the literature, which is valid across a wide range of metallicities for stars older than a few hundred million years. For the companions to stars in our sample that are outside the M-dwarf range, we used the mean values of \mathcal{R} and \mathcal{M} provided by Pecaut et al. (2012) and Pecaut & Mamajek (2013).

We did not tabulate the bolometric luminosity for 603 stars in our sample for two main reasons: Lack of trigonometric distances, or the presence of companion(s) at short angular separa-

¹¹ “A Modern Mean Dwarf Stellar Color and Effective Temperature Sequence”, http://www.pas.rochester.edu/~emamajek/EEM_dwarf_UBVIJHK_colors_Teff.txt

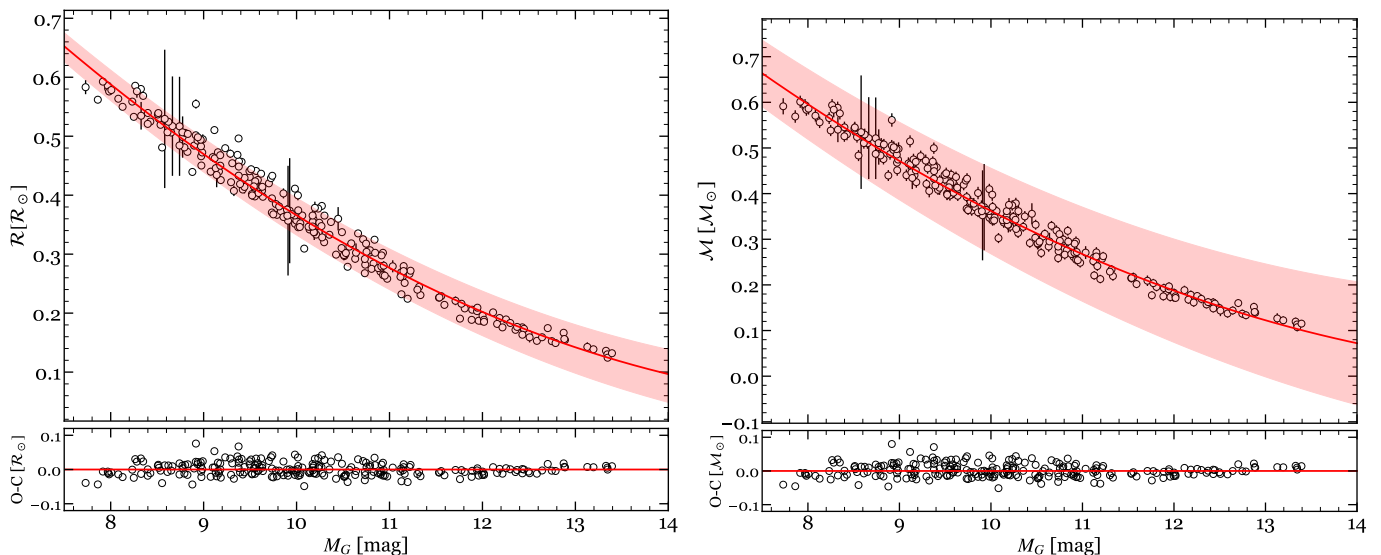


Fig. 10: Stellar radius (\mathcal{R} , left) and mass (\mathcal{M} , right) as a function of the absolute magnitude (M_G) valid in the M-dwarf domain. The red line represents the polynomial fit described in Table 4, and the red shaded area indicates the $1-\sigma$ level of uncertainty.

tions. *Gaia* data offer the capability to separate sub-arcsecond binaries that have not been resolved by other all-sky surveys (2MASS, WISE). Therefore, the individual components of stars without computed \mathcal{L} still have an M_G value, which we use as a proxy for luminosity (see Cifuentes et al. 2020). For those stars without luminosities and with components resolved by *Gaia* ('AB' or 'A+B' in our nomenclature; see Sect. 4.3), we estimated \mathcal{M} and \mathcal{R} using their M_G absolute magnitudes instead.

To do so, we fit ex professo $\mathcal{M}-M_G$ and $\mathcal{R}-M_G$ relations (Fig. 10) using the radii and masses derived from a subsample consisting of 240 M dwarfs with several restrictions: (i) they must be single (i.e. avoiding those in multiple systems, even with companions of large separation); (ii) they are not new binary candidates (Sect. 3.3); and (iii) they are not classified as young stellar objects or members of young kinematic groups (Sect. 4.5), for which the masses have been underestimated. Both fits are second-grade polynomials (degree determined by the Bayesian information criterion) with the coefficients given in Table 4 and Pearson's r equals 0.986 for both. They hold within the range $M_G \in [7.5, 14.0]$ mag or K7-M0 V to M7 V (Cifuentes et al. 2020). The $\mathcal{M}-\mathcal{R}$ relation from Schweitzer et al. (2019) links both fits, therefore the uncertainties of $\mathcal{M}-M_G$ are larger due to the error propagation. They can still be used up to $M_G = 16$ mag if necessary, but with extreme caution, being aware that the photometrically derived masses of ultra-cool dwarfs strongly depend on age (Soderblom 2010, and Fig. 13 of Sahlmann et al. 2020). For the stars outside our range of validity, we used the $M_G-\mathcal{M}$ and $M_G-\mathcal{R}$ relations by Pecaut & Mamajek (2013), where we assumed an uncertainty of at least 15%. Here, M_{K_s} is better correlated to \mathcal{M} and less dependent on metallicity and age than M_G (Mann et al. 2015). However, we used M_G to maximise the number of stars with homogeneous \mathcal{M} and \mathcal{R} determination, as there is a large number of close pairs resolved by *Gaia* (AB), but unresolved by 2MASS (A+B; Sect. 4.3).

For white dwarfs, we retrieved the masses from the literature when possible (see Sect. 4.4.2) or assigned a mean mass of $0.6 M_\odot$ otherwise (Kepler et al. 2007; Bédard et al. 2020). For objects cooler than L2, we did not estimate their masses or radii.

4.3. Description of the systems

Table A.1 displays all the M dwarfs in Carmencita plus their companions (in the case of multiple systems) resolved by *Gaia*. It contains a total of 2634 rows (2214 M dwarfs in the study sample plus 420 resolved companions) and 131 columns. Its structure is meant to be both human- and machine-readable. For the former, the systems are displayed with one component of the systems resolved by *Gaia* per row. A few notable cases lack *Gaia* identification, such as the very bright Capella or the very faint Wolf 1130 B, but they still have their rows assigned in the table. The stars are sorted by right ascension, but ensuring that those that belong to the same system are consecutive, in order of decreasing brightness.

The nomenclature of the system follows the scheme shown in Fig. 11. The primary components ('A', or their variations) are the most massive ones of the systems, which are typically the brightest ones. However, white dwarfs are an exception. Although they are dimmer than M-dwarf companions in most cases (see again Fig. 9), white dwarfs are known to be the remnants of late B to early G main sequence stars, which were more massive than M dwarfs. However, for historical reasons, we considered white dwarfs as companions in all the instances found in this work (see more details in Sect. 4.4.2). A comparison of the different surveys (WISE, *Gaia*, and 2MASS) and techniques (AO, LI, SB), with a focus on their ability to identify resolved binaries, is shown in the upper panel of Fig. 12; the lower panel shows the difference in magnitude (in general, *Gaia*'s G) as a function of the angular separation. The resolving capabilities of *Gaia* DR3 do not only depend on the separation, but also on the flux ratio, with considerable difficulty involved in telling individual sources apart with $\rho \lesssim 0.6$ arcsec and $\Delta G > 0.1$ mag. In addition, it is known that the rectangular pixels of *Gaia* induce a dependence on the position angle between the two stars, influenced by the scanning direction (de Bruijne et al. 2015); however, this fact is alleviated by the large number of transits at different scanning directions.

Figure 12 also helps to shed light on the boundary between 'close' and 'wide' pairs. These terms are generally defined in a static way, with separations that depend on the context of the

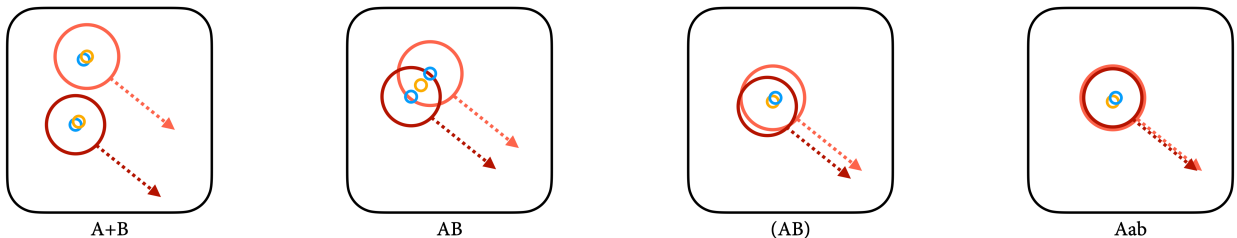


Fig. 11: Nomenclature of multiple systems based on the resolution of *Gaia* DR3 (blue circles) and 2MASS (orange circles). *From left to right*: ‘A+B’ (resolved in both surveys), ‘AB’ (only resolved in *Gaia*), ‘(AB)’ (not resolved either in *Gaia* or 2MASS, but resolved by adaptive optics, lucky imaging, or space imaging), and ‘Aab’ (spectroscopic binaries). Multiple systems can often be a combination of these cases.

study. However, the distinction between close and wide should be dynamic rather than static, based on the detection limits and spatial resolution of the used facilities. A practical definition of wide pairs could be those that can be resolved using natural seeing conditions (1–2 arcsec) without the need for advanced techniques such as AO and LI. The 2MASS survey, with a spatial resolution of 2–4 arcsec, can serve as a useful gauge to define these ‘wide’ pairs. In this work, we aim to adhere to this definition. However, the terms ‘wide’ and ‘close’ may occasionally be used to define specific separations, particularly when referencing the literal works of others.

An adapted version of the complete table can be found in the Appendix as Table A.1, which provides: numerical ID for each star and system, Karman, common name, and GJ identifiers, coordinates, spectral type, multiplicity type (single, part of multiple systems, or new unresolved binary candidates), and availability in other tables of this work. We give a column-by-column description in Table A.6. A comma-separated values (csv) file of the complete table is available on a dedicated GitHub repository¹².

4.3.1. Physical separations

Projected angular separation, ρ , and projected linear separation, s , relate as $s = \rho \cdot d$ under the small-angle approximation ($\sin \rho \approx \rho$, with an error below 1% for $\rho < 0.24$ radians or 14 deg). The coverage in projected linear separation, $s = \rho \cdot d$ (or a), of this work extends from $2.8 \cdot 10^{-3}$ au to $2.7 \cdot 10^5$ au, spanning eight orders of magnitude; namely, from close spectroscopic binaries to ultra-wide systems (Fig. 13). The smallest orbital separation in our sample corresponds to a double-lined spectroscopic binary (SB2), with a minimum value of $a \sin i = 0.002797$ au (1RXS J070005.1–190115, Baroch et al. 2021). On the other hand, the largest orbital separation (273 660 au) corresponds to the widest pair, which is part of a quadruple system (GJ 282 A+B+Cab, Poveda et al. 2009; Baroch et al. 2021) in the Ursa Major stellar kinematic group (Tabernero et al. 2017); therefore, its actual binding may be called into question. The widest pair not associated to any stellar kinematic group is in the quintuple system σ CrB, which consists of three Sun-like main-sequence stars and two low-mass stars: One of them, the M2.5 V σ CrB C star is at 14 346 au to the bright central star.

In terms of angular separation in resolved pairs, the range is 0.020–12 954 arcsec (or 3.6 deg). If we extrapolated to non-resolved systems such as SBs, the minimum separation would be as short as 0.0003 arcsec. G 146–35 B is the known equal-mass pair (Lamman et al. 2020) with the smallest angular separation

that *Gaia* DR3 resolves, with just $\rho \approx 0.196$ arcsec. Among those reported for the first time, LP 780-23 B is the star (\sim M3.0 V) with the smallest separation from an M dwarf primary, with $\rho = 0.199$ arcsec. In cases like these, the advantage of being able to resolve the pairs with *Gaia* comes at the cost of being significantly limited by problems affecting the astrometric measurements. In a few cases we identified members of stellar kinematic groups or associations that were either previously known (therefore confirming their membership) or unknown (therefore assigning them for the first time). These young stars are V1221 Tau with $s \approx 52\,000$ au (in the β Pictoris moving group, Gagné & Faherty 2018), and PM J18542+1058 with $s \approx 10\,000$ au (primary in the Carina moving group, Gagné & Faherty 2018), proposed for the first time in this work.

In the study of binaries, we faced the problem of translating projected angular separation, ρ , to the actual semimajor axis, a (see e.g. Kuiper 1935; Couteau 1960; van Albada 1968b). For circular orbits, s is always equal or smaller than a ; for eccentric orbits, it is the opposite case. The approximation to this problem varies between authors. Many incorporate a fixed correction factor, such as $\pi/2 \approx 1.57$ (Abt & Levy 1976) or 1.26 (Fischer & Marcy 1992, and later Dhital et al. 2010). In contradiction with previous works (e.g. Halbwachs 1983), Torres (1999) suggested that this factor varies with eccentricity. Dupuy & Liu (2011) incorporated this notion (as well as a discovery bias) to yield a factor of $1.16^{+0.81}_{-0.31}$. Other investigations have supported the assumption that s serves as a reasonable estimate for a when there is not enough information about the orbital elements of the system. For instance, Kuiper (1942) derived empirically, from 62 known orbits, a relation between the semimajor axis and the projected separation on the sky that $E(\log a) - E(\log s) = -0.11$, where E indicates the expectation value. A similar result was later obtained by Couteau (1960) using 410 orbits. When the eccentricity is taken into account, van Albada (1968b) calculated the expectation values between 0.0 (for $e = 1$) and -0.133 (for $e = 0$). More recently, Jiang & Tremaine (2010) stated that for a population of binaries at a given a , the median projected separation is $0.978a$. Given the broad scope intended for this work (we refer to the title) and the need for a proper comparison with previous work, we did not apply a conversion factor between a and s , while also assuming random orbital plane orientations.

4.3.2. Öpik’s law

It has been observed in a variety of ranges of separation that the number of pairs per unit of logarithmic separation remains roughly constant (Öpik 1924; Vereshchagin et al. 1988; Close et al. 1990; Allen et al. 2000; Poveda & Allen 2004; Poveda et al. 2007; Lépine & Bongiorno 2007). This empirical relation,

¹² <https://github.com/ccifuentesr/CARMENES-IX>

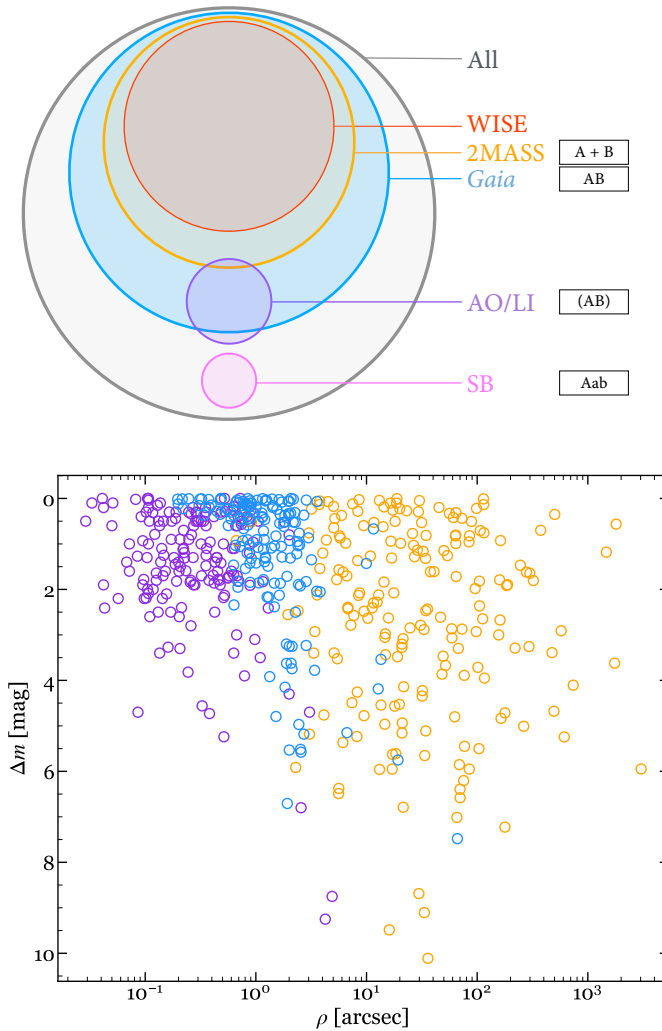


Fig. 12: Schematic of the capabilities to identify binaries of the surveys and techniques exploited in this work (*top*) and difference in G magnitude as a function of angular separation for pairs that *Gaia* resolves (“AB” or “A+B”) and those for which WDS tabulated magnitude difference (*bottom*). Both figures follow the same scheme of colours. The nomenclature assigned to each scenario (see again Fig. 11) is also displayed.

often referred to as Öpik’s law, captures the intuitive idea that the probability of finding a bound companion decreases as we go to larger separations. It admits different formulations, either through the frequency distribution $f(a) \propto a^{-1}$ or $f(s) \propto s^{-1}$, or via the cumulative distribution, which increases linearly on a logarithmic scale $N(\log a) \propto \log a$ or $N(\log s) \propto \log s$, where a and s can be used indistinctly (e.g. Allen et al. 2000).

We show in Fig. 14 the cumulative (top panel) and non-cumulative (bottom panel) distributions of projected physical separations between pairs in our sample. These data include all the possible separations between the elements in each system, namely, $n - 1$ measurements for a system of n components. We fit two well-sampled ranges in the cumulative distribution, delimited by vertical dashed lines, in which the number of multiple stars is uniformly distributed, separated by a change in slope at $s \sim 80$ au. We did not make any assumption on the optimal fitting intervals beforehand. Rather, we chose the optimal limits

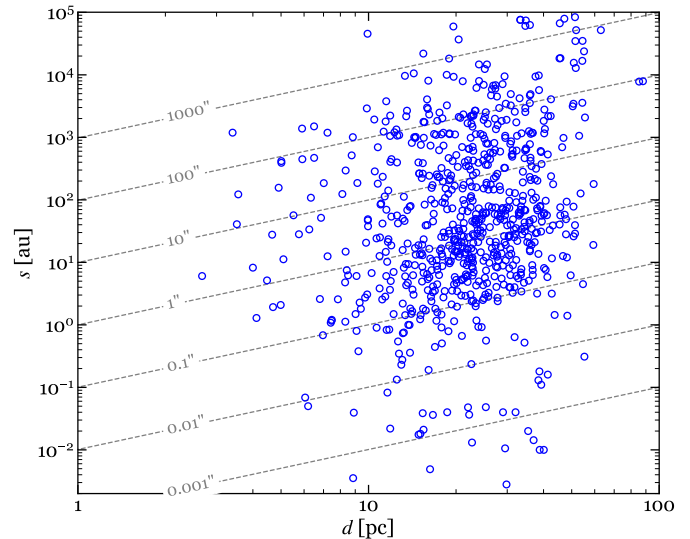


Fig. 13: Physical separation as a function of the distance for all the pairs in our sample. The grey dashed lines represent projected angular separations, $\rho = s/d$, in dex.

based on the maximisation of the χ^2 value. Following Öpik’s law, which states that there are roughly equal numbers of binaries (n_0) in each logarithmic interval of s , we expressed the parametrisation as:

$$N(s) = C + n_0(\log s - \log s_0), \quad (6)$$

where s_0 corresponds to the smallest s value in each range, and C and n_0 are free parameters. Obtaining very discrepant values for these parameters between both ranges points to a break in Öpik’s law. This behaviour had been already described (e.g. Lépine & Bongiorno 2007), with variations observed across studies due to differences in population characteristics, sample size, and data completeness. For instance, Allen et al. (2000) found that ‘wide binaries’ ($a > 25$ au, as defined by the authors) follow Öpik’s law all the way up to 10 000 au (and up to 20 000 au for those with the most halo-like orbits). Meanwhile, Poveda et al. (2007) found binaries in the field following Öpik’s law in the separation range $100 \text{ au} \leq a \leq 3000 \text{ au}$, which corresponds to the second range in our plot.

The cumulative distribution shown in Fig. 14 departs from Öpik’s at very close ($s \lesssim 1$ au) and very wide ($s \gtrsim 10^4$ au) orbital separations, a fact repeatedly observed in empirical studies (e.g. Poveda & Allen 2004, but see Poveda et al. 2007 for the exception of very young populations of binaries). The upper limit of Öpik’s law decreases with increasing system age as older systems tend to have fewer wide binaries, simply because they have had more time to be disrupted (see e.g. Weinberg et al. 1987). More recently, King et al. (2012), who studied the separation distributions in young star-forming regions, found an excess of binaries with $s < 100$ au when compared to the field population. As Lépine & Bongiorno (2007) pointed out that even if a population initially follows the canonical form of Öpik’s law, it will eventually exhibit a truncated distribution with a steeper power law, $f(s) \propto s^{-\lambda}$, where $\lambda > 1$.

It has been argued (e.g. Allen et al. 1997) that it might be preferable to describe this distribution function in accordance with the two main mechanisms of binary formation: disk fragmentation for the close systems, and first-collapse (or turbulent)

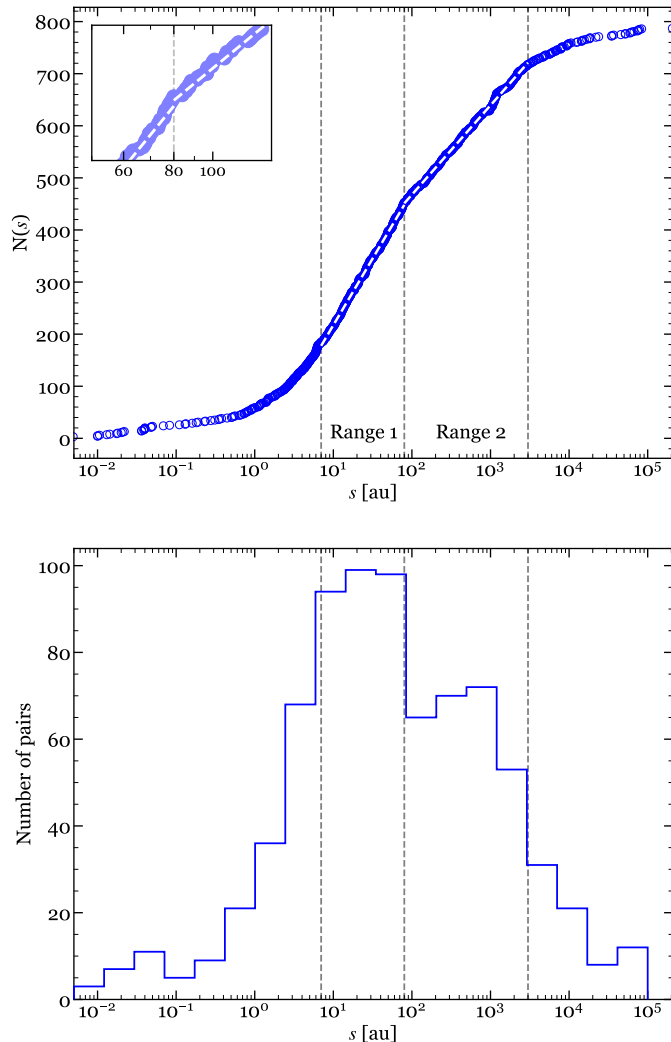


Fig. 14: Cumulative (top) and non-cumulative (bottom) distribution of physical separations for all the pairs in our sample. The white dashed lines in the upper panel are power-law fits for the ranges 7–80 au and 80–3000 au, respectively. The grey vertical dashed lines delimit these ranges.

fragmentation or the dynamical unfolding of compact triples for wider systems. Some authors (e.g. El-Badry & Rix 2018; Tian et al. 2020) have adopted a ‘broken’ power law instead. The existence of two formation mechanisms dominating in different separation regimes was also suggested by Tokovinin (2020) and Hwang et al. (2022) when studying the distribution of eccentricities. This observational result alleviates the problem that a single theory (namely, disk fragmentation) faces when explaining the existence of binaries with very wide separations. This behaviour has been observed both in pre-main and in main sequence stars (Poveda 1988; Poveda et al. 1982, 1994; Poveda & Allen 2004). All in all, it is accepted that multiple systems are formed through different processes and that the statistical properties of these systems are influenced by the environment in which they form.

The broad peak around 20 au (Fig. 14, bottom panel) was identified by Winters et al. (2019a), who noted that many stars could potentially harbour close companions, eventually altering the multiplicity rate and shifting the most common separations to smaller orbital sizes, once their orbital semimajor axes are determined. For 89 unresolved systems they adopted fixed

projected separations of 1 arcsec, which substantially underestimate the number of very close companions (at sub-Solar System scales, or less than 1 au). The authors noted that their distribution figures differed from that of Janson et al. (2014a), but highlighted the methodological differences between the two; this specifically includes the primary mass (Janson et al. 2014a focussed on M5–9 V). Our study cannot be compared directly with those above, since our distribution cannot be described with a single Gaussian given the broad range of separations that we cover.

Regarding the observed flattening of the distribution at very short and very wide separations, we assert that the former is caused by a fundamental limitation of the main high-resolution techniques (AO, LI, SI), while the latter is a consequence of the difficulty of the formation and eventual survival of the most separated binary systems, rather than observational constraints (see e.g. Poveda & Allen 2004; Lépine & Bongiorno 2007; Caballero 2009; González-Payo et al. 2023). Indeed, *Gaia* DR3 is complete for separations above 1.5–2.0 arcsec (Fabricius et al. 2021) and so, we did not expect to miss the most separated binaries in our search. The evidence shows that in binaries of $a \lesssim 50$ au, disruption by dynamical influences is negligible. They evolve essentially unaffected, either in the field or inside clusters (see e.g. Moeckel & Bate 2010). Parker et al. (2009) referred to these close-in pairs as ‘hard binaries’, while ‘intermediate binaries’ was used to refer to those with $50 \text{ au} < a < 1000$ au; the latter are severely affected by dynamical processes, especially when formed in dense star clusters. Unevolved ‘wide binaries’ with $s > 1000$ au can only originate in low-density star-forming regions with less than a few stars per cubic parsec (‘isolated star formation mode’, Goodwin 2010) or, in the words of Deacon & Kraus (2020), ‘wide binaries are rare in open clusters’. Early investigations, such as those by van Albada (1968a), suggested that binaries observed at separations greater than about 1000 au must be either ‘escaping’ double stars (or run-away stars; see also Poveda et al. 1967) or one of the components is actually a double star (yielding to a triple system) that supplies more mass (and therefore more gravitational support) to the system (Reipurth & Mikkola 2012; Cifuentes et al. 2021).

The non-cumulative distribution (Fig. 14, bottom panel) exhibits a rather bimodal shape, peaking at ~ 10 –100 au and around $\sim 10^3$ au, respectively, which roughly correspond to the changes in slope in the cumulative distribution, as marked by the range boundaries. It also shows that a large percentage of M dwarf companions are found to be as close as $s \lesssim 50$ au. Studies such as Hwang (2023) found that the fraction of wide (10^3 – 10^4 au) triple systems increases with decreasing orbital periods of the inner binaries, and the authors also found a tentative excess at $\sim 10^4$ au for tertiaries of eclipsing binaries. The bimodality in this distribution of separations has been reported before in the literature for wide ($s > 10^3$ au) binaries (e.g. Dhital et al. 2010; Oelkers et al. 2017; Jiménez-Esteban et al. 2019) and also for close ($< 10^3$ au) binaries (Kouwenhoven et al. 2010, see their Fig. 8). Dhital et al. (2010) suggested that this bimodality most likely reveals two distinct populations of wide binaries, possibly representing systems that form or dissipate through differing mechanisms: (1) systems of stars that formed with sufficient binding energy to survive for the age of the Galaxy, and (2) relatively young systems that formed within the past 1–2 Ga but that are not likely to survive much longer. The authors noted their high confidence that the bimodal structure is not due to a large contamination of very wide chance pairs, but likely that this bimodality reveals these two distinct populations of wide binaries. Oelkers et al. (2017) noted that the bimodality is split near separations of $10^{4.7}$ au, also suggesting two separate binary

populations, which follow different formation and evolutionary paths. Using *Gaia* DR2 data, Jiménez-Esteban et al. (2019) correlated the number of false positives with the separation of the system, estimating that it is $\sim 1\text{--}5\%$ of the candidate pairs with $s < 50\,000$ au, $\sim 10\text{--}18\%$ for s between 50 000 and 100 000 au, and increasing to $\sim 40\text{--}51\%$ for the largest separations, therefore resulting in most of their comoving candidate binaries with $s \lesssim 10^4$ au being real.

Before the *Gaia* mission, only relatively small samples of nearby and bright stars had useful parallaxes. Foundational works such as Kuiper (1942) only had limited data available, but recognised the limitations due to the ‘incomplete discoveries of spectroscopic and close visual binaries’ [sic]. More recently, Lépine & Bongiorno (2007) suggested that, using CCD imaging and AO, it should be possible to perform a complete census of common proper motion companions of Hipparcos stars down to angular separations of a fraction of an arcsecond, underlining the usefulness in extending the census to pairs with smaller orbital separations ($s < 1000$ au) and verify whether this regime can be consistently modelled with Öpik’s law.

Pre-*Gaia* investigations were fundamentally limited by the astrometric accuracy (in distance measurements and proper motion data), which made the characterisation of binary stars much more challenging. For example, the SLoWPoKES catalogues I and II (Dhital et al. 2010, 2015) were based on Sloan Digital Sky Survey (SDSS) data limited by their use of distance–colour relations rather than direct distance measurements. The SLoWPoKES extension catalogue, GAMBLES (Oelkers et al. 2017), used the published distances and proper motions from the Tycho–*Gaia* Astrometric Solution (TGAS), which was based on the first data release of *Gaia* and on the Tycho-2 catalogue, although also relied on SDSS data. TGAS uncertainties are typically around 0.3 mas a^{-1} , with positional uncertainties around 1–2 mas. *Gaia* DR3 significantly improved these measurements, with typical uncertainties for parallaxes around 0.02–0.03 mas, and 0.01–0.02 mas for positional measurements. Recent catalogues have used *Gaia* DR1 (Oh et al. 2017), DR2 (Tian et al. 2020; Harris et al. 2020), and EDR3 (El-Badry et al. 2021), which compile hundreds of thousands of pairs with different levels of contamination by chance alignments, sometimes using Bayesian formulation in the process.

Also using TGAS astrometry, Andrews et al. (2017) recognised that the excess of the distribution at $s \sim 10^4$ au corresponds to the transition from genuine binaries to random alignments, implying that the reported bimodality within separations of 1 pc in samples of wide binaries is most likely due to contamination from random alignments. El-Badry et al. (2021) showed that the contamination rate from chance alignments increases rapidly with separation. For instance, they distinguished between ‘initial candidate pairs’ and ‘high bound probability pairs’ (see their Fig. 2), suggesting that most initial candidates are chance alignments, which dominate at $s \gtrsim 3000$ au. They concluded that the separation distribution of binaries with high probability of being bound falls off steeply at wide separations. In particular, they suggested that at wide separations (meaning $10^{4.5}$ au) most candidates are chance alignments, an observation already made by Tian et al. (2020) relying on data from *Gaia* DR2 (see their Fig. 4). Prior to that study, the results from detailed works on the probabilities of chance alignments by Lépine & Bongiorno (2007) displayed an agreement with these results. By using astrometric data with unprecedented accuracy, the evidence presented here (see Sect. 4.3.4 for the study of binding energies and see again Figure 14) also suggests that some of the ultra-wide

binaries ($s \gtrsim 10^4$ au) claimed to be genuine are, in fact, random alignments.

4.3.3. Orbital periods

Orbital periods (P_{orb}) relate to the semimajor axis, a , and the total mass of the system, M_T , via Kepler’s third law:

$$P_{\text{orb}} = 2\pi \sqrt{\frac{a^3}{GM_T}}. \quad (7)$$

As stated above, the impact of the correction factor between a and s can be neglected. As mentioned in Sect. 1, close compact arrangements of stars can be adequately treated as a single star (with the aggregated masses) when considered from a distance much larger than the separation between its components. In this sense, triple, quadruple, or even higher order systems can be treated as binaries in the majority of cases. Therefore, we estimated orbital periods of the pairs in our sample only for the systems with available masses for all the components, either measured dynamically in the past or estimated by us (see Sect. 4.2), and with the suitable hierarchical arrangement.

Almost all the estimated P_{orb} lie between 10 a and 10^5 a, with 40 % of the total corresponding to periods of less than 10^3 a (given the dependence of P_{orb} on s , we omit the corresponding histogram, but the bottom panel of Fig. 14 may serve as a representative plot). Without the information about their orbital eccentricity and orientation, these values could be over- as well as under-estimated. For the vast majority of pairs in our sample, the orbital periods are measured by millennia, so the prospect of following them during one single orbit is unrealistic in practice. As an example, we refer again to Proxima Centauri, which has an estimated orbital period $P_{\text{orb}} \sim 5.5 \cdot 10^5$ a (Kervella et al. 2017). One consequence is that, in most cases, it will not be possible to discriminate among actual bound multiple systems and disintegrating clusters.

The largest orbital periods estimated correspond to GJ 1284 and GJ 282 C, with extreme values of $\sim 10^8$ a. On the other hand, several systems have estimated periods of less than half a century. Table 5 lists these systems, along with their masses and separations, both at the epoch of *Gaia* and at the time of the first satisfactory observation as listed by the WDS. In all cases these systems are binaries resolved by *Gaia* with angular separations $\rho \lesssim 2$ arcsec. One exception could be the system GJ 400, which might be a triple system made of HO 532 (shown in Table 5) and the innermost CHR 191 ($\rho \sim 0.37$ arcsec), but that has been poorly investigated (McAlister et al. 1987). If the system were triple, the orbital period would be of about 20 a.

In addition to the periods estimated by us, we also collected those reported in the literature, mainly derived from the study of spectroscopic binaries. Most of these are measured by days, or even by hours, such as that of LP 86-173 (LHS 1817), an M4.5-dwarf in a 7 h orbit with a possible white dwarf (Newton et al. 2016; Winters et al. 2020). The periods computed by us, as well as those collected from the literature, are included in the full version of Table A.1 (see Sect. 4.3).

4.3.4. Binding energies

The gravitational binding energy of a binary system is a measure of the strength of their attachment. In this sense, Heggie (1975) introduced the categories ‘soft’ and ‘hard’ binaries as a broad classification for the class of attachment that stellar pairs

Table 5: Systems with estimated minimum orbital periods of less than 50 years.

| Name | Comp. | Spectral Type | ρ (J2016.0) [arcsec] | ρ (epoch) [arcsec] | \mathcal{M} [\mathcal{M}_\odot] | $P_{\text{orb}}^{\text{min}}$ [a] |
|------------------------------|-------|---------------|------------------------------|----------------------------|--|--------------------------------------|
| BL Cet | A | M5.0 V | | | 0.129 ± 0.044 | |
| UV Cet | B | M6.0 V | 2.259 | 1.4 (1935) | 0.118 ± 0.045 | 29.9 ± 3.8 |
| HD 32450 A | A | M0.0 V | | | 0.611 ± 0.027 | |
| HD 32450 B | B | M3.0 V | 0.888 | 0.5 (1929) | 0.372 ± 0.032 | 20.60 ± 0.44 |
| V577 Mon | A | M4.5 V | | | 0.230 ± 0.037 | |
| Ross 614 B | B | M4.5 V | 0.313 | 1.3 (1939) | 0.228 ± 0.037 | 2.16 ± 0.12 |
| LP 780–32 | A | M4.0 V | | | 0.326 ± 0.013 | |
| Gaia DR3 2926756741750933120 | B | M4.0 V | 0.556 | 0.6 (2016) | 0.266 ± 0.036 | 32.30 ± 1.0 |
| GJ 400 A | A | M0.5 V | | | 0.642 ± 0.027 | |
| Gaia DR3 776067093937332992 | B | M2.5 V | 0.684 | 1.2 (1896) | 0.393 ± 0.032 | 28.22 ± 0.57 |
| GJ 3673 | A | M3.5 V | | | 0.386 ± 0.033 | |
| G 122–34 B | B | M3.0 V | 0.339 | 0.2 (2012) | 0.346 ± 0.034 | 42.2 ± 1.4 |
| Wolf 424 A | A | M5.0 V | | | 0.140 ± 0.043 | |
| Wolf 424 B | B | M5.5 V | 1.149 | 0.7 (1938) | 0.143 ± 0.042 | 21.9 ± 2.3 |
| GJ 3760 A | A | M2.5 V | | | 0.464 ± 0.030 | |
| GJ 3760 B | B | M2.0 V | 0.477 | 0.4 (1991) | 0.463 ± 0.030 | 49.9 ± 1.2 |
| GJ 3775 | A | M3.5 V | | | 0.218 ± 0.038 | |
| Gaia DR3 3688439268658769408 | B | M4.5 V | 0.701 | 0.6 (2012) | 0.211 ± 0.038 | 44.2 ± 2.8 |
| Ross 52 A | A | M3.5 V | | | 0.327 ± 0.034 | |
| Ross 52 B | B | M4.5 V | 0.880 | 0.9 (1940) | 0.238 ± 0.037 | 43.3 ± 1.9 |
| HD 239960 A | A | M3.0 V | | | 0.306 ± 0.034 | |
| DO Cep | B | M4.0 V | 2.052 | 2.3 (1890) | 0.199 ± 0.039 | 33.2 ± 1.7 |

Notes. Values for the orbital periods are published for some of these stars, namely: BL Cet + UV Cet: 26.380 ± 0.002 a ([Gravity Collaboration et al. 2024](#)); HD 32450 AB: 43.55 ± 0.27 a ([Hartkopf et al. 2001](#)); V577 Mon + Ross 614: 16.5777 ± 0.0027 a ([Mann et al. 2019](#)); GJ 400 AB: 160.67 a ([Mante 2000](#)); Wolf 424 AB: 15.826 ± 0.017 a ([Mann et al. 2019](#)); Ross 52 AB: 31.45 ± 0.42 a ([Mason et al. 2018](#)); HD 239960 A + DO Cep: 44.5814 ± 0.0345 a ([Izmailov 2019](#)).

can experience: The former are fragile and easy to break, while the latter are highly resilient to encounters. These definitions resemble those of ‘intermediate’ and ‘hard’ binaries as used by [Parker et al. \(2009\)](#) and summarised in Sect. 4.3.2. The reduced binding energy of a binary system of masses \mathcal{M}_1 and \mathcal{M}_2 , with a projected physical separation s , can be written as [Caballero \(2009\)](#):

$$U_g^* = -G \frac{\mathcal{M}_1 \mathcal{M}_2}{s}, \quad (8)$$

where the asterisk denotes the use of projected separation instead of the actual one, r , as the latter is unknown in most cases. Given that always $r \geq s$, the computed U_g^* values represent upper limits to the actual binding energies. Eq. 8 also applies for triple and higher order systems, with \mathcal{M}_1 and \mathcal{M}_2 corresponding to aggregated masses. This is, binding energies of high-order systems can be computed as long as they dynamically behave like a binary (as we proceeded when estimating the orbital periods). Figure 15 shows s and $|U_g^*|$ as a function of the total stellar mass, $\mathcal{M}_T = \mathcal{M}_1 + \mathcal{M}_2$, in the top and bottom panels, respectively.

The dynamical evolution of the stars over time, determined by their environment, sets a time limit for the stability of multiple systems, especially in the case of the most separated pairs. For example, [El-Badry & Rix \(2018\)](#) suggested that most wide

binaries with separations exceeding a few thousand au may become unbound during post-main sequence evolution. However, a binary never decays without neighbours. While catastrophic encounters such as collisions are not common, there is a myriad of subtle chances to disrupt their balance. The gravitational interaction with nearby stars can be disruptive in the long term, as shown by [Weinberg et al. \(1987\)](#). Considering the encounters with stars, the estimated average lifetime of a binary (Eq. 28 of their work) is:

$$t_*(a) = 1.8 \times 10^4 \text{ Ma} \left(\frac{n_*}{0.05 \text{ pc}^{-3}} \right)^{-1} \left(\frac{\mathcal{M}_T}{\mathcal{M}_\odot} \right) \left(\frac{\mathcal{M}_*}{\mathcal{M}_\odot} \right)^{-2} \times \left(\frac{\langle 1/V_{\text{rel}} \rangle^{-1}}{20 \text{ km s}^{-1}} \right) \left(\frac{a}{0.1 \text{ pc}} \right)^{-1} \ln^{-1} \Lambda, \quad (9)$$

where n_* and \mathcal{M}_* account for number density and mass of stellar perturbers, V_{rel} is the relative velocity between the binary and the perturber, \mathcal{M}_T and a refer to the total mass and semimajor axis of the binary, and Λ is the Coulomb logarithm. The expression accounts for the stochastic gravitational perturbations and the encounters with passing stars. Assuming an average perturber mass of $0.7 \mathcal{M}_\odot$, $V_{\text{rel}} = 20 \text{ km s}^{-1}$, $\Lambda = 1$, and using the average Galactic disk mass density of $0.11 \mathcal{M}_\odot \text{ pc}^{-3}$ ([Close et al. 2007; Dhital et al. 2010](#)), Eq. 9 can be greatly simplified as:

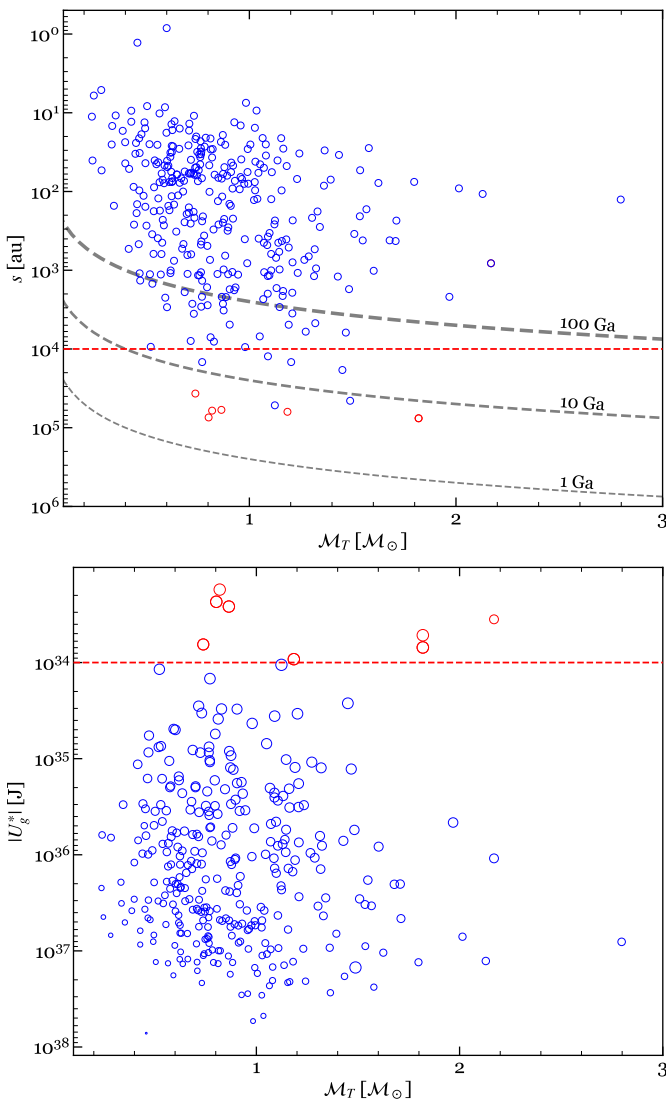


Fig. 15: Physical separation (top) and binding energy (bottom) as a function of system total mass. In the bottom panel, sizes are proportional to the physical separation from the primary. Red open circles highlight in both panels the most fragile pairs ($|U_g^*| < 10^{34}$ J – In the upper panel two of the datapoints overlap, as they share a common M_T and roughly equal separation.) The grey dashed lines mark the maximum separation, s , for expected survival in the case of 100, 10, and 1 Ga (from top to bottom). The red horizontal dashed lines mark the representative limits of 10^4 au (top) and 10^{34} J (bottom).

$$s_{\max} \approx 1.212 \frac{M_T}{t_\star} \cdot 206\,265 \text{ au.} \quad (10)$$

Here, s_{\max} represents the maximum separation for a total mass M_T in solar masses, to survive for a given age t_\star in gigayears. The separations that correspond to ages of 1, 10, and 100 Ga are plotted in Fig. 15.

Parker et al. (2009) suggested that in high- to moderate-density environments, most binaries with separations ranging from a few hundred to a few thousand au are disrupted within a few million years. Conversely, in lower density regions, galactic tides and weak interactions with passing stars gradually separate binaries with separations of around 10^4 au over approxi-

mately 10 Ga (Heggie 1975; Weinberg et al. 1987). The majority of pairs, separated some dozens or hundreds of au, are expected to be stable for hundreds of gigayears, assuming a negligible occurrence of catastrophic encounters. However, there are eight pairs in our sample with expected survival periods ranging from 1 Ga to 10 Ga. Among them there are the most weakly bound systems, with $|U_g^*| < 10^{34}$ J, highlighted in red in both panels of Fig. 15. The smallest binding energy, of $|U_g^*| = 1.74 \pm 0.21 \cdot 10^{33}$ J, corresponds to LP 404–54, a resolved component of the M3.5 dwarf primary GJ 3022 at an orbital separation of 60 680 au in a hierarchical triple system. These configurations are remarkably fragile and, therefore, more susceptible to be unbound by dynamical encounters with a plethora of sources of perturbation, such as stars, molecular clouds, clusters, and even stellar-mass black holes (Hills 1975; Ritterer & King 1982; Weinberg et al. 1987; Jiang & Tremaine 2010; Parker et al. 2011; Deacon & Kraus 2020; Ryu et al. 2022).

During our search for physical pairs resolved with *Gaia* up to 10^5 au, we found some physically bound components with $s > 10^4$ au. There are 24 systems with at least one companion of this kind in our sample. Among them there are the eight pairs with the most fragile bindings ($|U_g^*| < 10^{34}$ J), as defined above. They are collected in Table A.7, along with the most relevant parameters. Two of them (V1221 Tau and PMJ18542+1058) are identified as comoving pairs in this work for the first time (see also Table A.3). Among them, PM J18542+1058 is assigned by us as a new member of the Carina association.

4.3.5. Mass ratios

The mass ratio is defined as the fraction $q = M_B/M_A$, where ‘A’ refers to the primary component and ‘B’ refers generically to the remaining components. Given that a large number of the masses of the components of multiple systems are known or, in most cases, estimated when possible (see Sect. 4.2), we were able to calculate q for a considerable fraction of the pairs. We did not compute mass ratios for the M dwarf-white dwarf pairs (Sect. 4.4.2), given the special nature of these configurations, in which one of the components has lost much of its mass during the post-main-sequence evolution. Moreover, many q values involving spectroscopic binaries in one of the components may be absent given that only lower limits of the mass of the SB are often available.

The top panel of Fig. 16 displays the mass ratios of 424 pairs as a function of the physical separation and the primary mass¹³. An absence of small q for small primary masses (bottom right corner in the panel) has been observed in previous studies (e.g. Bergfors et al. 2010; Janson et al. 2012; Cortés-Contreras et al. 2017). This is arguably an observational bias, either because most surveys systematically miss either the least massive (faintest) companions ($M \lesssim 0.1 M_\odot$) or the most compact binaries ($a \lesssim 10$ au).

In the bottom panel of Fig. 16, the latter observational selection effect is visible, with a remarkable scarcity of data for the closest pairs. This lack of information prevents from testing if near equal-mass pairs ($q \gtrsim 0.8$) are typically found at smaller separations (Jódar et al. 2013; Janson et al. 2014b), or if on the contrary mass ratio distributions are independent of separation (Duquennoy & Mayor 1991; Fischer & Marcy 1992; Reggiani

¹³ Goodwin (2013) proposed that the total mass of the system (M_T) should replace the primary masses in the study of binary systems. They suggested that the mass ratio, q , aligns with a universal, flat distribution of M_T . For the sake of comparison, we used the primary mass, M_A .

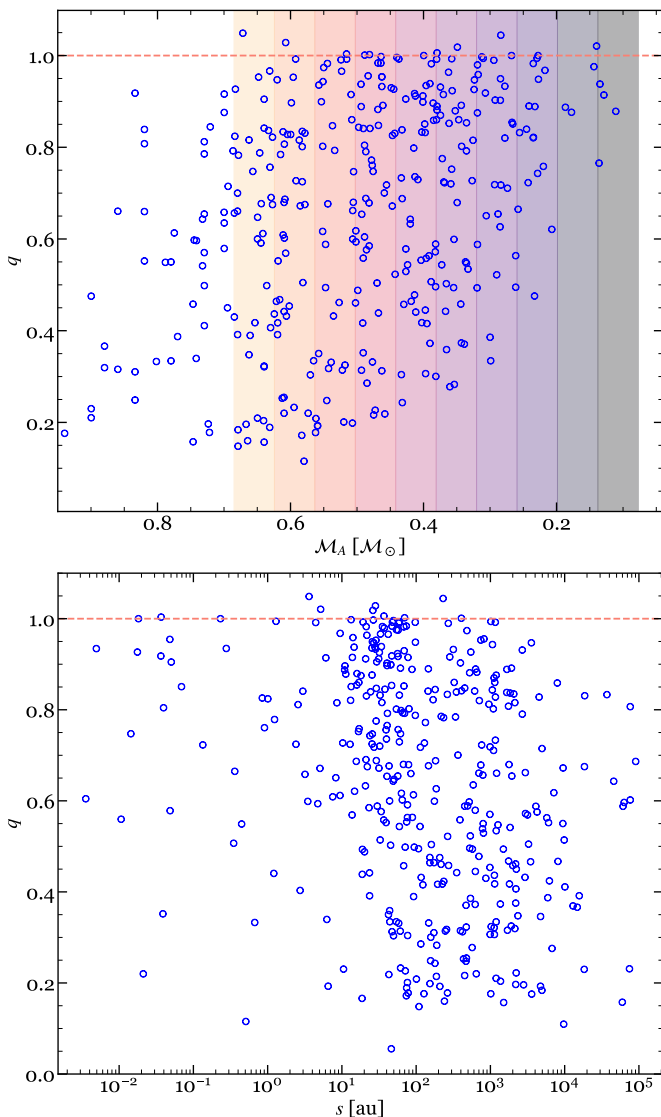


Fig. 16: Mass ratios as a function of primary star mass (top) and projected physical separation (bottom), only for M-dwarf primaries. The red dashed line marks $q = 1$. The gradient map in the background represents the spectral types from M0.0 V to M9.0 V (Cifuentes et al. 2020) following the same scheme as in Fig. 1.

& Meyer 2011). Nevertheless, based on the analysis of high-resolution images of 201 nearby systems collected with the *Hubble* Space Telescope, Dieterich et al. (2012) showed that the mass ratios of low-mass binaries tend to approach to unity as masses approach the hydrogen burning limit at about $0.07 M_{\odot}$, which means that brown dwarf companions are scarce. Studies involving the mass-ratio distribution in M dwarf binaries suggest that the formation mechanisms might differ from those of more massive stars, potentially involving more complex interactions and accretion processes (we refer to several of the studies in Table 1). In this sense, we are unable to reproduce the results by Goldberg et al. (2003), who analysed 162 SBs and observed two distinct populations ($q \sim 0.2$ and $q \sim 0.8$). But similarly to Winters et al. (2019a), we found no preference for equal-mass systems. When complemented with other orbital parameters, q also conveys important information regarding the long-term dynamical stability of these systems.

Table 6: Companions to M dwarfs found in our sample.

| Type | Number of systems | Tables |
|-------------------|-------------------|--------|
| M dwarfs | 720 | ... |
| OBA stars | 3 | ... |
| FGK stars | 60 | A.8 |
| White dwarfs | 28 | A.9 |
| Ultra-cool dwarfs | 16 | A.10 |
| Exoplanet hosts | 99 | A.11 |

In both panels of Fig. 16, some values of q are slightly larger than unity, which at first glance seems contradictory. The most plausible reason has to do with the definition of primary (component ‘A’) as the brightest in the *Gaia G* magnitude that we followed in this work. This definition can disagree with the original nomenclature of some systems, which based this naming convention typically in Johnson *V* filter, a narrower passband in comparison with *Gaia*’s. Another reason could involve a secondary that is actually a binary system of two equal-mass stars, which together could indeed be more massive than the primary, but a more detailed investigation of these secondaries is needed to clarify this hypothesis.

4.4. Companions to M dwarfs

M dwarfs can be found with a variety of stellar and substellar companions, ranging from massive OBA stars to ultra-cool dwarfs and planets. In particular, in our sample, only two M dwarfs are companions to A-type stars: Castor, an A1 V spectroscopic binary in a hierarchical sextuple system, and τ^{07} Ser, an A8 V star in a triple system. There are no earlier OB-type primaries. This lack of OBA+M systems is a direct consequence of the initial mass function and the short life of massive stars in the main sequence. The vast majority of M dwarfs in our sample (around 93 %) are found to be paired with other M dwarfs. Table 6 displays a summary of the different types of companions to our M dwarfs. A given system can harbour more than one type of companion. We describe below the systems with FGK-type primaries, white and ultra-cool dwarf companions, and, for completeness, exoplanets.

4.4.1. FGK primaries

Modelling the atmospheres of a star is a challenging task, and the cooler the star, the harder it becomes (see e.g. Valenti et al. 1998; Woolf & Wallerstein 2006; Önehag et al. 2012). Consequently, advances in new grids of theoretical models (MARCS: Gustafsson et al. 1975, 2008 – PHOENIX: Hauschildt et al. 1997; Husser et al. 2013 – NextGen: Hauschildt et al. 1999 – BT-Settl: Baraffe et al. 1998; Allard et al. 2012), lists of atomic and molecular lines and opacities, computational efficiency, and high-resolution spectroscopy are needed to determine effective temperatures, surface gravities, and, especially, element abundances. Gaining precision in the determination of stellar abundances is important for various reasons, including better constraints on planet formation, mantle composition, and relative core size (Dorn et al. 2017). As a result, the CARMENES Consortium has devoted efforts in the precise determination of abundances in M dwarfs (Abia et al. 2020; Marfil et al. 2021; Passegger et al. 2022; Tabernero et al. 2024).

In this effort of calibrating the metallicity of the coolest stars, solar-type physical companions can provide a shortcut because their abundances are much easier to determine (Nordström et al. 2004; Adibekyan et al. 2012; Benítez et al. 2014). A few investigations have estimated M-dwarf metallicities using wide binary pairs with FGK primaries (e.g. Rojas-Ayala et al. 2012; Montes et al. 2018; Birkby et al. 2020; Ishikawa et al. 2022; Lim et al. 2024). Among them, Montes et al. (2018) presented a relatively large sample of 192 wide visual binaries covering a reasonably broad range in metallicity and spectral type, with atmospheric parameters of the primaries homogeneously derived with the StePar code (Tabernero et al. 2019), and chemical abundances for 13 atomic species. We expect the list of investigated systems and species to increase in the near future, partly because of this work.

In Table A.8 we list 60 systems that contain 64 stars with spectral types between F5 and K5, and 70 M-dwarf companions. Earlier F and later K stars are either too hot or too cool for precise abundance determinations. Besides, the FGK stars are either dwarfs (60) or giants and subgiants (7). We tabulate the systems, their main astrometric properties, and their iron abundance ([Fe/H] as a proxy of metallicity) from the literature. The abundances of some FGK+M systems in Table A.8 were investigated for the first time by Duque-Arribas et al. (2023).

4.4.2. White dwarfs

White dwarfs (WDs) are remnants of stars less massive than $8-10 M_{\odot}$ and represent the final evolutionary stage for the majority of the stars in the Milky Way (Fontaine et al. 2001; Catalán et al. 2008; Doherty et al. 2015). When physically paired with M dwarfs, WDs are a valuable source of information because their modelling is easier (Bergeron et al. 1995; Renedo et al. 2010). For instance, WD companions can serve as effective chronometers for their hosts (Monteiro et al. 2006; Fouesneau et al. 2019; Qiu et al. 2021; Kiman et al. 2021) because the age estimation for WDs is based on their cooling, which is governed by well-understood physics, but one has to add the main-sequence life of the progenitor to get the total age (see Soderblom 2010).

The white dwarfs observed today are probably the remnants of F to late-B main sequence stars ($\sim 1.2-8 M_{\odot}$), with the number of cool unevolved dwarf companions peaking at mid-M type (Farihi et al. 2005). M dwarfs are the most common type of star, yet they do not seem to often pair with white dwarfs. According to Ferrario (2012), this might indicate that the way binary star systems form tends to avoid pairing them with stars that were originally F to late B-type stars. Regarding this observed deficit, Williams (2004) suggested that a large portion of the missing white dwarfs might be explained if these are part of unresolved systems (e.g. Morales-Rueda et al. 2005; Toonen et al. 2017). Ferrario (2012) estimated that there must be an additional $\sim 30\%$ of as yet undiscovered white dwarfs hidden within some kind of binaries. Also, studying wide binary systems from the Sloan Digital Sky Survey, Ferrario (2012) noted that if both M dwarfs and white dwarfs were drawn from the same initial mass function, the number of such systems would be significantly higher than observed, suggesting a different distribution of masses for M dwarf companions. Due to the limited number of WD+M systems, this specific aspect is not addressed in the present work (refer to Sect. 4.3.1).

Table A.9 displays the 28 systems in our sample that have at least one WD component, namely 21 binaries, 6 triples, and 1 quadruple. We tabulate ρ and θ with respect to the WD, as the progenitor was originally the most massive and, thus, brightest star in the system. The quadruple system contains two white dwarfs (G 107–70 A and G 107–70 B, Limoges et al. 2015) and a resolved ($\rho \sim 105$ arcsec) equal-mass M4 V binary companion (GJ 275.2 AB, Giclas et al. 1961). Among the triple systems is σ^2 Eri B, arguably the first white dwarf discovered (Adams 1914; Holberg 2005, and refer to the previous foundational work by Russell and Hertzsprung). It orbits the solar-type star σ^2 Eri A in close binarity with the M4.5 dwarf DY Eri (or σ^2 Eri C; Herschel 1785).

The object *Gaia* DR3 2005884249925303168, a physical companion of the M0.0 V star LF 4+54 152, is several magnitudes fainter than a main-sequence star of the same colour based on its position in the Hertzsprung-Russell diagram (Fig. 9). Although it has not been spectroscopically confirmed, Jiménez-Esteban et al. (2018) and Gentile Fusillo et al. (2019) classified it as an astro-photometric WD candidate, as we also do. All the remaining WDs have been spectroscopically investigated, and many of them are tabulated by the Montreal White Dwarf Database¹⁴ (MWDD). Masses, luminosities, and effective temperatures from evolutionary models are available for several of them in the MWDD, which we retrieved and incorporated in our study.

There have been several observational claims on the projected physical separation distribution of stellar systems with WDs. For example, El-Badry & Rix (2018) suggested that the distribution of s of systems of WDs and main-sequence stars breaks at ~ 3000 au, twice the break of WD+WD pairs. Unfortunately, the population of binaries in our sample is not sufficiently large to perform an analogous study (there are only five systems with $s > 3000$ au), but will allow to determine ages complementary to the kinematic study of Cortés-Contreras et al. (2024).

4.4.3. Ultra-cool dwarfs

Ultra-cool dwarfs (UCDs) are a mixture of very low-mass stars and brown dwarfs with spectral types M7.0 V and later. UCDs can provide important insights into the formation and evolution of low-mass stars and brown dwarfs, and can also help quantifying properties such as masses and ages, eventually testing the accuracy of ultra-cool evolutionary models.

In our sample, there are 16 systems with M dwarfs and UCDs, shown in Table A.10. The spectral types of the UCDs were taken from the literature, except for five, which we derived from *G*-band absolute magnitudes and the relationships of Cifuentes et al. (2020) and Pecaut & Mamajek (2013). The list of UCDs contains 1 late-M-, 7 L-, and 8 T-type UCDs, including the cornerstone late T8.0–8.5 dwarfs Ross 458C (Wolf 462 C), GJ 570 D, Wolf 1130 B, and Wolf 940 B, which were not detected in our *Gaia* search. Projected physical separations vary from roughly 25 au of the GJ 9492 system to over 3000 au of the Wolf 1130 AB system.

We provide astrometric measurements of two pairs for the first time: an \sim L4 dwarf at just ~ 0.53 arcsec to the X-ray M2.0 V star 1RXS J190405.9+211030, and an \sim L2 dwarf at ~ 11 arcsec to the the M3.0+M3.5: double star LP 395–8 AB. The \sim L2 dwarf is reported here for the first time, while the \sim L4 dwarf would need an independent astrometric confirmation given its close separation to the brighter primary and lack of five-parameter *Gaia* solution.

Our collection of systems is smaller than the recent and comprehensive work by Baig et al. (2024), who compiled 278 systems with UCDs at $d < 100$ pc, or the encyclopedic work by

¹⁴ <https://www.montrealwhitedwarfdatabase.org>

Kirkpatrick et al. (2024), who tabulated all known UCDs (either single or in multiple systems) at $d < 20$ pc. However, all primaries in Table A.10 (except for the system containing GJ 570 D, whose primary is a K4 V star – Table A.8) are nearby, bright, Carmencita M dwarfs, some of them with CARMENES monitoring and, therefore, high signal-to-noise ratio, high-resolution spectroscopy. As a result, our collection of systems with well-investigated M dwarfs and UCDs can be of help for forthcoming ultra-cool studies (metallicity, kinematics, age dating, dynamical mass determination, etc.).

4.4.4. Exoplanets

On one hand, the multiplicity of stars with exoplanets comes with an inherent observational bias (Lillo-Box et al. 2012; Ciardi et al. 2015; Fontanive & Bardalez Gagliuffi 2021; Mulders et al. 2021; González-Payo et al. 2024), although close stellar companions can also modify the formation, migration, or dynamical evolution of planets (Holman & Wiegert 1999; Mathieu et al. 2000; Desidera & Barbieri 2007; Kaib et al. 2013; Kraus et al. 2016). On the other hand, the discovery of exoplanets around M dwarfs is a relatively new topic in astrophysics, since at the end of the first decade of the 21st century only a bunch such systems were known (e.g. GJ 876 bcd – Marcy et al. 1998, 2001; Rivera et al. 2005, GJ 436 b – Butler et al. 2004, GJ 581 bce – Bonfils et al. 2005; Udry et al. 2007; Mayor et al. 2009).

It was only after the advent of new dedicated extreme precision spectrographs (e.g. CARMENES) and the TESS space mission that the ‘M-dwarf Opportunity’ was eventually made possible. Nowadays, there are hundreds of M dwarfs with known exoplanets (e.g. TRAPPIST-1 a-g – Gillon et al. 2016, LTT 1445 A bc – Winters et al. 2019b, GJ 3929 b – Kemmer et al. 2022, GJ 486 b – Trifonov et al. 2021, Barnard b – González Hernández et al. 2024). However, the multiplicity of M dwarfs with exoplanets has not yet been investigated in detail.

Here, we pave the way for future analyses on this topic by compiling the 99 stars in our initial sample that have exoplanets, 91 of which are M dwarfs, 8 are FGK stars (3 of them non-MS stars), and one is a WD (LP 141–14). We list the planet host stars together with the multiplicity status, number of planets, and corresponding references in Table A.11. For building it, we removed those that have been challenged by CARMENES (see Table 5 of Ribas et al. 2023) or by other authors (Brandt et al. 2020; Šubjak et al. 2023). We identified 73 single- and 28 multiple-star planetary systems. The eight FGK stars and one white dwarf with planets but without a Karman identifier are companions to Carmencita stars. Not by chance, a significant fraction of the exoplanets in multiple systems in Table A.11 were discovered by CARMENES (Reiners et al. 2018a; Kaminski et al. 2018; Perger et al. 2019; González-Álvarez et al. 2020, 2021; Kemmer et al. 2020; Nowak et al. 2020; Stock et al. 2020b; Kossakowski et al. 2021; Espinoza et al. 2022). This observational bias is due to the careful preparation of the input catalogue, by which only systems with companions at $\rho < 5$ arcsec that could contaminate the target’s optical fibre aperture were discarded from the RV survey (Cortés-Contreras et al. 2017).

4.5. Young systems

Stellar associations and moving groups are loose unbound star agglomerations that contain from dozens to hundreds of stars with a common origin in space (Eggen 1958, 1975; Montes et al. 2001; Zuckerman & Song 2004; Gagné 2024). Since young stars

in stellar kinematic groups (SKGs) represent a transitional stage between the original birthplace and the field, so do young multiple stellar systems in SKGs. Likewise, since wide multiple systems are disrupted by the galactic gravitational potential (Bahcall & Soneira 1980; Weinberg et al. 1987), youth is a common characteristic of the widest pairs (e.g. Caballero 2010; Shaya & Olling 2011; González-Payo et al. 2024).

Recently, Cortés-Contreras et al. (2024) characterised the kinematic properties of the CARMENES input catalogue, identified M-dwarf members in the different galactic populations (thin, transition, and thick discs and halo) and in young SKGs, stellar associations, superclusters, and open clusters with ages from 1 Ma to 800 Ma. They used the public codes SteParKin¹⁵ (Montes et al. 2001), LACEWING (Riedel et al. 2017), and BANYAN Σ (Malo et al. 2013; Gagné et al. 2018) for the identification. We assigned the same kinematic properties as Cortés-Contreras et al. (2024), and extrapolated them to their physical companions not listed in Carmencita. After cross-matching with the literature, we found 7 new SKG members in 5 systems from this extrapolation. We list them in Table 7 (see Alonso-Floriano et al. 2015b for an extrapolation example in the β Pictoris moving group).

Table 8 summarises the number of stars classified as kinematically young by Cortés-Contreras et al. (2024) that are part of our input sample (Carmencita M dwarfs plus confirmed resolved companions, N_{input}) and of multiple systems (N_{system}). Of the 352 young stars in our input sample ($\Sigma N_{\text{input},i}$), flagged in Table A.1 with the corresponding SKG descriptor, a total of 201 are part of multiple systems ($\Sigma N_{\text{system},i}$). The large corresponding proportion of young multiple systems is due to the our wide angular search radius, which corresponds to projected physical separations of 10^5 au (~ 0.5 pc). At these separations, it is difficult to delimit the boundary between relatively close, but unbound, SKG members and actual very wide binaries, especially in the core of the Hyades supercluster, which is the Hyades cluster itself (see the series of papers started by Caballero 2009). As a result, many of the systems in Table 8 should be taken with a grain a salt. However, as discussed in Sect. 4.3.4 and by González-Payo et al. (2024), binding energies above a certain limit (e.g. 10^{33} – 10^{34} J) could discriminate among actually bound systems and coincidental common proper motion pairs in SKGs. Delimiting such a boundary is beyond the scope of this work.

5. Conclusions

In this work, we explore the prevalence of M dwarfs as part of stellar systems based on a comprehensive photometric and astrometric characterisation. We examined individually each of the 2214 stars in the CARMENES input catalogue in search for known and potential physical companions. We identified a total of 835 M dwarfs as part of 720 multiple systems, predominantly binaries. Additionally, we take advantage of the statistical products of Gaia to propose another 327 candidates to binaries. They are found to exhibit astrometric and photometric anomalies compatible with the presence of an unresolved companion. They should be discarded from input target lists of exoplanet searches with forthcoming space missions (Tuchow et al. 2024; Harada et al. 2024; Menti et al. 2024).

Our findings translate into a minimum multiplicity fraction of 27.8 %, which is comparable to the binarity rates reported in previous studies of M dwarfs, although differences in methodology and sample make this comparison somewhat nuanced. Despite this, we suggest that the actual multiplicity fraction of M

¹⁵ <https://github.com/dmontesg/SteParKin>

Table 7: System components with new assignments to SKGs.

| Star | Comp. | α | δ | SKG | Ref. ^a |
|--|-------|-------------|-------------|-------|-------------------|
| 1RXS J011549.5+470159 LP 151-21 | AB | 01:15:50.51 | +47:02:02.1 | (Hya) | This work |
| | CD | 01:15:49.20 | +47:02:25.7 | Hya | Lod19, Fre20 |
| LP 296-57 LP 296-56 | A | 01:56:45.99 | +30:33:28.6 | (Hya) | This work |
| | B | 01:56:41.74 | +30:28:34.6 | Hya | Ros11 |
| PM J06102+2234 LP 362-121 Gaia DR3 3425067888342287616 | A | 06:10:17.81 | +22:34:17.2 | Hya | Ros11 |
| | B | 06:10:22.52 | +22:34:18.1 | (Hya) | This work |
| | C | 06:10:22.50 | +22:34:17.9 | (Hya) | This work |
| HD 230017A HD 230017B PM J18542+1058 | A | 18:54:53.67 | +10:58:42.4 | (Car) | This work |
| | B | 18:54:53.86 | +10:58:45.1 | Car | Gag18b |
| | C | 18:54:17.14 | +10:58:11.0 | (Car) | This work |
| GJ 9721 DENIS J210844.8-042517 | AB | 21:08:45.41 | -04:25:36.7 | UMa | Mon01 |
| | C | 21:08:44.75 | -04:25:18.3 | (UMa) | This work |

Notes. ^(a) Fre20: [Freund et al. \(2020\)](#); Gag18b: [Gagné & Faherty \(2018\)](#); Lod19: [Lodieu et al. \(2019\)](#); Mon01: [Montes et al. \(2001\)](#); Ros11: [Röser et al. \(2011\)](#).

Table 8: Number of kinematically young stars in multiple systems.

| SKG or assoc. | Descriptor | N_{input} | N_{system} |
|-----------------------|-------------|--------------------|---------------------|
| Taurus-Auriga | Tau | 7 | 5 |
| Upper Scorpius | USco | 3 | 1 |
| Argus | Arg | 10 | 5 |
| IC 2391 Supercluster | IC 2391 | 19 | 4 |
| Pleiades Supercluster | Ple | 6 | 4 |
| TW Hydreae | TWA | 2 | 2 |
| β Pictoris | β Pic | 64 | 44 |
| Columba | Col | 11 | 8 |
| Carina | Car | 13 | 9 |
| Tucana-Horologium | Tuc-Hor | 6 | 5 |
| AB Doradus | AB Dor | 39 | 28 |
| Hercules-Lyrae | Her-Lyr | 3 | 3 |
| Ursa Major | UMa | 35 | 18 |
| Castor | Cas | 34 | 16 |
| Hyades (Supercluster) | Hya | 100 | 49 |

Notes. Young SKG, stellar association, supercluster, or open cluster sorted by increasing age, descriptor in Table A.1, and number of stars in the input sample (N_{input}) and in multiple systems (in N_{system}).

dwarfs may be significantly higher, potentially reaching 40.3 %, if all newly proposed binary candidates are confirmed. This revised estimate brings M dwarf multiplicity more in line with the observed rates among Sun-like stars. Further high-resolution spectral and spatial follow-up studies are mandatory to capture the complete population of close companions. All these analyses will also be complemented with *Gaia* DR4 (second half of 2026) and DR5 (end of 2030).

A number of other conclusions can be derived from our analyses. In our sample a two-slope distribution of projected physical separations may support the idea that distinct formation mechanisms are at play for different separation regimes, as previous investigations have proposed: the wide-separation pairs suggest

a population of systems formed through dynamical interactions, while closer binaries may arise from more traditional fragmentation processes. Pre-*Gaia* investigations of ultra-wide physical pairs heavily relied on photometric distances due to the lack of precise astrometric data. Previous studies, while valuable, have often suggested the existence of a large number of very wide real binaries, but were dominated by chance alignments at $s \gtrsim 10^4$ au. The mass ratio distribution observed in our sample is slightly skewed towards equal-mass systems, compared to binaries of more massive stars; nonetheless, selection biases are likely to make us miss part of the picture. Given the significant binding energies computed for M-dwarf systems that have not been found to be young, they are likely to remain bound over tens of gigayears, enduring through the majority of the Galaxy's lifetime.

Finally, we identified remarkable systems with M dwarfs that have FGK star, white dwarf, ultra-cool dwarf, and exoplanet companions, and which belong to young stellar kinematic groups or associations. For these systems, we provide a homogeneous compilation of fundamental parameters and observables, and a detailed examination of architectures. These diverse pairings provide unique opportunities for deriving characteristics of M dwarfs that would be otherwise inaccessible or difficult to determine in M dwarfs that are single (e.g. ages, element abundances).

While our results are consistent with previous studies in terms of observed binary frequency, separation distributions, and mass ratio trends, they also highlight the need for continued investigation into close companions and the impact of observational biases. We expect that the data gathered in this work will serve as a valuable asset for testing and informing theoretical predictions, and for providing a foundation for future investigations on multiplicity.

Data availability

Tables A.1–A.12 are only available in electronic form at Zenodo. The full version of Table A.1 is available at the CDS via anonymous ftp to cdsarc.cds.unistra.fr (130.79.128.5) or via <http://cdsweb.u-strasbg.fr/cgi-bin/qcat?>

J/A+A/, and at the GitHub repository <https://github.com/ccfuentesr/CARMENES-IX>.

Acknowledgements. We are grateful to X. Delfosse, J. Gagné, C. Reylé, and, especially, A. Tokovinin and the reviewer Z. Zhang for their valuable suggestions, which have greatly enriched our work. We acknowledge financial support from the Agencia Estatal de Investigación of the Ministerio de Ciencia, Innovación y Universidades and the ERDF through projects 2023AT003 (PIE, CSIC) associated to RYC2021-031640-I, CNS2023-144309, PID2023-150468NB-I00, PID2022-137241NB-C4[1:4], PID2021-125627OB-C31, PID2019-107061GB-C61, BES-2017-080769, and the Centre of Excellence “Severo Ochoa” and “María de Maeztu” awards to the Instituto de Astrofísica de Canarias (CEX2019-000920-S), Instituto de Astrofísica de Andalucía (CEX2021-001131-S), Institut de Ciències de l’Espai (CEX2020-001058-M), and Centro de Astrobiología (MDM-2017-0737). CARMENES is an instrument at the Centro Astronómico Hispano en Andalucía (CAHA) at Calar Alto (Almería, Spain), operated jointly by the Junta de Andalucía and the Instituto de Astrofísica de Andalucía (CSIC). CARMENES was funded by the Max-Planck-Gesellschaft (MPG), the Consejo Superior de Investigaciones Científicas (CSIC), the Ministerio de Economía y Competitividad (MINECO) and the European Regional Development Fund (ERDF) through projects FICTS-2011-02, ICTS-2017-07-CAHA-4, and CAHA16-CE-3978, and the members of the CARMENES Consortium (Max-Planck-Institut für Astronomie, Instituto de Astrofísica de Andalucía, Landessternwarte Königstuhl, Institut de Ciències de l’Espai, Institut für Astrophysik Göttingen, Universidad Complutense de Madrid, Thüringer Landessternwarte Tautenburg, Instituto de Astrofísica de Canarias, Hamburger Sternwarte, Centro de Astrobiología and Centro Astronómico Hispano-Alemán), with additional contributions by the MINECO, the Deutsche Forschungsgemeinschaft through the Major Research Instrumentation Programme and Research Unit FOR2544 “Blue Planets around Red Stars”, the Klaus Tschira Stiftung, the states of Baden-Württemberg and Niedersachsen, and by the Junta de Andalucía. This work has made use of data from the European Space Agency (ESA) mission *Gaia* (<https://www.cosmos.esa.int/gaia>), processed by the *Gaia* Data Processing and Analysis Consortium (DPAC, <https://www.cosmos.esa.int/web/gaia/dpac/consortium>). Funding for the DPAC has been provided by national institutions, in particular the institutions participating in the *Gaia* Multilateral Agreement. This publication made use of the Washington Double Star Catalog maintained at the U.S. Naval Observatory, VOSA and the Filter Profile Service developed and maintained by the Spanish Virtual Observatory through grant AYA2017-84089, the SIMBAD database, the Aladin sky atlas, and the VizieR catalogue access tool developed at CDS, Strasbourg Observatory, France, the NASA Exoplanet Archive, which is operated by the California Institute of Technology, under contract with the National Aeronautics and Space Administration under the Exoplanet Exploration Program, and the Python libraries Matplotlib, NumPy, SciPy, Pandas and collection of software packages AstroPy.

References

- Abia, C., Tabernero, H. M., Korotin, S. A., et al. 2020, A&A, 642, A227
 Abt, H. A. 1970, ApJS, 19, 387
 Abt, H. A. 1981, ApJS, 45, 437
 Abt, H. A. 2008, ApJS, 176, 216
 Abt, H. A. & Levy, S. G. 1976, ApJS, 30, 273
 Adams, W. S. 1914, PASP, 26, 198
 Adams, W. S., Joy, A. H., Humason, M. L., & Brayton, A. M. 1935, ApJ, 81, 187
 Adibekyan, V. Z., Sousa, S. G., Santos, N. C., et al. 2012, A&A, 545, A32
 Affer, L., Damasso, M., Micela, G., et al. 2019, A&A, 622, A193
 Affer, L., Micela, G., Damasso, M., et al. 2016, A&A, 593, A117
 Allard, F., Homeier, D., & Freytag, B. 2012, Philosophical Transactions of the Royal Society of London Series A, 370, 2765
 Allen, C., Poveda, A., & Herrera, M. A. 1997, in Astrophysics and Space Science Library, Vol. 223, Visual Double Stars : Formation, Dynamics and Evolutionary Tracks, ed. J. A. Docobo, A. Elipe, & H. McAlister, 133
 Allen, C., Poveda, A., & Herrera, M. A. 2000, A&A, 356, 529
 Allison, R. J. & Goodwin, S. P. 2011, MNRAS, 415, 1967
 Alonso-Floriano, F. J., Caballero, J. A., Cortés-Contreras, M., Solano, E., & Montes, D. 2015a, A&A, 583, A85
 Alonso-Floriano, F. J., Morales, J. C., Caballero, J. A., et al. 2015b, A&A, 577, A128
 Amado, P. J., Bauer, F. F., Rodríguez López, C., et al. 2021, A&A, 650, A188
 Andersen, J. 1991, A&A Rev., 3, 91
 Andrews, J. J., Anguiano, B., Chanamé, J., et al. 2019, ApJ, 871, 42
 Andrews, J. J., Chanamé, J., & Agüeros, M. A. 2017, MNRAS, 472, 675
 Ansdel, M., Gaidos, E., Mann, A. W., et al. 2015, ApJ, 798, 41
 Apps, K., Clubb, K. I., Fischer, D. A., et al. 2010, PASP, 122, 156
 Arenou, F., Luri, X., Babusiaux, C., et al. 2018, A&A, 616, A17
 Arentsen, A., Prugniel, P., Gonçau, A., et al. 2019, A&A, 627, A138
 Astudillo-Defru, N., Díaz, R. F., Bonfils, X., et al. 2017a, A&A, 605, L11
 Astudillo-Defru, N., Forveille, T., Bonfils, X., et al. 2017b, A&A, 602, A88
 Auvergne, M., Bodin, P., Boisnard, L., et al. 2009, A&A, 506, 411
 Bahcall, J. N. & Soneira, R. M. 1980, ApJS, 44, 73
 Baig, S., Smart, R. L., Jones, H. R. A., et al. 2024, MNRAS, 533, 3784
 Baraffe, I., Chabrier, G., Allard, F., & Hauschildt, P. H. 1998, A&A, 337, 403
 Bardalez Gagliuffi, D. C., Burgasser, A. J., Gelino, C. R., et al. 2014, ApJ, 794, 143
 Baroch, D., Morales, J. C., Ribas, I., et al. 2021, A&A, 653, A49
 Baroch, D., Morales, J. C., Ribas, I., et al. 2018, A&A, 619, A32
 Barry, D. C. 1970, ApJS, 19, 281
 Basri, G. & Reiners, A. 2006, AJ, 132, 663
 Bate, M. R. 2012, MNRAS, 419, 3115
 Bate, M. R., Bonnell, I. A., & Bromm, V. 2003, MNRAS, 339, 577
 Batten, A. H. 1973, Binary and multiple systems of stars (Pergamon Press)
 Bauer, F. F., Zechmeister, M., Kamiński, A., et al. 2020, A&A, 640, A50
 Bayo, A., Rodrigo, C., Barrado y Navascués, D., et al. 2008, A&A, 492, 277
 Bean, J. L., Benedict, G. F., & Endl, M. 2006, ApJ, 653, L65
 Beard, C., Robertson, P., Kanodia, S., et al. 2022, ApJ, 936, 55
 Bédard, A., Bergeron, P., Brassard, P., & Fontaine, G. 2020, ApJ, 901, 93
 Bell, C. P. M., Murphy, S. J., & Mamajek, E. E. 2017, MNRAS, 468, 1198
 Belokurov, V., Penoyre, Z., Oh, S., et al. 2020, MNRAS, 496, 1922
 Belopolsky, A. 1897, ApJ, 5, 1
 Bender, C. F. & Simon, M. 2008, ApJ, 689, 416
 Benedict, G. F., Franz, O. G., Horch, E. P., et al. 2021, AJ, 161, 285
 Benedict, G. F., McArthur, B. E., Franz, O. G., Wasserman, L. H., & Henry, T. J. 2000, AJ, 120, 1106
 Benítez, N., Dupke, R., Moles, M., et al. 2014, arXiv e-prints, arXiv:1403.5237
 Berdyugina, S. V., Harrington, D. M., Kuzmychov, O., et al. 2017, ApJ, 847, 61
 Bergeron, P., Wesemael, F., & Beauchamp, A. 1995, PASP, 107, 1047
 Bergfors, C., Brandner, W., Janson, M., et al. 2010, A&A, 520, A54
 Bertout, C. & Genova, F. 2006, A&A, 460, 499
 Bessell, M. S. 1991, AJ, 101, 662
 Best, W. M. J., Liu, M. C., Magnier, E. A., et al. 2015, ApJ, 814, 118
 Best, W. M. J., Liu, M. C., Magnier, E. A., & Dupuy, T. J. 2020, AJ, 159, 257
 Bidelman, W. P. 1985, ApJS, 59, 197
 Biller, B. A., Liu, M. C., Wahaj, Z., et al. 2013, ApJ, 777, 160
 Binks, A. S. & Jeffries, R. D. 2016, MNRAS, 455, 3345
 Birkby, J., Nefs, B., Hodgkin, S., et al. 2012, MNRAS, 426, 1507
 Birkby, J., Hogg, D. W., Mann, A. W., & Burgasser, A. 2020, ApJ, 892, 31
 Blanco-Pozo, J., Perger, M., Damasso, M., et al. 2023, A&A, 671, A50
 Bluhm, P., Luque, R., Espinoza, N., et al. 2020, A&A, 639, A132
 Bluhm, P., Pallé, E., Molaverdikhani, K., et al. 2021, A&A, 650, A78
 Bochanski, J. J., Faherty, J. K., Gagné, J., et al. 2018, AJ, 155, 149
 Bochanski, J. J., Hawley, S. L., Covey, K. R., et al. 2010, AJ, 139, 2679
 Bochanski, J. J., Hawley, S. L., Reid, I. N., et al. 2005, AJ, 130, 1871
 Bonfils, X., Astudillo-Defru, N., Díaz, R., et al. 2018, A&A, 613, A25
 Bonfils, X., Delfosse, X., Udry, S., et al. 2013, A&A, 549, A109
 Bonfils, X., Forveille, T., Delfosse, X., et al. 2005, A&A, 443, L15
 Bonfils, X., Gillon, M., Udry, S., et al. 2012, A&A, 546, A27
 Bonnarel, F., Fernique, P., Bienaymé, O., et al. 2000, A&AS, 143, 33
 Bonnell, I. A., Bate, M. R., & Vine, S. G. 2003, MNRAS, 343, 413
 Bopp, B. W. & Fekel, F. C., J. 1977, PASP, 89, 65
 Borucki, W. J., Koch, D., Basri, G., et al. 2010, Science, 327, 977
 Bouy, H., Brandner, W., Martín, E. L., et al. 2003, AJ, 126, 1526
 Bowler, B. P., Liu, M. C., Shkolnik, E. L., & Tamura, M. 2015, ApJS, 216, 7
 Brandner, W., Calissendorff, P., & Kopytova, T. 2023, AJ, 165, 108
 Brandt, T. D. 2021, ApJS, 254, 42
 Brandt, T. D., Dupuy, T. J., Bowler, B. P., et al. 2020, AJ, 160, 196
 Buder, S., Lind, K., Ness, M. K., et al. 2019, A&A, 624, A19
 Buder, S., Sharma, S., Kos, J., et al. 2021, MNRAS, 506, 150
 Burgasser, A. J., Gillon, M., Melis, C., et al. 2015, AJ, 149, 104
 Burgasser, A. J., Kirkpatrick, J. D., Cutri, R. M., et al. 2000, ApJ, 531, L57
 Burgasser, A. J., Kirkpatrick, J. D., Reid, I. N., et al. 2003, ApJ, 586, 512
 Burgasser, A. J., Logsdon, S. E., Gagné, J., et al. 2015, ApJS, 220, 18
 Burgasser, A. J., Reid, I. N., Siegler, N., et al. 2007, in Protostars and Planets V, ed. B. Reipurth, D. Jewitt, & K. Keil, 427
 Burningham, B., Cardoso, C. V., Smith, L., et al. 2013, MNRAS, 433, 457
 Burningham, B., Leggett, S. K., Homeier, D., et al. 2011, MNRAS, 414, 3590
 Burt, J., Vogt, S. S., Butler, R. P., et al. 2014, ApJ, 789, 114
 Butler, R. P., Johnson, J. A., Marcy, G. W., et al. 2006, PASP, 118, 1685
 Butler, R. P., Marcy, G. W., Williams, E., Hauser, H., & Shirts, P. 1997, ApJ, 474, L115
 Butler, R. P., Vogt, S. S., Marcy, G. W., et al. 2004, ApJ, 617, 580
 Caballero, J. A. 2007, A&A, 462, L61
 Caballero, J. A. 2009, A&A, 507, 251
 Caballero, J. A. 2010, A&A, 514, A98

- Caballero, J. A., Cortés-Contreras, M., Alonso-Floriano, F. J., et al. 2016, in 19th Cambridge Workshop on Cool Stars, Stellar Systems, and the Sun (CS19), Cambridge Workshop on Cool Stars, Stellar Systems, and the Sun, 148
- Caballero, J. A., González-Álvarez, E., Brady, M., et al. 2022, *A&A*, 665, A120
- Caballero, J. A., Montes, D., Klutsch, A., et al. 2010, *A&A*, 520, A91
- Cadieux, C., Doyon, R., Plotnykov, M., et al. 2022, *AJ*, 164, 96
- Cannon, A. J. & Pickering, E. C. 1993, VizieR Online Data Catalog: Henry Draper Catalogue and Extension (Cannon+ 1918-1924; ADC 1989), VizieR On-line Data Catalog: II/135A. Originally published in: *Harv. Ann.* 91-100 (1918-1924)
- Cardona Guillén, C., Lodieu, N., Béjar, V. J. S., et al. 2021, *A&A*, 654, A134
- Casewell, S. L., Dobbie, P. D., Hodgkin, S. T., et al. 2007, *MNRAS*, 378, 1131
- Castro-Ginard, A., Penoyre, Z., Casey, A. R., et al. 2024, *A&A*, 688, A1
- Catala, C., Forveille, T., & Lai, O. 2006, *AJ*, 132, 2318
- Catalán, S., Isern, J., García-Berro, E., & Ribas, I. 2008, *MNRAS*, 387, 1693
- Chabrier, G. 2003, *PASP*, 115, 763
- Chanamé, J. & Gould, A. 2004, *ApJ*, 601, 289
- Chanamé, J. & Ramírez, I. 2012, *ApJ*, 746, 102
- Charbonneau, D., Berta, Z. K., Irwin, J., et al. 2009, *Nature*, 462, 891
- Chaturvedi, P., Bluhm, P., Nagel, E., et al. 2022, *A&A*, 666, A155
- Chen, Y.-P., Yan, R., Maraston, C., et al. 2020, *ApJ*, 899, 62
- Chevalier, S., Babusiaux, C., Merle, T., & Arenou, F. 2023, *A&A*, 678, A19
- Chini, R., Hoffmeister, V. H., Nasseri, A., Stahl, O., & Zinnecker, H. 2012, *MNRAS*, 424, 1925
- Christie, W. H. & Wilson, O. C. 1938, *ApJ*, 88, 34
- Christy, J. W. 1978, *AJ*, 83, 1225
- Chulkov, D. & Malkov, O. 2022, *MNRAS*, 517, 2925
- Ciardi, D. R., Beichman, C. A., Horch, E. P., & Howell, S. B. 2015, *ApJ*, 805, 16
- Cifuentes, C., Caballero, J. A., & Agustí, S. 2021, *RNAAS*, 5, 129
- Cifuentes, C., Caballero, J. A., Cortés-Contreras, M., et al. 2020, *A&A*, 642, A115
- Clark, B. M., Blake, C. H., & Knapp, G. R. 2012, *ApJ*, 744, 119
- Clark, C. A., van Belle, G. T., Horch, E. P., et al. 2024, *AJ*, 167, 174
- Clark, C. A., van Belle, G. T., Horch, E. P., et al. 2022, *AJ*, 164, 33
- Close, L. M., Richer, H. B., & Crabtree, D. R. 1990, *AJ*, 100, 1968
- Close, L. M., Siegler, N., Freed, M., & Biller, B. 2003, *ApJ*, 587, 407
- Close, L. M., Zuckerman, B., Song, I., et al. 2007, *ApJ*, 660, 1492
- Cloutier, R., Astudillo-Defru, N., Doyon, R., et al. 2017, *A&A*, 608, A35
- Cloutier, R., Eastman, J. D., Rodriguez, J. E., et al. 2020a, *AJ*, 160, 3
- Cloutier, R., Rodriguez, J. E., Irwin, J., et al. 2020b, *AJ*, 160, 22
- Cortés-Contreras, M., Béjar, V. J. S., Caballero, J. A., et al. 2017, *A&A*, 597, A47
- Cortés-Contreras, M., Caballero, J. A., Montes, D., et al. 2024, arXiv e-prints, arXiv:2411.06825
- Couteau, P. 1960, *Journal des Observateurs*, 43, 41
- Cruz, K. L., Kirkpatrick, J. D., & Burgasser, A. J. 2009, *AJ*, 137, 3345
- Cruz, K. L. & Reid, I. N. 2002, *AJ*, 123, 2828
- Cruz, K. L., Reid, I. N., Liebert, J., Kirkpatrick, J. D., & Lowrance, P. J. 2003, *AJ*, 126, 2421
- Curiel, S., Ortiz-León, G. N., Mioduszewski, A. J., & Sanchez-Bermudez, J. 2022, *AJ*, 164, 93
- Curtis, H. D. 1906, *ApJ*, 23, 351
- Cutri et al., R. M. 2014, VizieR Online Data Catalog, II/328
- Cvetković, Z., Pavlović, R., Ninković, S., & Stojanović, M. 2012, *AJ*, 144, 80
- Czavalainga, D. R., Mitnyan, T., Rappaport, S. A., et al. 2023, *A&A*, 670, A75
- Daemgen, S., Siegler, N., Reid, I. N., & Close, L. M. 2007, *ApJ*, 654, 558
- Dai, F., Howard, A. W., Halverson, S., et al. 2024, *AJ*, 168, 101
- Damasso, M., Perger, M., Almenara, J. M., et al. 2022, *A&A*, 666, A187
- David, T. J., Hillenbrand, L. A., Petigura, E. A., et al. 2016, *Nature*, 534, 658
- Davison, C. L., White, R. J., Henry, T. J., et al. 2015, *AJ*, 149, 106
- Davison, C. L., White, R. J., Jao, W. C., et al. 2014, *AJ*, 147, 26
- Dawson, P. C. & De Robertis, M. M. 2005, *PASP*, 117, 1
- de Bruijne, J. H. J., Allen, M., Azaz, S., et al. 2015, *A&A*, 576, A74
- Deacon, N. R. & Kraus, A. L. 2020, *MNRAS*, 496, 5176
- Deacon, N. R., Liu, M. C., Magnier, E. A., et al. 2014, *ApJ*, 792, 119
- Deacon, N. R., Liu, M. C., Magnier, E. A., et al. 2012, *ApJ*, 757, 100
- Dedrick, C. M., Fulton, B. J., Knutson, H. A., et al. 2021, *AJ*, 161, 86
- Deka-Szymankiewicz, B., Niedzielski, A., Adamczyk, M., et al. 2018, *A&A*, 615, A31
- Delfosse, X., Forveille, T., Beuzit, J. L., et al. 1999a, *A&A*, 344, 897
- Delfosse, X., Forveille, T., Mayor, M., Burnet, M., & Perrier, C. 1999b, *A&A*, 341, L63
- Delfosse, X., Forveille, T., Perrier, C., & Mayor, M. 1998, *A&A*, 331, 581
- Delfosse, X., Forveille, T., Udry, S., et al. 1999c, *A&A*, 350, L39
- Delgado-Donate, E. J., Clarke, C. J., & Bate, M. R. 2003, *MNRAS*, 342, 926
- Delorme, P., Albert, L., Forveille, T., et al. 2010, *A&A*, 518, A39
- Demory, B. O., Pozuelos, F. J., Gómez Maqueo Chew, Y., et al. 2020, *A&A*, 642, A49
- Deshpande, R., Martín, E. L., Montgomery, M. M., et al. 2012, *AJ*, 144, 99
- Desidera, S. & Barbieri, M. 2007, *A&A*, 462, 345
- Desidera, S., Gratton, R. G., Lucatello, S., & Claudi, R. U. 2006, *A&A*, 454, 581
- Desidera, S., Gratton, R. G., Scuderi, S., et al. 2004, *A&A*, 420, 683
- Dhital, S., West, A. A., Stassun, K. G., & Bochanski, J. J. 2010, *AJ*, 139, 2566
- Dhital, S., West, A. A., Stassun, K. G., Schluns, K. J., & Massey, A. P. 2015, *AJ*, 150, 57
- Dholakia, S., Palethorpe, L., Venner, A., et al. 2024, *MNRAS*, 531, 1276
- Díaz, M. R., Jenkins, J. S., Tuomi, M., et al. 2018, *AJ*, 155, 126
- Díaz, R. F., Delfosse, X., Hobson, M. J., et al. 2019, *A&A*, 625, A17
- Dieterich, S. B., Henry, T. J., Golinowski, D. A., Krist, J. E., & Tanner, A. M. 2012, *AJ*, 144, 64
- Dieterich, S. B., Henry, T. J., Jao, W.-C., et al. 2014, *AJ*, 147, 94
- Dittmann, J. A., Irwin, J. M., Charbonneau, D., & Berta-Thompson, Z. K. 2014, *ApJ*, 784, 156
- Dittmann, J. A., Irwin, J. M., Charbonneau, D., et al. 2017, *Nature*, 544, 333
- Doherty, C. L., Gil-Pons, P., Siess, L., Lattanzio, J. C., & Lau, H. H. B. 2015, *MNRAS*, 446, 2599
- Dorn, C., Venturini, J., Khan, A., et al. 2017, *A&A*, 597, A37
- Dreizler, S., Crossfield, I. J. M., Kossakowski, D., et al. 2020, *A&A*, 644, A127
- Dreizler, S., Luque, R., Ribas, I., et al. 2024, *A&A*, 684, A117
- Dressing, C. D., Hardegree-Ullman, K., Schlieder, J. E., et al. 2019, *AJ*, 158, 87
- Duchêne, G. & Kraus, A. 2013, *ARA&A*, 51, 269
- Dupuis, J., Vennes, S., Bowyer, S., Pradhan, A. K., & Thejll, P. 1994, in American Astronomical Society Meeting Abstracts, Vol. 184, American Astronomical Society Meeting Abstracts #184, 29.01
- Dupuy, T. J. & Liu, M. C. 2011, *ApJ*, 733, 122
- Dupuy, T. J. & Liu, M. C. 2012, *ApJS*, 201, 19
- Dupuy, T. J. & Liu, M. C. 2017, *ApJS*, 231, 15
- Dupuy, T. J., Liu, M. C., Best, W. M. J., et al. 2019, *AJ*, 158, 174
- Duque-Arribas, C., Montes, D., Tabernero, H. M., et al. 2023, *ApJ*, 944, 106
- Duquennoy, A. & Mayor, M. 1988, *A&A*, 200, 135
- Duquennoy, A. & Mayor, M. 1991, *A&A*, 248, 485
- Edwards, T. W. 1976, *AJ*, 81, 245
- Eggen, O. J. 1958, *MNRAS*, 118, 65
- Eggen, O. J. 1975, *PASP*, 87, 37
- El-Badry, K. 2024, *New A Rev.*, 98, 101694
- El-Badry, K. & Rix, H.-W. 2018, *MNRAS*, 480, 4884
- El-Badry, K., Rix, H.-W., & Heintz, T. M. 2021, *MNRAS*, 506, 2269
- Elliott, P., Bayo, A., Melo, C. H. F., et al. 2014, *A&A*, 568, A26
- Endl, M., Robertson, P., Cochran, W. D., et al. 2022, *AJ*, 164, 238
- Espinoza, N., Pallé, E., Kemmer, J., et al. 2022, *AJ*, 163, 133
- Evans, D. S. 1967, in IAU Symposium, Vol. 30, Determination of Radial Velocities and their Applications, ed. A. H. Batten & J. F. Heard, 57
- Evans, D. S. 1968, *QJRAS*, 9, 388
- Eyer, L., Audard, M., Holl, B., et al. 2023, *A&A*, 674, A13
- Eyer, L., Mowlavi, N., Evans, D. W., et al. 2017, arXiv e-prints, arXiv:1702.03295
- Fabricius, C., Høg, E., Makarov, V. V., et al. 2002, *A&A*, 384, 180
- Fabricius, C., Luri, X., Arenou, F., et al. 2021, *A&A*, 649, A5
- Faherty, J. K., Burgasser, A. J., Walter, F. M., et al. 2012, *ApJ*, 752, 56
- Faherty, J. K., Burgasser, A. J., West, A. A., et al. 2010, *AJ*, 139, 176
- Farihi, J., Becklin, E. E., & Zuckerman, B. 2005, *ApJS*, 161, 394
- Feng, F., Butler, R. P., Vogt, S. S., et al. 2022, *ApJS*, 262, 21
- Feng, F., Shectman, S. A., Clement, M. S., et al. 2020, *ApJS*, 250, 29
- Ferrario, L. 2012, *MNRAS*, 426, 2500
- Finch, C. T. & Zacharias, N. 2016, *AJ*, 151, 160
- Finch, C. T., Zacharias, N., & Jao, W.-C. 2018, *AJ*, 155, 176
- Fischer, D. A. & Marcy, G. W. 1992, *ApJ*, 396, 178
- Fischer, D. A., Marcy, G. W., Butler, R. P., et al. 2008, *ApJ*, 675, 790
- Fleming, T. A., Liebert, J., Gioia, I. M., & Maccacaro, T. 1988, *ApJ*, 331, 958
- Fontaine, G., Brassard, P., & Bergeron, P. 2001, *PASP*, 113, 409
- Fontanive, C., & Bardalez Gagliuffi, D. 2021, *Frontiers in Astronomy and Space Sciences*, 8, 16
- Fontanive, C., Biller, B., Bonavita, M., & Allers, K. 2018, *MNRAS*, 479, 2702
- Foreman-Mackey, D., Montet, B. T., Hogg, D. W., et al. 2015, *ApJ*, 806, 215
- Forveille, T., Bonfils, X., Delfosse, X., et al. 2009, *A&A*, 493, 645
- Forveille, T., Ségransan, D., Delorme, P., et al. 2004, *A&A*, 427, L1
- Fouesneau, M., Rix, H.-W., von Hippel, T., Hogg, D. W., & Tian, H. 2019, *ApJ*, 870, 9
- Fouqué, P., Moutou, C., Malo, L., et al. 2018, *MNRAS*, 475, 1960
- Freund, S., Robrade, J., Schneider, P. C., & Schmitt, J. H. M. M. 2020, *A&A*, 640, A66
- Frith, J., Pinfield, D. J., Jones, H. R. A., et al. 2013, *MNRAS*, 435, 2161
- Fukui, A., Kimura, T., Hirano, T., et al. 2022, *PASJ*, 74, L1
- Gagné, J. 2024, *PASP*, 136, 063001
- Gagné, J. & Faherty, J. K. 2018, *ApJ*, 862, 138
- Gagné, J., Lafrenière, D., Doyon, R., Malo, L., & Artigau, É. 2015, *ApJ*, 798, 73
- Gagné, J., Mamajek, E. E., Malo, L., et al. 2018, *ApJ*, 856, 23
- Gaia Collaboration. 2022, VizieR Online Data Catalog: Gaia DR3 Part 3. Non-single stars (Gaia Collaboration, 2022). VizieR On-line Data Catalog: I/357. Originally published in: *Astron. Astrophys.*, in prep. (2022)

- Gaia Collaboration, Arenou, F., Babusiaux, C., et al. 2023a, A&A, 674, A34
 Gaia Collaboration, Brown, A. G. A., Vallenari, A., et al. 2018, A&A, 616, A1
 Gaia Collaboration, Brown, A. G. A., Vallenari, A., et al. 2021a, A&A, 649, A1
 Gaia Collaboration, Prusti, T., de Bruijne, J. H. J., et al. 2016, A&A, 595, A1
 Gaia Collaboration, Smart, R. L., Sarro, L. M., et al. 2021b, A&A, 649, A6
 Gaia Collaboration, Vallenari, A., Brown, A. G. A., et al. 2023b, A&A, 674, A1
 Gaidos, E., Mann, A. W., Lépine, S., et al. 2014, MNRAS, 443, 2561
 Gallenne, A., Desgrange, C., Milli, J., et al. 2022, A&A, 665, A41
 Gandhi, P., Buckley, D. A. H., Charles, P. A., et al. 2022, MNRAS, 510, 3885
 Garcés, A., Catalán, S., & Ribas, I. 2011, A&A, 531, A7
 Geballe, T. R., Knapp, G. R., Leggett, S. K., et al. 2002, ApJ, 564, 466
 Gebran, M., Farah, W., Paletou, F., Monier, R., & Watson, V. 2016, A&A, 589, A83
 Gentile Fusillo, N. P., Tremblay, P.-E., Gänsicke, B. T., et al. 2019, MNRAS, 482, 4570
 Gianninas, A., Bergeron, P., & Ruiz, M. T. 2011, ApJ, 743, 138
 Giclas, H. L., Burnham, R., & Thomas, N. G. 1961, Lowell Observatory Bulletin, 6, 61
 Gilhooley, S. H., Blake, C. H., Terrien, R. C., et al. 2018, AJ, 155, 38
 Gillon, M., Jehin, E., Lederer, S. M., et al. 2016, Nature, 533, 221
 Gillon, M., Triaud, A. H. M. J., Demory, B.-O., et al. 2017, Nature, 542, 456
 Gizis, J. E. 1997, AJ, 113, 806
 Gizis, J. E., Monet, D. G., Reid, I. N., et al. 2000, AJ, 120, 1085
 Gizis, J. E. & Reid, I. N. 1996, AJ, 111, 365
 Gizis, J. E. & Reid, I. N. 1997, PASP, 109, 849
 Gizis, J. E., Reid, I. N., & Hawley, S. L. 2002, AJ, 123, 3356
 Gliese, W. 1957, Astronomisches Rechen-Institut Heidelberg Mitteilungen Serie A, 8, 1
 Gliese, W. 1969, Veroeffentlichungen des Astronomischen Rechen-Instituts Heidelberg, 22, 1
 Gliese, W. & Jahreß, H. 1979, A&AS, 38, 423
 Gliese, W. & Jahreß, H. 1991, Preliminary Version of the Third Catalogue of Nearby Stars, On: The Astronomical Data Center CD-ROM: Selected Astronomical Catalogs, Vol. I; L.E. Brotzmann, S.E. Gesser (eds.), NASA/Astronomical Data Center, Goddard Space Flight Center, Greenbelt, MD
 Goffo, E., Chaturvedi, P., Murgas, F., et al. 2024, A&A, 685, A147
 Goldberg, D., Mazeh, T., & Latham, D. W. 2003, ApJ, 591, 397
 Goldman, B., Marsat, S., Henning, T., Clemens, C., & Greiner, J. 2010, MNRAS, 405, 1140
 Golovin, A., Reffert, S., Just, A., et al. 2023, A&A, 670, A19
 Gómez de Castro, A. I., López-Santiago, J., López-Martínez, F., et al. 2015, ApJS, 216, 26
 Gontcharov, G. A. 2006, Astronomy Letters, 32, 759
 González-Álvarez, E., Kemmer, J., Chaturvedi, P., et al. 2023a, A&A, 675, A141
 González-Álvarez, E., Petralia, A., Micela, G., et al. 2021, A&A, 649, A157
 González-Álvarez, E., Zapatero Osorio, M. R., Caballero, J. A., et al. 2023b, A&A, 675, A177
 González-Álvarez, E., Zapatero Osorio, M. R., Caballero, J. A., et al. 2020, A&A, 637, A93
 González-Álvarez, E., Zapatero Osorio, M. R., Sanz-Forcada, J., et al. 2022, A&A, 658, A138
 González Hernández, J. I., Suárez Mascareño, A., Silva, A. M., et al. 2024, A&A, 690, A79
 González-Payo, J., Caballero, J. A., & Cortés-Contreras, M. 2023, A&A, 670, A102
 González-Payo, J., Caballero, J. A., Gorgas, J., et al. 2024, A&A, 689, A302
 Goodwin, S. P. 2010, Philosophical Transactions of the Royal Society of London Series A, 368, 851
 Goodwin, S. P. 2013, MNRAS, 430, L6
 Goodwin, S. P. & Kroupa, P. 2005, A&A, 439, 565
 Goodwin, S. P., Kroupa, P., Goodman, A., & Burkert, A. 2007, in Protostars and Planets V, 133
 Gravity Collaboration, Abuter, R., Amorim, A., et al. 2024, A&A, 685, L9
 Gray, R. O., Corbally, C. J., Garrison, R. F., et al. 2006, AJ, 132, 161
 Gray, R. O., Corbally, C. J., Garrison, R. F., McFadden, M. T., & Robinson, P. E. 2003, AJ, 126, 2048
 Gray, R. O., Napier, M. G., & Winkler, L. I. 2001, AJ, 121, 2148
 Greenstein, J. L. 1984, ApJ, 276, 602
 Greenstein, J. L. & Liebert, J. W. 1990, ApJ, 360, 662
 Griffin, R. F., Gunn, J. E., Zimmerman, B. A., & Griffin, R. E. M. 1985, AJ, 90, 609
 Guillout, P., Klutsch, A., Frasca, A., et al. 2009, A&A, 504, 829
 Gustafsson, B., Bell, R. A., Eriksson, K., & Nordlund, A. 1975, A&A, 42, 407
 Gustafsson, B., Edvardsson, B., Eriksson, K., et al. 2008, A&A, 486, 951
 Haghhighipour, N., Vogt, S. S., Butler, R. P., et al. 2010, ApJ, 715, 271
 Halbwachs, J. L. 1983, A&A, 128, 399
 Halbwachs, J. L., Mayor, M., & Udry, S. 2018, A&A, 619, A81
 Harada, C. K., Dressing, C. D., Kane, S. R., & Ardestani, B. A. 2024, ApJS, 272, 30
 Harakawa, H., Takarada, T., Kasagi, Y., et al. 2022, PASJ, 74, 904
 Harlan, E. A. & Taylor, D. C. 1970, AJ, 75, 507
 Harlow, J. J. B. 1996, AJ, 112, 2222
 Harrington, R. S. 1972, Celestial Mechanics, 6, 322
 Harrington, R. S., Christy, J. W., & Strand, K. A. 1981, AJ, 86, 909
 Harris, C. R., Millman, K. J., van der Walt, S. J., et al. 2020, Nature, 585, 357
 Hartigan, P., Strom, K. M., & Strom, S. E. 1994, ApJ, 427, 961
 Hartkopf, W. I., McAlister, H. A., & Mason, B. D. 2001, AJ, 122, 3480
 Hartkopf, W. I., Tokovinin, A., & Mason, B. D. 2012, AJ, 143, 42
 Hartman, J. D., Bakos, G. Á., Noyes, R. W., et al. 2011, AJ, 141, 166
 Hartman, Z. D. & Lépine, S. 2020, ApJS, 247, 66
 Hauschildt, P. H., Allard, F., & Baron, E. 1999, ApJ, 512, 377
 Hauschildt, P. H., Baron, E., & Allard, F. 1997, ApJ, 483, 390
 Hawkins, K., Lucey, M., Ting, Y.-S., et al. 2020, MNRAS, 492, 1164
 Hawley, S. L., Gizis, J. E., & Reid, I. N. 1996, AJ, 112, 2799
 Heggie, D. C. 1975, MNRAS, 173, 729
 Henry, T. J. 1991, PhD thesis, University of Arizona, USA
 Henry, T. J., Jao, W.-C., Subasavage, J. P., et al. 2006, AJ, 132, 2360
 Henry, T. J., Jao, W.-C., Winters, J. G., et al. 2018, AJ, 155, 265
 Henry, T. J., Kirkpatrick, J. D., & Simons, D. A. 1994, AJ, 108, 1437
 Henry, T. J. & McCarthy, D. W. J. 1990, ApJ, 350, 334
 Henry, T. J., Walkowicz, L. M., Barto, T. C., & Goliowski, D. A. 2002, AJ, 123, 2002
 Herbig, G. H. & Moorhead, J. M. 1965, ApJ, 141, 649
 Herczeg, G. J. & Hillenbrand, L. A. 2014, ApJ, 786, 97
 Herschel, W. 1785, Philosophical Transactions of the Royal Society of London Series I, 75, 40
 Herschel, W. 1803, Philosophical Transactions of the Royal Society of London Series I, 93, 339
 Hills, J. G. 1975, AJ, 80, 809
 Hirsch, L. A., Rosenthal, L., Fulton, B. J., et al. 2021, AJ, 161, 134
 Hobson, M. J., Delfosse, X., Astudillo-Defru, N., et al. 2019, A&A, 625, A18
 Hojjatpanah, S., Figueira, P., Santos, N. C., et al. 2019, A&A, 629, A80
 Holberg, J. B. 2005, in American Astronomical Society Meeting Abstracts, Vol. 207
 Holl, B., Fabricius, C., Portell, J., et al. 2023, A&A, 674, A25
 Holman, M. J. & Wiebert, P. A. 1999, AJ, 117, 621
 Houdebine, E. R., Mullan, D. J., Paletou, F., & Gebran, M. 2016, ApJ, 822, 97
 Houk, N. & Smith-Moore, M. 1988, Michigan Catalogue of Two-dimensional Spectral Types for the HD Stars. Volume 4, Declinations -26°.0 to -12°.0., Vol. 4
 Houk, N. & Swift, C. 1999, Michigan Spectral Survey, 5, 0
 Howard, A. W., Johnson, J. A., Marcy, G. W., et al. 2010, ApJ, 721, 1467
 Howell, S. B., Sobeck, C., Haas, M., et al. 2014, PASP, 126, 398
 Huang, S. S. & Struve, O. 1956, AJ, 61, 300
 Hubbard-James, H.-S., Lesley, D. X., Henry, T. J., Paredes, L. A., & Nisak, A. H. 2022, AJ, 164, 174
 Husser, T. O., Wende-von Berg, S., Dreizler, S., et al. 2013, A&A, 553, A6
 Hwang, H.-C. 2023, MNRAS, 518, 1750
 Hwang, H.-C., Ting, Y.-S., & Zakamska, N. L. 2022, MNRAS, 512, 3383
 Høg, E., Fabricius, C., Makarov, V. V., et al. 2000, A&A, 355, L27
 Ireland, M. J., Kraus, A., Martinache, F., Lloyd, J. P., & Tuthill, P. G. 2008, ApJ, 678, 463
 Irwin, J., Charbonneau, D., Berta, Z. K., et al. 2009, ApJ, 701, 1436
 Ishikawa, H. T., Aoki, W., Hirano, T., et al. 2022, AJ, 163, 72
 Izmailov, I. S. 2019, Astronomy Letters, 45, 30
 Jackson, R. J., Deliyannis, C. P., & Jeffries, R. D. 2018, MNRAS, 476, 3245
 Jahreß, H., Meusinger, H., Scholz, R. D., & Stecklum, B. 2008, A&A, 484, 575
 Jameson, R. F., Casewell, S. L., Bannister, N. P., et al. 2008, MNRAS, 384, 1399
 Janson, M., Bergfors, C., Brandner, W., et al. 2014a, ApJS, 214, 17
 Janson, M., Bergfors, C., Brandner, W., et al. 2014b, ApJ, 789, 102
 Janson, M., Durkan, S., Hippler, S., et al. 2017, A&A, 599, A70
 Janson, M., Hormuth, F., Bergfors, C., et al. 2012, ApJ, 754, 44
 Jeffers, S. V., Schöfer, P., Lamert, A., et al. 2018, A&A, 614, A76
 Jenkins, J. S., Ramsey, L. W., Jones, H. R. A., et al. 2009, ApJ, 704, 975
 Jiang, Y.-F. & Tremaine, S. 2010, MNRAS, 401, 977
 Jiménez-Esteban, F. M., Solano, E., & Rodrigo, C. 2019, AJ, 157, 78
 Jiménez-Esteban, F. M., Torres, S., Rebassa-Mansergas, A., et al. 2018, MNRAS, 480, 4505
 Jódar, E., Pérez-Garrido, A., Díaz-Sánchez, A., et al. 2013, MNRAS, 429, 859
 Joergens, V. 2008, A&A, 492, 545
 Johnson, J. A., Butler, R. P., Marcy, G. W., et al. 2007, ApJ, 670, 833
 Johnson, J. A., Howard, A. W., Marcy, G. W., et al. 2010, PASP, 122, 149
 Jørgensen, B. R. & Lindegren, L. 2005, A&A, 436, 127
 Joy, A. H. 1947, ApJ, 105, 96
 Joy, A. H. & Abt, H. A. 1974, ApJS, 28, 1
 Joy, A. H. & Sanford, R. F. 1926, ApJ, 64, 250
 Joy, A. H. & Wilson, R. E. 1949, ApJ, 109, 231
 Jónsson, H., Holtzman, J. A., Allende Prieto, C., et al. 2020, AJ, 160, 120
 Kaib, N. A., Raymond, S. N., & Duncan, M. 2013, Nature, 493, 381

- Kaminski, A., Trifonov, T., Caballero, J. A., et al. 2018, *A&A*, 618, A115
 Karataş, Y., Bilar, S., Eker, Z., & Demircan, O. 2004, *MNRAS*, 349, 1069
 Katoh, N., Itoh, Y., Toyota, E., & Sato, B. 2013, *AJ*, 145, 41
 Katz, D., Sartoretti, P., Guerrier, A., et al. 2023, *A&A*, 674, A5
 Keenan, P. C. & McNeil, R. C. 1989, *ApJS*, 71, 245
 Kemmer, J., Dreizler, S., Kossakowski, D., et al. 2022, *A&A*, 659, A17
 Kemmer, J., Stock, S., Kossakowski, D., et al. 2020, *A&A*, 642, A236
 Kepler, S. O., Kleinman, S. J., Nitta, A., et al. 2007, *MNRAS*, 375, 1315
 Kervella, P., Arenou, F., Mignard, F., & Thévenin, F. 2019, *A&A*, 623, A72
 Kervella, P., Thévenin, F., & Lovis, C. 2017, *A&A*, 598, L7
 Kesseli, A. Y., Muirhead, P. S., Mann, A. W., & Mace, G. 2018, *AJ*, 155, 225
 Khrutskaya, E. V., Izmailov, I. S., & Khovrichev, M. Y. 2010, *Astronomy Letters*, 36, 576
 Kiman, R., Faherty, J. K., Cruz, K. L., et al. 2021, *AJ*, 161, 277
 King, R. R., Goodwin, S. P., Parker, R. J., & Patience, J. 2012, *MNRAS*, 427, 2636
 Kirk, B., Conroy, K., Prša, A., et al. 2016, *AJ*, 151, 68
 Kirkpatrick, J. D., Cushing, M. C., Gelino, C. R., et al. 2011, *ApJS*, 197, 19
 Kirkpatrick, J. D., Gelino, C. R., Cushing, M. C., et al. 2012, *ApJ*, 753, 156
 Kirkpatrick, J. D., Henry, T. J., & McCarthy, D. W. J. 1991, *ApJS*, 77, 417
 Kirkpatrick, J. D., Marocco, F., Gelino, C. R., et al. 2024, *ApJS*, 271, 55
 Kirkpatrick, J. D., Martin, E. C., Smart, R. L., et al. 2019, *ApJS*, 240, 19
 Kirkpatrick, J. D., McGraw, J. T., Hess, T. R., Liebert, J., & McCarthy, D. W. J. 1994, *ApJS*, 94, 749
 Kiyaeva, O. V., Zhuchkov, R. Y., & Izmailov, I. S. 2020, *Astrophysical Bulletin*, 75, 425
 Klutsch, A., Frasca, A., Guillout, P., et al. 2020, *A&A*, 637, A43
 Koen, C., Kilkenney, D., van Wyk, F., & Marang, F. 2010, *MNRAS*, 403, 1949
 Kopparapu, R. K., Ramirez, R., Kasting, J. F., et al. 2013, *ApJ*, 765, 131
 Kopytova, T. G., Brandner, W., Tognelli, E., et al. 2016, *A&A*, 585, A7
 Kossakowski, D., Kemmer, J., Bluhm, P., et al. 2021, *A&A*, 656, A124
 Kossakowski, D., Kürster, M., Trifonov, T., et al. 2023, *A&A*, 670, A84
 Kounkel, M., Covey, K., Moe, M., et al. 2019, *AJ*, 157, 196
 Kouwenhoven, M. B. N., Brown, A. G. A., Portegies Zwart, S. F., & Kaper, L. 2007, *A&A*, 474, 77
 Kouwenhoven, M. B. N., Goodwin, S. P., Parker, R. J., et al. 2010, *MNRAS*, 404, 1835
 Kozai, Y. 1962, *AJ*, 67, 591
 Kraus, A. L., Herczeg, G. J., Rizzuto, A. C., et al. 2017, *ApJ*, 838, 150
 Kraus, A. L. & Hillenbrand, L. A. 2009, *ApJ*, 704, 531
 Kraus, A. L., Ireland, M. J., Cieza, L. A., et al. 2014a, *ApJ*, 781, 20
 Kraus, A. L., Ireland, M. J., Huber, D., Mann, A. W., & Dupuy, T. J. 2016, *AJ*, 152, 8
 Kraus, A. L., Shkolnik, E. L., Allers, K. N., & Liu, M. C. 2014b, *AJ*, 147, 146
 Krupa, P., Tout, C. A., & Gilmore, G. 1991, *MNRAS*, 251, 293
 Kuiper, G. P. 1935, *PASP*, 47, 121
 Kuiper, G. P. 1942, *ApJ*, 95, 201
 Kuznetsov, M. K., del Burgo, C., Pavlenko, Y. V., & Frith, J. 2019, *ApJ*, 878, 134
 Kuzuhara, M., Fukui, A., Livingston, J. H., et al. 2024, *ApJ*, 967, L21
 Lada, C. J. 2006, *ApJ*, 640, L63
 Lafrenière, D., Doyon, R., Marois, C., et al. 2007, *ApJ*, 670, 1367
 Lalitha, S., Baroch, D., Morales, J. C., et al. 2019, *A&A*, 627, A116
 Lamman, C., Baranec, C., Berta-Thompson, Z. K., et al. 2020, *AJ*, 159, 139
 Lane, B. F., Zapatero Osorio, M. R., Britton, M. C., Martín, E. L., & Kulkarni, S. R. 2001, *ApJ*, 560, 390
 Law, N. M., Hodgkin, S. T., & Mackay, C. D. 2006, *MNRAS*, 368, 1917
 Law, N. M., Hodgkin, S. T., & Mackay, C. D. 2008, *MNRAS*, 384, 150
 Lee, S. G. 1984, *AJ*, 89, 702
 Leigh, N. W. C. & Geller, A. M. 2013, *MNRAS*, 432, 2474
 Leinert, C., Henry, T., Glindemann, A., & McCarthy, D. W. J. 1997, *A&A*, 325, 159
 Leinert, C., Zinnecker, H., Weitzel, N., et al. 1993, *A&A*, 278, 129
 Lépine, S. & Bongiorno, B. 2007, *AJ*, 133, 889
 Lépine, S., Hilton, E. J., Mann, A. W., et al. 2013, *AJ*, 145, 102
 Lépine, S., Rich, R. M., & Shara, M. M. 2003, *AJ*, 125, 1598
 Lépine, S., Rich, R. M., & Shara, M. M. 2007, *ApJ*, 669, 1235
 Lépine, S. & Shara, M. M. 2005, *AJ*, 129, 1483
 Lépine, S., Shara, M. M., & Rich, R. M. 2002, *AJ*, 123, 3434
 Lépine, S., Thorstensen, J. R., Shara, M. M., & Rich, R. M. 2009, *AJ*, 137, 4109
 Lidov, M. L. 1962, *Planet. Space Sci.*, 9, 719
 Lillo-Box, J., Barrado, D., & Bouy, H. 2012, *A&A*, 546, A10
 Lim, D., Koch-Hansen, A. J., Hong, S., Chun, S.-H., & Lee, Y.-W. 2024, *AJ*, 167, 3
 Limoges, M. M., Bergeron, P., & Lépine, S. 2015, *ApJS*, 219, 19
 Limoges, M. M., Lépine, S., & Bergeron, P. 2013, *AJ*, 145, 136
 Lindegren, L., Hernández, J., Bombrun, A., et al. 2018, *A&A*, 616, A2
 Lindegren, L., Klioner, S. A., Hernández, J., et al. 2021, *A&A*, 649, A2
 Lindegren, L., Lammers, U., Bastian, U., et al. 2016, *A&A*, 595, A4
 Lindegren, L., Lammers, U., Hobbs, D., et al. 2012, *A&A*, 538, A78
 Lingam, M. & Loeb, A. 2018, *Astrobiology*, 18, 967
 Lodieu, N., Scholz, R. D., McCaughrean, M. J., et al. 2005, *A&A*, 440, 1061
 Lodieu, N., Smart, R. L., Pérez-Garrido, A., & Silvotti, R. 2019, *A&A*, 623, A35
 López-Santiago, J., Montes, D., Crespo-Chacón, I., & Fernández-Figueroa, M. J. 2006, *ApJ*, 643, 1160
 Loth, A. L. & Bidelman, W. P. 1998, *PASP*, 110, 268
 Luck, R. E. 2017, *AJ*, 153, 21
 Luck, R. E. 2018, *AJ*, 155, 111
 Luhman, K. L., Loutrel, N. P., McCurdy, N. S., et al. 2012, *ApJ*, 760, 152
 Luque, R., Nowak, G., Hirano, T., et al. 2022, *A&A*, 666, A154
 Luque, R., Nowak, G., Pallé, E., et al. 2018, *A&A*, 620, A171
 Luque, R., Pallé, E., Kossakowski, D., et al. 2019, *A&A*, 628, A39
 Mace, G. N., Kirkpatrick, J. D., Cushing, M. C., et al. 2013, *ApJ*, 777, 36
 Mace, G. N., Mann, A. W., Skiff, B. A., et al. 2018, *ApJ*, 854, 145
 Macintosh, B., Graham, J. R., Barman, T., et al. 2015, *Science*, 350, 64
 Mahadevan, S., Stefánsson, G., Robertson, P., et al. 2021, *ApJ*, 919, L9
 Maíz Apellániz, J., Holgado, G., Pantaleoni González, M., & Caballero, J. A. 2023, *A&A*, 677, A137
 Maíz Apellániz, J., Negueruela, I., & Caballero, J. A. 2024, arXiv e-prints, arXiv:2410.07301
 Makarov, V. V., Zacharias, N., & Hennessy, G. S. 2008, *ApJ*, 687, 566
 Maldonado, J., Micela, G., Baratella, M., et al. 2020, *A&A*, 644, A68
 Maldonado, J., Petralia, A., Damasso, M., et al. 2021, *A&A*, 651, A93
 Malkov, O. Y., Oblak, E., Snegireva, E. A., & Torra, J. 2006, *A&A*, 446, 785
 Malkov, O. Y., Tamazian, V. S., Docobo, J. A., & Chulkov, D. A. 2012, *A&A*, 546, A69
 Mallorquin, M., Béjar, V. J. S., Lodieu, N., et al. 2024, *A&A*, 689, A132
 Malo, L., Artigau, É., Doyon, R., et al. 2014a, *ApJ*, 788, 81
 Malo, L., Doyon, R., Feiden, G. A., et al. 2014b, *ApJ*, 792, 37
 Malo, L., Doyon, R., Lafrenière, D., et al. 2013, *ApJ*, 762, 88
 Mamajek, E. E., Kenworthy, M. A., Hinz, P. M., & Meyer, M. R. 2010, *AJ*, 139, 919
 Mann, A. W., Deacon, N. R., Gaidos, E., et al. 2014, *AJ*, 147, 160
 Mann, A. W., Dupuy, T., Kraus, A. L., et al. 2019, *ApJ*, 871, 63
 Mann, A. W., Feiden, G. A., Gaidos, E., Boyajian, T., & von Braun, K. 2015, *ApJ*, 804, 64
 Mante, R. 2000, IAU Commission on Double Stars, 140, 1
 Marcy, G. W., Butler, R. P., Fischer, D. A., et al. 2002, *ApJ*, 581, 1375
 Marcy, G. W., Butler, R. P., Fischer, D. A., et al. 2001, *ApJ*, 556, 296
 Marcy, G. W., Butler, R. P., Vogt, S. S., Fischer, D., & Lissauer, J. J. 1998, *ApJ*, 505, L147
 Marcy, G. W., Lindsay, V., & Wilson, K. 1987, *PASP*, 99, 490
 Marfil, E., Tabernero, H. M., Montes, D., et al. 2021, *A&A*, 656, A162
 Martín, E. L., Koresko, C. D., Kulkarni, S. R., Lane, B. F., & Wizinowich, P. L. 2000, *ApJ*, 529, L37
 Martinache, F., Lloyd, J. P., Ireland, M. J., Yamada, R. S., & Tuthill, P. G. 2007, *ApJ*, 661, 496
 Martioli, E., Hébrard, G., Correia, A. C. M., Laskar, J., & Lecavelier des Etangs, A. 2021, *A&A*, 649, A177
 Mason, B. D., Hartkopf, W. I., Gies, D. R., Henry, T. J., & Helsel, J. W. 2009, *AJ*, 137, 3358
 Mason, B. D., Hartkopf, W. I., Miles, K. N., et al. 2018, *AJ*, 155, 215
 Mason, B. D., Wycoff, G. L., Hartkopf, W. I., Douglass, G. G., & Worley, C. E. 2001, *AJ*, 122, 3466
 Massarotti, A., Latham, D. W., Stefanik, R. P., & Fogel, J. 2008, *AJ*, 135, 209
 Mathieu, R. D., Ghez, A. M., Jensen, E. L. N., & Simon, M. 2000, in *Protostars and Planets IV*, 703
 Matthews, R. & Gilmore, G. 1993, *MNRAS*, 261, L5
 Mayor, M., Bonfils, X., Forveille, T., et al. 2009, *A&A*, 507, 487
 Mazeh, T. 1990, *AJ*, 99, 675
 Mazeh, T., Latham, D. W., Goldberg, E., et al. 2001, *MNRAS*, 325, 343
 McAlister, H. A., Hartkopf, W. I., Hutter, D. J., & Franz, O. G. 1987, *AJ*, 93, 688
 McArthur, B. E., Endl, M., Cochran, W. D., et al. 2004, *ApJ*, 614, L81
 McCaughrean, M. J., Scholz, R. D., & Lodieu, N. 2002, *A&A*, 390, L27
 Medan, I. & Lépine, S. 2023, *AJ*, 166, 218
 Ment, K., Dittmann, J. A., Astudillo-Defru, N., et al. 2019, *AJ*, 157, 32
 Menti, F., Caballero, J. A., Wyatt, M. C., et al. 2024, *Research Notes of the American Astronomical Society*, 8, 267
 Mermilliod, J. C., Mayor, M., & Udry, S. 2009, *A&A*, 498, 949
 Miret-Roig, N., Galli, P. A. B., Brandner, W., et al. 2020, *A&A*, 642, A179
 Mishenina, T., Gorbaneva, T., Pignatari, M., Thielemann, F. K., & Korotin, S. A. 2015, *MNRAS*, 454, 1585
 Mochnicki, S. W., Gladders, M. D., Thomson, J. R., et al. 2002, *AJ*, 124, 2868
 Moekkel, N. & Bate, M. R. 2010, *MNRAS*, 404, 721
 Moharana, A., Helminiak, K. G., Marcadon, F., et al. 2024, *A&A*, 690, A153
 Monet, D. G., Levine, S. E., Canzian, B., et al. 2003, *AJ*, 125, 984
 Monteiro, H., Jao, W.-C., Henry, T., Subasavage, J., & Beaulieu, T. 2006, *ApJ*, 638, 446
 Montes, D., González-Peinado, R., Tabernero, H. M., et al. 2018, *MNRAS*, 479, 1332

- Montes, D., López-Santiago, J., Gálvez, M. C., et al. 2001, MNRAS, 328, 45
- Montet, B. T., Crepp, J. R., Johnson, J. A., Howard, A. W., & Marcy, G. W. 2014, ApJ, 781, 28
- Morales, J. C., Gallardo, J., Ribas, I., et al. 2010, ApJ, 718, 502
- Morales, J. C., Mustill, A. J., Ribas, I., et al. 2019, Science, 365, 1441
- Morales, J. C., Ribas, I., Jordi, C., et al. 2009, ApJ, 691, 1400
- Morales-Rueda, L., Marsh, T. R., Maxted, P. F. L., et al. 2005, MNRAS, 359, 648
- Morgan, W. W. & Hiltner, W. A. 1965, ApJ, 141, 177
- Morgan, W. W. & Keenan, P. C. 1973, ARA&A, 11, 29
- Mowlavi, N., Holl, B., Lecoeur-Taïbi, I., et al. 2023, A&A, 674, A16
- Mulders, G. D., Drażkowska, J., van der Marel, N., Ciesla, F. J., & Pascucci, I. 2021, ApJ, 920, L1
- Muterspaugh, M. W., Hartkopf, W. I., Lane, B. F., et al. 2010, AJ, 140, 1623
- Naef, D., Mayor, M., Korzennik, S. G., et al. 2003, A&A, 410, 1051
- Nagel, E., Czesla, S., Schmitt, J. H. M. M., et al. 2019, A&A, 622, A153
- Napiwotzki, R., Karl, C. A., Lisker, T., et al. 2020, A&A, 638, A131
- Nesterov, V. V., Kuzmin, A. V., Ashimbaeva, N. T., et al. 1995, A&AS, 110, 367
- Newton, E. R., Charbonneau, D., Irwin, J., et al. 2014, AJ, 147, 20
- Newton, E. R., Irwin, J., Charbonneau, D., et al. 2016, ApJ, 821, 93
- Nidever, D. L., Marcy, G. W., Butler, R. P., Fischer, D. A., & Vogt, S. S. 2002, ApJS, 141, 503
- Nordström, B., Mayor, M., Andersen, J., et al. 2004, A&A, 418, 989
- Nowak, G., Luque, R., Parviainen, H., et al. 2020, A&A, 642, A173
- Oelkers, R. J., Stassun, K. G., & Dhital, S. 2017, AJ, 153, 259
- Offner, S. S. R., Moe, M., Kratter, K. M., et al. 2023, in Astronomical Society of the Pacific Conference Series, Vol. 534, Protostars and Planets VII, ed. S. Inutsuka, Y. Aikawa, T. Muto, K. Tomida, & M. Tamura, 275
- Oh, S., Price-Whelan, A. M., Hogg, D. W., Morton, T. D., & Spergel, D. N. 2017, AJ, 153, 257
- Önehag, A., Heiter, U., Gustafsson, B., et al. 2012, A&A, 542, A33
- Öpik, E. 1924, Publications of the Tartu Astrofizika Observatory, 25, 1
- Oswalt, T. D., Hintzen, P. M., & Luyten, W. J. 1988, ApJS, 66, 391
- Palle, E., Nortmann, L., Casasayas-Barris, N., et al. 2020, A&A, 638, A61
- Palle, E., Orell-Miquel, J., Brady, M., et al. 2023, A&A, 678, A80
- Parker, R. J., Goodwin, S. P., & Allison, R. J. 2011, MNRAS, 418, 2565
- Parker, R. J., Goodwin, S. P., Kroupa, P., & Kouwenhoven, M. B. N. 2009, MNRAS, 397, 1577
- Parker, R. J. & Meyer, M. R. 2014, MNRAS, 442, 3722
- Parsons, S. G., Gänsicke, B. T., Marsh, T. R., et al. 2018, MNRAS, 481, 1083
- Passegger, V. M., Bello-García, A., Ordieres-Meré, J., et al. 2022, A&A, 658, A194
- Passegger, V. M., Reiners, A., Jeffers, S. V., et al. 2018, A&A, 615, A6
- Paulson, D. B. & Yelda, S. 2006, PASP, 118, 706
- Pecaut, M. J. & Mamajek, E. E. 2013, ApJS, 208, 9
- Pecaut, M. J., Mamajek, E. E., & Bubar, E. J. 2012, ApJ, 746, 154
- Penoyre, Z., Belokurov, V., & Evans, N. W. 2022a, MNRAS, 513, 2437
- Penoyre, Z., Belokurov, V., & Evans, N. W. 2022b, MNRAS, 513, 5270
- Penoyre, Z., Belokurov, V., Wyn Evans, N., Everall, A., & Koposov, S. E. 2020, MNRAS, 495, 321
- Perger, M., Ribas, I., Damasso, M., et al. 2017, A&A, 608, A63
- Perger, M., Scandariato, G., Ribas, I., et al. 2019, A&A, 624, A123
- Perryman, M. A. C., Lindegren, L., Kovalevsky, J., et al. 1997, A&A, 323, L49
- Pesch, P. & Bidelman, W. 1997, PASP, 109, 643
- Pettersen, B. R., Evans, D. S., & Coleman, L. A. 1984, ApJ, 282, 214
- Phan-Bao, N. & Bessell, M. S. 2006, A&A, 446, 515
- Phan-Bao, N., Forveille, T., Martín, E. L., & Delfosse, X. 2006, ApJ, 645, L153
- Pinamonti, M., Damasso, M., Marzari, F., et al. 2018, A&A, 617, A104
- Pinamonti, M., Sozzetti, A., Giacobbe, P., et al. 2019, A&A, 625, A126
- Piskunov, A. E. & Mal'Kov, O. I. 1991, A&A, 247, 87
- Plavchan, P., Barclay, T., Gagné, J., et al. 2020, Nature, 582, 497
- Popper, D. M. 1980, ARA&A, 18, 115
- Pourbaix, D., Arenou, F., Gavras, P., et al. 2022, Gaia DR3 documentation Chapter 7: Non-single stars
- Pourbaix, D., Tokovinin, A. A., Batten, A. H., et al. 2004, A&A, 424, 727
- Poveda, A. 1988, Ap&SS, 142, 67
- Poveda, A. & Allen, C. 2004, in Revista Mexicana de Astronomía y Astrofísica Conference Series, Vol. 21, 49–57
- Poveda, A., Allen, C., Costero, R., Echevarría, J., & Hernández-Alcántara, A. 2009, ApJ, 706, 343
- Poveda, A., Allen, C., & Hernández-Alcántara, A. 2007, in IAU Symposium, Vol. 240, Binary Stars as Critical Tools & Tests in Contemporary Astrophysics, ed. W. I. Hartkopf, P. Harmanec, & E. F. Guinan, 417
- Poveda, A., Allen, C., & Parrao, L. 1982, ApJ, 258, 589
- Poveda, A., Herrera, M. A., Allen, C., Cordero, G., & Lavalle, C. 1994, Rev. Mexicana Astron. Astrofis., 28, 43
- Poveda, A., Ruiz, J., & Allen, C. 1967, Boletín de los Observatorios Tonantzintla y Tacubaya, 4, 86
- Powell, B. P., Kostov, V. B., & Tokovinin, A. 2023, MNRAS, 524, 4296
- Pozuelos, F. J., Suárez, J. C., de Elía, G. C., et al. 2020, A&A, 641, A23
- Preibisch, T., Brown, A. G. A., Bridges, T., Guenther, E., & Zinnecker, H. 2002, AJ, 124, 404
- Pribulla, T. & Rucinski, S. M. 2006, AJ, 131, 2986
- Prša, A., Kochoska, A., Conroy, K. E., et al. 2022, ApJS, 258, 16
- Putney, A. 1997, ApJS, 112, 527
- Qiu, D., Tian, H.-J., Wang, X.-D., et al. 2021, ApJS, 253, 58
- Quirrenbach, A., Amado, P. J., Caballero, J. A., et al. 2014, in SPIE Conference Series, Vol. 9147, Ground-based and Airborne Instrumentation for Astronomy V
- Quirrenbach, A., Passegger, V. M., Trifonov, T., et al. 2022, A&A, 663, A48
- Raghavan, D., McAlister, H. A., Henry, T. J., et al. 2010, ApJS, 190, 1
- Raghavan, D., McAlister, H. A., Torres, G., et al. 2009, ApJ, 690, 394
- Rajpurohit, A. S., Allard, F., Teixeira, G. D. C., et al. 2018, A&A, 610, A19
- Rappaport, S., Deck, K., Levine, A., et al. 2013, ApJ, 768, 33
- Rebassa-Mansergas, A., Anguiano, B., García-Berro, E., et al. 2016, MNRAS, 463, 1137
- Rebolo, R., Zapatero Osorio, M. R., Madruga, S., et al. 1998, Science, 282, 1309
- Reefe, M. A., Luque, R., Gaidos, E., et al. 2022, AJ, 163, 269
- Reggiani, M. M. & Meyer, M. R. 2011, ApJ, 738, 60
- Reid, I. N. & Cruz, K. L. 2002, AJ, 123, 2806
- Reid, I. N., Cruz, K. L., Allen, P., et al. 2003, AJ, 126, 3007
- Reid, I. N., Cruz, K. L., Allen, P., et al. 2004, AJ, 128, 463
- Reid, I. N., Cruz, K. L., & Allen, P. R. 2007, AJ, 133, 2825
- Reid, I. N. & Gizis, J. E. 1997, AJ, 113, 2246
- Reid, I. N. & Gizis, J. E. 2005, PASP, 117, 676
- Reid, I. N., Gizis, J. E., Cohen, J. G., et al. 1997, PASP, 109, 559
- Reid, I. N., Hawley, S. L., & Gizis, J. E. 1995, AJ, 110, 1838
- Reiners, A. & Basri, G. 2009, ApJ, 705, 1416
- Reiners, A., Joshi, N., & Goldman, B. 2012, AJ, 143, 93
- Reiners, A., Ribas, I., Zechmeister, M., et al. 2018a, A&A, 609, L5
- Reiners, A., Zechmeister, M., Caballero, J. A., et al. 2018b, A&A, 612, A49
- Reipurth, B., Clarke, C. J., Boss, A. P., et al. 2014, in Protostars and Planets VI, 267
- Reipurth, B. & Mikkola, S. 2012, Nature, 492, 221
- Reipurth, B. & Zinnecker, H. 1993, A&A, 278, 81
- Renedo, I., Althaus, L. G., Miller Bertolami, M. M., et al. 2010, ApJ, 717, 183
- Retterer, J. M. & King, I. R. 1982, ApJ, 254, 214
- Reylé, C., Jardine, K., Fouqué, P., et al. 2021, A&A, 650, A201
- Reylé, C., Jardine, K., Fouqué, P., et al. 2022, in The 21st Cambridge Workshop on Cool Stars, Stellar Systems, and the Sun, Cambridge Workshop on Cool Stars, Stellar Systems, and the Sun, 218
- Riaz, B., Gizis, J. E., & Harvin, J. 2006, AJ, 132, 866
- Ribas, I. 2003, A&A, 398, 239
- Ribas, I., Reiners, A., Zechmeister, M., et al. 2023, A&A, 670, A139
- Rice, M. & Brewer, J. M. 2020, ApJ, 898, 119
- Ricker, G. R., Winn, J. N., Vanderspek, R., et al. 2014, in Society of Photo-Optical Instrumentation Engineers (SPIE) Conference Series, Vol. 9143, Proc. SPIE, 914320
- Riedel, A. R., Alam, M. K., Rice, E. L., Cruz, K. L., & Henry, T. J. 2017, ApJ, 840, 87
- Riedel, A. R., Blunt, S. C., Lambrides, E. L., et al. 2017, AJ, 153, 95
- Rivera, E. J., Laughlin, G., Butler, R. P., et al. 2010, ApJ, 719, 890
- Rivera, E. J., Lissauer, J. J., Butler, R. P., et al. 2005, ApJ, 634, 625
- Riviere-Marichalar, P., Ménard, F., Thi, W. F., et al. 2012, A&A, 538, L3
- Roberts, Lewis C. J., Rice, E. L., Beichman, C. A., et al. 2012, AJ, 144, 14
- Robertson, P., Endl, M., Cochran, W. D., MacQueen, P. J., & Boss, A. P. 2013, ApJ, 774, 147
- Rodgers, A. W. & Eggen, O. J. 1974, PASP, 86, 742
- Rojas-Ayala, B., Covey, K. R., Muirhead, P. S., & Lloyd, J. P. 2010, ApJ, 720, L113
- Rojas-Ayala, B., Covey, K. R., Muirhead, P. S., & Lloyd, J. P. 2012, ApJ, 748, 93
- Rosenthal, L. J., Fulton, B. J., Hirsch, L. A., et al. 2021, ApJS, 255, 8
- Röser, S., Schilbach, E., Piskunov, A. E., Kharchenko, N. V., & Scholz, R. D. 2011, A&A, 531, A92
- Ryu, T., Perna, R., & Wang, Y.-H. 2022, MNRAS, 516, 2204
- Sabotta, S., Schlecker, M., Chaturvedi, P., et al. 2021, A&A, 653, A114
- Sadavoy, S. I. & Stahler, S. W. 2017, MNRAS, 469, 3881
- Sahlmann, J., Burgasser, A. J., Bardalez Gagliuffi, D. C., et al. 2020, MNRAS, 495, 1136
- Salama, M., Ziegler, C., Baranec, C., et al. 2022, AJ, 163, 200
- Samus, N. N., Kazarovets, E. V., Durlevich, O. V., Kireeva, N. N., & Pastukhova, E. N. 2017, Astronomy Reports, 61, 80
- Sarkis, P., Henning, T., Kürster, M., et al. 2018, AJ, 155, 257
- Scalo, J., Kaltenegger, L., Segura, A. G., et al. 2007, Astrobiology, 7, 85
- Schanche, N., Collier Cameron, A., Almenara, J. M., et al. 2019, MNRAS, 488, 4905
- Schilbach, E. & Röser, S. 2012, A&A, 537, A129
- Schlieder, J. E., Lépine, S., & Simon, M. 2012, AJ, 143, 80

- Schmidt, S. J., Cruz, K. L., Bongiorno, B. J., Liebert, J., & Reid, I. N. 2007, AJ, 133, 2258
- Schneider, A. C., Meisner, A. M., Gagné, J., et al. 2021, ApJ, 921, 140
- Schneider, A. C., Shkolnik, E. L., Allers, K. N., et al. 2019, AJ, 157, 234
- Scholz, R. D., Meusinger, H., & Jahreiß, H. 2005, A&A, 442, 211
- Schweitzer, A., Passegger, V. M., Cifuentes, C., et al. 2019, A&A, 625, A68
- Shahaf, S., Bashir, D., Mazeh, T., et al. 2023, MNRAS, 518, 2991
- Shan, Y., Johnson, J. A., & Morton, T. D. 2015, ApJ, 813, 75
- Shan, Y., Yee, J. C., Bowler, B. P., et al. 2017, ApJ, 846, 93
- Shaya, E. J. & Olling, R. P. 2011, ApJS, 192, 2
- Shen, L. Z., Beavers, W. I., Eitter, J. J., & Salzer, J. J. 1985, AJ, 90, 1503
- Shkolnik, E., Liu, M. C., & Reid, I. N. 2009, ApJ, 699, 649
- Shkolnik, E. L., Allers, K. N., Kraus, A. L., Liu, M. C., & Flagg, L. 2017, AJ, 154, 69
- Shkolnik, E. L., Anglada-Escudé, G., Liu, M. C., et al. 2012, ApJ, 758, 56
- Shkolnik, E. L., Hebb, L., Liu, M. C., Reid, I. N., & Collier Cameron, A. 2010, ApJ, 716, 1522
- Simon, M. & Schaefer, G. H. 2011, ApJ, 743, 158
- Simons, D. A., Henry, T. J., & Kirkpatrick, J. D. 1996, AJ, 112, 2238
- Sion, E. M., Holberg, J. B., Oswalt, T. D., McCook, G. P., & Wasatonic, R. 2009, AJ, 138, 1681
- Sion, E. M., Kenyon, S. J., & Aannestad, P. A. 1990, ApJS, 72, 707
- Skinner, J., Covey, K. R., Bender, C. F., et al. 2018, AJ, 156, 45
- Skrutskie, M. F., Cutri, R. M., Stiening, R., et al. 2006, AJ, 131, 1163
- Skrutskie, M. F., Forrest, W. J., & Shure, M. 1989, AJ, 98, 1409
- Skrzypinski, S. L. 2021, MSc thesis, Universidad Complutense de Madrid, Spain
- Smith, L., Lucas, P. W., Birmingham, B., et al. 2014, MNRAS, 437, 3603
- Soderblom, D. R. 2010, ARA&A, 48, 581
- Soto, M. G., Anglada-Escudé, G., Dreizler, S., et al. 2021, A&A, 649, A144
- Soubiran, C., Bienaymé, O., Mishenina, T. V., & Kovtyukh, V. V. 2008, A&A, 480, 91
- Soubiran, C., Jasniewicz, G., Chemin, L., et al. 2018, A&A, 616, A7
- Sperauskas, J., Bartasiūtė, S., Boyle, R. P., et al. 2016, A&A, 596, A116
- Sperauskas, J., Deveikis, V., & Tokovinin, A. 2019, A&A, 626, A31
- Spina, L., Ting, Y. S., De Silva, G. M., et al. 2021, MNRAS, 503, 3279
- Stassun, K. G., Mathieu, R. D., & Valenti, J. A. 2006, Nature, 440, 311
- Stassun, K. G., Oelkers, R. J., Paegert, M., et al. 2019, AJ, 158, 138
- Stauffer, J. R., Balachandran, S. C., Krishnamurthi, A., et al. 1997, ApJ, 475, 604
- Stebbins, J. 1914, ApJ, 39, 459
- Stefansson, G., Cañas, C., Wisniewski, J., et al. 2020, AJ, 159, 100
- Steinmetz, M., Guiglion, G., McMillan, P. J., et al. 2020, AJ, 160, 83
- Stephenson, C. B. 1986a, AJ, 92, 139
- Stephenson, C. B. 1986b, AJ, 91, 144
- Stock, S., Kemmer, J., Reffert, S., et al. 2020a, A&A, 636, A119
- Stock, S., Nagel, E., Kemmer, J., et al. 2020b, A&A, 643, A112
- Stonkutė, E., Chorniy, Y., Tautvaisiene, G., et al. 2020, AJ, 159, 90
- Strassmeier, K. G. 1994, A&AS, 103, 413
- Strassmeier, K. G., Hall, D. S., Fekel, F. C., & Scheck, M. 1993, A&AS, 100, 173
- Strassmeier, K. G. & Rice, J. B. 2003, A&A, 399, 315
- Suárez Mascareño, A., González-Álvarez, E., Zapatero Osorio, M. R., et al. 2023, A&A, 670, A5
- Suárez Mascareño, A., González Hernández, J. I., Rebolo, R., et al. 2017a, A&A, 597, A108
- Suárez Mascareño, A., González Hernández, J. I., Rebolo, R., et al. 2017b, A&A, 605, A92
- Susemehl, N. & Meyer, M. R. 2022, A&A, 657, A48
- Tabernero, H. M., Marfil, E., Montes, D., & González Hernández, J. I. 2019, A&A, 628, A131
- Tabernero, H. M., Montes, D., González Hernández, J. I., & Ammler-von Eiff, M. 2017, A&A, 597, A33
- Tabernero, H. M., Shan, Y., Caballero, J. A., et al. 2024, A&A, 689, A223
- Tamazian, V. S., Docobo, J. A., & Balega, Y. Y. 2008, in Multiple Stars Across the H-R Diagram, ed. S. Hubrig, M. Petr-Gotzens, & A. Tokovinin, 71
- Tamazian, V. S., Docobo, J. A., Melikian, N. D., & Karapetian, A. A. 2006, PASP, 118, 814
- Tautvaisiene, G., Mikolaitis, S., Drazdauskas, A., et al. 2020, ApJS, 248, 19
- Taylor, M. B. 2005, in Astronomical Data Analysis Software and Systems XIV, Vol. 347, 29
- Terrien, R. C., Mahadevan, S., Bender, C. F., Deshpande, R., & Robertson, P. 2015a, ApJ, 802, L10
- Terrien, R. C., Mahadevan, S., Deshpande, R., & Bender, C. F. 2015b, ApJS, 220, 16
- Tian, H.-J., El-Badry, K., Rix, H.-W., & Gould, A. 2020, ApJS, 246, 4
- Ting, Y.-S., Conroy, C., Rix, H.-W., & Cargile, P. 2019, ApJ, 879, 69
- Tokovinin, A. 2008, MNRAS, 389, 925
- Tokovinin, A. 2014, AJ, 147, 87
- Tokovinin, A. 2017, MNRAS, 468, 3461
- Tokovinin, A. 2018, ApJS, 235, 6
- Tokovinin, A. 2020, MNRAS, 496, 987
- Tokovinin, A. 2022, AJ, 163, 127
- Tokovinin, A. 2023, AJ, 165, 180
- Tokovinin, A., Thomas, S., Sterzik, M., & Udry, S. 2006, A&A, 450, 681
- Tokovinin, A. A. 1997, A&AS, 121, 71
- Toledo-Padrón, B., Suárez Mascareño, A., González Hernández, J. I., et al. 2021, A&A, 648, A20
- Tomkin, J. & Pettersen, B. R. 1986, AJ, 92, 1424
- Toonen, S., Hollands, M., Gänsicke, B. T., & Boekholt, T. 2017, A&A, 602, A16
- Torres, C. A. O., Quast, G. R., da Silva, L., et al. 2006, A&A, 460, 695
- Torres, G. 1999, PASP, 111, 169
- Torres, G., Andersen, J., & Giménez, A. 2010, A&A Rev., 18, 67
- Torres, G., Claret, A., & Young, P. A. 2009, ApJ, 700, 1349
- Torres, G. & Ribas, I. 2002, ApJ, 567, 1140
- Torres, G., Schaefer, G. H., Monnier, J. D., et al. 2022, ApJ, 941, 8
- Tremblay, P. E., Hollands, M. A., Gentile Fusillo, N. P., et al. 2020, MNRAS, 497, 130
- Trifonov, T., Caballero, J. A., Morales, J. C., et al. 2021, Science, 371, 1038
- Trifonov, T., Kürster, M., Zechmeister, M., et al. 2018, A&A, 609, A117
- Tuchow, N. W., Stark, C. C., & Mamajek, E. 2024, AJ, 167, 139
- Tuomi, M., Jones, H. R. A., Barnes, J. R., Anglada-Escudé, G., & Jenkins, J. S. 2014, MNRAS, 441, 1545
- Udry, S., Bonfils, X., Delfosse, X., et al. 2007, A&A, 469, L43
- Valenti, J. A., Piskunov, N., & Johns-Krull, C. M. 1998, ApJ, 498, 851
- van Albada, T. S. 1968a, Bull. Astron. Inst. Netherlands, 19, 479
- van Albada, T. S. 1968b, Bull. Astron. Inst. Netherlands, 20, 57
- van Altena, W. F., Lee, J. T., & Hoffleit, E. D. 1995
- van Belle, G. T. & von Braun, K. 2009, ApJ, 694, 1085
- Van der Swaelmen, M., Merle, T., Van Eck, S., et al. 2023, arXiv e-prints, arXiv:2312.04721
- van Leeuwen, F. 2007, A&A, 474, 653
- Vanderburg, A., Rappaport, S. A., Xu, S., et al. 2020, Nature, 585, 363
- Vereshchagin, S., Tutukov, A., Iungelson, L., Kraicheva, Z., & Popova, E. 1988, Ap&SS, 142, 245
- Vinagre Maqueda, A. R. 2023, MSc thesis, Universidad Complutense de Madrid, Spain
- Vogt, S. S., Butler, R. P., Marcy, G. W., et al. 2005, ApJ, 632, 638
- Vogt, S. S., Butler, R. P., Marcy, G. W., et al. 2002, ApJ, 568, 352
- Vrijmoet, E. H., Henry, T. J., Jao, W.-C., & Dieterich, S. B. 2020, AJ, 160, 215
- Šubjak, J., Lodieu, N., Kabáth, P., et al. 2023, A&A, 671, A10
- Wang, Y.-F., Luo, A. L., Chen, W.-P., et al. 2022, A&A, 660, A38
- Ward-Duong, K., Patience, J., De Rosa, R. J., et al. 2015, MNRAS, 449, 2618
- Wasserman, I. & Weinberg, M. D. 1987, ApJ, 312, 390
- Weinberg, M. D., Shapiro, S. L., & Wasserman, I. 1987, ApJ, 312, 367
- Weinberger, A. J., Boss, A. P., Keiser, S. A., et al. 2016, AJ, 152, 24
- Wenger, M., Ochsenbein, F., Egret, D., et al. 2000, A&AS, 143, 9
- Wertheimer, J. G. & Laughlin, G. 2006, AJ, 132, 1995
- Wesemael, F., Greenstein, J. L., Liebert, J., et al. 1993, PASP, 105, 761
- West, A. A., Morgan, D. P., Bochanski, J. J., et al. 2011, AJ, 141, 97
- White, R. J., Gabor, J. M., & Hillenbrand, L. A. 2007, AJ, 133, 2524
- White, R. J. & Ghez, A. M. 2001, ApJ, 556, 265
- Williams, K. A. 2004, ApJ, 601, 1067
- Wilson, E. B. 1927, Journal of the American Statistical Association, 22, 209
- Wilson, R. E. 1953, Carnegie Institute Washington D.C. Publication, 0
- Winters, J. G., Cloutier, R., Medina, A. A., et al. 2022, AJ, 163, 168
- Winters, J. G., Henry, T. J., Jao, W.-C., et al. 2019a, AJ, 157, 216
- Winters, J. G., Henry, T. J., Lurie, J. C., et al. 2015, AJ, 149, 5
- Winters, J. G., Irwin, J. M., Charbonneau, D., et al. 2020, AJ, 159, 290
- Winters, J. G., Medina, A. A., Irwin, J. M., et al. 2019b, AJ, 158, 152
- Winters, J. G., Sevrinsky, R. A., Jao, W.-C., et al. 2017, AJ, 153, 14
- Woolf, V. M. & Wallerstein, G. 2006, PASP, 118, 218
- Woolley, R., Epps, E. A., Penston, M. J., & Pocock, S. B. 1970, Royal Observatory Annals, 5
- Wright, D. J., Wittenmyer, R. A., Tinney, C. G., Bentley, J. S., & Zhao, J. 2016, ApJ, 817, L20
- Xuan, J. W., Mérard, A., Thompson, W., et al. 2024, Nature, 634, 1070
- Yi, Z., Luo, A., Song, Y., et al. 2014, AJ, 147, 33
- Yoo, J., Chanamé, J., & Gould, A. 2004, ApJ, 601, 311
- Zacharias, N., Finch, C., Girard, T., et al. 2010, AJ, 139, 2184
- Zacharias, N., Finch, C. T., Girard, T. M., et al. 2012, VizieR Online Data Catalog, 1322
- Zakhzhaj, V. A. 1979, Vestnik Khar'kovskogo Universiteta, 190, 52
- Zakhzhaj, O. V., Launhardt, R., Müller, A., et al. 2022, A&A, 667, A63
- Zapatero Osorio, M. R., Lane, B. F., Pavlenko, Y., et al. 2004, ApJ, 615, 958
- Zboril, M. & Byrne, P. B. 1998, MNRAS, 299, 753
- Zechmeister, M., Dreizler, S., Ribas, I., et al. 2019, A&A, 627, A49
- Zhang, Z. H., Raddi, R., Burgasser, A. J., et al. 2024, MNRAS, 533, 1654
- Zhao, G., Zhao, Y.-H., Chu, Y.-Q., Jing, Y.-P., & Deng, L.-C. 2012, Research in Astronomy and Astrophysics, 12, 723
- Ziegler, C., Law, N. M., Baranec, C., et al. 2018, AJ, 156, 259
- Zong, W., Fu, J.-N., De Cat, P., et al. 2020, ApJS, 251, 15
- Zuckerman, B. & Song, I. 2004, ARA&A, 42, 685

Appendix A: Online material

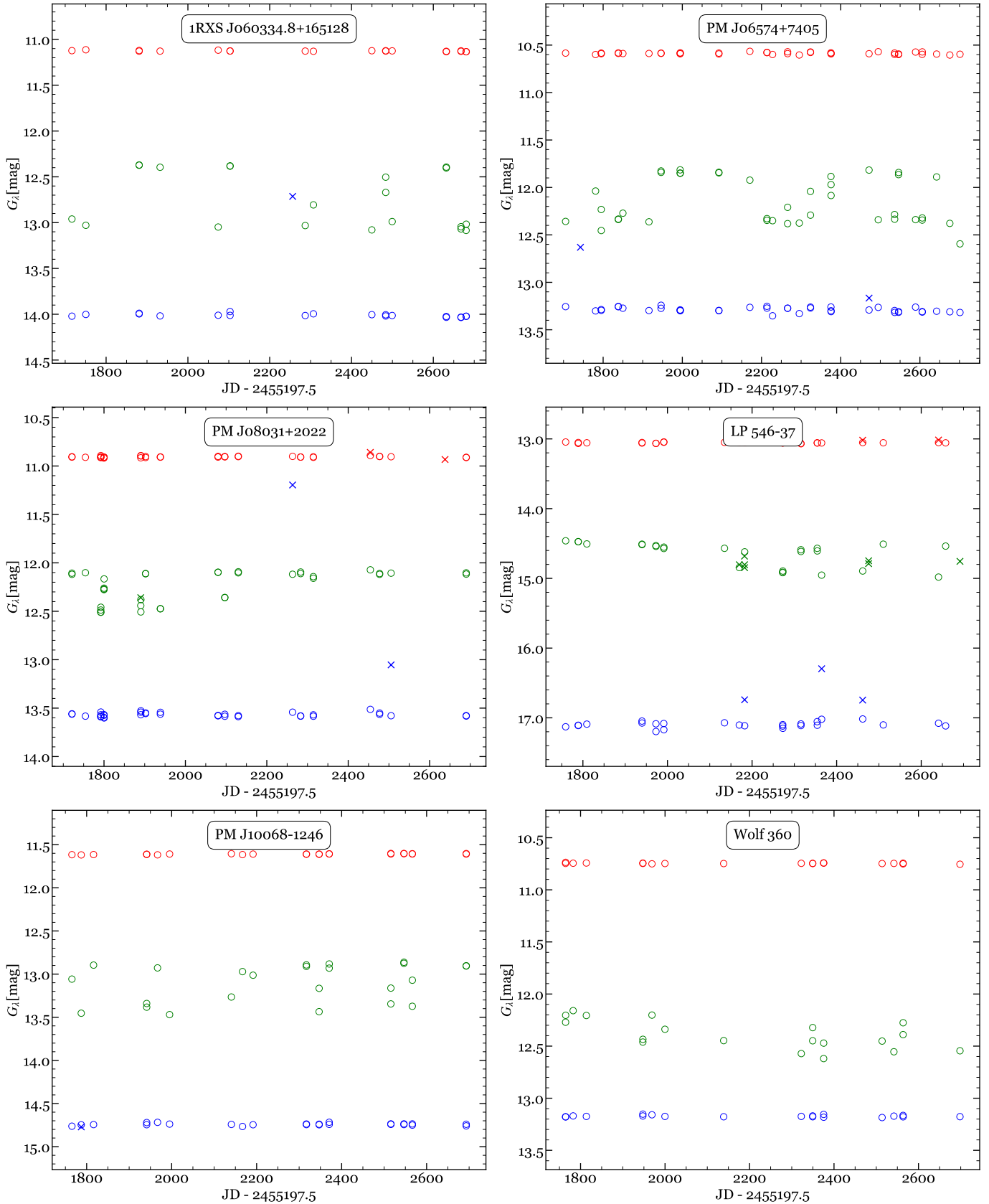


Fig. A.1: Same as Fig. 7 for single stars reported in this work as unresolved binary candidates.

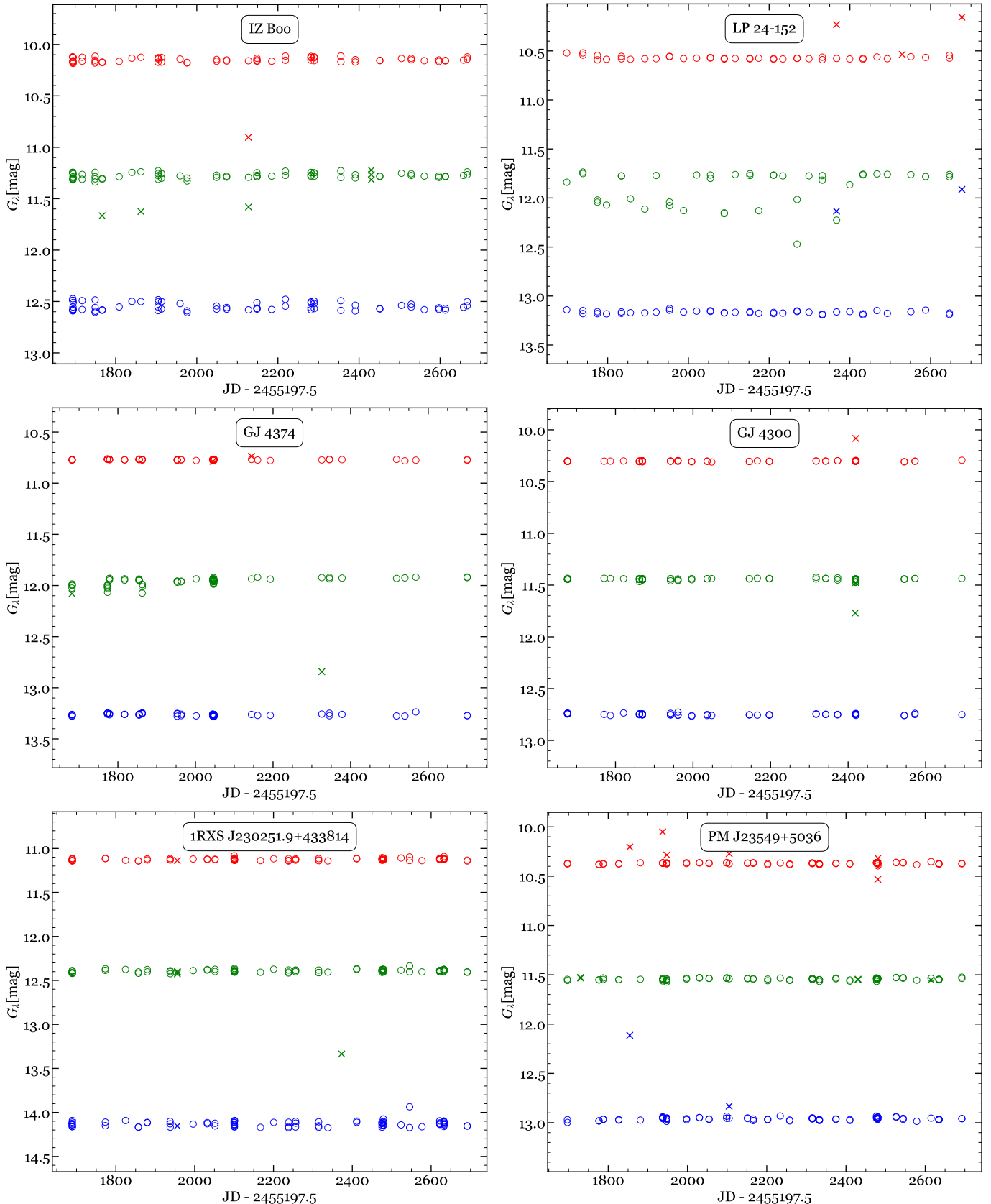


Fig. A.1: Same as Fig. 7 for the single stars reported in this work as candidates to unresolved binaries (cont.).

Table A.1: Complete sample studied in this work^a.

| Star id. | System id. | Karmn | Name | GJ | α (J2016.0) | δ (J2016.0) | Spectral type | Multiplicity type | In tables |
|----------|------------|-------------|-----------------------|--------|-----------------------|-----------------------|---------------|-------------------|-----------|
| 1 | 1 | J00012+139N | BD+13 5195A | | 00:01:13.21 | +13:58:32.7 | M0.5 V | Multiple | |
| 2 | 1 | J00012+139S | BD+13 5195B | | 00:01:12.89 | +13:58:22.0 | M0.0 V | Multiple | |
| 3 | 2 | J00026+383 | PM J00026+3821A | | 00:02:40.00 | +38:21:44.1 | M4.0 V | Multiple | |
| 4 | 2 | | PM J00026+3821B | | 00:02:40.05 | +38:21:45.3 | M3.5 V | Multiple | |
| 5 | | J00033+046 | StKM 1-2199 | | 00:03:18.97 | +04:41:11.6 | M1.5 V | Single | A.2 |
| 6 | 3 | | HD 38A | 4 A | 00:05:42.38 | +45:48:40.9 | K7 V | Multiple | A.4 |
| 7 | 3 | J00056+458 | HD 38B | 4 B | 00:05:42.30 | +45:48:35.0 | M0.0 V | Multiple | |
| 8 | 3 | J00051+457 | GJ 2 | 2 | 00:05:12.22 | +45:47:09.2 | M1.0 V | Multiple | |
| 9 | | J00067-075 | GJ 1002 | 1002 | 00:06:42.32 | -07:32:47.3 | M5.5 V | Single | A.11 |
| 10 | 4 | J00077+603 | G 217-32A | | 00:07:43.28 | +60:22:54.0 | M4.0 V | Multiple | |
| 11 | 4 | | G 217-32B | | 00:07:43.40 | +60:22:53.8 | M5.0 V | Multiple | A.2 |
| 12 | | J00078+676 | PM J00078+6736 | | 00:07:50.65 | +67:36:23.9 | M2.0 V | Candidate | |
| 13 | | J00079+080 | GJ 3007 | 3007 | 00:07:58.74 | +08:00:12.8 | M3.0 V | Candidate | |
| 14 | 5 | J00081+479 | IRXS J000806.3+475659 | | 00:08:06.23 | +47:57:02.4 | M4.0 V | Multiple | A.4 |
| 15 | | J00084+174 | GJ 3008 | 3008 | 00:08:27.18 | +17:25:26.4 | M0.0 V | Single | |
| 16 | 6 | J00088+208 | GJ 3010 | 3010 | 00:08:53.86 | +20:50:21.4 | M4.5 V | Multiple | |
| 17 | | J00110+052 | G 31-29 | | 00:11:04.89 | +05:12:33.4 | M1.0 V | Candidate | |
| 18 | | J00115+591 | LSPM J0011+5908 | | 00:11:29.94 | +59:08:21.2 | M5.5 V | Single | |
| 19 | | J00118+229 | LP 348-40 | | 00:11:53.17 | +22:59:01.2 | M3.5 V | Candidate | |
| 20 | | J00119+330 | G 130-53 | | 00:11:55.73 | +33:03:10.7 | M3.5 V | Single | |
| 21 | | J00122+304 | IRXS J001213.6+302906 | | 00:12:13.49 | +30:28:43.8 | M4.5 V | Candidate | |
| 22 | | J00131+703 | TYC 4298-613-1 | | 00:13:11.68 | +70:23:54.9 | M1.0 V | Single | |
| 23 | 7 | J00132+693 | GJ 11 A | 11 A | 00:13:18.00 | +69:19:32.4 | M3.0 V | Multiple | |
| 24 | 7 | | GJ 11 B | 11 B | 00:13:18.21 | +69:19:32.3 | M3.0 V | Multiple | |
| 25 | | J00133+275 | UPM J0013+2733 | | 00:13:19.55 | +27:33:29.1 | M4.5 V | Candidate | |
| 26 | 8 | J00136+806 | GJ 3014 | 3014 | 00:13:40.36 | +80:39:59.8 | M1.5 V | Multiple | |
| 27 | 8 | J00137+806 | GJ 3015 | 3015 | 00:13:44.59 | +80:39:52.3 | M5.0 V | Multiple | |
| 28 | 9 | J00154-161 | GJ 1005 | 1005 | 00:15:28.77 | -16:08:11.7 | M4.0 V | Multiple | |
| 29 | | J00156+722 | LP 49-338 | | 00:15:37.59 | +72:17:03.5 | M2.0 V | Single | |
| 30 | | J00158+135 | GJ 12 | 12 | 00:15:49.92 | +13:33:27.6 | M3.0 V | Single | A.11 |
| 31 | 10 | J00159-166 | IRXS J001557.5-163659 | | 00:15:57.94 | -16:36:57.5 | M4.0 V | Multiple | |
| 32 | 11 | J00162+198W | EZ Psc | 1006 A | 00:16:15.44 | +19:51:25.3 | M4.0 V | Multiple | A.4 |
| 33 | 11 | J00162+198E | GJ 1006 B | 1006 B | 00:16:16.96 | +19:51:38.5 | M4.0 V | Multiple | |
| 34 | | J00169+051 | GJ 1007 | 1007 | 00:16:56.20 | +05:07:16.4 | M4.5 V | Single | |
| 35 | 12 | J00169+200 | GJ 3022 | 3022 | 00:16:57.03 | +20:03:55.7 | M3.5 V | Multiple | A.7 |
| 36 | 12 | | G 131-47B | | 00:16:57.10 | +20:03:55.4 | M3.5 V | Multiple | A.7 |
| 37 | 12 | | LP 404-54 | | 00:15:13.81 | +19:47:40.5 | M5.0 V | Multiple | A.7 |
| 38 | | J00173+291 | Ross 680 | 3023 | 00:17:21.17 | +29:11:05.7 | M2.0 V | Single | |
| 39 | | J00176-086 | GJ 3025 | 3025 | 00:17:41.23 | -08:40:55.8 | M0.0 V | Candidate | |
| 40 | 13 | J00179+209 | LP 404-81 | | 00:17:58.87 | +20:57:18.6 | M1.0 V | Multiple | |
| 41 | 13 | | LP 404-80 | | 00:17:58.33 | +20:57:13.0 | M3.0 V | Multiple | |
| 42 | | J00182+102 | GJ 16 | 16 | 00:18:16.59 | +10:12:09.6 | M1.5 V | Single | |
| 43 | 14 | J00183+440 | GX And | 15 A | 00:18:27.17 | +44:01:29.2 | M1.0 V | Multiple | A.11 |
| 44 | 14 | J00184+440 | GQ And | 15 B | 00:18:30.07 | +44:01:43.5 | M3.5 V | Multiple | |
| 45 | | J00188+278 | GJ 3027 | 3027 | 00:18:54.07 | +27:48:48.1 | M4.0 V | Single | |
| 46 | | J00190-099 | GJ 1008 | 1008 | 00:19:05.52 | -09:57:58.3 | M0.0 V | Single | |
| 47 | | J00201-170 | GJ 2003 | 2003 | 00:20:08.54 | -17:03:41.2 | M1.0 V | Single | |
| 48 | | J00204+330 | GJ 3028 | 3028 | 00:20:30.78 | +33:04:52.6 | M5.5 V | Single | |
| 49 | | J00207+596 | [I81] M 134 | | 00:20:47.70 | +59:36:15.6 | M2.5 V | Single | |
| 50 | | J00209+176 | StKM 1-25 | | 00:20:57.24 | +17:38:14.7 | M0.0 V | Single | |
| 51 | | J00210+557 | G 217-43 | | 00:21:05.02 | +55:43:55.6 | M2.0 V | Single | |
| 52 | | J00218+382 | G 171-51 | | 00:21:54.79 | +38:16:24.2 | M3.0 V | Single | |
| 53 | 15 | J00219+492 | GJ 3030 | 3030 | 00:21:58.20 | +49:12:37.3 | M2.5 V | Multiple | |
| 54 | 15 | | LP 149-56 B | | 00:21:58.00 | +49:12:38.4 | M5.0 V | Multiple | |
| 55 | | J00234+243 | GJ 1011 | 1011 | 00:23:27.73 | +24:18:26.5 | M4.0 V | Single | |
| 56 | 16 | J00234+771 | GJ 1010 A | 1010 A | 00:23:24.80 | +77:11:22.2 | M1.5 V | Multiple | |
| 57 | 16 | J00235+771 | GJ 1010 B | 1010 B | 00:23:27.78 | +77:11:27.5 | M4.0 V | Multiple | |
| 58 | | J00240+264 | LSPM J0024+2626 | | 00:24:03.96 | +26:26:28.9 | M4.0 V | Candidate | |
| 59 | | J00244+360 | G 130-67 | | 00:24:26.30 | +36:03:54.0 | M1.0 V | Single | |
| 60 | | J00245+300 | GJ 3033 | 3033 | 00:24:35.60 | +30:02:29.7 | M4.5 V | Single | |
| 61 | | J00253+228 | GJ 3034 | 3034 | 00:25:20.33 | +22:53:03.7 | M4.0 V | Single | |
| 62 | | J00268+701 | GJ 21 | 21 | 00:26:52.27 | +70:08:30.4 | M0.5 V | Single | |
| 63 | | J00271+496 | GJ 3035 | 3035 | 00:27:07.39 | +49:41:49.3 | M4.5 V | Single | |
| 64 | 17 | J00279+223 | LP 349-25 | | 00:27:56.46 | +22:19:29.7 | M8.0 V | Multiple | |
| 65 | | J00286-066 | GJ 1012 | 1012 | 00:28:39.11 | -06:40:02.0 | M4.0 V | Single | |
| 66 | 18 | J00288+503 | GJ 3036 | 3036 | 00:28:54.66 | +50:22:35.3 | M4.0 V | Multiple | |
| 67 | | J00315-058 | GJ 1013 | 1013 | 00:31:35.79 | -05:52:30.0 | M3.5 V | Single | |
| 68 | | J00322+544 | G 217-56 | | 00:32:15.34 | +54:28:55.3 | M4.5 V | Single | |
| 69 | 19 | J00324+672N | V547 Cas | 22A | 00:32:34.33 | +67:14:03.6 | M2.0 V | Multiple | |
| 70 | 19 | J00324+672S | GJ 22 B | 22 B | 00:32:34.28 | +67:13:59.8 | M3.0 V | Multiple | |
| 71 | 20 | J00325+074 | LP 525-39 A | 3039 | 00:32:34.91 | +07:29:25.7 | M4.0 V | Multiple | |
| 72 | 20 | | LP 525-39 B | | 00:32:34.89 | +07:29:26.4 | M3.0 V | Multiple | |
| 73 | 21 | J00328-045 | GR* 50 | | 00:32:53.21 | -04:34:09.4 | M4.5 V | Multiple | |
| 74 | | J00333+368 | G 132-4 | | 00:33:21.17 | +36:50:28.6 | M3.0 V | Single | |
| 75 | 22 | J00341+253 | V493 AndA | | 00:34:08.48 | +25:23:48.5 | M0.0 V | Multiple | |
| 76 | 22 | | V493 AndB | | 00:34:08.59 | +25:23:48.2 | K7 V | Multiple | A.7 |
| 77 | 22 | | UCAC4 578-001365 | | 00:34:20.04 | +25:28:12.9 | M4.0 V | Multiple+ | A.7 |
| 78 | | J00346+711 | GJ 3040 | 3040 | 00:34:39.40 | +71:11:36.6 | M3.5 V | Single | |
| 79 | 23 | J00357+025 | LP 585-55 | | 00:35:43.30 | +02:33:10.9 | M5.0 V | Multiple | |
| 80 | 24 | J00358+526 | G 172-11 | | 00:35:54.70 | +52:41:09.3 | M2.5 V | Multiple | |

Table A.1: Complete sample studied in this work^a (cont.).

| Star id. | System id. | Karmn | Name | GJ | α (J2016.0) | δ (J2016.0) | Spectral type | Multiplicity type | In tables |
|----------|------------|-------------|----------------------------|--------|-----------------------|-----------------------|---------------|-------------------|-----------|
| 81 | 24 | | G 217–59 | | 00:35:55.04 | +52:41:33.7 | M3.0 V | Multiple | |
| 82 | | J00359+104 | GJ 1014 | 1014 | 00:35:56.70 | +10:28:29.4 | M5.0 V | Single | |
| 83 | 25 | J00361+455 | G 172–013 | 3042 | 00:36:08.05 | +45:30:55.3 | M2.5 V | Multiple | |
| 84 | | J00374+515 | G 172–14 | | 00:37:25.07 | +51:33:06.8 | M0.5 V | Candidate | |
| 85 | | J00380+169 | PM J00380+1656 | | 00:38:03.75 | +16:56:01.3 | M3.0 V | Single | |
| 86 | | J00382+523 | GJ 3044 | 3044 | 00:38:15.16 | +52:19:53.3 | M0.0 V | Single | |
| 87 | | J00385+514 | GJ 3045 | 3045 | 00:38:33.48 | +51:27:58.4 | M2.5 V | Single | |
| 88 | | J00389+306 | Wolf 1056 | 26 | 00:39:00.98 | +30:36:58.8 | M2.5 V | Single | |
| 89 | 26 | J00395+149S | LP 465–061 | | 00:39:33.91 | +14:54:19.6 | M4.0 V | Multiple | |
| 90 | 26 | J00395+149N | LP 465–62 | | 00:39:34.16 | +14:54:35.4 | M4.5 V | Multiple | |
| 91 | | J00395+605 | Wolf 10 | 3046 | 00:39:33.51 | +60:33:10.9 | M2.5 V | Candidate | |
| 92 | | J00403+612 | TOI–1470 | | 00:40:21.40 | +61:12:48.2 | M2.0 V | Single | A.11 |
| 93 | | J00409+313 | GJ 3047 | 3047 | 00:40:56.19 | +31:22:51.2 | M4.0 V | Single | |
| 94 | 27 | | GJ 1015 B | 1015 B | 00:41:22.64 | +55:50:07.2 | DBQ5 | Multiple | A.9 |
| 95 | 27 | J00413+558 | GJ 1015 A | 1015 A | 00:41:21.44 | +55:50:03.2 | M4.0 V | Multiple | A.9 |
| 96 | | J00427+438 | PM J00427+4349 | | 00:42:47.79 | +43:49:24.0 | M2.5 V | Single | |
| 97 | 28 | J00428+355 | FF And | 9022 A | 00:42:48.59 | +35:32:56.9 | M1.0 V | Multiple | A.4 |
| 98 | | J00435+284 | GJ 1019 | 1019 | 00:43:35.44 | +28:26:24.4 | M4.0 V | Single | |
| 99 | | J00443+091 | GJ 3052 | 3052 | 00:44:21.54 | +09:07:34.5 | M4.5 V | Candidate | |
| 100 | | J00443+126 | GJ 3051 | 3051 | 00:44:19.64 | +12:36:59.8 | M3.5 V | Candidate | |
| 101 | | J00449–152 | GJ 3053 | 3053 | 00:44:59.68 | -15:16:27.1 | M4.5 V | Single | A.11 |
| 102 | 29 | J00459+337 | G 132–25 | | 00:45:57.01 | +33:47:11.3 | M4.5 V | Multiple | |
| 103 | | J00463+353 | PM J00463+3522 | | 00:46:21.76 | +35:22:10.6 | M1.5 V | Single | |
| 104 | | J00464+506 | G 172–22 | | 00:46:30.66 | +50:38:35.3 | M4.0 V | Single | |
| 105 | | J00468+160 | PM J00468+1603 | | 00:46:53.16 | +16:03:01.8 | M2.0 V | Single | |
| 106 | | J00484+753 | LSPM J0048+7518 | | 00:48:30.66 | +75:18:47.2 | M3.0 V | Single | |
| 107 | | J00487+270 | GJ 3057 | 3057 | 00:48:45.34 | +27:01:04.4 | M2.5 V | Single | |
| 108 | 30 | J00489+445 | LP 193–564 A | 3058 | 00:48:58.46 | +44:35:06.9 | M3.0 V | Multiple | |
| 109 | 30 | | LP 193–564 B | | 00:48:58.37 | +44:35:06.6 | M3.0 V | Multiple | |
| 110 | | J00490+657 | PM J00490+6544 | | 00:49:05.09 | +65:44:36.8 | M2.5 V | Single | |
| 111 | 31 | J00502+086 | RX J0050.2+0837 | | 00:50:17.59 | +08:37:33.6 | M4.5 V | Multiple | A.4 |
| 112 | 32 | J00505+248 | FT Psc A | | 00:50:33.49 | +24:48:59.7 | M3.5 V | Multiple | |
| 113 | 32 | | FT Psc B | | 00:50:33.45 | +24:49:00.4 | M4.5 V | Multiple | |
| 114 | | J00511+225 | BPM 84579 | | 00:51:10.71 | +22:34:43.8 | M1.5 V | Candidate | |
| 115 | | J00514+583 | Wolf 33 | 38 | 00:51:33.02 | +58:18:13.8 | M0.0 V | Single | |
| 116 | 33 | | HD 4967 | 40 A | 00:51:34.73 | -22:54:40.7 | K5 V | Multiple | A.8 |
| 117 | 33 | J00515–229 | HD 4967B | 40 B | 00:51:35.91 | -22:54:35.4 | M5.5 V | Multiple | A.8 |
| 118 | | J00520+205 | G 69–27 | | 00:52:00.27 | +20:34:56.6 | M1.0 V | Single | |
| 119 | | J00532+190 | LSPM J0053+1903 | | 00:53:12.84 | +19:03:25.0 | M2.5 V | Single | |
| 120 | | J00538+459 | G 172–28 | | 00:53:53.72 | +45:56:41.6 | M0.0 V | Single | |
| 121 | | J00540+691 | Ross 317 | | 00:54:00.72 | +69:10:56.9 | M2.0 V | Candidate | |
| 122 | | J00548+275 | G 69–32 | | 00:54:48.49 | +27:31:03.9 | M4.5 V | Candidate | |
| 123 | | J00566+174 | GJ 1024 | 1024 | 00:56:39.14 | +17:27:30.3 | M4.0 V | Single | |
| 124 | | J00570+450 | G 172–30 | | 00:57:03.64 | +45:05:08.7 | M3.0 V | Single | |
| 125 | | J00577+058 | BD+05 127 | | 00:57:44.49 | +05:51:20.6 | M0.0 V | Single | |
| 126 | | J00580+393 | 1RXS J005802.4+391912 | | 00:58:01.01 | +39:19:11.5 | M4.5 V | Single | |
| 127 | | J01008+669 | GJ 3068 | 3068 | 01:00:48.83 | +66:56:53.8 | M3.5 V | Single | |
| 128 | | J01009–044 | GJ 1025 | 1025 | 01:00:57.71 | -04:26:49.5 | M4.0 V | Single | |
| 129 | | J01013+613 | Wolf 44 | 47 | 01:01:20.86 | +61:21:43.7 | M2.0 V | Single | |
| 130 | | J01019+541 | GJ 3069 | 3069 | 01:01:58.94 | +54:10:55.8 | M5.0 V | Candidate | |
| 131 | | J01023–104 | GJ 3072 | 3072 | 01:02:21.16 | -10:25:28.7 | M0.0 V | Single | A.11 |
| 132 | | J01025+716 | Ross 318 | 48 | 01:02:38.16 | +71:40:41.2 | M3.0 V | Single | |
| 133 | 34 | J01026+623 | Wolf 46 | 49 | 01:02:40.55 | +62:20:43.6 | M1.5 V | Multiple | A.11 |
| 134 | 34 | J01033+623 | V388 Cas | 51 | 01:03:21.51 | +62:21:57.2 | M5.0 V | Multiple | |
| 135 | 35 | J01032+200 | GJ 1026 A | 1026 A | 01:03:14.92 | +20:05:53.1 | M2.0 V | Multiple | |
| 136 | 35 | | GJ 1026 B | 1026 B | 01:03:15.07 | +20:05:54.5 | M3.5 V | Multiple | |
| 137 | 36 | J01032+316 | GJ 3073 | 3073 | 01:03:14.23 | +31:40:59.7 | M3.5 V | Multiple | |
| 138 | 37 | J01032+712 | LP 29–70 | | 01:03:16.13 | +71:13:11.8 | M4.0 V | Multiple | |
| 139 | 38 | J01036+408 | G 132–50 | | 01:03:40.31 | +40:51:26.6 | M0.0 V | Multiple | |
| 140 | 38 | J01037+408 | G 132–51A | | 01:03:42.24 | +40:51:13.5 | M2.5 V | Multiple | |
| 141 | 38 | | LP 194–20 | | 01:03:42.46 | +40:51:13.1 | M4.0 V | Multiple | |
| 142 | | J01041+108 | StKM 1–112 | | 01:04:11.07 | +10:51:35.4 | M1.0 V | Single | |
| 143 | | J01048–181 | GJ 1028 | 1028 | 01:04:55.25 | -18:07:20.8 | M5.0 V | Single | |
| 144 | 39 | J01056+284 | GJ 1029 | 1029 | 01:05:39.97 | +28:29:30.6 | M5.0 V | Multiple | A.4 |
| 145 | | J01066+152 | GJ 1030 | 1030 | 01:06:41.39 | +15:16:18.1 | M2.0 V | Single | |
| 146 | | J01066+192 | LSPM J0106+1913 | | 01:06:36.93 | +19:13:29.6 | M3.0 V | Single | A.11 |
| 147 | | J01069+804 | LP 12–502 | | 01:06:56.00 | +80:27:34.0 | M4.5 V | Candidate | |
| 148 | | J01078+128 | G 2–21 | | 01:07:52.53 | +12:52:51.4 | M1.5 V | Single | |
| 149 | | J01102–118 | LP 707–16 | | 01:10:17.75 | -11:51:19.3 | M3.0 V | Candidate | |
| 150 | 40 | J01114+154 | GJ 3076 | 3076 | 01:11:25.63 | +15:26:19.9 | M5.0 V | Multiple | |
| 151 | | J01116+120 | LP 467–15 | | 01:11:36.66 | +12:05:02.3 | M2.0 V | Single | |
| 152 | 41 | J01119+049N | GJ 3077 | 3077 | 01:11:56.01 | +04:54:56.6 | M3.0 V | Multiple | |
| 153 | 41 | J01119+049S | GJ 3078 | 3078 | 01:11:58.39 | +04:54:04.0 | M3.5 V | Multiple | |
| 154 | | J01125–169 | YZ Cet | 54.1 | 01:12:31.98 | -16:59:46.2 | M4.5 V | Single | |
| 155 | 42 | J01133+589 | Wolf 58 | | 01:13:20.12 | +58:55:20.3 | M1.5 V | Multiple | |
| 156 | 42 | | Gaia DR3 41410814095410872 | | 01:13:19.97 | +58:55:18.6 | M5.0 V | Multiple | |
| 157 | | J01134–229 | GJ 1033 | 1033 | 01:13:24.20 | -22:54:07.3 | M4.0 V | Single | |
| 158 | | J01141+790 | PM J01141+7904 | | 01:14:06.69 | +79:04:01.9 | M3.0 V | Candidate | |
| 159 | | J01147+253 | LP 351–6 | | 01:14:49.86 | +25:18:57.6 | M1.5 V | Single | |
| 160 | 43 | J01158+470 | 1RXS J011549.5+470159 | | 01:15:50.51 | +47:02:02.1 | M4.5 V | Multiple | 7 |
| 161 | 43 | | LP 151–21 | | 01:15:49.20 | +47:02:25.7 | M5.0 V | Multiple | 7 |
| 162 | | J01161+601 | Wolf 59 | | 01:16:10.94 | +60:09:09.6 | M0.5 V | Single | |

Table A.1: Complete sample studied in this work^a (cont.).

| Star id. | System id. | Karmn | Name | GJ | α (J2016.0) | δ (J2016.0) | Spectral type | Multiplicity type | In tables |
|----------|------------|-------------|------------------------------|--------|-----------------------|-----------------------|---------------|-------------------|-----------|
| 163 | | J01178+054 | GJ 3084 | 3084 | 01:17:53.34 | +05:28:16.0 | M0.5 V | Single | |
| 164 | | J01178+286 | Ross 324 | 3083 | 01:17:50.21 | +28:40:09.6 | M0.5 V | Single | |
| 165 | | J01182-128 | GJ 56.1 | 56.1 | 01:18:16.20 | -12:54:10.2 | M2.0 V | Single | |
| 166 | | J01198+841 | GJ 1035 | 1035 | 01:19:41.88 | +84:09:40.4 | M5.0 V | Single | |
| 167 | | J01214+243 | Ross 788 | | 01:21:29.78 | +24:19:50.2 | M0.0 V | Single | |
| 168 | 44 | J01221+221 | LP 351-34 | | 01:22:10.58 | +22:09:00.6 | M4.5 V | Multiple | |
| 169 | 45 | J01227+005 | GJ 3093 | 3093 | 01:22:44.77 | +00:31:55.7 | M4.5 V | Multiple | |
| 170 | 45 | | GJ 3094 | 3094 | 01:22:44.83 | +00:31:56.5 | M5.0 V | Multiple | |
| 171 | 46 | J01256+097 | Wolf 66 A | 3097 A | 01:25:36.89 | +09:45:18.5 | M4.0 V | Multiple | |
| 172 | 46 | | Wolf 66 B | 3097 B | 01:25:36.86 | +09:45:18.0 | M4.5 V | Multiple | |
| 173 | | J01317+209 | Wolf 1523 | | 01:32:44.80 | +20:59:13.5 | M2.0 V | Single | |
| 174 | | J01324-219 | GJ 3098 | 3098 | 01:32:25.53 | -21:54:32.7 | M1.5 V | Single | |
| 175 | | J01339-176 | LP 768-113 | | 01:33:58.05 | -17:38:26.8 | M4.0 V | Single | |
| 176 | | J01352-072 | IRXS J013514.2-071254 | | 01:35:14.03 | -07:12:52.2 | M4.0 V | Single | |
| 177 | 47 | | EX Cet | | 01:37:35.65 | -06:45:39.1 | K0.5 V | Multiple | A.7 A.8 |
| 178 | 47 | J01369-067 | LP 648-20 | | 01:36:55.36 | -06:47:39.6 | M3.5 V | Multiple | A.7 A.8 |
| 179 | | J01373+610 | TYC 4031-2527-1 | | 01:37:21.44 | +61:05:27.6 | M1.5 V | Candidate | |
| 180 | | J01383+572 | Ross 10 | 63 | 01:38:21.23 | +57:13:51.4 | M2.5 V | Single | |
| 181 | | J01384+006 | GJ 3103 | 3103 | 01:38:30.49 | +00:39:08.4 | M2.0 V | Single | |
| 182 | 48 | J01390-179 | BL Cet | 65 A | 01:39:05.17 | -17:56:53.9 | M5.0 V | Multiple | 5 |
| 183 | 48 | | UV Cet | 65 B | 01:39:05.20 | -17:56:51.7 | M6.0 V | Multiple | 5 |
| 184 | 49 | J01395+050 | GJ 3104 | 3104 | 01:39:31.32 | +05:03:20.3 | M3.0 V | Multiple | |
| 185 | | J01402+317 | GJ 3105 | 3105 | 01:40:17.16 | +31:47:30.4 | M4.0 V | Candidate | |
| 186 | 50 | J01431+210 | RX J0143.1+2101 | | 01:43:11.75 | +21:01:10.4 | M4.0 V | Multiple | |
| 187 | | J01432+278 | GJ 3108 | 3108 | 01:43:16.64 | +27:50:31.1 | M0.0 V | Single | |
| 188 | | J01433+043 | GJ 70 | 70 | 01:43:19.73 | +04:19:05.7 | M2.0 V | Single | |
| 189 | 51 | J01437-060 | PM J01437-0602 | | 01:43:45.20 | -06:02:40.6 | M3.5 V | Multiple | A.4 |
| 190 | | J01449+163 | Wolf 1530 | 73 | 01:44:57.63 | +16:20:32.5 | M4.0 V | Single | |
| 191 | 52 | J01466-086 | GJ 3113 | 3113 | 01:46:37.29 | -08:39:00.5 | M4.0 V | Multiple | |
| 192 | 53 | J01453+465 | G 173-18 | | 01:45:18.81 | +46:32:11.3 | M2.0 V | Multiple | A.4 |
| 193 | | J01480+212 | Wolf 87 | 3114 | 01:48:04.37 | +21:12:20.8 | M2.5 V | Single | |
| 194 | | J01510-061 | GJ 3119 | 3119 | 01:51:04.69 | -06:07:09.3 | M4.5 V | Single | |
| 195 | | J01514+213 | Wolf 90 | 3120 | 01:51:24.17 | +21:23:33.9 | M4.0 V | Single | |
| 196 | 54 | | GJ 3118 | 3118 | 01:51:51.69 | +64:25:49.3 | DA5.6 | Multiple | A.9 |
| 197 | 54 | J01518+644 | GJ 3117 | 3117 | 01:51:51.72 | +64:26:02.8 | M2.5 V | Multiple | A.9 |
| 198 | | J01518-108 | Ross 555 | 78 | 01:51:49.30 | -10:48:21.1 | M2.0 V | Single | |
| 199 | 55 | J01531-210 | BD-21 332 | | 01:53:11.67 | -21:05:42.2 | M2.0 V | Multiple | A.4 |
| 200 | 56 | J01538-149 | PM J01538-1459A | | 01:53:50.97 | -14:59:51.5 | M3.0 V | Multiple | |
| 201 | 56 | | PM J01538-1459B | | 01:53:50.79 | -14:59:50.5 | M1.5 V | Multiple | |
| 202 | 57 | J01544+576 | IRXS J015426.6+574136 | | 01:54:28.04 | +57:41:27.7 | M3.5 V | Multiple | |
| 203 | 57 | | LSPM J0154+5741N | | 01:54:28.05 | +57:41:36.4 | M4.5 V | Multiple | |
| 204 | | J01550+379 | LSPM J0155+3758 | | 01:55:02.64 | +37:57:54.6 | M5.0 V | Candidate | |
| 205 | | J01556+028 | G 73-5 | | 01:55:36.98 | +02:52:53.8 | M1.5 V | Candidate | |
| 206 | 58 | J01567+305 | LP 296-57 | | 01:56:45.99 | +30:33:28.6 | M4.5 V | Multiple+ | 7 |
| 207 | 58 | | LP 296-56 | | 01:56:41.74 | +30:28:34.6 | M5.0 V | Multiple | A.2.7 |
| 208 | 59 | J01592+035E | GJ 1041 A | 1041 A | 01:59:12.66 | +03:31:09.6 | M2.5 V | Multiple | |
| 209 | 59 | J01592+035W | GJ 1041 B | 1041 B | 01:59:12.89 | +03:31:12.1 | M2.5 V | Multiple | A.4 |
| 210 | | J01593+585 | V596 Cas | 82 | 01:59:24.17 | +58:31:13.0 | M4.0 V | Single | |
| 211 | | J02000+437 | GJ 3123 | 3123 | 02:00:03.00 | +43:45:23.9 | M2.5 V | Single | |
| 212 | | J02001+366 | GJ 3124 | 3124 | 02:00:07.50 | +36:39:43.8 | M3.5 V | Single | |
| 213 | | J02002+130 | TZ Ari | 9066 | 02:00:14.16 | +13:02:38.7 | M3.5 V | Single | |
| 214 | | J02007-103 | GJ 3127 | 3127 | 02:00:46.86 | -10:21:26.6 | M3.5 V | Candidate | |
| 215 | | J02015+637 | GJ 3126 | 3126 | 02:01:34.72 | +63:46:10.5 | M3.0 V | Single | |
| 216 | 60 | J02019+735 | GJ 3125 | 3125 | 02:01:55.13 | +73:32:30.2 | M4.5 V | Multiple | |
| 217 | 60 | | Gaia DR3 55861149099229480 | | 02:01:55.18 | +73:32:30.4 | M5.5 V | Multiple | |
| 218 | 61 | | Wolf 109 | 9067 A | 02:02:02.81 | +03:56:20.0 | K5 V | Multiple | A.8 |
| 219 | 61 | J02020+039 | Wolf 109 B | 9067 B | 02:02:03.11 | +03:56:37.4 | M2.0 V | Multiple | A.8 |
| 220 | 61 | | Gaia DR3 2517912315149114240 | | 02:02:03.16 | +03:56:36.9 | M5.0 V | Multiple | A.8 |
| 221 | | J02022+103 | GJ 3128 | 3128 | 02:02:15.51 | +10:20:09.4 | M5.5 V | Single | |
| 222 | 62 | J02026+105 | PM J02024+1034B | | 02:02:28.15 | +10:34:51.9 | M4.5 V | Multiple | |
| 223 | 62 | | PM J02024+1034A | | 02:02:28.18 | +10:34:52.7 | M4.5 V | Multiple | A.2 |
| 224 | 63 | J02027+135 | GJ 3129 | 3129 | 02:02:44.86 | +13:34:31.9 | M4.5 V | Multiple | A.4 |
| 225 | | J02028+047 | RX J0202.8+0446 | | 02:02:52.00 | +04:47:00.4 | M3.5 V | Single | |
| 226 | 64 | J02033-212 | GJ 3131 | 3131 | 02:03:20.52 | -21:13:50.2 | M2.5 V | Multiple | A.4 A.10 |
| 227 | 64 | | GJ 3131 B | 3131 B | 02:03:20.25 | -21:13:51.5 | L0 | Multiple | A.10 |
| 228 | | J02044-018 | GJ 3132 | 3132 | 02:04:26.87 | -01:53:06.0 | M4.0 V | Single | |
| 229 | 65 | J02050-176 | GJ 84 | 84 | 02:05:06.31 | -17:36:55.5 | M2.5 V | Multiple | |
| 230 | | J02055+056 | Wolf 116 | | 02:05:30.35 | +05:41:43.0 | M1.0 V | Single | |
| 231 | 66 | J02069+451 | V374 And | 9071 A | 02:06:57.61 | +45:10:56.9 | M0.0 V | Multiple | A.4 |
| 232 | | J02070+496 | G 173-37 | | 02:07:04.24 | +49:38:36.6 | M3.5 V | Single | |
| 233 | | J02071+642 | GJ 3134 | 3134 | 02:07:10.89 | +64:17:08.7 | M4.0 V | Single | |
| 234 | | J02082+802 | G 242-81 | | 02:08:18.76 | +80:13:11.1 | M0.0 V | Single | |
| 235 | | J02088+494 | GJ 3136 | 3136 | 02:08:54.01 | +49:26:51.8 | M3.5 V | Candidate | |
| 236 | | J02096-143 | GJ 3139 | 3139 | 02:09:36.70 | -14:21:38.2 | M2.5 V | Single | |
| 237 | | J02116+185 | G 35-32 | | 02:11:41.19 | +18:33:42.3 | M3.0 V | Single | |
| 238 | | J02123+035 | Wolf 124 | 87 | 02:12:19.10 | +03:34:02.6 | M1.5 V | Single | |
| 239 | 67 | J02133+368 | IRXS J021320.6+364837 | | 02:13:20.68 | +36:48:51.6 | M4.5 V | Multiple | |
| 240 | | J02129+000 | GJ 3142 | 3142 | 02:12:55.22 | +00:00:17.3 | M4.0 V | Single | |
| 241 | | J02142-039 | LP 649-72 | | 02:14:13.11 | -03:57:46.1 | M5.5 V | Single | |
| 242 | | J02149+174 | GJ 1045 | 1045 | 02:15:00.20 | +17:25:00.8 | M4.0 V | Single | |
| 243 | | J02153+074 | Wolf 127 | | 02:15:22.39 | +07:29:32.5 | M1.5 V | Single | |
| 244 | | J02155+339 | GJ 3143 | 3143 | 02:15:34.63 | +33:57:35.0 | M3.5 V | Candidate | |

Table A.1: Complete sample studied in this work^a (cont.).

| Star id. | System id. | Karmn | Name | GJ | α (J2016.0) | δ (J2016.0) | Spectral type | Multiplicity type | In tables |
|----------|------------|-------------|-------------------------|--------|-----------------------|-----------------------|---------------|-------------------|-----------|
| 245 | | J02158-126 | GJ 3145 | 3145 | 02:15:49.43 | -12:40:24.2 | M3.5 V | Single | |
| 246 | | J02164+135 | GJ 3146 | 3146 | 02:16:30.40 | +13:35:05.9 | M5.5 V | Single | |
| 247 | | J02171+354 | GJ 3147 | 3147 | 02:17:10.74 | +35:26:28.4 | M5.0 V | Single | |
| 248 | | J02185+207 | G 35-39 | | 02:18:35.93 | +20:47:44.8 | M2.5 V | Single | |
| 249 | | J02186+123 | RX J0218.6+1219 | | 02:18:36.75 | +12:18:56.0 | M2.5 V | Single | |
| 250 | | J02190+238 | GJ 3150 | 3150 | 02:19:02.67 | +23:52:53.7 | M4.0 V | Single | |
| 251 | | J02190+353 | Ross 19 | 94 | 02:19:03.89 | +35:21:11.8 | M3.5 V | Single | A.11 |
| 252 | 68 | J02204+377 | GJ 3151 | 3151 | 02:20:25.74 | +37:47:29.6 | M2.5 V | Multiple | A.9 |
| 253 | | J02207+029 | GJ 3153 | 3153 | 02:20:46.42 | +02:58:32.9 | M4.5 V | Single | |
| 254 | 69 | J02210+368 | GJ 1047 A | 1047 A | 02:21:05.05 | +36:52:55.2 | M3.0 V | Multiple | |
| 255 | 69 | | GJ 1047 B | 1047 B | 02:21:05.01 | +36:52:56.4 | M4.5 V | Multiple | |
| 256 | 69 | | GJ 1047 C | 1047 C | 02:21:02.88 | +36:52:38.6 | M3.5 V | Multiple | |
| 257 | | J02222+478 | GJ 96 | 96 | 02:22:14.99 | +47:52:48.8 | M0.5 V | Single | |
| 258 | | J02230+181 | StKM 1-261 | | 02:23:06.15 | +18:10:31.6 | M0.5 V | Candidate | |
| 259 | | J02234+227 | LP 353-51 | | 02:23:26.76 | +22:44:05.0 | M0.5 V | Single | |
| 260 | | J02247+259 | GJ 3156 | 3156 | 02:24:46.00 | +25:58:31.5 | M0.5 V | Single | |
| 261 | | J02254+246 | StKM 1-265 | | 02:25:28.00 | +24:40:36.9 | M2.0 V | Single | |
| 262 | | J02256+375 | GJ 3157 | 3157 | 02:25:38.83 | +37:32:32.8 | M4.0 V | Single | |
| 263 | 70 | J02272+545 | IRXS J022716.4+543258 | | 02:27:17.31 | +54:32:46.1 | M4.5 V | Multiple | |
| 264 | | J02274+031 | PM J02274+0310 | | 02:27:27.43 | +03:10:54.7 | M4.0 V | Candidate | |
| 265 | 71 | J02277+044 | HD 15285 | 98 | 02:27:46.05 | +04:25:58.8 | M1.0 V | Multiple | |
| 266 | | J02282+014 | GJ 3159 | 3159 | 02:28:17.41 | +01:26:29.0 | M3.0 V | Single | |
| 267 | | J02283+219 | TYC 1221-1171-1 | | 02:28:22.17 | +21:59:45.3 | M0.5 V | Candidate | |
| 268 | 72 | J02285-200 | HD 15468 | 100 B | 02:29:02.40 | -19:58:40.8 | K4.5 V | Multiple | A.8 |
| 269 | 72 | J02287+156 | GJ 100 C | 100 C | 02:28:32.62 | -20:02:22.5 | M2.5 V | Multiple | A.8 |
| 270 | 73 | J02287+156 | LSPM J0228+1538 | | 02:28:47.15 | +15:38:53.6 | M2.0 V | Multiple | |
| 271 | 73 | | StKM 2-212B | | 02:28:47.18 | +15:38:52.9 | M4.0 V | Multiple | |
| 272 | 74 | J02289+120 | GJ 3160 | 3160 | 02:28:54.68 | +12:05:22.3 | M2.0 V | Multiple | A.4 |
| 273 | 75 | J02289+226 | StKM 2-213A | | 02:28:58.41 | +22:36:24.5 | M2.0 V | Multiple | |
| 274 | 75 | | StKM 2-213B | | 02:28:58.52 | +22:36:21.9 | M0.5 V | Multiple | |
| 275 | | J02292+195 | LP 410-33 | | 02:29:14.32 | +19:32:31.9 | M2.5 V | Candidate | |
| 276 | | J02293+884 | GJ 3137 | 3137 | 02:29:14.09 | +88:24:20.3 | M3.5 V | Single | |
| 277 | | J02314+573 | Ross 21 | 101 | 02:31:29.87 | +57:22:43.3 | M3.5 V | Single | |
| 278 | | J02330+078 | LP 530-26 | | 02:33:04.78 | +07:49:41.0 | M2.0 V | Candidate | |
| 279 | | J02336+249 | GJ 102 | 102 | 02:33:37.23 | +24:55:26.9 | M4.0 V | Single | |
| 280 | | J02337+150 | GJ 3165 | 3165 | 02:33:47.96 | +15:00:17.8 | M3.0 V | Single | |
| 281 | | J02340+417 | GJ 3164 | 3164 | 02:34:00.46 | +41:46:50.4 | M3.0 V | Single | |
| 282 | | J02345+566 | G 174-4 | | 02:34:34.87 | +56:36:42.1 | M2.0 V | Single | |
| 283 | | J02353+235 | GJ 3166 | 3166 | 02:35:22.50 | +23:34:29.5 | M3.5 V | Candidate | |
| 284 | | J02358+202 | GJ 104 | 104 | 02:35:53.59 | +20:13:09.3 | M2.0 V | Single | |
| 285 | 76 | | HD 16160 | 105 A | 02:36:06.81 | +06:53:36.0 | K3 V | Multiple | A.8 |
| 286 | 76 | J02362+068 | BX Cet | 105 B | 02:36:17.20 | +06:52:41.1 | M4.0 V | Multiple | A.8 |
| 287 | | J02364+554 | GJ 3168 | 3168 | 02:36:26.63 | +55:28:30.2 | M3.0 V | Candidate | |
| 288 | | J02367+226 | G 36-26 | | 02:36:44.08 | +22:40:20.2 | M5.0 V | Candidate | |
| 289 | 77 | J02367+320 | GJ 3169 | 3169 | 02:36:47.30 | +32:04:18.9 | M3.5 V | Multiple | |
| 290 | 77 | | GJ 3170 | 3170 | 02:36:47.44 | +32:04:20.0 | M3.0 V | Multiple | |
| 291 | | J02392+074 | GJ 3174 | 3174 | 02:39:17.85 | +07:28:14.9 | M4.0 V | Single | |
| 292 | | J02412-045 | G 75-35 | | 02:41:15.51 | -04:32:18.8 | M4.5 V | Single | |
| 293 | | J02419+435 | StKM 1-291 | | 02:41:58.94 | +43:34:19.0 | M1.0 V | Candidate | |
| 294 | | J02424+182 | LP 410-81 | | 02:42:25.80 | +18:14:44.0 | M1.5 V | Single | |
| 295 | | J02438-088 | Wolf 1132 | 1051 | 02:43:53.88 | -08:49:57.8 | M1.5 V | Single | |
| 296 | 78 | | HD 16895 | 107 A | 02:44:12.53 | +49:13:41.0 | F8 V | Multiple+ | A.8 |
| 297 | 78 | J02441+492 | GJ 107 B | 107 B | 02:44:10.79 | +49:13:53.0 | M1.5 V | Multiple | A.8 |
| 298 | | J02442+255 | VX Ari | 109 | 02:44:16.53 | +25:31:18.3 | M3.0 V | Single | |
| 299 | 79 | J02443+109W | MCC 401 | | 02:44:21.45 | +10:57:40.2 | M1.0 V | Multiple | |
| 300 | 79 | J02443+109E | 2MASS J02442272+1057349 | | 02:44:22.81 | +10:57:34.2 | M5.0 V | Multiple | |
| 301 | 80 | J02456+449 | GJ 3178 | 3178 | 02:45:40.30 | +44:56:53.5 | M0.5 V | Multiple | |
| 302 | 80 | | GJ 3179 | 3179 | 02:45:41.85 | +44:57:00.8 | M5.0 V | Multiple | |
| 303 | | J02462-049 | GJ 3180 | 3180 | 02:46:16.73 | -04:59:50.7 | M6.0 V | Single | |
| 304 | | J02465+164 | GJ 3181 | 3181 | 02:46:33.79 | +16:25:01.1 | M6.0 V | Single | |
| 305 | | J02486+621 | 2MASS J02483695+6211228 | | 02:48:37.25 | +62:11:21.3 | M5.5 V | Single | |
| 306 | 81 | J02489-145W | PM J02489-1432W | | 02:48:59.45 | -14:32:14.2 | M2.0 V | Multiple | A.11 |
| 307 | 81 | J02489-145E | PM J02489-1432E | | 02:49:00.02 | -14:32:15.5 | M2.5 V | Multiple | |
| 308 | | J02502+628 | G 246-12 | | 02:50:16.95 | +62:51:16.4 | M2.5 V | Single | |
| 309 | | J02518+062 | GJ 3184 | 3184 | 02:51:51.15 | +06:13:39.6 | M3.0 V | Single | |
| 310 | 82 | J02518+294 | GJ 3183 | 3183 | 02:51:49.63 | +29:29:10.4 | M4.0 V | Multiple | |
| 311 | | J02519+224 | RBS 365 | | 02:51:54.22 | +22:27:28.2 | M4.0 V | Single | |
| 312 | | J02524+269 | GJ 3186 | 3186 | 02:52:25.03 | +26:58:26.2 | M1.0 V | Single | |
| 313 | | J02530+168 | Teegarden's Star | | 02:53:04.71 | +16:51:51.7 | M7.0 V | Single | A.11 |
| 314 | | J02534+174 | LP 411-18 | | 02:53:26.14 | +17:24:28.4 | M3.5 V | Candidate | |
| 315 | 83 | | HD 18143A | 9105 A | 02:55:39.38 | +26:52:20.5 | K2 IV | Multiple | A.8 A.11 |
| 316 | 83 | | HD 18143B | 9105 B | 02:55:39.14 | +26:52:16.9 | K7 V | Multiple | A.8 |
| 317 | 83 | J02555+268 | HD 18143C | 9105 C | 02:55:36.11 | +26:52:17.6 | M4.0 V | Multiple | A.8 |
| 318 | | J02560-006 | LP 591-156 | | 02:56:04.17 | -00:36:32.0 | M5.0 V | Single | |
| 319 | 84 | J02562+239 | LSPM J0256+2359 | | 02:56:14.06 | +23:59:07.4 | M5.0 V | Multiple | |
| 320 | 85 | J02565+554W | Ross 364 | 119 A | 02:56:35.79 | +55:26:06.8 | M1.0 V | Multiple | |
| 321 | 85 | J02565+554E | Ross 365 | 119 B | 02:56:36.49 | +55:26:22.3 | M3.0 V | Multiple | |
| 322 | | J02573+765 | LP 14-53 | | 02:57:21.43 | +76:33:04.9 | M4.0 V | Single | A.11 |
| 323 | | J02575+107 | Ross 791 | 120 | 02:57:32.96 | +10:47:17.9 | M3.0 V | Single | |
| 324 | | J02581-128 | GJ 3189 | 3189 | 02:58:10.53 | -12:52:57.4 | M2.5 V | Single | |
| 325 | 86 | J02591+366 | Ross 331 | 3190 | 02:59:11.44 | +36:36:35.7 | M3.5 V | Multiple | |
| 326 | 86 | | Ross 331B | | 02:59:11.45 | +36:36:37.6 | M6.0 V | Multiple | |

Table A.1: Complete sample studied in this work^a (cont.).

| Star id. | System id. | Karmn | Name | GJ | α (J2016.0) | δ (J2016.0) | Spectral type | Multiplicity type | In tables |
|----------|------------|-------------|-----------------------------|--------|-----------------------|-----------------------|---------------|-------------------|-----------|
| 327 | | J02592+317 | GJ 3191 | 3191 | 02:59:16.77 | +31:46:27.8 | M3.5 V | Single | |
| 328 | 87 | J02597+389 | G 134–63 | | 02:59:46.67 | +38:55:34.6 | M4.5 V | Multiple | |
| 329 | 88 | J03018–165S | GJ 3193 | 3193 | 03:01:50.98 | -16:35:40.3 | M3.5 V | Multiple | A.11 |
| 330 | 88 | J03018–165N | GJ 3192 | 3192 | 03:01:50.63 | -16:35:35.2 | M3.0 V | Multiple | |
| 331 | | J03026–181 | GJ 9108 | 9108 | 03:02:38.51 | -18:09:56.1 | M2.5 V | Candidate | |
| 332 | | J03033–080 | StM 20 | | 03:03:21.47 | -08:05:16.0 | M3.0 V | Candidate | |
| 333 | 89 | J03037–128 | GJ 3197 | 3197 | 03:03:48.10 | -12:51:21.0 | M3.0 V | Multiple+ | |
| 334 | 89 | J03036–128 | GJ 3196 | 3196 | 03:03:40.99 | -12:50:33.7 | M3.0 V | Multiple | |
| 335 | | J03040–203 | GJ 3198 | 3198 | 03:04:05.05 | -20:22:50.7 | M3.5 V | Single | |
| 336 | 90 | | HD 18757 | 3194 | 03:04:11.26 | +61:42:09.9 | G1.5 V | Multiple | A.8 |
| 337 | 90 | J03047+617 | GJ 3195 | 3195 | 03:04:45.06 | +61:43:57.7 | M3.0 V | Multiple | A.8 |
| 338 | 91 | J03075–039 | GJ 3202 | 3202 | 03:07:33.51 | -03:58:23.2 | M0.0 V | Multiple | |
| 339 | | J03077+249 | LP 355–27 | | 03:07:47.13 | +24:57:53.3 | M4.5 V | Single | |
| 340 | | J03090+100 | GJ 1055 | 1055 | 03:09:00.48 | +10:01:16.3 | M5.0 V | Single | |
| 341 | 92 | J03095+457 | GJ 125 | 125 | 03:09:30.17 | +45:43:52.7 | M2.0 V | Multiple | |
| 342 | | J03102+059 | EK Cet | 3205 | 03:10:15.34 | +05:54:22.5 | M2.0 V | Single | |
| 343 | | J03104+584 | GJ 3204 | 3204 | 03:10:26.72 | +58:26:05.5 | M1.0 V | Single | |
| 344 | | J03109+737 | GJ 1053 | 1053 | 03:11:05.27 | +73:46:02.5 | M5.0 V | Single | |
| 345 | | J03110–046 | LP 652–62 | | 03:11:04.90 | -04:36:41.1 | M3.0 V | Single | |
| 346 | | J03112+011 | IRXS J031114.2+010655 | | 03:11:15.60 | +01:06:30.6 | M5.5 V | Single | |
| 347 | | J03118+196 | Wolf 132 | | 03:11:48.26 | +19:40:11.3 | M0.5 V | Candidate | |
| 348 | 93 | J03119+615 | GJ 3206 | 3206 | 03:11:56.89 | +61:31:14.6 | M0.0 V | Multiple | |
| 349 | | J03133+047 | CD Cet | 1057 | 03:13:24.78 | +04:46:30.7 | M5.0 V | Single | A.11 |
| 350 | | J03136+653 | LP 53–55 | | 03:13:37.88 | +65:21:19.5 | M1.5 V | Single | |
| 351 | | J03142+286 | GJ 3208 | 3208 | 03:14:12.85 | +28:40:27.6 | M6.0 V | Single | |
| 352 | 94 | J03145+594 | Ross 369A | | 03:14:33.17 | +59:26:13.8 | M2.5 V | Multiple | |
| 353 | 94 | | Ross 369B | | 03:14:33.10 | +59:26:13.2 | M3.0 V | Multiple | |
| 354 | | J03147+114 | RX J0314.7+1127 | | 03:14:47.26 | +11:27:26.7 | M2.0 V | Candidate | |
| 355 | | J03147+485 | Ross 346 | 3209 | 03:14:45.11 | +48:31:05.5 | M1.0 V | Candidate | |
| 356 | 95 | J03162+581S | Ross 370A | 9113 A | 03:16:14.73 | +58:09:57.3 | M2.0 V | Multiple | |
| 357 | 95 | J03162+581N | Ross 370B | 9113 B | 03:16:14.75 | +58:10:02.4 | M2.0 V | Multiple | |
| 358 | | J03167+389 | PM J03167+3855 | | 03:16:46.02 | +38:55:27.7 | M3.5 V | Candidate | |
| 359 | 96 | J03172+453 | GJ 3213 | 3213 | 03:17:11.82 | +45:22:20.9 | M3.0 V | Multiple | |
| 360 | | J03177+252 | GJ 3215 | 3215 | 03:17:46.17 | +25:15:00.6 | M2.5 V | Single | |
| 361 | | J03181+382 | HD 275122 | 134 | 03:18:08.09 | +38:14:58.3 | M1.5 V | Single | |
| 362 | | J03181+426 | Wolf 140 | | 03:18:07.31 | +42:40:06.8 | M3.5 V | Single | |
| 363 | | J03185+103 | StKM 1–354 | | 03:18:35.36 | +10:18:43.2 | M1.5 V | Single | |
| 364 | | J03186+326 | GJ 3216 | 3216 | 03:18:38.59 | +32:39:55.3 | M0.0 V | Single | |
| 365 | | J03187+606 | Ross 371 | 3214 | 03:18:43.66 | +60:36:21.1 | M3.0 V | Candidate | |
| 366 | 97 | J03194+619 | G 246–33 | | 03:19:29.28 | +61:56:01.5 | M4.0 V | Multiple | |
| 367 | 98 | J03207+397 | LP 198–637 A | | 03:20:45.42 | +39:42:59.3 | M1.5 V | Multiple | |
| 368 | 98 | | LP 198–637 B | | 03:20:45.35 | +39:42:59.6 | M1.5 V | Multiple | A.2 |
| 369 | | J03213+799 | GJ 133 | 133 | 03:21:24.29 | +79:58:06.8 | M2.0 V | Single | |
| 370 | | J03217–066 | GJ 3218 | 3218 | 03:21:47.27 | -06:40:25.0 | M2.0 V | Single | |
| 371 | | J03220+029 | GJ 1058 | 1058 | 03:22:04.46 | +02:56:22.7 | M4.5 V | Single | |
| 372 | | J03224+271 | GJ 3219 | 3219 | 03:22:28.40 | +27:09:20.8 | M0.0 V | Single | |
| 373 | | J03230+420 | GJ 1059 | 1059 | 03:23:02.16 | +42:00:15.8 | M5.0 V | Single | |
| 374 | | J03233+116 | GJ 3221 | 3221 | 03:23:22.15 | +11:41:11.0 | M2.5 V | Single | |
| 375 | | J03236+056 | IRXS J032338.7+054117 | | 03:23:39.25 | +05:41:14.1 | M4.5 V | Single | |
| 376 | 99 | J03241+237 | GJ 140 A | 140 A | 03:24:06.73 | +23:47:04.2 | M1.5 V | Multiple | |
| 377 | 99 | | GJ 140 B | 140 B | 03:24:06.67 | +23:47:06.6 | M3.0 V | Multiple | |
| 378 | 99 | J03242+237 | GJ 140 C | 140 C | 03:24:13.10 | +23:46:17.3 | M2.0 V | Multiple | |
| 379 | 100 | J03247+4447 | PM J03247+4447A | | 03:24:42.31 | +44:47:41.4 | M1.5 V | Multiple | |
| 380 | 100 | | PM J03247+4447B | | 03:24:42.23 | +44:47:39.7 | M3.5 V | Multiple | A.2 |
| 381 | 101 | J03257+058 | GJ 3224 | 3224 | 03:25:42.04 | +05:51:48.2 | M4.5 V | Multiple | |
| 382 | 102 | J03263+171 | PM J03263+1709 | | 03:26:23.74 | +17:09:30.1 | M4.0 V | Multiple | |
| 383 | | J03267+192 | GJ 3225 | 3225 | 03:26:44.97 | +19:14:37.7 | M4.5 V | Candidate | |
| 384 | | J03272+273 | CK Ari | | 03:27:14.22 | +27:23:07.8 | M1.0 V | Single | |
| 385 | | J03275+222 | ATO J051.8788+22.2102 | | 03:27:30.94 | +22:12:36.9 | M4.5 V | Single | |
| 386 | 103 | J03284+352 | LSPM J0328+3515A | | 03:28:29.35 | +35:15:18.6 | M2.0 V | Multiple | |
| 387 | 103 | | LSPM J0328+3515B | | 03:28:29.32 | +35:15:17.4 | M1.5 V | Multiple | |
| 388 | 104 | J03286–156 | GJ 3228 | 3228 | 03:28:39.18 | -15:37:16.4 | M3.5 V | Multiple+ | |
| 389 | 104 | | GJ 3229 | 3229 | 03:28:39.36 | -15:37:32.6 | M3.5 V | Multiple | |
| 390 | 105 | J03303+346 | IRXS J033021.4+344044 | | 03:30:23.37 | +34:40:31.7 | M4.0 V | Multiple | |
| 391 | 105 | | Gaia DR3 221088045766546816 | | 03:30:16.90 | +34:39:50.2 | M1.5 V | Multiple | |
| 392 | 105 | | Gaia DR3 221088050062935680 | | 03:30:16.80 | +34:39:49.2 | M3.0 V | Multiple | |
| 393 | | J03288+264 | GJ 3227 | 3227 | 03:28:49.84 | +26:29:10.2 | M3.0 V | Single | |
| 394 | | J03308+542 | LSPM J0330+5413 | | 03:30:48.61 | +54:13:55.1 | M5.0 V | Single | |
| 395 | 106 | J03309+706 | LP 31–368 | | 03:30:56.01 | +70:41:06.4 | M3.5 V | Multiple | |
| 396 | | J03317+143 | GJ 143.3 | 143.3 | 03:31:47.18 | +14:19:07.0 | M2.0 V | Single | |
| 397 | 107 | J03325+287 | RX J0332.6+2843 | | 03:32:35.85 | +28:43:54.1 | M4.5 V | Multiple | |
| 398 | 108 | | V577 Per | | 03:33:13.60 | +46:15:23.7 | K2 V | Multiple | A.8 |
| 399 | 108 | J03332+462 | HD 21845B | | 03:33:14.16 | +46:15:16.2 | M0.0 V | Multiple | A.8 |
| 400 | | J03340+585 | Ross 563 | | 03:34:01.11 | +58:35:52.3 | M0.5 V | Candidate | |
| 401 | 109 | J03346–048 | GJ 3235 | 3235 | 03:34:40.07 | -04:50:38.5 | M3.5 V | Multiple | A.4 |
| 402 | | J03361+313 | IRXS J033609.2+311853 | | 03:36:08.85 | +31:18:37.4 | M4.5 V | Single | |
| 403 | | J03366+034 | GJ 3237 | 3237 | 03:36:40.97 | +03:29:17.6 | M4.5 V | Candidate | |
| 404 | 110 | J03372+691 | GJ 3236 | 3236 | 03:37:14.55 | +69:10:47.9 | M3.5 V | Multiple | A.4 A.5 |
| 405 | 111 | J03375+178N | GJ 3239 | 3239 | 03:37:33.54 | +17:51:14.1 | M2.5 V | Multiple | A.4 |
| 406 | 111 | J03375+178S | GJ 3240 | 3240 | 03:37:34.09 | +17:51:00.0 | M3.5 V | Multiple | A.4 |
| 407 | | J03394+249 | KP Tau | 3241 | 03:39:29.85 | +24:58:05.7 | M3.0 V | Single | |
| 408 | 112 | J03396+254E | Wolf 204 | 3242 | 03:39:36.47 | +25:28:11.6 | M3.0 V | Multiple | |

Table A.1: Complete sample studied in this work^a (cont.).

| Star id. | System id. | Karmn | Name | GJ | α (J2016.0) | δ (J2016.0) | Spectral type | Multiplicity type | In tables |
|----------|------------|-------------|-------------------------------|---------|-----------------------|-----------------------|---------------|-------------------|--------------|
| 409 | 112 | J03396+254W | Wolf 205 | 9120 | 03:39:40.77 | +25:28:39.1 | M3.5 V | Multiple | |
| 410 | 113 | | HD 278874 | 9119 A | 03:39:48.92 | +33:28:24.3 | K2 V | Multiple | A.4 A.8 |
| 411 | 113 | J03397+334 | HD 278874B | 9119 B | 03:39:47.79 | +33:28:30.7 | M3.0 V | Multiple | A.8 |
| 412 | | J03416+552 | TYC 3720-426-1 | | 03:41:37.46 | +55:13:05.0 | M0.0 V | Single | |
| 413 | 114 | J03430+459 | LSPM J0343+4554A | | 03:43:01.79 | +45:54:17.4 | M4.0 V | Multiple | |
| 414 | 114 | | LSPM J0343+4554B | | 03:43:01.72 | +45:54:17.9 | M4.5 V | Multiple | |
| 415 | | J03433-095 | GJ 3247 | 3247 | 03:43:22.53 | -09:33:46.1 | M4.5 V | Candidate | |
| 416 | 115 | J03438+166 | GJ 150.1 A | 150.1 A | 03:43:52.74 | +16:40:14.2 | M0.0 V | Multiple | |
| 417 | 115 | J03437+166 | GJ 150.1 B | 150.1 B | 03:43:45.42 | +16:39:57.2 | M1.0 V | Multiple | |
| 418 | | J03445+349 | HD 278968 | | 03:44:31.21 | +34:58:20.8 | M0.0 V | Single | |
| 419 | 116 | J03454+729 | G 221-21 | | 03:45:28.68 | +72:59:25.2 | M1.5 V | Multiple | A.7 |
| 420 | 116 | | LP 31-200 | | 03:43:44.04 | +72:53:42.2 | M3.5 V | Multiple | A.7 |
| 421 | | J03455+703 | PM J03455+7018 | | 03:45:32.34 | +70:18:00.4 | M1.0 V | Single | |
| 422 | | J03459+147 | G 6-33 | | 03:45:54.96 | +14:42:47.2 | M1.5 V | Single | |
| 423 | | J03463+262 | HD 23453 | 154 | 03:46:20.60 | +26:12:52.7 | M0.0 V | Single | |
| 424 | | J03467+821 | TYC 4521-1342-1 | | 03:46:42.67 | +82:07:50.1 | M1.0 V | Single | |
| 425 | | J03467-112 | GJ 3249 | 3249 | 03:46:46.04 | -11:17:40.5 | M2.5 V | Candidate | |
| 426 | | J03473+086 | GJ 3250 | 3250 | 03:47:21.40 | +08:41:36.7 | M4.5 V | Single | |
| 427 | | J03473-019 | G 80-21 | | 03:47:23.53 | -01:58:24.3 | M3.0 V | Single | |
| 428 | | J03479+027 | Ross 588 | 9133 | 03:47:57.68 | +02:47:09.3 | M0.5 V | Single | |
| 429 | 117 | | HD 23189 | 153 A | 03:48:01.40 | +68:40:26.4 | K2 V | Multiple | A.8 |
| 430 | 117 | J03480+686 | GJ 153 C | 153 C | 03:48:02.08 | +68:40:42.9 | M1.5 V | Multiple | A.8 |
| 431 | | J03486+735 | GJ 3248 | 3248 | 03:48:39.73 | +73:32:30.9 | M1.0 V | Single | |
| 432 | | J03505+634 | GJ 3251 | 3251 | 03:50:33.69 | +63:27:14.9 | M1.5 V | Single | |
| 433 | | J03507-060 | GJ 1065 | 1065 | 03:50:43.81 | -06:06:03.6 | M3.0 V | Single | |
| 434 | 118 | J03510+142 | PM J03510+1413 | | 03:51:00.87 | +14:13:38.7 | M4.5 V | Multiple+ | |
| 435 | 118 | | UPM J0350+1414 | | 03:50:59.58 | +14:14:00.5 | M3.5 V | Multiple+ | |
| 436 | | J03510-008 | GJ 3252 | 3252 | 03:51:00.04 | -00:52:52.4 | M6.0 V | Single | |
| 437 | 119 | | HD 275867 | | 03:52:00.35 | +39:47:43.7 | K2 V | Multiple | A.8 |
| 438 | 119 | J03519+397 | TYC 2868-639-1 | | 03:51:58.19 | +39:46:55.8 | M0.0 V | Multiple+ | A.8 |
| 439 | 120 | J03526+170 | Wolf 227 | 3253 | 03:52:42.24 | +17:00:53.8 | M4.5 V | Multiple | A.4 |
| 440 | | J03531+625 | Ross 567 | | 03:53:10.51 | +62:34:03.8 | M3.0 V | Single | |
| 441 | | J03543-146 | 2MASS J03542008-1437388 | | 03:54:20.02 | -14:37:37.2 | M6.5 V | Candidate | |
| 442 | 121 | J03544-091 | GJ 3256 | 3256 | 03:54:25.52 | -09:09:29.2 | M1.0 V | Multiple | |
| 443 | 121 | | GJ 3256 B | 3256 B | 03:54:25.61 | -09:09:32.0 | M3.0 V | Multiple | |
| 444 | | J03548+163 | LP 413-108 | | 03:54:53.37 | +16:18:55.9 | M4.0 V | Candidate | |
| 445 | | J03565+319 | IRXS J035632.5+315746 | | 03:56:33.26 | +31:57:23.8 | M3.5 V | Candidate | |
| 446 | | J03567+039 | Ross 23 | 9138 | 03:56:47.95 | +53:33:30.5 | M1.5 V | Single | |
| 447 | 122 | | HD 24916 | 157 A | 03:57:28.50 | -01:09:36.4 | K4 V | Multiple | A.8 |
| 448 | 122 | J03574-011 | HD 24916B | 157 C | 03:57:28.68 | -01:09:25.7 | M2.5 V | Multiple | A.4 A.8 |
| 449 | | J03586+520 | Ross 24 | | 03:58:36.92 | +52:01:21.7 | M1.0 V | Single | |
| 450 | | J03588+125 | G 7-14 | | 03:58:49.38 | +12:30:18.3 | M4.0 V | Single | |
| 451 | | J03598+260 | Wolf 1322 | 9140 | 03:59:54.53 | +26:05:19.5 | M3.0 V | Candidate | |
| 452 | 123 | | LSPM J0401+5131 | | 04:01:02.14 | +51:31:17.2 | DC8 | Multiple | A.7 A.9 |
| 453 | 123 | J04011+513 | Ross 25 | 9141 | 04:01:08.18 | +51:23:06.4 | M3.5 V | Multiple | A.7 A.9 |
| 454 | 124 | J04056+057 | GJ 3261 | 3261 | 04:05:38.94 | +05:44:40.4 | M3.5 V | Multiple | A.7 |
| 455 | 124 | | Gaia DR 3 3296932486866670720 | | 04:05:38.89 | +05:44:40.1 | M4.0 V | Multiple | A.2 A.7 |
| 456 | 124 | | V1221 Tau | | 04:05:53.46 | +05:31:24.6 | M3.0 V | Multiple | A.3 A.7 |
| 457 | 125 | J04059+712E | LP 31-301 | | 04:05:58.09 | +71:16:34.7 | M4.0 V | Multiple | |
| 458 | 125 | J04059+712W | LP 31-302 A | | 04:05:57.21 | +71:16:32.4 | M5.0 V | Multiple | |
| 459 | 125 | | LP 31-302 B | | 04:05:57.02 | +71:16:31.9 | M6.0 V | Multiple | |
| 460 | | J04061-055 | PM J04061-0534 | | 04:06:06.90 | -05:34:46.9 | M3.5 V | Single | |
| 461 | 126 | J04077+142 | LP 474-123 | | 04:07:44.14 | +14:13:22.1 | M0.0 V | Multiple | |
| 462 | 126 | J04079+142 | LP 474-124 | | 04:07:54.99 | +14:12:58.2 | M2.5 V | Multiple | |
| 463 | | J04081+743 | LP 32-16 | | 04:08:13.87 | +74:22:51.6 | M3.5 V | Single | |
| 464 | | J04083+691 | LP 31-433 | | 04:08:24.60 | +69:10:57.9 | M4.5 V | Candidate | |
| 465 | 127 | J04086+336 | HD 281621 | 162 | 04:08:38.07 | +33:38:15.3 | M0.5 V | Multiple | |
| 466 | 128 | J04093+057 | LP 534-29 | | 04:09:22.50 | +05:46:25.2 | M4.5 V | Multiple | |
| 467 | 129 | J04108-128 | LP 714-37 | | 04:10:47.88 | -12:51:48.4 | M5.5 V | Multiple | |
| 468 | 129 | | LP 714-37 B | | 04:10:47.98 | -12:51:49.4 | M6.5 V | Multiple | |
| 469 | | J04112+495 | Ross 27 | 3265 | 04:11:13.29 | +49:31:45.0 | M3.5 V | Single | |
| 470 | | J04122+647 | GJ 3266 | 3266 | 04:12:18.25 | +64:43:48.7 | M4.0 V | Single | |
| 471 | 130 | J04123+162 | LP 414-117 | | 04:12:21.90 | +16:15:02.9 | M4.0 V | Multiple | A.4 A.7 |
| 472 | 130 | | LSPM J0409+1622 | | 04:09:57.30 | +16:22:41.3 | M5.5 V | Multiple | A.7 |
| 473 | 131 | J04129+526 | Ross 28 | 164 B | 04:12:58.22 | +52:36:28.9 | M4.5 V | Multiple | |
| 474 | 132 | J04131+505 | Ross 29A | | 04:13:09.43 | +50:31:38.0 | M4.0 V | Multiple | |
| 475 | 132 | | Ross 29B | | 04:13:09.56 | +50:31:39.1 | M4.5 V | Multiple | |
| 476 | | J04137+476 | LSPM J0413+4737E | | 04:13:47.70 | +47:37:42.5 | M2.5 V | Single | |
| 477 | | J04139+829 | GJ 3262 | 3262 | 04:13:56.69 | +82:55:03.0 | M0.0 V | Candidate | |
| 478 | | J04148+277 | G 39-3 | | 04:14:53.80 | +27:45:26.0 | M3.5 V | Single | |
| 479 | 133 | | σ^2 Eri B | 166 B | 04:15:19.39 | -07:40:22.6 | DA2.9 | Multiple | A.8 A.9 |
| 480 | 133 | | σ^2 Eri | 166 A | 04:15:13.91 | -07:40:05.1 | K0 V | Multiple | A.8 A.9 A.11 |
| 481 | 133 | J04153-076 | σ^2 Eri C | 166 C | 04:15:19.12 | -07:40:15.3 | M4.5 V | Multiple | A.8 A.9 |
| 482 | 134 | J04166-125 | GJ 2033 A | 2033 A | 04:16:41.59 | -12:33:19.3 | M1.0 V | Multiple | |
| 483 | 134 | | GJ 2033 B | 2033 B | 04:16:41.80 | -12:33:19.8 | M2.5 V | Multiple | A.2 |
| 484 | | J04167-120 | LP 714-47 | | 04:16:45.65 | -12:05:05.6 | M0.0 V | Single | A.11 |
| 485 | | J04173+088 | GJ 3270 | 3270 | 04:17:18.68 | +08:49:16.0 | M4.5 V | Candidate | |
| 486 | 135 | J04177+410 | LSPM J0417+4103A | | 04:17:44.44 | +41:03:10.1 | M3.5 V | Multiple | |
| 487 | 135 | | LSPM J0417+4103B | | 04:17:44.24 | +41:03:09.2 | M4.5 V | Multiple | |
| 488 | | J04188+013 | HIP 20122 | | 04:18:51.45 | +01:23:35.0 | M2.0 V | Candidate | |
| 489 | | J04191+097 | UPM J0419+0944 | | 04:19:08.15 | +09:44:50.2 | M3.0 V | Single | |
| 490 | | J04191-074 | LP 654-39 | | 04:19:06.41 | -07:27:43.6 | M3.5 V | Single | |

Table A.1: Complete sample studied in this work^a (cont.).

| Star id. | System id. | Karmn | Name | GJ | α (J2016.0) | δ (J2016.0) | Spectral type | Multiplicity type | In tables |
|----------|------------|--------------|-----------------------|---------|-----------------------|-----------------------|---------------|-------------------|-----------|
| 491 | | J04198+425 | LSPM J0419+4233 | | 04:19:52.90 | +42:33:07.4 | M8.5 V | Single | |
| 492 | | J04199+364 | Ross 592 | | 04:19:59.96 | +36:29:04.1 | M1.5 V | Single | |
| 493 | | J04205+815 | PM J04205+8131 | | 04:20:34.24 | +81:31:54.4 | M3.0 V | Candidate | |
| 494 | | J04206+272 | XEST 16–045 | | 04:20:39.20 | +27:17:31.4 | M4.5 V | Candidate | |
| 495 | 136 | J04207+152 | LP 415–363 | | 04:20:48.16 | +15:14:08.2 | M4.0 V | Multiple | |
| 496 | | J04218+213 | GJ 3274 | 3274 | 04:21:50.22 | +21:19:39.2 | M3.5 V | Single | |
| 497 | | J04219+751 | GJ 3271 | 3271 | 04:21:59.86 | +75:08:20.5 | M2.5 V | Single | |
| 498 | | J04221+192 | GJ 3275 | 3275 | 04:22:08.13 | +19:15:21.4 | M3.0 V | Single | |
| 499 | 137 | TYC 78–257–1 | | | 04:21:04.26 | +03:16:07.9 | K3.0 V | Multiple | A.7 A.8 |
| 500 | 137 | J04224+036 | RX J0422.4+0337 | | 04:22:25.19 | +03:37:08.5 | M3.5 V | Multiple+ | A.7 A.8 |
| 501 | | J04224+740 | LP 31–339 | | 04:22:28.52 | +74:01:21.5 | M1.5 V | Single | |
| 502 | | J04225+105 | LSPM J0422+1031 | | 04:22:32.25 | +10:31:19.3 | M3.5 V | Single | |
| 503 | | J04225+390 | GJ 1070 | 1070 | 04:22:34.31 | +39:00:34.0 | M5.0 V | Single | |
| 504 | | J04227+205 | LP 415–30 | | 04:22:42.99 | +20:34:11.9 | M4.0 V | Candidate | |
| 505 | | J04229+259 | G 8–31 | | 04:22:59.30 | +25:59:10.4 | M4.5 V | Single | |
| 506 | | J04234+495 | TYC 3337–1716–1 | | 04:23:26.84 | +49:34:15.6 | M2.5 V | Single | |
| 507 | | J04234+809 | 1RXS J042323.2+805511 | | 04:23:29.60 | +80:55:08.8 | M4.0 V | Candidate | |
| 508 | | J04238+092 | LP 535–73 | | 04:23:50.83 | +09:12:19.4 | M3.0 V | Single | |
| 509 | | J04238+149 | IN Tau | | 04:23:50.50 | +14:55:17.0 | M3.5 V | Candidate | |
| 510 | 138 | J04247–067 | 1RXS J042441.9–064725 | | 04:24:42.78 | -06:47:31.2 | M4.0 V | Multiple | A.4 |
| 511 | | J04248+324 | GJ 3280 | 3280 | 04:24:49.49 | +32:26:56.0 | M2.0 V | Single | |
| 512 | | J04251+515 | PM J04251+5131 | | 04:25:09.86 | +51:31:56.2 | M2.0 V | Candidate | |
| 513 | 139 | J04252+080S | GJ 3282 | 3282 | 04:25:15.25 | +08:02:55.8 | M2.5 V | Multiple | A.4 |
| 514 | 139 | J04252+080N | GJ 3283 | 3283 | 04:25:17.09 | +08:04:03.9 | M4.0 V | Multiple+ | |
| 515 | 140 | | HD 27848 | | 04:24:22.38 | +17:04:43.8 | F5 V | Multiple | A.7 A.8 |
| 516 | 140 | | V991 Tau | 3281 | 04:25:00.35 | +16:59:05.2 | K4 V | Multiple | A.7 A.8 |
| 517 | 140 | J04252+172 | V805 Tau | | 04:25:13.67 | +17:16:05.1 | M3.5 V | Multiple | A.7 A.8 |
| 518 | 140 | | LP 415–881 | | 04:26:19.16 | +17:03:01.7 | M7.0 V | Multiple | A.7 A.8 |
| 519 | | J04274+203 | TYC 1273–9–1 | | 04:27:24.97 | +20:22:44.5 | M1.5 V | Single | |
| 520 | 141 | J04276+595 | GJ 3287 | 3287 | 04:27:41.56 | +59:35:13.5 | M4.0 V | Multiple | |
| 521 | | J04278+117 | GJ 3291 | 3291 | 04:27:53.89 | +11:46:46.8 | M4.0 V | Single | |
| 522 | 142 | J04284+176 | V1102 Tau | | 04:28:28.89 | +17:41:44.9 | M2.0 V | Multiple | |
| 523 | 142 | | HG 7–232B | | 04:28:29.01 | +17:41:45.3 | M3.0 V | Multiple | A.2 |
| 524 | | J04290+219 | HD 28343 | 169 | 04:29:00.05 | +21:55:24.5 | M0.5 V | Single | |
| 525 | | J04293+142 | GJ 3292 | 3292 | 04:29:18.76 | +14:14:02.0 | M4.0 V | Single | |
| 526 | 143 | J04294+262 | FW Tau | | 04:29:29.71 | +26:16:52.8 | M5.5 V | Multiple | |
| 527 | | J04302+708 | PM J04302+7049 | | 04:30:11.72 | +70:49:14.3 | M1.5 V | Single | |
| 528 | | J04304+398 | V546 Per | 170 | 04:30:25.67 | +39:50:50.4 | M4.5 V | Single | |
| 529 | 144 | J04308–088 | LP 655–23 | | 04:30:52.04 | -08:49:22.0 | M4.0 V | Multiple+ | |
| 530 | 144 | | Koenigstuhl 2B | | 04:30:51.58 | -08:49:03.5 | M8.0 V | Multiple | |
| 531 | 145 | J04310+367 | PM J04310+3647A | | 04:30:59.95 | +36:47:54.7 | M3.0 V | Multiple | |
| 532 | 145 | | PM J04310+3647B | | 04:30:59.91 | +36:47:54.0 | M3.0 V | Multiple | |
| 533 | 146 | | GJ 169.1 B | 169.1 B | 04:31:15.33 | +58:58:10.1 | DC5 | Multiple | A.9 |
| 534 | 146 | J04311+589 | GJ 169.1 A | 169.1 A | 04:31:14.21 | +58:58:04.7 | M4.0 V | Multiple | A.9 |
| 535 | | J04312+422 | PM J04312+4217 | | 04:31:14.99 | +42:17:08.9 | M2.5 V | Single | |
| 536 | 147 | J04313+241 | V927 Tau | | 04:31:23.83 | +24:10:52.6 | M4.5 V | Multiple | |
| 537 | | J04326+098 | LP 475–1095 | | 04:32:37.96 | +09:51:06.5 | M1.5 V | Candidate | |
| 538 | 148 | J04329+001E | LP 595–23 | | 04:32:56.07 | +00:06:14.7 | M0.5 V | Multiple | |
| 539 | 148 | J04329+001S | G 82–28 | | 04:32:55.38 | +00:06:28.3 | M4.0 V | Multiple | |
| 540 | 148 | J04329+001N | LP 595–21 | | 04:32:55.32 | +00:06:33.2 | M4.0 V | Multiple | |
| 541 | 149 | J04333+239 | V697 TauA | | 04:33:23.91 | +23:59:26.0 | M3.0 V | Multiple | |
| 542 | 149 | | V697 TauB | | 04:33:23.87 | +23:59:26.5 | M1.5 V | Multiple | A.2 |
| 543 | | J04335+207 | GJ 3296 | 3296 | 04:33:34.48 | +20:44:40.7 | M4.0 V | Candidate | |
| 544 | | J04343+430 | PM J04343+4302 | | 04:34:22.55 | +43:02:13.3 | M2.5 V | Single | A.11 |
| 545 | | J04347–004 | LP 595–11 | | 04:34:45.24 | -00:26:50.2 | M4.0 V | Candidate | |
| 546 | 150 | J04350+086 | StKM 1–495 | | 04:35:02.65 | +08:39:30.5 | M1.0 V | Multiple | |
| 547 | 151 | J04352–161 | LP 775–31 | | 04:35:16.33 | -16:06:52.2 | M8.0 V | Multiple | A.4 |
| 548 | | J04366+112 | GJ 3302 | 3302 | 04:36:39.94 | +11:13:22.8 | M4.0 V | Single | |
| 549 | | J04369+593 | LP 84–34 | | 04:36:58.75 | +59:21:57.7 | M2.0 V | Single | |
| 550 | | J04369–162 | 1RXS J043657.1–161258 | | 04:36:57.49 | -16:13:07.0 | M3.5 V | Candidate | |
| 551 | | J04373+193 | LP 415–1644 | | 04:37:22.00 | +19:21:16.9 | M4.0 V | Candidate | |
| 552 | | J04376+528 | HD 232979 | 172 | 04:37:41.47 | +52:53:29.4 | M0.0 V | Single | |
| 553 | 152 | | HD 29391 | | 04:37:36.18 | -02:28:25.8 | F0 V | Multiple | A.11 |
| 554 | 152 | J04376–024 | GJ 3305 | 3305 | 04:37:37.51 | -02:29:29.7 | M1.0 V | Multiple | A.2 |
| 555 | | J04376–110 | GJ 173 | 173 | 04:37:41.62 | -11:02:23.1 | M1.5 V | Single | |
| 556 | 153 | J04382+282 | GJ 3304 A | 3304 A | 04:38:13.13 | +28:12:58.4 | M4.0 V | Multiple | |
| 557 | 153 | | GJ 3304 B | 3304 B | 04:38:13.05 | +28:12:59.0 | M4.5 V | Multiple | |
| 558 | | J04386–115 | LP 715–39 | | 04:38:36.86 | -11:30:18.6 | M3.5 V | Candidate | |
| 559 | 154 | J04388+217 | G 8–48A | | 04:38:53.72 | +21:47:51.7 | M3.5 V | Multiple | |
| 560 | 154 | | LP 358–478 | | 04:38:53.79 | +21:47:51.0 | M5.5 V | Multiple | |
| 561 | 154 | | G 8–48B | | 04:38:54.69 | +21:47:45.0 | M5.0 V | Multiple+ | |
| 562 | 155 | | V583 Aur | | 04:39:25.47 | +33:32:43.9 | K5 V | Multiple | A.8 |
| 563 | 155 | J04393+335 | PM J04393+3331 | | 04:39:23.22 | +33:31:48.7 | M4.0 V | Multiple | A.2 A.8 |
| 564 | | J04395+162 | LP 415–302 | | 04:39:31.54 | +16:15:30.2 | M5.5 V | Single | |
| 565 | | J04398+251 | PM J04398+2509 | | 04:39:48.86 | +25:09:25.4 | M3.5 V | Single | |
| 566 | | J04403–055 | LP 655–48 | | 04:40:23.63 | -05:30:06.1 | M6.0 V | Single | |
| 567 | 156 | J04404–091 | GJ 9163 A | 9163 A | 04:40:29.13 | -09:11:48.5 | M0.0 V | Multiple | |
| 568 | 156 | | GJ 9163 B | 9163 B | 04:40:29.15 | -09:11:46.8 | M1.0 V | Multiple | A.2 |
| 569 | | J04406–128 | TOI–2457 | | 04:40:40.16 | -12:53:26.6 | M0.0 V | Single | |
| 570 | | J04407+022 | GJ 3307 | 3307 | 04:40:42.67 | +02:13:52.7 | M1.5 V | Candidate | |
| 571 | 157 | J04413+327 | G 39–30A | | 04:41:24.22 | +32:42:19.9 | M4.0 V | Multiple | |
| 572 | 157 | | G 39–30B | | 04:41:24.22 | +32:42:21.4 | M4.0 V | Multiple | |

Table A.1: Complete sample studied in this work^a (cont.).

| Star id. | System id. | Karmn | Name | GJ | α (J2016.0) | δ (J2016.0) | Spectral type | Multiplicity type | In tables |
|----------|------------|-------------|------------------------------|--------|-----------------------|-----------------------|---------------|-------------------|-----------|
| 573 | 158 | J04414+132 | TYC 694–1183–1 | | 04:41:29.78 | +13:13:16.0 | M0.5 V | Multiple | A.4 |
| 574 | | J04422+577 | LP 84–59 | | 04:42:15.86 | +57:42:18.2 | M0.0 V | Candidate | |
| 575 | | J04423+207 | LP 415–1896 | | 04:42:23.76 | +20:46:34.9 | M2.0 V | Single | |
| 576 | 159 | J04425+204 | LP 415–345 | | 04:42:30.40 | +20:27:10.8 | M3.0 V | Multiple | A.4 A.7 |
| 577 | 159 | | LP 415–3051 | | 04:42:58.58 | +20:36:16.8 | M3.0 V | Multiple | A.7 |
| 578 | 159 | | Gaia DR2 341105484886601472 | | 04:43:55.36 | +20:08:40.5 | M6.0 V | Multiple | A.7 |
| 579 | 160 | J04429+095 | PM J04429+0935 | | 04:42:55.14 | +09:35:53.7 | M1.0 V | Multiple | |
| 580 | 160 | | Gaia DR3 3293060625388613248 | | 04:42:53.91 | +09:35:50.3 | M6.5 V | Multiple | |
| 581 | | J04429+189 | HD 285968 | 176 | 04:42:56.52 | +18:57:11.5 | M2.0 V | Single | A.11 |
| 582 | | J04429+214 | PM J04429+2128 | | 04:42:55.90 | +21:28:24.8 | M3.5 V | Single | |
| 583 | | J04433+296 | Haro 6–36 | | 04:43:20.23 | +29:40:05.7 | M5.5 V | Single | |
| 584 | | J04444+278 | HD 283779 | 3309 | 04:44:26.17 | +27:51:37.2 | M1.5 V | Single | |
| 585 | | J04458–144 | PM J04458–1426 | | 04:45:52.69 | -14:26:23.6 | M4.0 V | Candidate | |
| 586 | 161 | J04468–112 | PM J04468–1116A | | 04:46:51.63 | -11:16:48.6 | M3.0 V | Multiple | |
| 587 | 161 | | PM J04468–1116B | | 04:46:51.53 | -11:16:48.2 | M6.0 V | Multiple | |
| 588 | | J04471+021 | GJ 3313 | 3313 | 04:47:11.55 | +02:09:39.6 | M0.0 V | Single | |
| 589 | | J04472+206 | RX J04472+2038 | | 04:47:12.35 | +20:38:09.2 | M5.0 V | Candidate | |
| 590 | 162 | J04480+170 | LP 416–43 | | 04:48:00.98 | +17:03:21.1 | M0.5 V | Multiple | A.4 |
| 591 | 163 | J04488+100 | IRXS J04487.6+100302 | | 04:48:47.32 | +10:03:01.4 | M3.0 V | Multiple | A.4 |
| 592 | 164 | J04494+484 | G 81–34 | | 04:49:29.77 | +48:28:42.9 | M4.0 V | Multiple | |
| 593 | 165 | J04499+236 | EM* LkCa 18A | | 04:49:56.34 | +23:41:00.1 | M1.0 V | Multiple | |
| 594 | 165 | | EM* LkCa 18B | | 04:49:56.51 | +23:41:00.1 | M1.5 V | Multiple | |
| 595 | | J04499+711 | LP 32–204 | | 04:49:56.29 | +71:09:46.5 | M3.5 V | Single | |
| 596 | | J04502+459 | GJ 3315 | 3315 | 04:50:15.59 | +45:58:46.2 | M1.0 V | Single | |
| 597 | | J04504+199 | BPM 85800 | | 04:50:25.49 | +19:59:09.1 | M1.5 V | Single | |
| 598 | | J04508+221 | GJ 1072 | 1072 | 04:50:51.65 | +22:07:14.7 | M5.0 V | Single | |
| 599 | | J04508+261 | GJ 3316 | 3316 | 04:50:51.21 | +26:07:22.3 | M2.5 V | Single | |
| 600 | | J04520+064 | Wolf 1539 | 179 | 04:52:05.90 | +06:28:30.7 | M3.5 V | Single | |
| 601 | | J04524–168 | LP 776–25 | | 04:52:24.55 | -16:49:25.3 | M3.5 V | Candidate | A.11 |
| 602 | | J04525+407 | GJ 1073 | 1073 | 04:52:36.26 | +40:42:06.6 | M4.0 V | Single | |
| 603 | | J04536+623 | LP 84–48 | | 04:53:40.79 | +62:18:59.9 | M3.5 V | Single | |
| 604 | | J04538+158 | LSPM J0453+1549 | | 04:53:50.10 | +15:49:12.6 | M2.5 V | Single | |
| 605 | | J04538–177 | GJ 180 | 180 | 04:53:50.44 | -17:46:34.6 | M2.0 V | Single | A.11 |
| 606 | | J04544+650 | IRXS J045430.9+650451 | | 04:54:29.98 | +65:04:39.5 | M4.0 V | Single | |
| 607 | 166 | | HD 31412 | 9169 | 04:55:56.03 | +04:40:10.5 | F9.5 V | Multiple | A.8 |
| 608 | 166 | J04559+046 | HD 31412B | | 04:55:54.60 | +04:40:13.5 | M2.0 V | Multiple | A.8 |
| 609 | | J04560+432 | LP 202–2 | | 04:56:04.12 | +43:13:53.0 | M4.0 V | Single | |
| 610 | | J04587+509 | GJ 1074 | 1074 | 04:58:46.84 | +50:56:32.4 | M0.5 V | Single | |
| 611 | | J04588+498 | GJ 181 | 181 | 04:58:50.76 | +49:50:55.6 | M0.0 V | Single | |
| 612 | | J04595+017 | GJ 182 | 182 | 04:59:34.88 | +01:46:59.2 | M0.0 V | Single | |
| 613 | | J05012+248 | Ross 794 | 3320 | 05:01:15.79 | +24:52:18.2 | M2.0 V | Single | |
| 614 | | J05013+226 | LSPM J0501+2237 | | 05:01:17.95 | +22:36:55.3 | M4.5 V | Single | |
| 615 | | J05018+037 | GJ 3321 | 3321 | 05:01:50.71 | +03:45:53.1 | M1.0 V | Single | |
| 616 | | J05019+011 | IRXS J050156.7+010845 | | 05:01:56.70 | +01:08:41.4 | M4.0 V | Single | |
| 617 | 167 | J05019+099 | GJ 3322 A | 3322 A | 05:01:58.83 | +09:58:57.1 | M4.0 V | Multiple | A.4 |
| 618 | 167 | | GJ 3322 B | 3322 B | 05:01:58.89 | +09:58:55.9 | M2.5 V | Multiple | A.2 |
| 619 | | J05019–069 | GJ 3323 | 3323 | 05:01:56.83 | -06:56:54.9 | M4.0 V | Single | A.11 |
| 620 | 168 | J05024–212 | HD 32450A | 185 A | 05:02:28.28 | -21:15:28.4 | M0.0 V | Multiple | 5 |
| 621 | 168 | | HD 32450B | 185 B | 05:02:28.26 | -21:15:27.5 | M3.0 V | Multiple | 5 A.2 |
| 622 | 169 | J05032+213 | HD 285190 | | 05:03:16.21 | +21:23:54.0 | M1.5 V | Multiple | A.4 |
| 623 | 169 | J05030+213 | LP 359–186 | | 05:03:05.77 | +21:22:33.8 | M5.0 V | Multiple | A.2 |
| 624 | | J05033–173 | GJ 3325 | 3325 | 05:03:19.83 | -17:22:31.8 | M3.0 V | Single | |
| 625 | 170 | J05034+531 | GJ 184 | 184 | 05:03:26.22 | +53:07:17.9 | M0.5 V | Multiple | |
| 626 | 170 | | BD+52 911B | | 05:03:25.60 | +53:07:18.7 | M7.5 V | Multiple | |
| 627 | | J05042+110 | GJ 3326 | 3326 | 05:04:14.69 | +11:03:27.0 | M4.0 V | Single | |
| 628 | | J05050+442 | UPM J0505+4414 | | 05:05:06.06 | +44:14:03.3 | M5.0 V | Single | |
| 629 | | J05051–120 | GJ 3327 | 3327 | 05:05:11.55 | -12:00:30.9 | M3.0 V | Single | |
| 630 | | J05060+043 | GJ 3328 | 3328 | 05:06:04.44 | +04:20:16.1 | M1.0 V | Single | |
| 631 | | J05062+046 | RX J0506.2+0439 | | 05:06:12.96 | +04:39:25.7 | M4.0 V | Candidate | |
| 632 | 171 | J05068–215E | GJ 3331 | 3331 | 05:06:49.97 | -21:35:09.4 | M1.5 V | Multiple | |
| 633 | 171 | J05068–215W | GJ 3332 | 3332 | 05:06:49.48 | -21:35:04.3 | M3.5 V | Multiple | A.2 |
| 634 | 171 | | BD–21 1074C | | 05:06:49.55 | -21:35:04.7 | M2.5 V | Multiple | A.2 |
| 635 | 172 | J05072+375 | RX J0507.2+3731A | | 05:07:14.33 | +37:30:42.1 | M5.0 V | Multiple | |
| 636 | 172 | | RX J0507.2+3731B | | 05:07:14.37 | +37:30:42.1 | M5.0 V | Multiple | A.3 |
| 637 | | J05076+275 | TYC 1853–1649–1 | | 05:07:36.74 | +27:30:03.8 | M0.5 V | Candidate | |
| 638 | 173 | J05078+179 | Wolf 230 | 3333 | 05:07:49.34 | +17:58:53.5 | M3.0 V | Multiple | |
| 639 | 174 | J05083+756 | LP 15–315 | | 05:08:19.36 | +75:38:13.3 | M4.5 V | Multiple | |
| 640 | 175 | J05084–210 | 2MASS J05082729–2101444 | | 05:08:27.34 | -21:01:44.6 | M5.0 V | Multiple | |
| 641 | 176 | J05085–181 | GJ 190 | 190 | 05:08:35.61 | -18:10:41.8 | M3.5 V | Multiple | |
| 642 | | J05091+154 | Ross 388 | 3335 | 05:09:10.11 | +15:27:22.8 | M3.0 V | Candidate | |
| 643 | | J05103+095 | G 97–23 | | 05:10:18.12 | +09:30:01.8 | M2.0 V | Single | |
| 644 | | J05103+272 | LSPM J0510+2714 | | 05:10:19.83 | +27:13:51.8 | M7.0 V | Single | |
| 645 | 177 | J05103+488 | GJ 3336 A | 3336 A | 05:10:22.30 | +48:50:26.3 | M2.5 V | Multiple | |
| 646 | 177 | | GJ 3336 B | 3336 B | 05:10:22.48 | +48:50:25.5 | M2.0 V | Multiple | |
| 647 | | J05106+297 | G 86–28 | | 05:10:39.22 | +29:46:48.9 | M3.0 V | Single | |
| 648 | | J05109+186 | GJ 3337 | 3337 | 05:10:57.16 | +18:37:24.1 | M3.5 V | Single | |
| 649 | | J05111+158 | StKM 1–549 | | 05:11:09.78 | +15:48:57.0 | M1.0 V | Candidate | |
| 650 | | J05114+101 | LP 477–36 | | 05:11:29.68 | +10:07:12.2 | M1.0 V | Candidate | |
| 651 | | J05127+196 | GJ 192 | 192 | 05:12:42.54 | +19:40:00.2 | M2.0 V | Single | |
| 652 | | J05151–073 | GJ 3340 | 3340 | 05:15:08.33 | -07:20:55.4 | M1.0 V | Single | |
| 653 | | J05152+236 | UPM J0515+2336 | | 05:15:17.58 | +23:36:25.2 | M5.0 V | Candidate | |
| 654 | | J05155+591 | LSPM J0515+5911 | | 05:15:31.19 | +59:11:01.3 | M7.5 V | Candidate | |

Table A.1: Complete sample studied in this work^a (cont.).

| Star id. | System id. | Karmn | Name | GJ | α (J2016.0) | δ (J2016.0) | Spectral type | Multiplicity type | In tables |
|----------|------------|-------------|------------------------------|--------|-----------------------|-----------------------|---------------|-------------------|-----------|
| 655 | 178 | J05173+321 | G 86–37 | | 05:17:20.09 | +32:07:29.7 | M3.5 V | Multiple | |
| 656 | 179 | | Capella | 194 B | 05:16:41.36 | +45:59:52.8 | G3 III | Multiple | A.4 A.8 |
| 657 | 179 | J05173+458 | Capella H | 195 A | 05:17:24.00 | +45:50:16.1 | M2.5 V | Multiple | A.8 |
| 658 | 179 | | Capella L | 195 B | 05:17:24.04 | +45:50:12.6 | M4.0 V | Multiple | A.8 |
| 659 | | J05173+721 | TYC 4351–466–1 | | 05:17:21.23 | +72:10:49.8 | M1.0 V | Single | |
| 660 | | J05187+464 | PM J05187+4629 | | 05:18:44.62 | +46:29:57.9 | M4.5 V | Candidate | |
| 661 | | J05195+649 | IRXS J051929.3+645435 | | 05:19:31.21 | +64:54:36.2 | M3.5 V | Candidate | |
| 662 | 180 | J05206+587N | GJ 3342 | 3342 | 05:20:41.70 | +58:47:25.2 | M3.5 V | Multiple+ | |
| 663 | 180 | J05206+587S | GJ 3343 | 3343 | 05:20:41.05 | +58:47:12.0 | M3.5 V | Multiple | A.2 |
| 664 | | J05211+557 | GJ 3345 | 3345 | 05:21:10.47 | +55:45:46.5 | M3.0 V | Single | |
| 665 | | J05223+305 | PM J05223+3031 | | 05:22:20.65 | +30:31:08.3 | M3.0 V | Single | |
| 666 | | J05226+795 | TYC 4532–731–1 | | 05:22:39.87 | +79:34:30.3 | M0.5 V | Single | |
| 667 | 181 | J05228+202 | PM J05228+2016 | | 05:22:50.18 | +20:16:36.5 | M2.5 V | Multiple | |
| 668 | 181 | | Gaia DR3 3402193923314210944 | | 05:22:50.43 | +20:16:36.6 | M4.5 V | Multiple | |
| 669 | 182 | J05243–160 | PM J05243–1601A | | 05:24:19.14 | -16:01:15.8 | M4.5 V | Multiple | |
| 670 | 182 | | PM J05243–1601B | | 05:24:19.17 | -16:01:15.6 | M3.5 V | Multiple | A.2 |
| 671 | 183 | J05256–091 | LP 717–36 | | 05:25:41.70 | -09:09:15.8 | M3.5 V | Multiple | |
| 672 | 183 | | Gaia DR3 3014628959425010688 | | 05:25:41.73 | -09:09:15.3 | M3.5 V | Multiple | |
| 673 | | J05280+096 | Ross 41 | 203 | 05:27:59.94 | +09:38:26.0 | M3.5 V | Single | |
| 674 | 184 | J05282+029 | GJ 1080 | 1080 | 05:28:14.24 | +02:57:56.6 | M3.0 V | Multiple | A.4 |
| 675 | 184 | | GJ 1080 B | 1080 B | 05:28:14.27 | +02:57:51.9 | M6.0 V | Multiple | |
| 676 | 185 | | HD 35956 | 3347 | 05:28:51.74 | +12:32:59.6 | G0 V | Multiple | A.4 A.8 |
| 677 | 185 | | HD 35956B | | 05:28:52.11 | +12:33:01.4 | M1.0 V | Multiple | A.8 |
| 678 | 185 | J05289+125 | G 102–4A | 3348 | 05:28:56.61 | +12:31:50.4 | M4.0 V | Multiple | A.2 A.8 |
| 679 | 185 | | G 102–4B | | 05:28:56.61 | +12:31:50.2 | M4.0 V | Multiple | A.8 |
| 680 | 186 | J05294+155E | GJ 2043 | 2043 | 05:29:26.92 | +15:34:36.2 | M0.0 V | Multiple | |
| 681 | 186 | J05294+155W | GJ 2043 B | 2043 B | 05:29:26.02 | +15:34:43.4 | M4.0 V | Multiple | |
| 682 | | J05298+320 | Ross 406 | 3349 | 05:29:52.40 | +32:04:40.4 | M3.0 V | Single | |
| 683 | | J05298–034 | Wolf 1450 | 9182 | 05:29:51.70 | -03:26:37.6 | M2.5 V | Single | |
| 684 | | J05306+152 | LSPM J0530+1514 | | 05:30:37.09 | +15:14:26.3 | M3.0 V | Single | |
| 685 | | J05314–036 | HD 36395 | 205 | 05:31:28.21 | -03:41:11.5 | M1.5 V | Single | |
| 686 | 187 | J05320–030 | V1311 Ori | | 05:32:04.51 | -03:05:30.0 | M2.0 V | Multiple | |
| 687 | 187 | | PM J05319–0303W | | 05:31:57.88 | -03:03:37.6 | M5.0 V | Multiple | A.2 |
| 688 | 187 | | 2MASS J05315816–0303397 | | 05:31:58.17 | -03:03:40.7 | M3.5 V | Multiple | A.2 |
| 689 | 187 | | ESO–HA 737 | | 05:32:05.97 | -03:01:16.8 | M5.0 V | Multiple | A.2 |
| 690 | 188 | J05322+098 | Ross 42 | 206 | 05:32:14.46 | +09:49:11.5 | M3.5 V | Multiple | A.4 |
| 691 | | J05328+338 | G 98–7 | | 05:32:51.57 | +33:49:39.8 | M3.5 V | Single | |
| 692 | 189 | J05333+448 | GJ 1081 | 1081 | 05:33:19.20 | +44:48:52.9 | M3.5 V | Multiple | |
| 693 | 190 | J05337+019 | V371 Ori | 9183 | 05:33:44.55 | +01:56:41.0 | M2.5 V | Multiple | A.4 |
| 694 | | J05339–023 | RX J0534.0–0221 | | 05:33:59.83 | -02:21:33.3 | M3.0 V | Single | |
| 695 | 191 | | PM J05334+4809 | | 05:33:28.97 | +48:09:26.2 | M0.0 V | Multiple | A.7 |
| 696 | 191 | J05341+475 | PM J05341+4732A | | 05:34:10.56 | +47:32:02.8 | M2.5 V | Multiple | A.7 |
| 697 | 191 | | PM J05341+4732B | | 05:34:10.62 | +47:32:05.2 | M3.0 V | Multiple | A.7 |
| 698 | 191 | | UPM J0533+4809 | | 05:33:16.22 | +48:09:23.3 | M3.5 V | Multiple+ | A.7 |
| 699 | | J05341+512 | GJ 3352 | 3352 | 05:34:08.57 | +51:12:52.8 | M0.5 V | Single | |
| 700 | 192 | J05342+103N | Ross 45 | 3353 | 05:34:15.05 | +10:19:08.0 | M3.0 V | Multiple | |
| 701 | 192 | J05342+103S | Ross 45B | 3354 | 05:34:15.00 | +10:19:03.0 | M4.5 V | Multiple | A.4 |
| 702 | | J05348+138 | Ross 46 | 3356 | 05:34:51.99 | +13:52:40.4 | M3.5 V | Single | |
| 703 | | J05360–076 | Wolf 1457 | 3357 | 05:36:00.20 | -07:38:51.0 | M4.0 V | Single | |
| 704 | 193 | J05365+113 | V2689 Ori | 208 | 05:36:30.99 | +11:19:39.4 | M0.0 V | Multiple | |
| 705 | 193 | J05366+112 | PM J05366+1117 | | 05:36:38.46 | +11:17:47.8 | M4.0 V | Multiple | |
| 706 | | J05394+406 | LSPM J0539+4038 | | 05:39:25.71 | +40:38:29.5 | M8.0 V | Candidate | |
| 707 | | J05394+747 | LP 33–191 | | 05:39:25.44 | +74:46:02.6 | M3.5 V | Single | |
| 708 | 194 | J05402+126 | V1402 Ori | 3362 | 05:40:16.07 | +12:38:56.4 | M1.0 V | Multiple | A.4 |
| 709 | 195 | | V538 Aur | 211 | 05:41:20.34 | +53:28:43.4 | K1 V | Multiple | A.8 |
| 710 | 195 | J05415+534 | HD 233153 | 212 | 05:41:30.74 | +53:29:15.0 | M1.0 V | Multiple | A.8 |
| 711 | 196 | J05404+248 | V780 Tau | 1083 | 05:40:25.82 | +24:48:02.0 | M5.5 V | Multiple | |
| 712 | | J05419+153 | GJ 9188 | 9188 | 05:41:58.95 | +15:20:13.3 | M0.0 V | Single | |
| 713 | | J05421+124 | V1352 Ori | 213 | 05:42:11.45 | +12:28:56.5 | M4.0 V | Single | |
| 714 | | J05422–054 | GJ 2045 | 2045 | 05:42:12.53 | -05:27:40.3 | M5.0 V | Single | |
| 715 | | J05425+154 | IRXS J054232.1+152459 | | 05:42:31.70 | +15:25:00.2 | M3.5 V | Candidate | |
| 716 | 197 | J05456+729 | PM J05456+7255 | | 05:45:39.09 | +72:55:14.6 | M3.0 V | Multiple | |
| 717 | 197 | J05455–119 | PM J05455–1158 | | 05:45:32.04 | -11:58:02.3 | M4.5 V | Multiple | |
| 718 | | J05458+729 | PM J05458+7254 | | 05:45:50.02 | +72:54:09.0 | M2.5 V | Single | |
| 719 | 198 | J05466+441 | Wolf 237 | 3365 | 05:46:37.60 | +44:07:14.0 | M4.0 V | Multiple | A.4 |
| 720 | | J05468+665 | TYC 4106–420–1 | | 05:46:48.92 | +66:30:13.1 | M0.5 V | Candidate | |
| 721 | | J05471–052 | GJ 3366 | 3366 | 05:47:09.69 | -05:12:20.3 | M4.5 V | Single | |
| 722 | | J05472–000 | GJ 3367 | 3367 | 05:47:17.89 | -00:00:49.9 | M0.0 V | Single | |
| 723 | | J05484+077 | GJ 3368 | 3368 | 05:48:24.15 | +07:45:34.3 | M4.0 V | Single | |
| 724 | | J05511+122 | PM J05511+1216 | | 05:51:10.51 | +12:16:09.4 | M4.0 V | Candidate | |
| 725 | 199 | J05530+047 | G 106–7 | | 05:53:04.75 | +04:43:02.6 | M1.5 V | Multiple | |
| 726 | 199 | | G 106–7B | | 05:53:04.65 | +04:43:02.8 | M5.5 V | Multiple | |
| 727 | 200 | J05530+251 | LSPM J0553+2507 | | 05:53:01.92 | +25:07:40.9 | M3.0 V | Multiple | |
| 728 | 201 | J05532+242 | Ross 59 | 220 | 05:53:14.24 | +24:15:22.1 | M1.5 V | Multiple | |
| 729 | | J05547+109 | RX J0554.7+1055 | | 05:54:45.58 | +10:55:55.9 | M3.0 V | Candidate | |
| 730 | 202 | J05558+406 | PM J05558+4036 | | 05:55:48.31 | +40:36:48.0 | M1.0 V | Multiple | |
| 731 | 202 | | Gaia DR3 3458612029599345664 | | 05:55:48.41 | +40:36:47.7 | M3.0 V | Multiple | |
| 732 | | J05566–103 | IRXS J055641.0–101837 | | 05:56:40.63 | -10:18:35.8 | M3.5 V | Single | |
| 733 | | J05587+259 | PM J05587+2557 | | 05:58:47.68 | +25:57:40.1 | M1.0 V | Single | |
| 734 | 203 | J05588+213 | G 104–9 | | 05:58:53.53 | +21:20:54.5 | M5.0 V | Multiple | |
| 735 | 204 | J05596+585 | EG Cam | 3371 | 05:59:37.77 | +58:35:30.8 | M0.5 V | Multiple | |
| 736 | 204 | J05599+585 | GJ 3372 | 3372 | 05:59:55.68 | +58:34:11.2 | M4.0 V | Multiple | |

Table A.1: Complete sample studied in this work^a (cont.).

| Star id. | System id. | Karmn | Name | GJ | α (J2016.0) | δ (J2016.0) | Spectral type | Multiplicity type | In tables |
|----------|------------|------------|------------------------------|---------|-----------------------|-----------------------|---------------|-------------------|-----------|
| 737 | | J06000+027 | GJ 3379 | 3379 | 06:00:03.83 | +02:42:22.9 | M4.0 V | Single | |
| 738 | 205 | J06008+681 | GJ 3373 | 3373 | 06:00:50.71 | +68:09:05.3 | M3.5 V | Multiple | |
| 739 | 205 | J06007+681 | GJ 3374 | 3374 | 06:00:47.81 | +68:08:11.6 | M4.0 V | Multiple | |
| 740 | | J06011+595 | GJ 3378 | 3378 | 06:01:10.82 | +59:35:35.0 | M3.5 V | Single | |
| 741 | | J06017+130 | LSPM J0601+1305 | | 06:01:45.54 | +13:05:00.7 | M2.5 V | Single | |
| 742 | | J06023–203 | GJ 3382 | 3382 | 06:02:22.56 | -20:19:35.3 | M3.5 V | Single | |
| 743 | | J06024+498 | GJ 3380 | 3380 | 06:02:29.31 | +49:51:42.6 | M5.0 V | Single | |
| 744 | | J06024+663 | LP 57–46 | | 06:02:26.51 | +66:20:32.3 | M4.5 V | Single | |
| 745 | | J06025+371 | PM J06025+3707 | | 06:02:35.46 | +37:07:36.2 | M1.0 V | Candidate | |
| 746 | | J06034+478 | Wolf 261 | 3381 | 06:03:29.48 | +47:48:06.0 | M4.0 V | Single | |
| 747 | | J06035+155 | 1RXS J060335.0+153132 | | 06:03:34.74 | +15:31:30.4 | M0.0 V | Candidate | |
| 748 | | J06035+168 | 1RXS J060334.8+165128 | | 06:03:34.49 | +16:51:45.4 | M4.0 V | Candidate | |
| 749 | | J06039+261 | Ross 60 | 9197 | 06:03:54.54 | +26:08:46.0 | M3.0 V | Single | |
| 750 | 206 | J06054+608 | LP 86–173 | | 06:05:30.04 | +60:49:09.8 | M4.5 V | Multiple | A.4 |
| 751 | 207 | J06066+465 | PM J06066+4633A | | 06:06:37.78 | +46:33:47.0 | M3.0 V | Multiple | |
| 752 | 207 | | PM J06066+4633B | | 06:06:37.77 | +46:33:45.2 | M3.5 V | Multiple | A.2 |
| 753 | | J06071+335 | Ross 70 | 3384 | 06:07:11.91 | +33:32:30.9 | M2.5 V | Single | |
| 754 | | J06075+472 | 1RXS J060732.5+471154 | | 06:07:31.91 | +47:12:23.3 | M4.5 V | Candidate | |
| 755 | | J06097+001 | HD 291290 | | 06:09:46.30 | +00:09:30.8 | M0.0 V | Single | |
| 756 | 208 | J06102+225 | PM J06102+2234 | | 06:10:17.81 | +22:34:17.2 | M4.0 V | Multiple | 7 |
| 757 | 208 | J06103+225 | LP 362–121 | | 06:10:22.52 | +22:34:18.1 | M5.0 V | Multiple | A.2 7 |
| 758 | 208 | | Gaia DR3 3425067888342287616 | | 06:10:22.50 | +22:34:17.9 | M5.5 V | Multiple | 7 |
| 759 | | J06103+722 | LSPM J0610+7212 | | 06:10:18.09 | +72:11:58.0 | M2.5 V | Single | |
| 760 | | J06103+821 | GJ 226 | 226 | 06:10:20.24 | +82:06:02.9 | M2.0 V | Single | |
| 761 | | J06105+024 | TYC 135–239–1 | | 06:10:31.41 | +02:25:30.3 | M0.0 V | Candidate | |
| 762 | 209 | J06105–218 | GJ 229 | 229 | 06:10:34.46 | -21:52:04.2 | M0.5 V | Multiple | A.11 |
| 763 | | J06107+259 | Wolf 1058 | 3385 | 06:10:46.51 | +25:55:53.3 | M1.5 V | Candidate | |
| 764 | 210 | J06109+103 | Ross 79 | 228 | 06:10:54.88 | +10:18:50.6 | M2.5 V | Multiple | |
| 765 | | J06140+516 | GJ 3388 | 3388 | 06:14:01.72 | +51:40:06.5 | M3.5 V | Single | |
| 766 | | J06145+025 | G 106–35 | | 06:14:34.76 | +02:30:19.7 | M3.0 V | Single | |
| 767 | 211 | | HD 43587 | 231.1 A | 06:17:15.90 | +05:06:02.6 | G0 V | Multiple | A.8 |
| 768 | 211 | J06171+051 | GJ 231.1 B | 231.1 B | 06:17:10.42 | +05:07:05.3 | M3.5 V | Multiple | A.8 |
| 769 | | J06151–164 | LP 779–34 | | 06:15:11.90 | -16:26:21.4 | M4.0 V | Single | |
| 770 | 212 | J06171+751 | TYC 4525–194–1 | | 06:18:07.08 | +75:06:04.3 | M2.0 V | Multiple | A.4 |
| 771 | | J06171+838 | LSPM J0617+8353 | | 06:17:04.81 | +83:53:32.5 | M3.5 V | Candidate | |
| 772 | | J06185+250 | G 103–29 | | 06:18:34.83 | +25:03:00.6 | M4.0 V | Single | |
| 773 | | J06193–066 | Ross 417 | 9211 | 06:19:20.74 | -06:39:32.1 | M3.0 V | Single | |
| 774 | | J06194+139 | TYC 743–1836–1 | | 06:19:29.61 | +13:57:02.3 | M0.5 V | Single | |
| 775 | 213 | J06212+442 | GJ 3391 | 3391 | 06:21:13.26 | +44:14:26.7 | M2.0 V | Multiple | |
| 776 | 213 | | Gaia DR3 962141157559432064 | | 06:21:13.21 | +44:14:25.5 | M5.0 V | Multiple | |
| 777 | 214 | J06216+163 | LP 420–5 | | 06:21:36.85 | +16:18:33.8 | M1.0 V | Multiple | |
| 778 | 214 | J06217+163 | LP 420–6 | | 06:21:44.17 | +16:19:19.9 | M2.5 V | Multiple | |
| 779 | | J06218–227 | GJ 2049 | 2049 | 06:21:53.08 | -22:43:19.7 | M1.0 V | Single | |
| 780 | | J06223+334 | TYC 2425–1286–1 | | 06:22:20.65 | +33:26:54.6 | M1.0 V | Candidate | |
| 781 | 215 | J06236–096 | LP 720–10 | | 06:23:38.41 | -09:38:51.5 | M3.5 V | Multiple | |
| 782 | 215 | | LP 720–10 B | | 06:23:38.29 | -09:38:51.4 | M8.0 V | Multiple | |
| 783 | | J06237+020 | TYC 141–24–1 | | 06:23:46.49 | +05:02:40.1 | M1.5 V | Single | |
| 784 | 216 | J06238+456 | LP 160–22 | | 06:23:51.20 | +45:40:00.0 | M5.0 V | Multiple | |
| 785 | | J06246+234 | Ross 64 | 232 | 06:24:41.93 | +23:25:50.8 | M4.0 V | Single | |
| 786 | | J06258+561 | GJ 3393 | 3393 | 06:25:53.21 | +56:10:16.9 | M4.0 V | Single | |
| 787 | | J06262+238 | 1RXS J062614.2+234942 | | 06:26:14.52 | +23:49:36.4 | M1.5 V | Single | |
| 788 | 217 | J06277+093 | Ross 603A | | 06:27:43.80 | +09:23:51.3 | M2.0 V | Multiple | |
| 789 | 217 | | Ross 603B | | 06:27:43.74 | +09:23:50.5 | M3.5 V | Multiple | A.2 5 |
| 790 | 218 | J06293–028 | V577 Mon | 234 A | 06:29:24.18 | -02:49:01.9 | M4.5 V | Multiple | 5 |
| 791 | 218 | | Ross 614 B | 234 B | 06:29:24.19 | -02:49:01.7 | M4.5 V | Multiple | 5 |
| 792 | 219 | J06298–027 | G 108–4 | | 06:29:50.47 | -02:47:49.0 | M4.0 V | Multiple | A.4 |
| 793 | | J06306+456 | PM J06306+4539 | | 06:30:37.39 | +45:39:23.0 | M1.0 V | Single | |
| 794 | | J06307+397 | PM J06307+3947 | | 06:30:47.39 | +39:47:38.5 | M2.0 V | Single | |
| 795 | | J06310+500 | GJ 3395 | 3395 | 06:31:00.97 | +50:02:45.5 | M0.5 V | Single | |
| 796 | | J06318+414 | GJ 3396 | 3396 | 06:31:50.73 | +41:29:42.2 | M5.0 V | Candidate | |
| 797 | | J06322+378 | TYC 2928–1568–1 | | 06:32:14.91 | +37:48:10.6 | M1.5 V | Candidate | |
| 798 | | J06323–097 | PM J06323–0943 | | 06:32:20.28 | -09:43:29.9 | M4.5 V | Candidate | |
| 799 | | J06325+641 | LP 57–192 | | 06:32:31.27 | +64:06:12.2 | M4.0 V | Single | |
| 800 | | J06345+315 | G 103–41 | | 06:34:33.48 | +31:30:05.1 | M3.5 V | Single | |
| 801 | 220 | J06354–040 | 1RXS J06351.2–040314 | | 06:35:29.75 | -04:03:17.2 | M5.5 V | Multiple | |
| 802 | | J06361+116 | GJ 3398 | 3398 | 06:36:06.16 | +11:36:49.5 | M4.5 V | Single | |
| 803 | | J06361+201 | LP 420–4 | | 06:36:12.05 | +20:08:10.3 | M2.5 V | Single | |
| 804 | | J06371+175 | HD 260655 | 239 | 06:37:09.94 | +17:33:58.7 | M0.0 V | Single | A.11 |
| 805 | 221 | J06396–210 | LP 780–32 | | 06:39:37.20 | -21:01:32.4 | M4.0 V | Multiple | 5 |
| 806 | 221 | | Gaia DR3 2926756741750933120 | | 06:39:37.22 | -21:01:31.9 | M4.0 V | Multiple | 5 A.2 |
| 807 | 222 | J06400+285 | GJ 3399 | 3399 | 06:40:05.54 | +28:35:10.5 | M2.0 V | Multiple | |
| 808 | 223 | J06401–164 | LP 780–23 | | 06:40:08.72 | -16:27:21.5 | M2.5 V | Multiple | |
| 809 | 223 | | LP 780–23 B | | 06:40:08.72 | -16:27:21.7 | M2.5 V | Multiple | A.3 |
| 810 | | J06414+157 | Wolf 289 | 3402 | 06:41:28.23 | +15:45:42.6 | M4.0 V | Single | |
| 811 | 224 | J06421+035 | GJ 3404 | 3404 | 06:42:11.24 | +03:34:48.5 | M3.5 V | Multiple | |
| 812 | 224 | J06422+035 | GJ 3405 | 3405 | 06:42:13.39 | +03:35:26.8 | M4.0 V | Multiple | |
| 813 | | J06435+166 | G 110–14 | | 06:43:34.53 | +16:41:35.5 | M4.5 V | Candidate | |
| 814 | 225 | J06438+511 | G 192–39A | 3406A | 06:43:49.95 | +51:08:06.0 | M2.5 V | Multiple | |
| 815 | 225 | | G 192–39B | 3406B | 06:43:49.77 | +51:08:05.8 | M4.5 V | Multiple | |
| 816 | 226 | J06447+718 | GJ 2050 | 2050 | 06:44:45.25 | +71:53:06.7 | M0.5 V | Multiple | |
| 817 | 227 | | HD 263175 | 3408 | 06:46:04.47 | +32:33:22.0 | K3 V | Multiple | A.8 |
| 818 | 227 | J06461+325 | HD 263175B | 3409 | 06:46:06.88 | +32:33:16.6 | M1.0 V | Multiple | A.8 |

Table A.1: Complete sample studied in this work^a (cont.).

| Star id. | System id. | Karmn | Name | GJ | α (J2016.0) | δ (J2016.0) | Spectral type | Multiplicity type | In tables |
|----------|------------|-------------|----------------------------|---------|-----------------------|-----------------------|---------------|-------------------|-----------|
| 819 | | J06467+159 | IRXS J064645.7+155739 | | 06:46:45.62 | +15:57:41.8 | M1.0 V | Single | |
| 820 | | J06474+054 | G 108–27 | | 06:47:27.57 | +05:24:23.3 | M4.0 V | Single | |
| 821 | | J06486+532 | LP 121–58 | | 06:48:38.72 | +53:17:24.3 | M1.5 V | Single | |
| 822 | | J06489+211 | IRXS J064855.9+210754 | | 06:48:55.18 | +21:08:02.8 | M2.5 V | Single | |
| 823 | | J06490+371 | GJ 1092 | 1092 | 06:49:05.73 | +37:06:25.0 | M4.0 V | Single | |
| 824 | | J06509–091 | LP 661–2 | | 06:50:59.37 | -09:10:59.3 | M3.5 V | Single | |
| 825 | 228 | | HD 50281 | 250 A | 06:52:17.47 | -05:10:25.4 | K3.5 V | Multiple | A.8 |
| 826 | 228 | J06523–051 | HD 50281B | 250 B | 06:52:17.42 | -05:11:24.3 | M2.0 V | Multiple | A.8 |
| 827 | | J06524+182 | GJ 3413 | 3413 | 06:52:24.45 | +18:17:06.9 | M4.0 V | Single | |
| 828 | 229 | J06540+608 | GJ 3412 | 3412 | 06:54:05.43 | +60:52:02.4 | M3.0 V | Multiple | |
| 829 | | J06548+332 | HD 265866 | 251 | 06:54:48.03 | +33:15:59.1 | M3.0 V | Single | A.11 |
| 830 | | J06564+121 | TYC 756–1685–1 | | 06:56:25.84 | +12:07:31.4 | M1.0 V | Candidate | |
| 831 | 230 | | GJ 3415 | 3415 | 06:56:28.28 | +40:04:20.6 | K4.5 V | Multiple | A.8 |
| 832 | 230 | J06564+400 | GJ 3416 | 3416 | 06:56:28.64 | +40:04:58.3 | M0.5 V | Multiple | A.8 |
| 833 | | J06564+759 | LP 34–110 | | 06:53:24.30 | +72:55:09.3 | M1.0 V | Candidate | |
| 834 | | J06565+440 | G 107–36 | | 06:56:31.24 | +44:01:45.0 | M4.5 V | Single | |
| 835 | | J06574+740 | PM J06574+7405 | | 06:57:25.77 | +74:05:26.1 | M4.0 V | Candidate | |
| 836 | 231 | J06579+623 | GJ 3417 A | 3417 A | 06:57:57.83 | +62:19:11.0 | M4.5 V | Multiple | |
| 837 | 231 | | GJ 3417 B | 3417 B | 06:57:57.66 | +62:19:10.5 | M5.0 V | Multiple | |
| 838 | | J06582+511 | G 192–59 | | 06:58:12.70 | +51:08:32.4 | M2.0 V | Single | |
| 839 | | J06594+193 | GJ 1093 | 1093 | 06:59:29.84 | +19:20:41.5 | M5.0 V | Single | |
| 840 | | J06594+195 | G 88–2 | | 06:59:28.65 | +19:30:30.4 | M3.0 V | Single | |
| 841 | | J06596+057 | PM J06596+0545 | | 06:59:41.55 | +05:45:38.9 | M2.5 V | Single | |
| 842 | 232 | J07001–190 | IRXS J070005.1–190115 | | 07:00:07.00 | -19:01:25.1 | M5.0 V | Multiple | A.4 |
| 843 | | J07009–023 | PM J07009–0221 | | 07:00:59.74 | -02:21:32.2 | M3.0 V | Single | |
| 844 | | J07012+008 | PM J07012+0052 | | 07:01:15.54 | +00:52:40.4 | M2.5 V | Candidate | |
| 845 | | J07033+346 | GJ 3423 | 3423 | 07:03:23.09 | +34:41:53.6 | M4.0 V | Single | |
| 846 | | J07034+767 | LP 16–379 | | 07:03:29.98 | +76:46:21.9 | M3.5 V | Single | |
| 847 | 233 | J07039+527 | GJ 3421 | 3421 | 07:03:56.92 | +52:41:51.8 | M5.0 V | Multiple | |
| 848 | 234 | J07042–105 | Ross 54 | 263 B | 07:04:17.55 | -10:30:44.6 | M3.5 V | Multiple | |
| 849 | | J07044+682 | GJ 258 | 258 | 07:04:26.94 | +68:17:20.5 | M3.0 V | Single | |
| 850 | | J07047+249 | Ross 874 | 3424 | 07:04:49.44 | +24:59:50.6 | M1.5 V | Single | |
| 851 | | J07051–101 | IRXS J070511.2–100801 | | 07:05:12.10 | -10:07:51.6 | M5.0 V | Single | |
| 852 | | J07052+084 | G 108–52 | | 07:05:12.39 | +08:25:45.7 | M2.0 V | Single | |
| 853 | | J07076+486 | GJ 3426 | 3426 | 07:07:37.70 | +48:41:08.6 | M3.5 V | Single | |
| 854 | | J07078+672 | GJ 3425 | 3425 | 07:07:49.68 | +67:12:03.7 | M1.0 V | Candidate | |
| 855 | | J07081–228 | LP 840–16 | | 07:08:06.53 | -22:48:51.0 | M2.0 V | Candidate | |
| 856 | | J07086+307 | GJ 3429 | 3429 | 07:08:39.72 | +30:42:51.6 | M0.0 V | Single | |
| 857 | | J07095+698 | GJ 3427 | 3427 | 07:09:31.85 | +69:50:53.1 | M2.5 V | Single | |
| 858 | 235 | J07100+385 | QY Aur | 268 | 07:10:01.23 | +38:31:31.0 | M4.5 V | Multiple | A.4 |
| 859 | 236 | | GJ 3431 | 3431 | 07:10:14.04 | +37:40:15.0 | DQ8 | Multiple | A.9 |
| 860 | 236 | J07102+376 | GJ 3430 | 3430 | 07:10:13.32 | +37:40:05.9 | M4.0 V | Multiple+ | A.9 |
| 861 | | J07105–087 | IRXS J071032.6–084232 | | 07:10:31.37 | -08:42:46.7 | M3.5 V | Single | |
| 862 | 237 | J07111+434 | LP 206–11 | | 07:11:11.97 | +43:29:49.0 | M5.5 V | Multiple | |
| 863 | 237 | | LP 206–11 B | | 07:11:12.02 | +43:29:49.3 | M5.5 V | Multiple | |
| 864 | 238 | J07119+773 | TYC 4530–1414–1 | | 07:11:57.13 | +77:21:57.4 | M1.5 V | Multiple | A.4 |
| 865 | | J07121+522 | GJ 3432 | 3432 | 07:12:11.14 | +52:16:20.4 | M1.0 V | Single | |
| 866 | | J07129+357 | IRXS J071259.5+354655 | | 07:12:59.62 | +35:47:03.1 | M2.5 V | Single | |
| 867 | 239 | J07140+507 | G 193–39 | | 07:14:04.29 | +50:43:28.9 | M0.5 V | Multiple | |
| 868 | 239 | | G 193–39B | | 07:14:04.09 | +50:43:28.4 | M5.0 V | Multiple | |
| 869 | 240 | J07163+271 | GJ 268.3 | 268.3 | 07:16:19.73 | +27:08:29.9 | M2.5 V | Multiple | |
| 870 | | J07163+331 | GJ 1096 | 1096 | 07:16:17.89 | +33:09:03.4 | M4.0 V | Single | |
| 871 | | J07172–050 | PM J07172–0501 | | 07:17:17.54 | -05:01:09.8 | M3.5 V | Single | |
| 872 | | J07174+195 | GJ 3437 | 3437 | 07:17:29.57 | +19:34:12.4 | M2.5 V | Single | |
| 873 | 241 | J07181+392 | Ross 987 | 3438 | 07:18:07.89 | +39:16:27.4 | M0.0 V | Multiple | |
| 874 | | J07182+137 | PM J07182+1342 | | 07:18:12.86 | +13:42:16.2 | M3.5 V | Single | |
| 875 | | J07195+328 | GJ 270 | 270 | 07:19:31.79 | +32:49:42.8 | M0.0 V | Single | |
| 876 | | J07199+840 | TYC 4618–116–1 | | 07:19:57.65 | +84:04:36.8 | M2.5 V | Single | |
| 877 | 242 | J07200–087 | Scholz's star | | 07:20:03.21 | -08:46:51.9 | M9.5 V | Multiple | |
| 878 | | J07212+005 | TYC 178–2187–1 | | 07:31:12.97 | +00:33:13.8 | M0.5 V | Single | |
| 879 | | J07227+306 | GJ 3439 | 3439 | 07:22:41.50 | +30:40:02.3 | M3.5 V | Single | |
| 880 | | J07232+460 | GJ 272 | 272 | 07:23:14.71 | +46:05:10.9 | M0.5 V | Single | |
| 881 | | J07274+052 | Luyten's Star | 273 | 07:27:25.11 | +05:12:33.8 | M3.5 V | Single | A.11 |
| 882 | | J07274+220 | Ross 878 | 3441 | 07:27:28.31 | +22:02:35.6 | M1.5 V | Single | |
| 883 | | J07282–187 | GJ 3442 | 3442 | 07:28:13.09 | -18:47:25.2 | M4.5 V | Candidate | |
| 884 | | J07287–032 | GJ 1097 | 1097 | 07:28:45.91 | -03:18:05.9 | M3.0 V | Single | |
| 885 | 243 | J07295+359 | IRXS J072931.4+355607 | | 07:29:31.04 | +35:55:58.5 | M1.5 V | Multiple | |
| 886 | 243 | | 2MASS J07293670+3554531 | | 07:29:36.67 | +35:54:51.3 | M3.0 V | Multiple | A.2 |
| 887 | 244 | G 107–70A | | 275.2 B | 07:30:46.99 | +48:10:05.7 | DA | Multiple | A.9 |
| 888 | 244 | G 107–70B | | | 07:30:46.96 | +48:10:06.3 | DA | Multiple | A.9 |
| 889 | 244 | J07307+481 | GJ 275.2 A | 275.2 A | 07:30:42.46 | +48:11:38.2 | M4.0 V | Multiple | A.9 |
| 890 | 245 | | IRXS J073138.4+455718 | | 07:31:38.47 | +45:57:15.8 | M3.0 V | Multiple | A.4 A.7 |
| 891 | 245 | J07310+460 | IRXS J073101.9+460030 | | 07:31:01.27 | +46:00:24.8 | M4.0 V | Multiple+ | A.7 |
| 892 | 245 | | Gaia DR3 97531298903090560 | | 07:31:09.03 | +45:56:55.6 | M4.5 V | Multiple | A.7 |
| 893 | 246 | J07319+362S | VV LynA | 277 | 07:31:57.38 | +36:13:06.2 | M2.5 V | Multiple | |
| 894 | 246 | J07319+362N | BL Lyn | 277 B | 07:31:56.97 | +36:13:43.2 | M3.5 V | Multiple | |
| 895 | 246 | | VV LynB | | 07:31:57.36 | +36:13:04.6 | M5.0 V | Multiple | |
| 896 | | J07319+392 | GJ 3445 | 3445 | 07:31:56.74 | +39:13:34.0 | M3.0 V | Candidate | |
| 897 | 247 | J07320+173E | GJ 3447 | 3447 | 07:32:02.63 | +17:19:07.0 | M0.0 V | Multiple | |
| 898 | 247 | J07320+173W | GJ 3448 | 3448 | 07:32:01.87 | +17:19:09.4 | M3.0 V | Multiple | |
| 899 | | J07320+686 | GJ 9235 | 9235 | 07:32:01.51 | +68:37:13.6 | M1.0 V | Single | |
| 900 | | J07325+248 | G 88–37 | | 07:32:30.71 | +24:53:42.4 | M3.0 V | Single | |

Table A.1: Complete sample studied in this work^a (cont.).

| Star id. | System id. | Karmn | Name | GJ | α (J2016.0) | δ (J2016.0) | Spectral type | Multiplicity type | In tables |
|----------|------------|-------------|------------------------------|--------|-----------------------|-----------------------|---------------|-------------------|-------------|
| 901 | | J07342+009 | GJ 1099 | 1099 | 07:34:17.57 | +00:58:59.7 | M2.5 V | Single | |
| 902 | | J07344+629 | GJ 9236 | 9236 | 07:34:26.27 | +62:56:27.6 | M0.5 V | Single | |
| 903 | | J07346+223 | GJ 3453 | 3453 | 07:34:39.31 | +22:20:13.9 | M1.0 V | Single | |
| 904 | 248 | | Castor | 278.0 | 07:34:35.95 | +31:53:18.6 | A1 V | Multiple | A.4 |
| 905 | 248 | J07346+318 | Castor C | 278 D | 07:34:37.19 | +31:52:08.6 | M0.5 V | Multiple | A.2 A.4 A.5 |
| 906 | 249 | J07349+147 | TYC 777-141-1 | | 07:34:56.25 | +14:45:52.5 | M3.0 V | Multiple | |
| 907 | 249 | | Gaia DR3 3165346543026736512 | | 07:34:56.18 | +14:45:52.9 | M4.5 V | Multiple | |
| 908 | | J07353+548 | GJ 3452 | 3452 | 07:35:21.67 | +54:50:59.2 | M2.0 V | Single | |
| 909 | | J07354+482 | LP 162-39 | | 07:35:26.96 | +48:14:33.0 | M1.0 V | Single | |
| 910 | | J07359+785 | LP 17-66 | | 07:35:57.31 | +78:32:49.7 | M3.0 V | Single | |
| 911 | 250 | | V869 Mon | 282 A | 07:39:59.40 | -03:35:55.5 | K3 V | Multiple | A.7 A.8 |
| 912 | 250 | | HD 6106B | 282 B | 07:40:02.97 | -03:36:17.8 | K7 V | Multiple | A.7 A.8 |
| 913 | 250 | J07361-031 | GJ 282 C | 282 C | 07:36:07.15 | -03:06:43.4 | M1.0 V | Multiple | A.4 A.7 A.8 |
| 914 | 251 | J07364+070 | GJ 3454 | 3454 | 07:36:25.37 | +07:04:38.2 | M5.0 V | Multiple | |
| 915 | | J07365-006 | PM J07365-0039 | | 07:36:30.27 | -00:39:37.3 | M3.5 V | Candidate | |
| 916 | 252 | J07366+440 | G 111-20 | | 07:36:39.13 | +44:04:43.5 | M3.5 V | Multiple | |
| 917 | 252 | | G 111-20B | | 07:36:38.87 | +44:04:46.5 | M6.5 V | Multiple | |
| 918 | | J07383+344 | TYC 2461-826-1 | | 07:38:19.92 | +34:27:00.6 | M0.0 V | Candidate | |
| 919 | | J07384+240 | IRXS J073829.3+240014 | | 07:38:29.32 | +24:00:07.1 | M3.5 V | Single | |
| 920 | | J07386-212 | GJ 3459 | 3459 | 07:38:41.48 | -21:13:36.1 | M3.0 V | Single | |
| 921 | | J07393+021 | Ross 880 | 281 | 07:39:22.88 | +02:10:57.3 | M0.0 V | Single | |
| 922 | 253 | J07395+334 | GJ 3457 | 3457 | 07:39:35.62 | +33:27:42.6 | M2.0 V | Multiple+ | |
| 923 | 253 | | GJ 3458 | 3458 | 07:39:36.51 | +33:27:49.5 | M6.0 V | Multiple | |
| 924 | 254 | | GJ 283 A | 283 A | 07:40:22.06 | -17:24:57.8 | DZQA6 | Multiple | A.9 |
| 925 | 254 | J07403-174 | GJ 283 B | 283 B | 07:40:20.66 | -17:24:54.5 | M6.0 V | Multiple | A.9 |
| 926 | 255 | J07418+050 | GJ 3461 | 3461 | 07:41:52.56 | +05:02:23.1 | M2.5 V | Multiple | A.4 |
| 927 | 255 | | G 50-1B | | 07:41:52.61 | +05:02:22.4 | M7.0 V | Multiple | |
| 928 | | J07421+500 | LP 162-55 | | 07:42:10.07 | +50:04:28.5 | M2.5 V | Candidate | |
| 929 | | J07431+181 | GJ 3462 | 3462 | 07:43:11.67 | +18:10:34.8 | M1.0 V | Candidate | |
| 930 | | J07446+035 | YZ CMi | 285 | 07:44:39.80 | +03:33:01.7 | M4.5 V | Single | |
| 931 | | J07467+574 | G 193-65 | | 07:46:41.97 | +57:26:49.5 | M4.5 V | Candidate | |
| 932 | | J07470+760 | LP 17-75 | | 07:47:06.48 | +76:03:13.1 | M4.0 V | Single | |
| 933 | | J07472+503 | IRXS J074714.1+502032 | | 07:47:13.84 | +50:20:39.8 | M4.0 V | Single | |
| 934 | | J07482+203 | Wolf 1421 | 289 | 07:48:18.04 | +20:21:49.4 | M1.0 V | Single | |
| 935 | | J07493+849 | GJ 3456 | 3456 | 07:49:17.72 | +84:58:32.5 | M3.0 V | Single | |
| 936 | | J07497-033 | PM J07497-0320 | | 07:49:41.97 | -03:20:34.9 | M3.5 V | Candidate | |
| 937 | | J07518+055 | GJ 3463 | 3463 | 07:51:51.86 | +05:32:50.6 | M4.5 V | Single | |
| 938 | | J07519-000 | GJ 1103 A | 1103 A | 07:51:54.95 | -00:00:24.4 | M4.5 V | Single | |
| 939 | | J07523+162 | LP 423-31 | | 07:52:24.13 | +16:12:09.4 | M6.0 V | Single | |
| 940 | 256 | J07545+085 | IRXS J075434.3+083213 | | 07:54:33.90 | +08:32:25.5 | M2.5 V | Multiple | A.4 |
| 941 | | J07525+063 | GJ 3465 | 3465 | 07:52:33.63 | +06:18:22.0 | M3.0 V | Candidate | |
| 942 | 257 | J07545-096 | PM J07545-0941 | | 07:54:32.60 | -09:41:47.9 | M3.5 V | Multiple | |
| 943 | 257 | | PM J07545-0941B | | 07:54:32.66 | -09:41:48.7 | M4.5 V | Multiple | |
| 944 | | J07558+833 | GJ 1101 | 1101 | 07:55:51.23 | +83:22:55.4 | M4.5 V | Single | |
| 945 | | J07581+072 | GJ 3467 | 3467 | 07:58:08.74 | +07:17:00.9 | M4.0 V | Single | |
| 946 | | J07582+413 | GJ 1105 | 1105 | 07:58:13.01 | +41:18:02.3 | M3.5 V | Single | |
| 947 | | J07583+496 | LP 163-47 | | 07:58:23.26 | +49:39:41.3 | M3.5 V | Single | |
| 948 | 258 | J07585+155N | GJ 3468 | 3468 | 07:58:30.88 | +15:30:12.6 | M3.5 V | Multiple | |
| 949 | 258 | J07585+155S | GJ 3469 A | 3469 A | 07:58:30.37 | +15:29:58.8 | M4.5 V | Multiple | |
| 950 | 258 | | GJ 3469 B | 3469 B | 07:58:30.34 | +15:29:57.8 | M5.0 V | Multiple | |
| 951 | | J07590+153 | GJ 3470 | 3470 | 07:59:05.63 | +15:23:28.3 | M1.5 V | Single | A.11 |
| 952 | | J07591+173 | IRXS J075908.2+171957 | | 07:59:07.07 | +17:19:46.8 | M4.0 V | Candidate | |
| 953 | | J08005+258 | TYC 1930-667-1 | | 08:00:34.87 | +25:53:32.6 | M2.0 V | Candidate | |
| 954 | | J08017+237 | TYC 1926-794-1 | | 08:01:43.44 | +23:42:25.3 | M1.5 V | Candidate | |
| 955 | 259 | J08023+033 | GJ 3473 | 3473 | 08:02:22.45 | +03:20:13.6 | M4.0 V | Multiple | A.11 |
| 956 | 259 | | GJ 3474 | 3474 | 08:02:20.22 | +03:19:37.4 | M6.0 V | Multiple | |
| 957 | | J08025-130 | LP 724-16 | | 08:02:33.09 | -13:05:33.4 | M2.5 V | Candidate | |
| 958 | 260 | J08031+203 | PM J08031+2022 | | 08:03:10.06 | +20:22:14.3 | M3.5 V | Multiple | |
| 959 | 261 | J08033+528 | G 194-7 | | 08:03:20.18 | +52:50:27.3 | M1.5 V | Multiple | |
| 960 | 262 | J08066+558 | GJ 3477 | 3477 | 08:06:36.75 | +55:53:37.1 | M2.0 V | Multiple | |
| 961 | | J08068+367 | GJ 3479 | 3479 | 08:06:48.21 | +36:45:32.5 | M3.0 V | Single | |
| 962 | | J08069+422 | G 111-56 | | 08:06:54.99 | +42:17:28.7 | M4.0 V | Single | |
| 963 | 263 | | GJ 3481 | 3481 | 08:08:12.85 | +21:06:12.6 | K7 V | Multiple | |
| 964 | 263 | J08082+211 | GJ 3482 | 3482 | 08:08:13.29 | +21:06:03.9 | M3.0 V | Multiple | |
| 965 | | J08083+585 | GJ 3480 | 3480 | 08:08:17.82 | +58:31:08.4 | M3.0 V | Single | |
| 966 | 264 | | FP Cnc | 1108 A | 08:08:56.33 | +32:49:08.3 | K7 V | Multiple | |
| 967 | 264 | J08089+328 | FP CncB | | 08:08:55.38 | +32:49:01.4 | M3.0 V | Multiple | A.2 A.4 |
| 968 | | J08095+219 | GJ 3484 | 3484 | 08:09:30.59 | +21:54:16.2 | M1.5 V | Single | |
| 969 | | J08103+095 | PM J08103+0935 | | 08:10:20.65 | +09:35:15.4 | M2.5 V | Single | |
| 970 | 265 | | HD 68146 | 9255 A | 08:10:39.55 | -13:47:56.2 | F6.5 V | Multiple | A.8 |
| 971 | 265 | J08105-138 | L 818-40 A | | 08:10:34.02 | -13:48:50.1 | M2.5 V | Multiple | A.8 |
| 972 | 265 | | L 818-40 B | | 08:10:33.96 | -13:48:49.9 | M4.0 V | Multiple | A.8 |
| 973 | | J08108+039 | GJ 3485 | 3485 | 08:10:53.75 | +03:58:28.2 | M3.5 V | Single | |
| 974 | | J08117+531 | G 194-14 | | 08:11:47.07 | +53:11:48.4 | M2.5 V | Candidate | |
| 975 | | J08119+087 | Ross 619 | 299 | 08:11:58.72 | +08:45:01.4 | M4.5 V | Candidate | |
| 976 | | J08126-215 | GJ 300 | 300 | 08:12:40.90 | -21:33:18.1 | M4.0 V | Single | |
| 977 | | J08158+346 | LP 311-8 | | 08:15:53.78 | +31:36:35.8 | M1.0 V | Candidate | |
| 978 | | J08161+013 | GJ 2066 | 2066 | 08:16:07.58 | +01:18:10.2 | M2.0 V | Single | |
| 979 | | J08175+209 | LP 367-67 | | 08:17:31.31 | +20:59:48.7 | M2.5 V | Single | |
| 980 | | J08178+311 | GJ 3491 | 3491 | 08:17:51.20 | +31:07:49.4 | M1.0 V | Single | |
| 981 | | J08202+055 | PM J08202+0532 | | 08:20:13.29 | +05:32:08.2 | M2.0 V | Single | |
| 982 | | J08258+690 | GJ 3497 | 3497 | 08:25:50.76 | +69:01:40.7 | M5.5 V | Candidate | |

Table A.1: Complete sample studied in this work^a (cont.).

| Star id. | System id. | Karmn | Name | GJ | α (J2016.0) | δ (J2016.0) | Spectral type | Multiplicity type | In tables |
|----------|------------|-------------|-----------------------------|--------|-----------------------|-----------------------|---------------|-------------------|-----------|
| 983 | | J08282+201 | GJ 1110 | 1110 | 08:28:12.37 | +20:08:11.4 | M2.5 V | Single | |
| 984 | 266 | J08283+350 | GJ 308 | 308 | 08:28:20.83 | +35:00:53.6 | M0.0 V | Multiple | |
| 985 | 266 | | Gaia DR3 903444927988618752 | | 08:28:20.82 | +35:00:54.0 | M0.0 V | Multiple | |
| 986 | | J08283+553 | PM J08283+5522 | | 08:28:18.75 | +55:22:40.6 | M2.5 V | Single | |
| 987 | 267 | J08286+660 | 1RXS J082839.4+660229 | | 08:28:41.33 | +66:02:25.4 | M4.0 V | Multiple | |
| 988 | | J08293+039 | PM J08293+0355E | | 08:29:21.81 | +03:55:08.2 | M2.5 V | Single | |
| 989 | | J08298+267 | DX Cnc | 1111 | 08:29:48.02 | +26:46:23.8 | M6.5 V | Single | |
| 990 | 268 | J08313-060 | GJ 3501 | 3501 | 08:31:21.14 | -06:02:02.8 | M1.5 V | Multiple | |
| 991 | 268 | J08314-060 | GJ 3502 | 3502 | 08:31:26.75 | -06:02:13.6 | M3.0 V | Multiple | |
| 992 | | J08313-104 | GJ 3503 | 3503 | 08:31:22.81 | -10:29:58.9 | M4.0 V | Single | |
| 993 | | J08315+730 | LP 35-219 | | 08:31:32.36 | +73:03:50.1 | M4.0 V | Single | |
| 994 | 269 | J08316+193S | CU Cnc | 2069 A | 08:31:37.32 | +19:23:37.5 | M3.5 V | Multiple | A.4 A.5 |
| 995 | 269 | J08316+193N | CV Cnc A | 2069 B | 08:31:37.17 | +19:23:47.6 | M4.0 V | Multiple | |
| 996 | 269 | | CV Cnc B | | 08:31:37.16 | +19:23:46.7 | M5.0 V | Multiple | |
| 997 | | J08317+057 | 1RXS J083147.3+054504 | | 08:31:47.89 | +05:45:17.0 | M1.0 V | Candidate | |
| 998 | | J08321+844 | GJ 3496 | 3496 | 08:32:13.99 | +84:24:34.8 | M3.5 V | Single | |
| 999 | | J08325+451 | Wolf 312 | | 08:32:35.78 | +45:10:16.3 | M2.5 V | Single | |
| 1000 | | J08334+185 | GJ 3505 | 3505 | 08:33:25.06 | +18:31:34.9 | M4.5 V | Single | |
| 1001 | | J08344-011 | GJ 2070 | 2070 | 08:34:26.13 | -01:08:46.3 | M3.5 V | Single | |
| 1002 | 270 | J08353+141 | LSPM J0835+1408 | | 08:35:19.75 | +14:08:31.9 | M4.5 V | Multiple | A.4 |
| 1003 | | J08358+680 | GJ 3506 | 3506 | 08:35:46.65 | +68:04:00.1 | M2.5 V | Single | |
| 1004 | 271 | J08364+264 | LP 311-37 | | 08:36:26.45 | +26:28:18.9 | M2.0 V | Multiple | |
| 1005 | 271 | | LP 311-37 B | | 08:36:26.29 | +26:28:17.9 | M6.5 V | Multiple | |
| 1006 | 272 | J08364+672 | GJ 310 | 310 | 08:36:22.51 | +67:17:42.9 | M0.5 V | Multiple | |
| 1007 | | J08371+151 | GJ 3508 | 3508 | 08:37:07.82 | +15:07:31.2 | M2.5 V | Single | |
| 1008 | | J08375+035 | LSPM J0837+0333 | | 08:37:30.28 | +03:33:43.1 | M4.0 V | Single | |
| 1009 | | J08387+516 | StKM 1-711 | | 08:38:42.06 | +51:41:31.9 | M1.5 V | Single | |
| 1010 | 273 | J08398+089 | GJ 3510 | 3510 | 08:39:47.80 | +08:56:21.0 | M2.0 V | Multiple | |
| 1011 | 273 | | GJ 3511 | 3511 | 08:39:48.25 | +08:56:21.1 | M4.5 V | Multiple | |
| 1012 | | J08402+314 | LSPM J0840+3127 | | 08:40:16.24 | +31:27:08.7 | M3.5 V | Single | |
| 1013 | | J08404+184 | AZ Cnc | 9272 | 08:40:28.77 | +18:24:01.5 | M6.0 V | Single | |
| 1014 | | J08409-234 | GJ 317 | 317 | 08:40:58.67 | -23:27:09.7 | M3.5 V | Single | A.11 |
| 1015 | | J08410+676 | GJ 3509 | 3509 | 08:41:01.83 | +67:39:33.1 | M4.0 V | Single | |
| 1016 | | J08413+594 | GJ 3512 | 3512 | 08:41:19.58 | +59:29:30.0 | M5.5 V | Single | A.11 |
| 1017 | 274 | J08427+095 | GJ 319 A | 319 A | 08:42:44.77 | +09:33:14.0 | M0.0 V | Multiple | A.4 |
| 1018 | 274 | | GJ 319 B | 319 B | 08:42:44.84 | +09:33:15.1 | M4.0 V | Multiple | |
| 1019 | 274 | J08428+095 | GJ 319 C | 319 C | 08:42:52.47 | +09:33:01.3 | M2.5 V | Multiple | |
| 1020 | | J08443-104 | GJ 3513 | 3513 | 08:44:22.71 | -10:24:20.1 | M3.5 V | Single | |
| 1021 | | J08447+182 | G 9-19 | | 08:44:45.08 | +18:12:59.2 | M3.5 V | Candidate | |
| 1022 | 275 | J08449-066 | PM J08449-0637 | | 08:44:55.59 | -06:37:28.2 | M3.5 V | Multiple | |
| 1023 | | J08517+181 | Ross 622 | 1114 | 08:51:42.78 | +18:07:29.1 | M1.5 V | Single | |
| 1024 | 276 | | ρ^0 Cnc | 324 A | 08:52:35.22 | +28:19:47.2 | K0 IV/V | Multiple | A.8 A.11 |
| 1025 | 276 | J08526+283 | ρ^0 Cnc B | 324 B | 08:52:40.28 | +28:18:54.9 | M4.5 V | Multiple | A.8 |
| 1026 | | J08531-202 | PM J08531-2017 | | 08:53:10.96 | -20:17:19.3 | M3.0 V | Single | |
| 1027 | | J08536-034 | GJ 3517 | 3517 | 08:53:35.61 | -03:29:35.4 | M9.0 V | Single | |
| 1028 | | J08537+149 | StKM 1-730 | | 08:53:43.67 | +14:58:09.7 | M0.0 V | Candidate | |
| 1029 | 277 | J08540-131 | GJ 326 A | 326 A | 08:54:05.69 | -13:07:39.9 | M2.5 V | Multiple | |
| 1030 | 277 | | GJ 326 B | 326 B | 08:54:05.63 | -13:07:39.8 | M3.5 V | Multiple | |
| 1031 | | J08551+015 | Ross 623 | 328 | 08:55:07.67 | +01:32:30.7 | M0.0 V | Single | A.11 |
| 1032 | | J08555+664 | PM J08555+6628 | | 08:55:31.46 | +66:28:06.6 | M3.0 V | Single | |
| 1033 | 278 | J08563+126 | G 41-8 | | 08:56:19.49 | +12:39:45.8 | M6.0 V | Multiple | |
| 1034 | 279 | J08570+116 | GJ 330 | 330 | 08:57:04.65 | +11:38:43.9 | M1.0 V | Multiple | |
| 1035 | | J08572+194 | LP 426-35 | | 08:57:15.55 | +19:24:15.2 | M3.5 V | Candidate | |
| 1036 | 280 | J08582+197 | GJ 1116 A | 1116 A | 08:58:14.21 | +19:45:46.7 | M5.5 V | Multiple | |
| 1037 | 280 | | GJ 1116 B | 1116 B | 08:58:14.09 | +19:45:45.3 | M5.5 V | Multiple | A.2 |
| 1038 | | J08588+210 | G 41-13 | | 08:58:52.53 | +21:04:29.1 | M2.0 V | Single | A.11 |
| 1039 | 281 | J08595+537 | G 194-47 | | 08:59:35.41 | +53:43:47.5 | M3.5 V | Multiple | |
| 1040 | 282 | J08589+084 | GJ 3522 | 3522 | 08:58:56.73 | +08:28:20.8 | M3.5 V | Multiple | A.4 |
| 1041 | 282 | | Gaia DR3 585250248258396416 | 3522 B | 08:58:56.76 | +08:28:20.9 | M3.5 V | Multiple | |
| 1042 | | J08599+729 | GJ 3520 | 3520 | 08:59:59.70 | +72:57:35.8 | M4.0 V | Single | |
| 1043 | | J09003+218 | LP 368-128 | | 09:00:22.95 | +21:49:55.4 | M6.5 V | Single | |
| 1044 | | J09005+465 | GJ 1119 | 1119 | 09:00:31.74 | +46:35:02.7 | M4.5 V | Single | |
| 1045 | 283 | J09008+052W | Ross 686 | 9282 A | 09:00:48.25 | +05:14:38.1 | M3.0 V | Multiple | |
| 1046 | 283 | J09008+052E | Ross 687 | 9282 B | 09:00:50.05 | +05:14:26.3 | M3.5 V | Multiple | |
| 1047 | 284 | J09011+019 | Ross 625 | 3527 | 09:01:10.07 | +01:56:33.7 | M3.0 V | Multiple | |
| 1048 | 284 | | Ross 625B | 3527 B | 09:01:10.16 | +01:56:31.0 | M6.0 V | Multiple | |
| 1049 | | J09023+084 | GJ 3528 | 3528 | 09:02:20.55 | +08:28:03.3 | M2.5 V | Single | |
| 1050 | | J09023+177 | PM J09023+1746 | | 09:02:22.91 | +17:46:31.8 | M4.0 V | Single | |
| 1051 | | J09028+680 | GJ 3526 | 3526 | 09:02:53.41 | +68:03:52.1 | M4.0 V | Single | |
| 1052 | | J09029+716 | LSPM J0902+7138 | | 09:02:55.82 | +71:38:11.0 | M1.5 V | Single | |
| 1053 | | J09033+056 | LP 546-37 | | 09:03:20.91 | +05:40:08.5 | M7.0 V | Candidate | |
| 1054 | | J09037+520 | G 194-52 | | 09:03:43.39 | +52:02:49.1 | M3.5 V | Single | |
| 1055 | | J09038+129 | LP 486-43 | | 09:03:53.41 | +12:59:24.8 | M2.0 V | Candidate | |
| 1056 | 285 | | V405 Hya | | 09:04:20.57 | -15:54:51.8 | K2 V | Multiple | A.8 |
| 1057 | 285 | J09040-159 | 1RXS J090406.8-155512 | | 09:04:05.44 | -15:55:19.0 | M2.5 V | Multiple | A.8 |
| 1058 | 286 | J09050+028 | G 114-33A | 3530 | 09:05:04.11 | +02:50:03.9 | M1.5 V | Multiple | |
| 1059 | 286 | | G 114-33B | | 09:05:04.03 | +02:50:03.5 | M3.5 V | Multiple | |
| 1060 | | J09057+186 | LP 426-56 | | 09:05:43.02 | +18:36:27.6 | M2.5 V | Candidate | |
| 1061 | | J09062+128 | GJ 3531 | 3531 | 09:06:13.79 | +12:51:30.1 | M3.5 V | Candidate | |
| 1062 | | J09070-221 | GJ 3533 | 3533 | 09:07:02.40 | -22:08:56.6 | M4.5 V | Candidate | |
| 1063 | | J09087+665 | GJ 3532 | 3532 | 09:08:46.58 | +66:35:36.4 | M2.5 V | Candidate | |
| 1064 | | J09091+227 | 2MASS J09090798+2247413 | | 09:09:07.88 | +22:47:40.1 | M4.5 V | Candidate | |

Table A.1: Complete sample studied in this work^a (cont.).

| Star id. | System id. | Karmn | Name | GJ | α (J2016.0) | δ (J2016.0) | Spectral type | Multiplicity type | In tables |
|----------|------------|-------------|-----------------------------|--------|-----------------------|-----------------------|---------------|-------------------|-----------|
| 1065 | | J09093+401 | GJ 1121 | 1121 | 09:09:23.06 | +40:05:55.5 | M4.0 V | Candidate | |
| 1066 | 287 | J09095+328 | GJ 336 | 336 | 09:09:30.18 | +32:48:59.1 | M0.5 V | Multiple | |
| 1067 | 287 | | BD+33 1814B | | 09:09:30.17 | +32:48:59.5 | M0.0 V | Multiple | |
| 1068 | | J09096+067 | GJ 3537 | 3537 | 09:09:39.07 | +06:42:11.8 | M3.0 V | Single | |
| 1069 | | J09099+004 | G 46–24 | | 09:09:59.43 | +00:23:39.5 | M1.0 V | Single | |
| 1070 | | J09115+126 | LP 487–10 | | 09:11:32.14 | +12:37:18.3 | M2.5 V | Candidate | |
| 1071 | | J09115+466 | GJ 336.1 | 336.1 | 09:11:30.27 | +46:37:00.7 | M0.5 V | Single | |
| 1072 | 288 | J09120+279 | GJ 3540 | 3540 | 09:12:02.44 | +27:54:16.2 | M3.0 V | Multiple | A.4 |
| 1073 | 289 | J09133+688 | G 234–57A | | 09:13:23.43 | +68:52:27.1 | M2.5 V | Multiple | |
| 1074 | 289 | | G 234–57B | | 09:13:23.34 | +68:52:26.7 | M2.0 V | Multiple | |
| 1075 | 290 | J09140+196 | LP 427–16 | | 09:14:03.02 | +19:40:03.2 | M3.0 V | Multiple | A.4 |
| 1076 | 291 | J09143+526 | HD 79210 | 338 A | 09:14:20.05 | +52:41:02.7 | M0.0 V | Multiple | A.4 |
| 1077 | 291 | J09144+526 | HD 79211 | 338 B | 09:14:21.91 | +52:41:00.3 | M0.0 V | Multiple | A.11 |
| 1078 | 292 | J09156–105 | G 161–7 | | 09:15:35.96 | -10:35:50.2 | M5.0 V | Multiple | |
| 1079 | | J09160+293 | G 47–31 | | 09:16:05.04 | +29:19:36.3 | M2.0 V | Single | |
| 1080 | | J09161+018 | RX J0916.1+0153 | | 09:16:10.24 | +01:53:07.2 | M4.0 V | Single | |
| 1081 | | J09163–186 | GJ 3543 | 3543 | 09:16:20.29 | -18:37:30.6 | M1.5 V | Single | |
| 1082 | | J09165+841 | GJ 3536 | 3536 | 09:16:24.75 | +84:11:06.4 | M1.5 V | Candidate | |
| 1083 | | J09168+248 | 2MASS J09165078+2448559 | | 09:16:50.70 | +24:48:54.0 | M4.5 V | Single | |
| 1084 | 293 | J09177+462 | RX J0917.7+4612 | | 09:17:44.52 | +46:12:24.4 | M2.5 V | Multiple | |
| 1085 | | J09177+584 | GJ 3542 | 3542 | 09:17:46.04 | +58:25:02.7 | M4.5 V | Candidate | |
| 1086 | 294 | J09187+267 | GJ 3548 | 3548 | 09:18:45.99 | +26:45:05.4 | M1.5 V | Multiple | |
| 1087 | 294 | | GJ 3549 | 3549 | 09:18:41.19 | +26:45:46.6 | M5.0 V | Multiple | |
| 1088 | 295 | J09193+385S | G 115–68 | | 09:19:18.62 | +38:31:15.9 | M4.0 V | Multiple | |
| 1089 | 295 | J09193+385N | G 115–69 | | 09:19:18.71 | +38:31:23.3 | M4.0 V | Multiple | |
| 1090 | 296 | J09193+620 | GJ 3547 | 3547 | 09:19:22.21 | +62:03:10.7 | M1.0 V | Multiple | |
| 1091 | 297 | J09200+308 | TYC 2493–1386–1 | | 09:20:00.38 | +30:52:39.1 | M1.5 V | Multiple | |
| 1092 | 297 | | 2MASS J09195883+3052156 | | 09:19:58.74 | +30:52:15.0 | M5.0 V | Multiple | |
| 1093 | | J09201+037 | IRXS J092010.8+034731 | | 09:20:10.74 | +03:47:27.0 | M3.5 V | Candidate | |
| 1094 | | J09209+033 | GJ 3553 | 3553 | 09:20:58.28 | +03:21:48.3 | M3.5 V | Single | |
| 1095 | | J09213+731 | GJ 3550 | 3550 | 09:21:16.03 | +73:06:33.1 | M4.5 V | Single | |
| 1096 | 298 | J09218+435 | GJ 3554 | 3554 | 09:21:48.61 | +43:30:26.5 | M4.5 V | Multiple | |
| 1097 | | J09218–023 | RAVE J092148.1–021943 | | 09:21:48.32 | -02:19:43.2 | M2.5 V | Single | |
| 1098 | 299 | J09228+467 | G 115–72 | | 09:22:51.31 | +46:46:58.8 | M1.0 V | Multiple | |
| 1099 | 299 | | G 115–72B | | 09:22:51.44 | +46:47:02.0 | M4.5 V | Multiple | |
| 1100 | 300 | | BD+22 2086A | | 09:23:06.19 | +22:18:17.6 | K5 V | Multiple | A.8 |
| 1101 | 300 | J09231+223 | BD+22 2086B | | 09:23:06.01 | +22:18:25.6 | M0.0 V | Multiple | A.8 |
| 1102 | | J09238+001 | GJ 3555 | 3555 | 09:23:52.36 | +00:08:13.8 | M1.0 V | Single | |
| 1103 | | J09248+306 | LSPM J0924+3041 | | 09:24:50.68 | +30:41:34.2 | M3.5 V | Candidate | |
| 1104 | 301 | J09256+634 | G 235–25 | | 09:25:39.51 | +63:29:14.9 | M4.5 V | Multiple | |
| 1105 | | J09275+506 | GJ 3556 | 3556 | 09:27:30.19 | +50:39:10.1 | M1.5 V | Candidate | |
| 1106 | | J09286–121 | LP 727–31 | | 09:28:41.63 | -12:10:02.0 | M2.5 V | Single | A.11 |
| 1107 | 302 | J09288–073 | Ross 439 | 347 A | 09:28:53.16 | -07:22:27.2 | M2.5 V | Multiple | |
| 1108 | 302 | J09289–073 | GJ 347 B | 347 B | 09:28:55.53 | -07:22:23.3 | M4.5 V | Multiple | |
| 1109 | | J09291+259 | LP 370–26 | | 09:29:09.83 | +25:58:05.0 | M5.0 V | Single | |
| 1110 | | J09300+396 | GJ 3558 | 3558 | 09:30:01.84 | +39:37:21.1 | M2.5 V | Single | |
| 1111 | | J09302+265 | LSPM J0930+2630 | | 09:30:14.24 | +26:30:22.7 | M3.5 V | Single | |
| 1112 | | J09307+003 | GJ 1125 | 1125 | 09:30:43.98 | +00:19:12.8 | M3.5 V | Single | |
| 1113 | | J09308+024 | IRXS J093051.2+022741 | | 09:30:50.81 | +02:27:21.5 | M4.0 V | Candidate | |
| 1114 | 303 | J09313–134 | Ross 440 | 352 | 09:31:20.26 | -13:29:18.9 | M3.0 V | Multiple | |
| 1115 | 303 | | Gaia DR3 569003194858514368 | 352 A | 09:31:20.22 | -13:29:18.9 | M3.0 V | Multiple | |
| 1116 | | J09315+202 | Ross 84 | 9300 | 09:31:33.05 | +20:16:43.6 | M2.0 V | Single | |
| 1117 | | J09319+363 | GJ 353 | 353 | 09:31:56.06 | +36:19:04.4 | M0.0 V | Single | |
| 1118 | 304 | | DX Leo | 9301 A | 09:32:43.58 | +26:59:14.8 | G9 V | Multiple | A.8 |
| 1119 | 304 | J09328+269 | HD 82443B | 9301 B | 09:32:48.07 | +26:59:39.9 | M5.5 V | Multiple | A.8 |
| 1120 | | J09352+612 | GJ 3560 | 3560 | 09:35:13.45 | +61:14:37.6 | M2.0 V | Single | |
| 1121 | | J09360–061 | GJ 3561 | 3561 | 09:36:04.10 | -06:07:01.2 | M3.5 V | Single | |
| 1122 | | J09360–216 | GJ 357 | 357 | 09:36:01.80 | -21:39:54.7 | M2.5 V | Single | A.11 |
| 1123 | 305 | | HD 82939 | | 09:36:15.78 | +37:31:44.1 | G5 V | Multiple | A.8 |
| 1124 | 305 | J09362+375 | GJ 9303 | 9303 | 09:36:04.14 | +37:33:08.9 | M0.0 V | Multiple | A.4 A.8 |
| 1125 | | J09370+405 | GJ 3562 | 3562 | 09:37:03.29 | +40:34:37.7 | M4.0 V | Single | |
| 1126 | | J09394+146 | LP 428–20 | | 09:39:29.77 | +14:38:48.5 | M3.5 V | Single | |
| 1127 | 306 | J09394+317 | G 117–34 | | 09:39:24.04 | +31:45:13.7 | M1.5 V | Multiple | |
| 1128 | 306 | | G 117–34B | | 09:39:23.89 | +31:45:14.1 | M7.5 V | Multiple | |
| 1129 | | J09410+220 | Ross 92 | 359 | 09:41:02.58 | +22:01:20.5 | M4.5 V | Single | |
| 1130 | | J09411+132 | Ross 85 | 361 | 09:41:09.64 | +13:12:32.1 | M1.5 V | Single | |
| 1131 | | J09423+559 | GJ 363 | 363 | 09:42:21.84 | +55:58:53.1 | M3.5 V | Single | |
| 1132 | 307 | J09425+700 | GJ 360 | 360 | 09:42:32.74 | +70:01:57.6 | M2.0 V | Multiple | |
| 1133 | 307 | J09428+700 | GJ 362 | 362 | 09:42:49.63 | +70:02:17.6 | M3.0 V | Multiple | |
| 1134 | | J09425–192 | GJ 3563 | 3563 | 09:42:35.14 | -19:14:08.6 | M2.5 V | Single | |
| 1135 | 308 | J09430+237 | LP 370–35 | | 09:43:01.12 | +23:49:18.3 | M1.0 V | Multiple | |
| 1136 | 308 | | LSPM J0943+2349S | | 09:43:00.94 | +23:49:13.2 | M6.0 V | Multiple | |
| 1137 | 308 | | LP 370–34 | | 09:42:56.96 | +23:51:16.1 | M7.0 V | Multiple | |
| 1138 | | J09439+269 | Ross 93 | 3564 | 09:43:54.92 | +26:58:06.8 | M3.5 V | Single | |
| 1139 | | J09447–182 | GJ 1129 | 1129 | 09:44:45.55 | -18:12:51.7 | M4.0 V | Single | |
| 1140 | | J09449–123 | G 161–71 | | 09:44:53.83 | -12:20:53.7 | M5.0 V | Single | |
| 1141 | 309 | J09461–044 | GJ 3566 | 3566 | 09:46:08.66 | -04:25:40.6 | M4.0 V | Multiple | |
| 1142 | 309 | | G 161–74B | | 09:46:08.66 | -04:25:39.4 | M5.0 V | Multiple | |
| 1143 | | J09468+760 | Ross 434 | 366 | 09:46:48.87 | +76:02:22.1 | M1.5 V | Single | |
| 1144 | | J09473+263 | Ross 94 | | 09:47:22.15 | +26:18:06.9 | M0.0 V | Single | |
| 1145 | | J09475+129 | GJ 3568 | 3568 | 09:47:34.71 | +12:56:42.8 | M4.0 V | Single | |
| 1146 | 310 | J09506–138 | LP 728–70 | | 09:50:40.70 | -13:48:40.2 | M4.0 V | Multiple | A.4 |

Table A.1: Complete sample studied in this work^a (cont.).

| Star id. | System id. | Karmn | Name | GJ | α (J2016.0) | δ (J2016.0) | Spectral type | Multiplicity type | In tables |
|----------|------------|-----------------------------|-----------------|---------|-----------------------|-----------------------|---------------|-------------------|-----------|
| 1147 | | J09488+156 | G 43–2 | | 09:48:50.18 | +15:38:48.5 | M3.0 V | Single | |
| 1148 | | J09511–123 | GJ 369 | 369 | 09:51:10.88 | -12:20:10.8 | M0.5 V | Single | |
| 1149 | | J09526–156 | LP 728–71 | | 09:52:41.65 | -15:36:15.9 | M3.5 V | Single | |
| 1150 | 311 | J09527+554 | G 195–43 | | 09:52:45.26 | +55:28:16.2 | M1.5 V | Multiple | |
| 1151 | 311 | | G 195–43B | | 09:52:45.16 | +55:28:18.8 | M6.0 V | Multiple | |
| 1152 | 312 | J09531–036 | GJ 372 | 372 | 09:53:11.67 | -03:41:31.8 | M2.0 V | Multiple | A.4 |
| 1153 | | J09535+507 | LP 126–73 | | 09:53:32.64 | +50:45:04.2 | M1.5 V | Single | |
| 1154 | | J09539+209 | GJ 3571 | 3571 | 09:53:54.78 | +20:56:53.1 | M4.5 V | Single | |
| 1155 | | J09557+353 | Wolf 330 | 3572 | 09:55:43.55 | +35:21:36.8 | M3.0 V | Single | |
| 1156 | 313 | J09561+627 | GJ 373 | 373 | 09:56:07.96 | +62:47:09.1 | M0.0 V | Multiple | A.4 |
| 1157 | | J09564+226 | GJ 3573 | 3573 | 09:56:26.42 | +22:38:56.9 | M4.0 V | Single | |
| 1158 | | J09579+118 | GJ 3576 | 3576 | 09:57:57.54 | +11:48:26.3 | M4.0 V | Candidate | |
| 1159 | | J09587+555 | G 196–1 | | 09:58:46.62 | +55:32:59.0 | M1.0 V | Candidate | |
| 1160 | | J09589+059 | LP 549–6 | | 09:58:56.31 | +05:57:58.8 | M4.5 V | Single | |
| 1161 | 314 | J09593+438W | GJ 3577 | 3577 | 09:59:18.65 | +43:50:21.9 | M3.5 V | Multiple+ | |
| 1162 | 314 | J09593+438E | GJ 3578 | 3578 | 09:59:20.78 | +43:50:22.1 | M4.0 V | Multiple | |
| 1163 | | J09597+472 | GJ 3579 | 3579 | 09:59:46.11 | +47:12:06.9 | M4.0 V | Single | |
| 1164 | | J09597+721 | PM J09597+7211 | | 09:59:45.30 | +72:12:01.3 | M3.5 V | Single | |
| 1165 | 315 | J10004+272 | GJ 375.2 | 375.2 | 10:00:26.69 | +27:16:03.5 | M0.5 V | Multiple | |
| 1166 | 315 | 2MASS J10003572+2717054 | | | 10:00:35.70 | +27:17:07.5 | M6.5 V | Multiple | |
| 1167 | 315 | Gaia DR3 740041664172917376 | | | 10:00:26.56 | +27:16:05.7 | M7.5 V | Multiple | A.3 |
| 1168 | | J10007+323 | Wolf 335 | | 10:00:43.01 | +32:18:23.1 | M1.0 V | Single | |
| 1169 | | J10020+697 | LP 37–57 | | 10:02:05.67 | +69:45:25.6 | M4.0 V | Single | |
| 1170 | | J10023+480 | GJ 378 | 378 | 10:02:20.74 | +48:04:56.1 | M1.0 V | Single | A.11 |
| 1171 | | J10027+149 | GJ 3582 | 3582 | 10:02:42.62 | +14:59:09.2 | M4.0 V | Candidate | |
| 1172 | 316 | J10028+484 | G 195–55 | | 10:02:48.79 | +48:27:28.7 | M5.5 V | Multiple | |
| 1173 | | J10035+059 | GJ 3583 | 3583 | 10:03:32.76 | +05:57:45.4 | M3.5 V | Single | |
| 1174 | 317 | J10040+187 | GJ 9312 | 9312 | 10:04:05.80 | +18:47:41.5 | M0.5 V | Multiple | |
| 1175 | 318 | J10043+503 | G 196–3 | | 10:04:21.23 | +50:23:10.1 | M2.5 V | Multiple | A.10 |
| 1176 | 318 | | G 196–3B | | 10:04:20.41 | +50:22:56.1 | L3beta | Multiple | A.10 |
| 1177 | | J10067+417 | GJ 3585 | 3585 | 10:06:43.45 | +41:42:46.1 | M0.5 V | Candidate | |
| 1178 | | J10068–127 | PM J10068–1246 | | 10:06:51.98 | -12:46:54.3 | M4.5 V | Candidate | |
| 1179 | | J10069+126 | LP 489–35 | | 10:06:57.49 | +12:40:51.6 | M1.5 V | Single | |
| 1180 | | J10079+692 | GJ 1131 | 1131 | 10:07:56.60 | +69:14:46.1 | M4.0 V | Single | |
| 1181 | | J10087+027 | LP 549–23 | | 10:08:44.52 | +02:43:49.6 | M3.0 V | Single | |
| 1182 | | J10087+355 | Wolf 346 | | 10:08:42.37 | +35:32:51.3 | M1.5 V | Single | |
| 1183 | | J10088+692 | TYC 4384–1735–1 | | 10:08:52.40 | +69:16:35.8 | M0.5 V | Single | A.11 |
| 1184 | | J10094+512 | GJ 3586 | 3586 | 10:09:29.22 | +51:17:06.4 | M4.0 V | Single | |
| 1185 | | J10094+544 | PM J10094+5424 | | 10:09:26.88 | +54:24:22.5 | M2.0 V | Single | |
| 1186 | 319 | J10120–026 | GJ 381 | 381 | 10:12:05.23 | -02:41:14.8 | M2.5 V | Multiple | |
| 1187 | | J10117+353 | Wolf 351 | 3587 | 10:11:44.11 | +35:18:40.1 | M4.0 V | Single | |
| 1188 | | J10122–037 | AN Sex | 382 | 10:12:17.50 | -03:44:48.3 | M1.5 V | Single | |
| 1189 | | J10125+570 | LP 92–48 | | 10:12:34.10 | +57:03:40.5 | M3.5 V | Single | |
| 1190 | 320 | J10130+233 | G 54–18 | | 10:13:00.45 | +23:20:45.9 | M3.5 V | Multiple | |
| 1191 | 321 | J10143+210 | DK Leo | 2079 | 10:14:19.03 | +21:04:26.8 | M0.5 V | Multiple | |
| 1192 | | J10133+467 | LP 167–17 | | 10:13:20.56 | +46:47:24.5 | M5.5 V | Single | |
| 1193 | | J10148+213 | G 54–19 | | 10:14:52.91 | +21:23:42.5 | M4.5 V | Candidate | |
| 1194 | 322 | J10151+314 | GJ 3590 | 3590 | 10:15:06.87 | +31:25:07.0 | M4.0 V | Multiple | |
| 1195 | 322 | | G 118–43B | | 10:15:06.76 | +31:25:08.1 | M3.5 V | Multiple | |
| 1196 | | J10155–164 | PM J10155–1628E | | 10:15:34.86 | -16:28:20.4 | M4.0 V | Candidate | |
| 1197 | | J10158+174 | LSPM J1015+1729 | | 10:15:54.26 | +17:29:27.2 | M3.5 V | Single | |
| 1198 | | J10167–119 | GJ 386 | 386 | 10:16:45.49 | -11:57:52.1 | M3.0 V | Single | |
| 1199 | 323 | J10182–204 | LP 790–2 | | 10:18:13.39 | -20:28:39.3 | M4.5 V | Multiple | A.4 |
| 1200 | 323 | | LP 790–1 | | 10:18:11.66 | -20:28:19.3 | M4.5 V | Multiple | |
| 1201 | 324 | J10185–117 | LP 729–54 | | 10:18:34.77 | -11:43:04.2 | M4.0 V | Multiple | A.11 |
| 1202 | 324 | | LP 729–55 | | 10:18:35.83 | -11:43:06.2 | M3.5 V | Multiple | |
| 1203 | | J10196+198 | AD Leo | 388 | 10:19:35.72 | +19:52:11.3 | M3.0 V | Single | |
| 1204 | | J10200+289 | G 118–51 | | 10:20:00.23 | +28:57:09.5 | M3.0 V | Single | |
| 1205 | | J10206+492 | GJ 3595 | 3595 | 10:20:37.15 | +49:17:43.2 | M2.5 V | Single | |
| 1206 | | J10238+438 | LP 212–62 | | 10:23:52.13 | +43:53:33.2 | M5.0 V | Single | |
| 1207 | | J10240+366 | PM J10240+3639 | | 10:24:05.04 | +36:39:30.2 | M3.5 V | Candidate | |
| 1208 | 325 | J10243+119 | GJ 3598 | 3598 | 10:24:20.16 | +11:57:23.5 | M2.0 V | Multiple | |
| 1209 | | J10251–102 | GJ 390 | 390 | 10:25:10.09 | -10:13:41.3 | M1.0 V | Single | |
| 1210 | | J10255+263 | GJ 3599 | 3599 | 10:25:29.93 | +26:23:09.8 | M3.5 V | Single | |
| 1211 | 326 | J10260+504W | GJ 3600 | 3600 | 10:26:01.99 | +50:27:00.0 | M4.0 V | Multiple | |
| 1212 | 326 | J10260+504E | GJ 3601 | 3601 | 10:26:02.64 | +50:27:13.0 | M4.0 V | Multiple | |
| 1213 | | J10273+799 | PM J10273+7959 | | 10:27:22.67 | +79:59:50.0 | M2.0 V | Candidate | |
| 1214 | | J10278+028 | G 44–19 | | 10:27:49.12 | +02:51:35.5 | M3.5 V | Candidate | |
| 1215 | 327 | J10284+482 | GJ 3602 | 3602 | 10:28:28.86 | +48:14:17.7 | M3.5 V | Multiple | |
| 1216 | 327 | | G 146–35B | | 10:28:28.87 | +48:14:17.8 | M3.5 V | Multiple | |
| 1217 | 328 | J10286+322 | GJ 3604 | 3604 | 10:28:40.73 | +32:14:21.7 | M2.5 V | Multiple | |
| 1218 | 328 | | G 118–61B | | 10:28:40.84 | +32:14:23.1 | M4.0 V | Multiple | |
| 1219 | | J10289+008 | Ross 446 | 393 | 10:28:54.91 | +00:50:15.9 | M2.0 V | Single | A.11 |
| 1220 | | J10303+328 | GJ 3607 | 3607 | 10:30:23.19 | +32:50:07.3 | M3.5 V | Single | |
| 1221 | 329 | | GJ 397.1 | 397.1 | 10:31:43.09 | +57:06:59.9 | K5 V | Multiple | A.8 |
| 1222 | 329 | J10315+570 | GJ 397.1 B | 397.1 B | 10:31:30.64 | +57:05:20.4 | M4.5 V | Multiple | A.2 A.8 |
| 1223 | | J10320+033 | PM J10320+0318 | | 10:32:02.31 | +03:18:54.9 | M2.0 V | Candidate | |
| 1224 | 330 | J10345+463 | GJ 3610 | 3610 | 10:34:29.53 | +46:18:07.2 | M3.0 V | Multiple | |
| 1225 | 330 | | GJ 3611 | 3611 | 10:34:25.22 | +46:18:20.8 | M4.5 V | Multiple | |
| 1226 | | J10350–094 | LP 670–17 | | 10:35:01.36 | -09:24:41.5 | M3.0 V | Single | |
| 1227 | 331 | J10354+694 | GJ 3612 | 3612 | 10:35:21.96 | +69:26:48.5 | M4.0 V | Multiple | |
| 1228 | | J10359+288 | RX J1035.9+2853 | | 10:35:57.12 | +28:53:30.3 | M3.0 V | Candidate | |

Table A.1: Complete sample studied in this work^a (cont.).

| Star id. | System id. | Karmn | Name | GJ | α (J2016.0) | δ (J2016.0) | Spectral type | Multiplicity type | In tables |
|----------|------------|-------------|------------------------------|--------|-----------------------|-----------------------|---------------|-------------------|-----------|
| 1229 | | J10360+051 | RY Sex | 398 | 10:36:00.52 | +05:07:14.8 | M3.5 V | Single | |
| 1230 | 332 | J10364+415 | G 146–48 | | 10:36:27.19 | +41:30:02.8 | M2.5 V | Multiple | |
| 1231 | 332 | | G 146–48B | | 10:36:27.02 | +41:30:01.8 | M5.5 V | Multiple | |
| 1232 | 333 | J10367+153 | PM J10367+1521A | | 10:36:44.96 | +15:21:38.6 | M3.5 V | Multiple | |
| 1233 | 333 | | PM J10367+1521B | | 10:36:44.92 | +15:21:37.9 | M4.5 V | Multiple | A.2 |
| 1234 | 334 | J10368+509 | LP 127–502 | | 10:36:48.58 | +50:55:00.7 | M4.5 V | Multiple | A.4 |
| 1235 | 335 | J10379+127 | LP 490–42 A | | 10:37:55.05 | +12:46:36.8 | M3.0 V | Multiple | |
| 1236 | 335 | | LP 490–42 B | | 10:37:55.03 | +12:46:37.6 | M3.0 V | Multiple | |
| 1237 | | J10384+485 | GJ 3613 | 3613 | 10:38:29.47 | +48:31:43.4 | M3.0 V | Single | |
| 1238 | | J10385+354 | LP 262–400 | | 10:38:32.66 | +35:29:53.7 | M2.5 V | Single | |
| 1239 | | J10389+250 | StKM 1–873 | | 10:38:56.64 | +25:05:39.0 | M2.0 V | Single | |
| 1240 | | J10396–069 | GJ 399 | 399 | 10:39:39.79 | -06:55:27.2 | M2.5 V | Single | |
| 1241 | | J10403+015 | TYC 254–88–1 | | 10:40:21.42 | +01:34:36.6 | M1.0 V | Single | |
| 1242 | | J10416+376 | GJ 1134 | 1134 | 10:41:35.91 | +37:36:33.4 | M4.5 V | Single | |
| 1243 | 336 | J10430–092 | PM J10430–0912 | | 10:43:00.72 | -09:12:35.0 | M5.5 V | Multiple | |
| 1244 | | J10443+124 | LP 490–63 | | 10:44:18.52 | +12:25:11.5 | M3.5 V | Single | |
| 1245 | 337 | J10448+324 | GJ 3616 A | 3616 A | 10:44:52.40 | +32:24:41.3 | M3.0 V | Multiple | A.2 |
| 1246 | 337 | | GJ 3616 B | 3616 B | 10:44:52.43 | +32:24:40.1 | M4.0 V | Multiple | A.2 |
| 1247 | 337 | | GJ 3617 | 3617 | 10:44:54.79 | +32:24:23.4 | M5.0 V | Multiple | A.2 |
| 1248 | 338 | J10453+385 | GJ 400 A | 400 A | 10:45:21.43 | +38:30:44.8 | M0.5 V | Multiple | 5 |
| 1249 | 338 | | Gaia DR3 776067093937332992 | | 10:45:21.39 | +38:30:44.4 | M2.5 V | Multiple | 5 |
| 1250 | 339 | | GJ 401 B | 401 B | 10:45:36.93 | -19:06:54.7 | DQ | Multiple | A.9 |
| 1251 | 339 | J10456–191 | GJ 401 | 401 | 10:45:36.98 | -19:07:01.3 | M0.5 V | Multiple | A.9 |
| 1252 | | J10460+096 | GJ 3619 | 3619 | 10:46:03.81 | +09:41:47.1 | M3.5 V | Single | |
| 1253 | 340 | J10472+404 | LP 213–67 | | 10:47:12.19 | +40:26:43.2 | M7.0 V | Multiple | |
| 1254 | 340 | | LP 213–68 | | 10:47:13.36 | +40:26:48.7 | M8.0 V | Multiple+ | |
| 1255 | 341 | J10474+025 | Ross 895 | | 10:47:24.47 | +02:35:32.7 | M2.0 V | Multiple | |
| 1256 | | J10482–113 | GJ 3622 | 3622 | 10:48:13.24 | -11:20:34.1 | M6.5 V | Single | |
| 1257 | | J10485+191 | GJ 3623 | 3623 | 10:48:32.84 | +19:09:00.3 | M3.0 V | Single | |
| 1258 | 342 | J10497+355 | GJ 1138 | 1138 | 10:49:44.71 | +35:32:34.3 | M4.5 V | Multiple | |
| 1259 | 343 | J10504+331 | GJ 3626 | 3626 | 10:50:26.08 | +33:05:54.0 | M4.0 V | Multiple | A.4 |
| 1260 | 344 | | LZ UMa | 3627 | 10:50:39.98 | +51:47:58.8 | G5 V | Multiple+ | A.8 |
| 1261 | 344 | J10506+517 | GJ 3628 | 3628 | 10:50:37.91 | +51:45:01.6 | M3.5 V | Multiple | A.2 A.8 |
| 1262 | 345 | J10508+068 | EE Leo | 402 | 10:50:51.11 | +06:48:16.2 | M4.0 V | Multiple | |
| 1263 | 346 | J10513+361 | GJ 3629 | 3629 | 10:51:20.33 | +36:07:24.5 | M3.0 V | Multiple | |
| 1264 | 347 | J10520+005 | GJ 3630 | 3630 | 10:52:02.83 | +00:32:38.5 | M4.0 V | Multiple | A.4 |
| 1265 | | J10520+139 | GJ 403 | 403 | 10:52:03.01 | +13:59:54.5 | M3.5 V | Single | |
| 1266 | | J10522+059 | GJ 3631 | 3631 | 10:52:13.50 | +05:55:08.9 | M5.0 V | Single | |
| 1267 | 348 | J10546–073 | LP 671–8 | | 10:54:41.77 | -07:18:39.4 | M4.0 V | Multiple | |
| 1268 | 348 | | Gaia DR3 3763681220170173952 | | 10:54:41.83 | -07:18:39.1 | M4.0 V | Multiple | |
| 1269 | | J10555–093 | GJ 3632 | 3632 | 10:55:34.19 | -09:21:18.7 | M3.5 V | Single | |
| 1270 | | J10563+042 | PM J10563+0415 | | 10:56:22.32 | +04:15:44.6 | M2.5 V | Single | |
| 1271 | | J10564+070 | CN Leo | 406 | 10:56:24.77 | +07:00:09.8 | M6.0 V | Single | |
| 1272 | | J10576+695 | Ross 447 | 9341 | 10:57:36.16 | +69:35:48.8 | M0.0 V | Single | |
| 1273 | | J10584–107 | LP 731–76 | | 10:58:27.78 | -10:46:31.8 | M5.0 V | Single | |
| 1274 | | J11000+228 | Ross 104 | 408 | 11:00:03.76 | +22:49:54.1 | M2.5 V | Single | |
| 1275 | 349 | J11003+728 | G 254–11A | | 11:00:23.29 | +72:52:17.6 | M2.0 V | Multiple | |
| 1276 | 349 | | G 254–11B | | 11:00:23.11 | +72:52:18.3 | M4.0 V | Multiple | |
| 1277 | | J11008+120 | GJ 3636 | 3636 | 11:00:50.58 | +12:04:08.7 | M5.0 V | Candidate | |
| 1278 | | J11013+030 | GJ 3637 | 3637 | 11:01:20.81 | +03:00:10.8 | M4.0 V | Single | |
| 1279 | | J11014+568 | StKM 1–902 | | 11:01:26.72 | +56:52:04.0 | M1.0 V | Single | |
| 1280 | 350 | J11023+165E | GJ 1141 A | 1141 A | 11:02:19.29 | +16:30:27.1 | M1.0 V | Multiple | |
| 1281 | 350 | J11023+165W | GJ 1141 B | 1141 B | 11:02:18.02 | +16:30:30.8 | M1.0 V | Multiple | |
| 1282 | | J11026+219 | DS Leo | 410 | 11:02:38.51 | +21:58:00.9 | M1.0 V | Single | |
| 1283 | | J11030+037 | Wolf 360 | | 11:03:04.39 | +03:44:19.2 | M2.5 V | Candidate | |
| 1284 | | J11031+152 | LP 431–50 | | 11:03:08.01 | +15:17:50.3 | M3.5 V | Candidate | |
| 1285 | | J11031+366 | GJ 3639 | 3639 | 11:03:09.74 | +36:39:09.1 | M3.5 V | Single | |
| 1286 | | J11033+359 | Lalande 21185 | 411 | 11:03:19.43 | +35:56:55.2 | M1.5 V | Single | A.11 |
| 1287 | 351 | J11036+136 | LP 491–51 | | 11:03:21.05 | +13:37:58.2 | M4.0 V | Multiple | A.4 |
| 1288 | | J11042+400 | GJ 3640 | 3640 | 11:04:15.64 | +40:00:15.1 | M0.0 V | Candidate | |
| 1289 | | J11044+304 | LSPM J1104+3027 | | 11:04:28.35 | +30:27:30.9 | M3.0 V | Single | |
| 1290 | 352 | J11054+435 | GJ 412 A | 412 A | 11:05:22.09 | +43:31:51.4 | M1.0 V | Multiple | |
| 1291 | 352 | J11055+435 | WX UMa | 412 B | 11:05:24.50 | +43:31:33.3 | M5.5 V | Multiple | |
| 1292 | 353 | J11055+450 | GJ 3641 | 3641 | 11:05:33.91 | +45:00:27.9 | M0.0 V | Multiple | |
| 1293 | 353 | | G 176–8B | | 11:05:33.92 | +45:00:30.5 | M6.0 V | Multiple | |
| 1294 | | J11057+102 | GJ 3643 | 3643 | 11:05:43.80 | +10:13:58.1 | M2.5 V | Single | |
| 1295 | | J11075+437 | PM J11075+4345 | | 11:07:31.88 | +43:45:56.3 | M3.0 V | Single | |
| 1296 | 354 | | GJ 1142 B | 1142 B | 11:07:59.89 | -05:09:33.1 | DA3 | Multiple | A.9 |
| 1297 | 354 | J11081–052 | GJ 1142 A | 1142 A | 11:08:06.48 | -05:13:54.2 | M3.0 V | Multiple | A.9 |
| 1298 | | J11108+479 | GJ 3646 | 3646 | 11:10:51.05 | +47:56:53.7 | M4.0 V | Single | |
| 1299 | 355 | J11110+304E | HD 97101 | 414 A | 11:11:05.90 | +30:26:42.5 | K7 V | Multiple | A.11 |
| 1300 | 355 | J11110+304W | HD 97101B | 414 B | 11:11:03.29 | +30:26:38.0 | M2.0 V | Multiple | |
| 1301 | 356 | J11113+434 | GJ 9351 A | 9351 A | 11:11:18.88 | +43:24:55.8 | M2.5 V | Multiple | |
| 1302 | 356 | | GJ 9351 B | 9351 B | 11:11:18.56 | +43:24:55.3 | M2.5 V | Multiple | |
| 1303 | | J11118+335 | CW Uma | 3647 | 11:11:51.52 | +33:32:13.1 | M3.5 V | Single | |
| 1304 | | J11126+189 | GJ 3649 | 3649 | 11:12:38.95 | +18:56:05.5 | M1.5 V | Single | |
| 1305 | 357 | J11131+002 | Wolf 370 | 3650 | 11:13:09.63 | +00:14:16.7 | M0.0 V | Multiple | |
| 1306 | 358 | | HD 97584 | 420 A | 11:15:10.39 | +73:28:32.5 | K4 V | Multiple | A.8 |
| 1307 | 358 | J11151+734 | HD 97584B | 420 B | 11:15:09.56 | +73:28:38.0 | M2.5 V | Multiple | A.8 |
| 1308 | | J11152+194 | GJ 3652 | 3652 | 11:15:12.62 | +19:27:04.3 | M3.5 V | Single | |
| 1309 | 359 | | GJ 421 A | 421 A | 11:15:20.90 | -18:08:49.2 | K7 V | Multiple | |
| 1310 | 359 | | GJ 421 B | 421 B | 11:15:19.61 | -18:08:52.0 | K5 V | Multiple | |

Table A.1: Complete sample studied in this work^a (cont.).

| Star id. | System id. | Karmn | Name | GJ | α (J2016.0) | δ (J2016.0) | Spectral type | Multiplicity type | In tables |
|----------|------------|------------|-----------------------------|---------|-----------------------|-----------------------|---------------|-------------------|-----------|
| 1311 | 359 | J11152-181 | GJ 421 C | 421 C | 11:15:15.67 | -18:07:47.8 | M3.0 V | Multiple | |
| 1312 | | J11154+410 | G 122-8 | | 11:15:26.72 | +41:05:12.5 | M3.5 V | Single | |
| 1313 | | J11159+553 | GJ 3653 | 3653 | 11:15:53.69 | +55:19:49.2 | M0.5 V | Candidate | |
| 1314 | | J11195+466 | LP 169-22 | | 11:19:31.09 | +46:41:33.4 | M5.5 V | Single | |
| 1315 | | J11200+658 | GJ 424 | 424 | 11:19:57.14 | +65:50:50.3 | M0.0 V | Single | |
| 1316 | | J11201-104 | LP 733-99 | | 11:20:05.89 | -10:29:46.4 | M2.0 V | Single | |
| 1317 | 360 | | HD 98712A | 425 A | 11:21:26.87 | -20:27:15.3 | K7 V | Multiple | |
| 1318 | 360 | J11214-204 | HD 98712B | 425 B | 11:21:26.84 | -20:27:11.5 | M2.5 V | Multiple | A.2 |
| 1319 | | J11216+061 | GJ 1146 | 1146 | 11:21:37.67 | +06:08:00.7 | M3.0 V | Single | |
| 1320 | 361 | J11231+258 | GJ 3657 | 3657 | 11:23:06.77 | +25:53:31.7 | M5.0 V | Multiple | A.10 |
| 1321 | 361 | | 2MASS J11225550+2550250 | | 11:22:55.50 | +25:50:25.1 | T6 | Multiple | A.10 |
| 1322 | | J11233+448 | GJ 3658 | 3658 | 11:23:20.14 | +44:48:36.5 | M2.5 V | Single | |
| 1323 | | J11237+085 | Wolf 386 | 2085 | 11:23:43.49 | +08:33:51.6 | M0.5 V | Single | |
| 1324 | 362 | | GJ 426.1 A | 426.1 A | 11:23:55.62 | +10:31:44.9 | F1 IV | Multiple | A.4 A.8 |
| 1325 | 362 | | GJ 426.1 B | 426.1 B | 11:23:55.75 | +10:31:44.7 | F5 V | Multiple | A.2 A.8 |
| 1326 | 362 | J11238+106 | LSPM J1123+1037 | | 11:23:50.12 | +10:37:07.0 | M0.5 V | Multiple+ | A.8 |
| 1327 | | J11239-183 | Ross 1002 | 3659 | 11:23:56.61 | -18:21:49.5 | M3.0 V | Candidate | |
| 1328 | | J11247+675 | Ross 448 | | 11:24:46.53 | +67:33:08.5 | M1.0 V | Single | |
| 1329 | | J11249+024 | StKM 1-941 | | 11:24:58.52 | +02:28:26.8 | M1.0 V | Single | |
| 1330 | 363 | J11240+381 | 1RXS J112405.0+380809 | | 11:24:04.53 | +38:08:10.7 | M4.5 V | Multiple | |
| 1331 | 363 | | 2MUCD 10984 | | 11:24:05.06 | +38:08:05.3 | M8.5 V | Multiple | |
| 1332 | 364 | J11254+782 | GJ 3660 | 3660 | 11:25:26.06 | +78:15:52.9 | M2.0 V | Multiple | |
| 1333 | 364 | | GJ 3661 | 3661 | 11:25:13.53 | +78:16:55.0 | M3.0 V | Multiple | |
| 1334 | 365 | J11266+379 | PM J11266+3756 | | 11:26:37.40 | +37:56:22.8 | M2.0 V | Multiple | |
| 1335 | 365 | | PM J11266+3756B | | 11:26:37.31 | +37:56:22.5 | M1.5 V | Multiple | |
| 1336 | | J11276+039 | GJ 3664 | 3664 | 11:27:38.47 | +03:58:36.1 | M0.0 V | Single | |
| 1337 | | J11289+101 | Wolf 398 | 3666 | 11:28:55.45 | +10:10:48.2 | M3.5 V | Single | |
| 1338 | | J11302+076 | K2-18 | | 11:30:14.43 | +07:35:16.1 | M3.0 V | Single | A.11 |
| 1339 | | J11306-080 | LP 672-42 | | 11:30:41.44 | -08:05:38.9 | M3.5 V | Single | |
| 1340 | 366 | J11307+549 | StKM 1-950 | | 11:30:43.80 | +54:57:29.1 | M1.0 V | Multiple | |
| 1341 | 366 | | Gaia DR3 844502037681090688 | | 11:30:42.66 | +54:56:57.0 | M6.0 V | Multiple | |
| 1342 | | J11311-149 | GJ 3668 | 3668 | 11:31:08.84 | -14:57:43.2 | M4.5 V | Single | |
| 1343 | | J11315+022 | LP 552-68 | | 11:31:32.21 | +02:13:34.8 | M2.5 V | Single | |
| 1344 | | J11317+226 | Ross 903 | 9365 | 11:31:42.72 | +22:40:02.2 | M0.5 V | Single | |
| 1345 | | J11351-056 | GJ 3672 | 3672 | 11:35:07.66 | -05:39:38.2 | M4.5 V | Single | |
| 1346 | 367 | J11355+389 | GJ 3673 | 3673 | 11:35:30.94 | +38:55:33.4 | M3.5 V | Multiple | 5 |
| 1347 | 367 | | G 122-34B | | 11:35:30.95 | +38:55:33.4 | M3.0 V | Multiple | 5 |
| 1348 | | J11376+587 | Ross 112 | 3676 | 11:37:38.30 | +58:42:38.2 | M2.5 V | Candidate | |
| 1349 | | J11404+770 | LP 19-403 | | 11:40:27.09 | +77:04:19.0 | M2.0 V | Single | |
| 1350 | | J11417+427 | Ross 1003 | 1148 | 11:41:43.80 | +42:45:05.7 | M4.0 V | Single | A.11 |
| 1351 | | J11420+147 | Ross 115 | 3681 | 11:42:01.43 | +14:46:39.9 | M3.0 V | Single | |
| 1352 | | J11421+267 | Ross 905 | 436 | 11:42:12.16 | +26:42:10.6 | M2.5 V | Single | A.11 |
| 1353 | 368 | J11423+230 | LP 375-23 | | 11:42:18.14 | +23:01:37.3 | M0.5 V | Multiple | A.11 |
| 1354 | 368 | | LP 375-24 | | 11:42:20.98 | +23:03:14.8 | M4.0 V | Multiple | |
| 1355 | | J11433+253 | GJ 3682 | 3682 | 11:43:23.27 | +25:18:13.2 | M4.0 V | Candidate | |
| 1356 | | J11451+183 | LP 433-47 | | 11:45:11.57 | +18:20:53.8 | M4.0 V | Single | |
| 1357 | | J11467-140 | GJ 443 | 443 | 11:46:43.69 | -14:01:04.4 | M3.0 V | Single | |
| 1358 | 369 | J11470+700 | GJ 3684 A | 3684 A | 11:47:04.37 | +70:01:57.7 | M4.0 V | Multiple | |
| 1359 | 369 | | GJ 3684 B | 3684 B | 11:47:04.25 | +70:01:58.4 | M3.5 V | Multiple | |
| 1360 | | J11474+667 | 1RXS J114728.8+664405 | | 11:47:28.27 | +66:44:02.6 | M5.0 V | Candidate | |
| 1361 | 370 | J11476+002 | GJ 3685 | 3685 | 11:47:40.41 | +00:15:18.5 | M4.0 V | Multiple | |
| 1362 | 370 | | GJ 3686 | 3686 | 11:47:41.77 | +00:15:04.4 | M5.0 V | Multiple | |
| 1363 | | J11476+786 | GJ 445 | 445 | 11:47:45.46 | +78:41:35.9 | M3.5 V | Single | |
| 1364 | | J11477+008 | Fl Vir | 447 | 11:47:45.05 | +00:47:56.8 | M4.0 V | Single | A.11 |
| 1365 | | J11483-112 | GJ 3688 | 3688 | 11:48:18.61 | -11:17:15.0 | M3.0 V | Single | |
| 1366 | | J11485+076 | G 10-52 | | 11:48:35.63 | +07:41:37.8 | M3.5 V | Single | |
| 1367 | | J11496+220 | BPM 87650 | | 11:49:40.33 | +22:03:52.5 | M0.0 V | Candidate | |
| 1368 | | J11509+483 | GJ 1151 | 1151 | 11:50:55.24 | +48:22:23.2 | M4.5 V | Single | |
| 1369 | | J11511+352 | GJ 450 | 450 | 11:51:06.98 | +35:16:23.3 | M1.5 V | Single | |
| 1370 | 371 | J11519+075 | RX J1151.9+0731 | | 11:51:56.69 | +07:31:25.2 | M2.5 V | Multiple | |
| 1371 | | J11529+244 | GJ 3691 | 3691 | 11:52:57.55 | +24:28:46.9 | M4.5 V | Single | |
| 1372 | | J11532-073 | GJ 452 | 452 | 11:53:15.91 | -07:22:35.8 | M2.5 V | Single | |
| 1373 | | J11533+430 | TYC 3016-577-1 | | 11:53:23.24 | +43:02:56.3 | M1.0 V | Single | |
| 1374 | | J11538+069 | GJ 3693 | 3693 | 11:53:53.01 | +06:59:41.9 | M6.0 V | Single | |
| 1375 | | J11541+098 | Ross 119 | 9375 | 11:54:07.98 | +09:48:10.0 | M3.5 V | Single | |
| 1376 | | J11549-021 | PM J11549-0206 | | 11:54:56.83 | -02:06:08.4 | M3.0 V | Single | |
| 1377 | | J11551+009 | Ross 129 | 9381 | 11:55:06.42 | +00:58:26.1 | M1.5 V | Single | |
| 1378 | | J11557-189 | GJ 3694 | 3694 | 11:55:44.87 | -18:54:36.6 | M3.5 V | Single | |
| 1379 | | J11557-227 | LP 851-346 | | 11:55:42.42 | -22:25:01.8 | M7.5 V | Single | |
| 1380 | | J11575+118 | Ross 122 | 3695 | 11:57:32.06 | +11:49:43.7 | M2.0 V | Single | |
| 1381 | | J11582+425 | GJ 3696 | 3696 | 11:58:17.81 | +42:34:23.0 | M4.0 V | Single | |
| 1382 | 372 | J11521+039 | StM 162 | | 11:52:09.87 | +03:57:21.4 | M4.0 V | Multiple | |
| 1383 | 373 | J11589+426 | GJ 3697 | 3697 | 11:58:58.99 | +42:39:40.8 | M1.5 V | Multiple | |
| 1384 | 374 | J11585+595 | G 197-38 | | 11:58:33.53 | +59:33:22.2 | M0.0 V | Multiple | |
| 1385 | 375 | J12006-138 | GJ 3698 | 3698 | 12:00:36.36 | -13:49:36.6 | M3.5 V | Multiple | |
| 1386 | 375 | | GJ 3699 | 3699 | 12:00:35.98 | -13:49:40.6 | M4.5 V | Multiple | |
| 1387 | 376 | J12016-122 | GJ 3700 | 3700 | 12:01:40.72 | -12:13:57.6 | M3.0 V | Multiple | |
| 1388 | 376 | | L 829-10 B | | 12:01:40.90 | -12:13:52.0 | M7.0 V | Multiple | |
| 1389 | | J12054+695 | Ross 689 | 3704 | 12:05:28.29 | +69:32:21.7 | M4.0 V | Single | |
| 1390 | | J12057+784 | LSPM J1205+7825 | | 12:05:45.99 | +78:25:51.6 | M2.5 V | Candidate | |
| 1391 | 377 | J12023+285 | GJ 455 | 455 | 12:02:17.12 | +28:35:13.4 | M2.5 V | Multiple | |
| 1392 | | J12088+303 | 1RXS J120847.7+302120 | | 12:08:49.63 | +30:21:00.5 | M2.5 V | Single | A.4 |

Table A.1: Complete sample studied in this work^a (cont.).

| Star id. | System id. | Karmn | Name | GJ | α (J2016.0) | δ (J2016.0) | Spectral type | Multiplicity type | In tables |
|----------|------------|-------------|------------------------------|--------|-----------------------|-----------------------|---------------|-------------------|-----------|
| 1393 | | J12093+210 | StM 165 | | 12:09:21.70 | +21:03:05.8 | M2.5 V | Candidate | |
| 1394 | | J12100-150 | GJ 3707 | 3707 | 12:10:05.54 | -15:04:28.4 | M3.5 V | Single | |
| 1395 | 378 | J12063-132 | 1RXS J120622.6-131453 | | 12:06:22.22 | -13:14:57.2 | M3.5 V | Multiple | |
| 1396 | | J12109+410 | GJ 9393 | 9393 | 12:10:56.90 | +41:03:31.7 | M0.0 V | Single | A.4 |
| 1397 | 379 | J12104-131 | LP 734-34 | | 12:10:28.65 | -13:10:29.5 | M4.5 V | Multiple | |
| 1398 | 380 | J12111-199 | GJ 3708 | 3708 | 12:11:11.52 | -19:57:41.0 | M3.0 V | Multiple | |
| 1399 | 380 | J12112-199 | GJ 3709 | 3709 | 12:11:16.71 | -19:58:24.7 | M3.5 V | Multiple | |
| 1400 | 381 | J12121+488 | GJ 3713 | 3713 | 12:12:11.68 | +48:48:58.3 | M2.5 V | Multiple | |
| 1401 | 381 | G 122-74B | | | 12:12:11.74 | +48:48:55.5 | M4.5 V | Multiple | |
| 1402 | | J12122+714 | LP 39-66 | | 12:12:13.89 | +71:25:26.2 | M3.0 V | Single | |
| 1403 | 382 | J12123+544S | HD 238090 | 458 A | 12:12:21.29 | +54:29:10.2 | M0.0 V | Multiple | A.11 |
| 1404 | 382 | J12123+544N | GJ 458 B | 458 B | 12:12:21.58 | +54:29:24.6 | M3.0 V | Multiple | |
| 1405 | | J12124+121 | PM J12124+1211 | | 12:12:25.99 | +12:11:38.2 | M2.0 V | Single | |
| 1406 | 383 | J12124+396 | GJ 3714 | 3714 | 12:12:29.65 | +39:40:25.2 | M1.0 V | Multiple | |
| 1407 | | J12133+166 | IV Com | 9397 | 12:13:19.91 | +16:41:32.3 | M1.0 V | Single | |
| 1408 | | J12144+245 | GJ 3717 | 3717 | 12:14:26.04 | +24:35:20.5 | M2.0 V | Single | |
| 1409 | | J12151+487 | GJ 458.2 | 458.2 | 12:15:08.46 | +48:43:56.4 | M0.5 V | Candidate | |
| 1410 | | J12154+391 | GJ 3718 | 3718 | 12:15:27.93 | +39:11:15.4 | M1.5 V | Single | |
| 1411 | | J12156+526 | StKM 2-809 | | 12:15:39.55 | +52:39:08.7 | M4.0 V | Candidate | |
| 1412 | | J12142+006 | GJ 1154 | 1154 | 12:14:15.53 | +00:37:21.8 | M5.0 V | Single | |
| 1413 | 384 | | Gaia DR3 1547529669400723968 | | 12:16:14.94 | +50:53:38.4 | M2.5 V | Multiple | |
| 1414 | 384 | J12162+508 | RX J1216.2+5053 | | 12:16:14.90 | +50:53:36.7 | M4.0 V | Multiple | |
| 1415 | 385 | | GJ 1155 B | 1155 B | 12:16:51.17 | +02:58:06.9 | DA | Multiple | A.9 |
| 1416 | 385 | J12168+029 | GJ 1155 A | 1155 A | 12:16:51.16 | +02:58:09.0 | M3.0 V | Multiple | A.9 |
| 1417 | | J12168+248 | PM J12168+2451E | | 12:16:52.62 | +24:51:06.0 | M1.5 V | Single | |
| 1418 | | J12189+111 | GL Vir | 1156 | 12:18:58.02 | +11:07:37.0 | M5.0 V | Single | |
| 1419 | 386 | J12169+311 | GJ 3719 | 3719 | 12:16:58.27 | +31:09:22.6 | M3.5 V | Multiple | A.4 |
| 1420 | 387 | J12191+318 | LP 320-626 | | 12:19:05.55 | +31:50:43.5 | M3.5 V | Multiple | A.4 |
| 1421 | 387 | | LP 320-626 | | 12:19:05.47 | +31:50:42.2 | M3.5 V | Multiple | |
| 1422 | | J12194+283 | Wolf 408 | 9404 | 12:19:23.31 | +28:22:57.8 | M0.0 V | Single | |
| 1423 | | J12198+527 | StKM 1-1007 | | 12:19:47.76 | +52:46:43.1 | M0.0 V | Single | |
| 1424 | | J12199+364 | G 123-36 | | 12:29:55.22 | +36:26:40.0 | M1.0 V | Candidate | |
| 1425 | 388 | J12204+005 | GJ 461 | 461 | 12:20:25.59 | +00:35:00.4 | M0.0 V | Multiple | |
| 1426 | 388 | | Gaia DR3 3699797155055781760 | | 12:20:25.60 | +00:35:01.3 | M2.5 V | Multiple | A.2 |
| 1427 | 389 | J12214+306W | G 148-48 | | 12:21:26.79 | +30:38:31.4 | M5.0 V | Multiple | |
| 1428 | 389 | J12214+306E | LP 320-416 | | 12:21:26.49 | +30:38:33.6 | M4.5 V | Multiple | |
| 1429 | | J12217+682 | LP 39-245 | | 12:21:46.41 | +68:16:07.3 | M3.0 V | Single | |
| 1430 | | J12223+251 | Wolf 409 | 3721 | 12:22:20.46 | +25:10:08.6 | M0.0 V | Single | |
| 1431 | | J12225+123 | BD+28 2110 | | 12:22:33.90 | +27:36:16.5 | M0.0 V | Single | |
| 1432 | | J12230+640 | Ross 690 | 463 | 12:22:58.52 | +64:01:56.9 | M3.0 V | Single | |
| 1433 | | J12235+279 | Wolf 411 | | 12:23:34.55 | +27:54:49.6 | M0.0 V | Single | |
| 1434 | 390 | J12228-040 | G 13-33 | | 12:22:50.33 | -04:04:47.5 | M4.5 V | Multiple | |
| 1435 | | J12238+125 | HD 107888 | 464 | 12:23:53.60 | +12:34:46.2 | M0.0 V | Single | |
| 1436 | | J12248-182 | Ross 695 | 465 | 12:24:53.73 | -18:15:09.2 | M2.0 V | Single | |
| 1437 | 391 | J12235+671 | GJ 3722 | 3722 | 12:23:33.85 | +67:11:16.4 | M2.5 V | Multiple | |
| 1438 | 392 | J12251+604 | LP 95-135 | | 12:25:05.64 | +60:25:06.0 | M1.0 V | Multiple | |
| 1439 | 392 | | LP 95-136 | | 12:25:08.10 | +60:25:14.3 | M1.5 V | Multiple | |
| 1440 | 393 | | HD 108421A | | 12:27:13.83 | +27:01:24.9 | K2 V | Multiple | A.8 |
| 1441 | 393 | | HD 108421B | | 12:27:13.84 | +27:01:27.6 | K4 V | Multiple | A.8 |
| 1442 | 393 | J12269+270 | CX Com | 3726 C | 12:26:57.47 | +27:00:49.7 | M4.5 V | Multiple+ | A.8 |
| 1443 | | J12274+374 | G 148-61 | | 12:27:29.12 | +37:26:35.1 | M1.5 V | Single | |
| 1444 | 394 | J12277-032 | G 13-39A | | 12:27:44.38 | -03:15:01.3 | M3.5 V | Multiple | |
| 1445 | 394 | | G 13-39B | | 12:27:44.41 | -03:14:59.9 | M4.5 V | Multiple | |
| 1446 | 395 | J12288-106N | Ross 948A | 3727 | 12:28:52.85 | -10:39:48.6 | M2.0 V | Multiple | |
| 1447 | 395 | J12288-106S | Ross 948B | 3728 | 12:28:52.65 | -10:39:50.8 | M2.0 V | Multiple | |
| 1448 | 396 | J12289+084 | Wolf 414 | 469 | 12:28:56.90 | +08:25:27.3 | M3.5 V | Multiple | |
| 1449 | 397 | J12290+417 | GJ 3729 | 3729 | 12:29:02.65 | +41:43:45.9 | M3.5 V | Multiple | |
| 1450 | 398 | J12292+535 | GJ 1159 A | 1159 A | 12:29:12.22 | +53:32:47.0 | M4.0 V | Multiple | |
| 1451 | 398 | | GJ 1159 B | 1159 B | 12:29:11.96 | +53:33:08.3 | M6.0 V | Multiple | |
| 1452 | | J12294+229 | GJ 3730 | 3730 | 12:29:26.92 | +22:59:46.4 | M4.0 V | Single | |
| 1453 | 399 | J12299-054W | GJ 3731 | 3731 | 12:29:53.57 | -05:27:29.2 | M3.5 V | Multiple | |
| 1454 | 399 | J12299-054E | GJ 3732 | 3732 | 12:29:54.05 | -05:27:25.2 | M4.0 V | Multiple | |
| 1455 | | J12312+086 | Wolf 417 | 471 | 12:31:15.12 | +08:48:29.8 | M0.5 V | Single | |
| 1456 | | J12323+315 | GJ 3733 | 3733 | 12:32:19.79 | +31:36:03.2 | M3.0 V | Candidate | |
| 1457 | | J12324+203 | GJ 3734 | 3734 | 12:32:26.37 | +20:23:28.0 | M2.5 V | Single | |
| 1458 | | J12327+682 | LP 39-249 | | 12:32:44.66 | +68:15:42.1 | M0.0 V | Single | |
| 1459 | 400 | J12332+090 | Wolf 424 A | 473 A | 12:33:15.48 | +09:01:19.5 | M5.0 V | Multiple | 5 |
| 1460 | 400 | | Wolf 424 B | 473 B | 12:33:15.52 | +09:01:18.6 | M5.5 V | Multiple | 5 |
| 1461 | | J12349+322 | PM J12349+3214 | | 12:34:54.03 | +32:14:29.2 | M3.5 V | Candidate | |
| 1462 | | J12350+098 | Wolf 427 | 476 | 12:35:00.22 | +09:49:37.5 | M2.5 V | Single | |
| 1463 | | J12363-043 | GJ 3736 | 3736 | 12:36:22.35 | -04:22:41.7 | M3.0 V | Single | |
| 1464 | | J12368-019 | PM J12368-0159 | | 12:36:51.96 | -01:59:02.0 | M3.5 V | Single | |
| 1465 | | J12373-208 | LP 795-38 | | 12:37:21.52 | -20:52:42.4 | M4.0 V | Single | |
| 1466 | | J12387-043 | GJ 1162 | 1162 | 12:38:46.47 | -04:19:20.2 | M3.5 V | Single | |
| 1467 | | J12388+116 | Wolf 433 | 480 | 12:38:51.18 | +11:41:42.1 | M3.0 V | Single | |
| 1468 | 401 | J12390+470 | G 123-049A | 3738 | 12:39:05.24 | +47:02:21.4 | M2.0 V | Multiple | |
| 1469 | 401 | | G 123-049B | | 12:39:05.30 | +47:02:21.2 | M2.0 V | Multiple | |
| 1470 | | J12397+255 | GJ 3739 | 3739 | 12:39:43.32 | +25:30:43.3 | M4.0 V | Single | |
| 1471 | | J12416+482 | GJ 3741 | 3741 | 12:41:38.24 | +48:14:22.3 | M1.0 V | Single | |
| 1472 | | J12417+567 | RX J1241.7+5645 | | 12:41:47.59 | +56:45:13.7 | M3.5 V | Single | |
| 1473 | | J12428+418 | G 123-55 | | 12:42:49.10 | +41:53:47.8 | M4.0 V | Single | |
| 1474 | | J12436+251 | GJ 1163 | 1163 | 12:43:35.62 | +25:06:21.1 | M3.0 V | Candidate | |

Table A.1: Complete sample studied in this work^a (cont.).

| Star id. | System id. | Karmn | Name | GJ | α (J2016.0) | δ (J2016.0) | Spectral type | Multiplicity type | In tables |
|----------|------------|-------------|------------------------------|--------|-----------------------|-----------------------|---------------|-------------------|-----------|
| 1475 | | J12440–111 | LP 735–29 | | 12:44:00.22 | -11:10:32.8 | M4.5 V | Single | |
| 1476 | | J12470+466 | Ross 991 | 3748 | 12:46:59.81 | +46:37:28.6 | M2.5 V | Single | |
| 1477 | | J12471–035 | GJ 3747 | 3747 | 12:47:09.24 | -03:34:18.0 | M3.0 V | Single | |
| 1478 | | J12479+097 | Wolf 437 | 486 | 12:47:55.53 | +09:44:57.7 | M3.5 V | Single | A.11 |
| 1479 | 402 | J12364+352 | G 123–45 | | 12:36:28.17 | +35:11:59.0 | M4.5 V | Multiple | A.4 |
| 1480 | | J12485+495 | RX J1248.5+4933 | | 12:48:34.67 | +49:33:53.8 | M3.5 V | Candidate | |
| 1481 | 403 | J12481+472 | GJ 3749 | 3749 | 12:48:10.07 | +47:13:23.2 | M3.5 V | Multiple | |
| 1482 | | J12495+094 | Wolf 439 | 3751 | 12:49:33.74 | +09:28:31.6 | M3.5 V | Single | |
| 1483 | | J12505+269 | GJ 3755 | 3755 | 12:50:34.35 | +26:55:20.3 | M3.5 V | Candidate | |
| 1484 | | J12508–213 | APMPM J1251–2121 | | 12:50:53.16 | -21:21:18.9 | M7.5 V | Candidate | |
| 1485 | 404 | J12490+661 | DP Dra | 487 | 12:49:01.61 | +66:06:35.2 | M3.0 V | Multiple | A.4 |
| 1486 | 405 | J12513+221 | GJ 1166A | 1166A | 12:51:23.71 | +22:06:15.7 | M3.0 V | Multiple | |
| 1487 | 405 | | LP 377–78 B | | 12:51:28.60 | +22:07:06.3 | M3.5 V | Multiple | |
| 1488 | 405 | | GJ 1166 B | 1166 B | 12:51:23.80 | +22:06:15.7 | M3.5 V | Multiple | |
| 1489 | 406 | J12576+352E | BF CVn | 490 A | 12:57:39.89 | +35:13:27.9 | M1.0 V | Multiple | |
| 1490 | 406 | J12576+352W | GJ 490 B | 490 B | 12:57:38.94 | +35:13:16.9 | M4.0 V | Multiple | A.2 |
| 1491 | | J12594+077 | GJ 3757 | 3757 | 12:59:23.31 | +07:43:54.8 | M5.0 V | Single | |
| 1492 | | J13000–056 | Ross 972 | 3758 | 13:00:03.58 | -05:37:47.1 | M3.0 V | Single | |
| 1493 | | J13005+056 | FN Vir | 493.1 | 13:00:32.51 | +05:41:11.6 | M4.5 V | Single | |
| 1494 | 407 | J12583+405 | LP 41–165 | | 12:58:21.97 | +40:33:20.7 | M1.5 V | Multiple | |
| 1495 | 408 | J13007+123 | Wolf 462 | 494 B | 13:00:45.87 | +12:22:32.1 | M1.5 V | Multiple | A.10 |
| 1496 | 408 | | Ross 458C | 494 C | 13:00:42.08 | +12:21:15.1 | T8.5p | Multiple | A.10 |
| 1497 | | J13019+335 | G 164–38 | | 13:01:55.96 | +33:35:23.0 | M1.0 V | Single | |
| 1498 | | J13027+415 | G 123–84 | | 13:02:46.65 | +41:31:06.6 | M3.5 V | Single | |
| 1499 | 409 | J13047+559 | GJ 497 A | 497 A | 13:04:46.29 | +55:54:10.6 | M0.5 V | Multiple | |
| 1500 | 409 | | GJ 497 B | 497 B | 13:04:46.36 | +55:54:08.7 | M1.0 V | Multiple | |
| 1501 | 410 | J13054+371 | GJ 3760 A | 3760 A | 13:05:29.44 | +37:08:07.6 | M2.5 V | Multiple | 5 |
| 1502 | 410 | | GJ 3760 B | 3760 B | 13:05:29.46 | +37:08:07.2 | M2.0 V | Multiple | 5 |
| 1503 | | J13068+308 | GJ 3762 | 3762 | 13:06:50.53 | +30:50:46.4 | M5.0 V | Candidate | |
| 1504 | | J13084+169 | GJ 9428 | 9428 | 13:08:24.64 | +16:58:18.5 | M1.0 V | Candidate | |
| 1505 | | J13088+163 | GJ 3763 | 3763 | 13:08:49.96 | +16:22:00.9 | M2.5 V | Candidate | |
| 1506 | | J13089+490 | GJ 3765 | 3765 | 13:08:55.46 | +49:04:50.3 | M0.5 V | Single | |
| 1507 | | J13102+477 | G 177–25 | | 13:10:11.62 | +47:45:08.8 | M5.0 V | Single | |
| 1508 | | J13113+285 | GJ 3766 | 3766 | 13:11:21.13 | +28:32:34.4 | M5.0 V | Single | |
| 1509 | | J13118+253 | GJ 3767 | 3767 | 13:11:51.24 | +25:20:48.1 | M5.0 V | Single | |
| 1510 | | J13119+658 | PM J13119+6550 | | 13:11:59.17 | +65:50:01.3 | M3.0 V | Single | A.11 |
| 1511 | | J13130+201 | GJ 1168 | 1168 | 13:13:04.08 | +20:11:29.0 | M3.5 V | Single | |
| 1512 | | J13140+038 | GJ 3772 | 3772 | 13:14:05.05 | +03:53:59.0 | M3.0 V | Single | |
| 1513 | | J13095+289 | GJ 1167 A | 1167 A | 13:09:34.56 | +28:59:03.1 | M4.0 V | Candidate | |
| 1514 | 411 | J13142+792 | G 255–29A | | 13:14:14.06 | +79:14:45.9 | M1.0 V | Multiple | |
| 1515 | 411 | | G 255–29B | | 13:14:13.78 | +79:14:47.1 | M2.0 V | Multiple | |
| 1516 | | J13165+278 | GJ 1169 | 1169 | 13:16:31.95 | +27:52:33.5 | M3.5 V | Single | |
| 1517 | | J13167–123 | LP 737–14 | | 13:16:45.10 | -12:20:21.2 | M3.5 V | Candidate | |
| 1518 | 412 | J13143+133 | LP 497–33 | | 13:14:20.08 | +13:19:57.9 | M6.0 V | Multiple | |
| 1519 | 413 | | HD 115404 | 505 A | 13:16:51.76 | +17:00:57.6 | K2 V | Multiple | A.8 A.11 |
| 1520 | 413 | J13168+170 | HD 115404B | 505 B | 13:16:52.28 | +17:00:55.7 | M0.5 V | Multiple | A.8 |
| 1521 | | J13168+231 | GJ 3774 | 3774 | 13:16:53.38 | +23:10:05.5 | M1.5 V | Single | |
| 1522 | | J13179+362 | GJ 1170 | 1170 | 13:17:58.30 | +36:17:51.5 | M1.0 V | Single | |
| 1523 | 414 | J13180+022 | GJ 3775 | 3775 | 13:18:01.42 | +02:14:00.4 | M3.5 V | Multiple | 5 |
| 1524 | 414 | | Gaia DR3 3688439268658769408 | | 13:18:01.41 | +02:14:00.2 | M4.5 V | Multiple | 5 |
| 1525 | 415 | J13182+733 | PM J13182+7322 | | 13:18:13.82 | +73:22:05.6 | M3.5 V | Multiple | |
| 1526 | 415 | | PM J13182+7322B | | 13:18:13.11 | +73:22:12.4 | M7.0 V | Multiple | |
| 1527 | 416 | J13195+351W | GJ 507 A | 507 A | 13:19:34.10 | +35:06:24.2 | M0.5 V | Multiple | |
| 1528 | 416 | J13195+351E | GJ 507 B | 507 B | 13:19:35.18 | +35:06:12.4 | M3.0 V | Multiple | A.4 |
| 1529 | 417 | J13197+477 | HD 115953 | 508.0 | 13:19:45.90 | +47:46:40.5 | M0.5 V | Multiple | |
| 1530 | 417 | | HD 115953B | 508 B | 13:19:45.97 | +47:46:40.6 | M2.0 V | Multiple | |
| 1531 | | J13196+333 | Ross 1007 | 9440 | 13:19:39.74 | +33:20:45.2 | M1.5 V | Single | |
| 1532 | | J13209+342 | Ross 1008 | 9442 | 13:20:58.67 | +34:16:39.4 | M1.0 V | Single | |
| 1533 | | J13215+035 | LSPM J1321+0332 | | 13:21:30.15 | +03:33:02.1 | M1.0 V | Single | |
| 1534 | | J13215+037 | GJ 3778 | 3778 | 13:21:34.69 | +03:45:54.5 | M1.0 V | Single | |
| 1535 | | J13229+244 | Ross 1020 | 3779 | 13:22:56.03 | +24:27:49.8 | M4.0 V | Single | A.11 |
| 1536 | 418 | J13235+292 | HD 116495A | 509 A | 13:23:32.21 | +29:14:18.9 | M0.0 V | Multiple | |
| 1537 | 418 | | HD 116495B | 509 B | 13:23:32.33 | +29:14:19.0 | K7 V | Multiple | |
| 1538 | | J13239+694 | LP 40–109 | | 13:23:56.16 | +69:27:03.5 | M0.0 V | Single | |
| 1539 | | J13247–050 | G 14–52 | | 13:24:46.56 | -05:04:24.8 | M4.0 V | Candidate | |
| 1540 | | J13251–114 | PM J13251–1126 | | 13:25:11.61 | -11:26:33.7 | M3.0 V | Single | |
| 1541 | 419 | J13254+377 | BD+38 2445 | | 13:25:28.07 | +37:43:10.9 | M0.0 V | Multiple | |
| 1542 | 419 | | BD+38 2445B | | 13:25:28.31 | +37:43:10.4 | M4.5 V | Multiple | |
| 1543 | | J13255+688 | TOI–1238 | | 13:25:31.76 | +68:50:09.8 | M0.0 V | Single | A.11 |
| 1544 | 420 | | PM J13255+2738 | | 13:25:35.66 | +27:38:08.9 | M1.0 V | Multiple | A.7 |
| 1545 | 420 | J13260+275 | PM J13260+2735A | | 13:26:02.70 | +27:35:03.7 | M3.0 V | Multiple | A.7 |
| 1546 | 420 | | PM J13260+2735B | | 13:26:02.63 | +27:35:02.5 | M2.5 V | Multiple | A.2 A.7 |
| 1547 | 421 | J13282+300 | BD+30 2400 | | 13:28:17.53 | +30:02:43.0 | M0.0 V | Multiple | |
| 1548 | 421 | | BD+30 2400B | | 13:28:17.48 | +30:02:44.1 | M4.5 V | Multiple | |
| 1549 | 421 | | LP 323–115 | | 13:28:20.69 | +30:03:15.8 | M7.0 V | Multiple | |
| 1550 | 422 | J13283–023W | Ross 486A | 512 A | 13:28:21.24 | -02:21:45.0 | M3.0 V | Multiple | |
| 1551 | 422 | J13283–023E | Ross 486B | 512 B | 13:28:21.68 | -02:21:39.6 | M4.0 V | Multiple | |
| 1552 | | J13293+114 | GJ 513 | 513 | 13:29:21.67 | +11:26:07.6 | M3.5 V | Single | |
| 1553 | | J13294–143 | 1RXS J132923.9–142206 | | 13:29:24.21 | -14:22:13.0 | M3.5 V | Single | |
| 1554 | | J13299+102 | Ross 490 | 514 | 13:30:01.01 | +10:22:20.6 | M0.5 V | Single | A.11 |
| 1555 | 423 | | Wolf 485 | 515 | 13:30:12.44 | -08:34:37.0 | DA3.5 | Multiple | A.9 |
| 1556 | 423 | J13300–087 | Ross 476 | 9447 | 13:30:01.59 | -08:42:33.0 | M4.0 V | Multiple | A.9 |

Table A.1: Complete sample studied in this work^a (cont.).

| Star id. | System id. | Karmn | Name | GJ | α (J2016.0) | δ (J2016.0) | Spectral type | Multiplicity type | In tables |
|----------|------------|-------------|------------------------------|---------|-----------------------|-----------------------|---------------|-------------------|-----------|
| 1557 | | J13305+191 | GJ 1171 | 1171 | 13:30:30.49 | +19:09:13.5 | M4.5 V | Candidate | |
| 1558 | | J13318+233 | GJ 3790 | 3790 | 13:31:50.26 | +23:23:21.1 | M2.0 V | Single | |
| 1559 | 424 | J13317+292 | DG CVn | 3789 | 13:31:46.33 | +29:16:34.3 | M4.0 V | Multiple | |
| 1560 | 425 | J13319+311 | GJ 9448 B | 9448 | 13:31:58.08 | +31:08:05.3 | M0.0 V | Multiple | |
| 1561 | 425 | | Gaia DR3 1468339715235126784 | | 13:31:58.10 | +31:08:05.6 | M0.0 V | Multiple | |
| 1562 | 426 | J13326+309 | LP 323–169 | | 13:32:38.85 | +30:59:05.3 | M4.5 V | Multiple | |
| 1563 | 427 | J13327+168 | VW Com | 516 A | 13:32:44.93 | +16:48:35.8 | M2.5 V | Multiple | |
| 1564 | 427 | | GJ 516 B | 516 B | 13:32:45.08 | +16:48:37.4 | M4.0 V | Multiple | |
| 1565 | | J13335+704 | PM J13335+7029 | | 13:33:33.27 | +70:29:41.6 | M3.5 V | Single | |
| 1566 | | J13343+046 | Wolf 1487 | 1172 | 13:34:21.67 | +04:40:00.7 | M0.0 V | Single | |
| 1567 | | J13348+201 | GJ 3793 | 3793 | 13:34:49.40 | +20:11:35.7 | M3.5 V | Candidate | |
| 1568 | 428 | | GJ 9453 | 9453 | 13:34:51.91 | +74:30:01.1 | K5 V | Multiple+ | A.8 |
| 1569 | 428 | J13348+745 | GJ 9453 B | 9453 B | 13:34:49.83 | +74:30:12.6 | M3.5 V | Multiple | A.8 |
| 1570 | | J13358+146 | G 150–17 | | 13:35:50.73 | +14:41:07.4 | M2.5 V | Single | |
| 1571 | | J13369+229 | Ross 1021 | 3794 | 13:36:55.35 | +22:57:58.2 | M2.5 V | Single | |
| 1572 | 429 | J13378+481 | GJ 520 A | 520 A | 13:37:50.84 | +48:08:14.8 | M0.0 V | Multiple | |
| 1573 | 429 | | GJ 520 B | 520 B | 13:37:50.77 | +48:08:16.3 | M1.5 V | Multiple | |
| 1574 | 429 | J13376+481 | GJ 520 C | 520 C | 13:37:40.09 | +48:07:52.0 | M4.0 V | Multiple+ | |
| 1575 | | J13386+258 | Ross 1022 | 3795 | 13:38:36.37 | +25:49:50.7 | M3.0 V | Single | |
| 1576 | | J13386–115 | IRXS J133841.3–113137 | | 13:38:41.05 | -11:32:09.1 | M4.5 V | Single | |
| 1577 | | J13388–022 | Ross 488 | 3796 | 13:38:53.11 | -02:15:48.5 | M2.0 V | Single | |
| 1578 | | J13401+437 | Ross 1026 | 1174 | 13:40:07.19 | +43:46:42.8 | M3.5 V | Candidate | |
| 1579 | | J13413–091 | PM J13413–0907 | | 13:41:21.33 | -09:07:16.4 | M2.5 V | Single | |
| 1580 | 430 | J13414+489 | StM 186 | | 13:41:27.84 | +48:54:43.4 | M3.5 V | Multiple | |
| 1581 | 431 | J13394+461 | GJ 521 | 521 | 13:39:24.04 | +46:11:17.6 | M1.5 V | Multiple | |
| 1582 | | J13415+148 | GJ 3799 | 3799 | 13:41:31.58 | +14:49:27.6 | M1.0 V | Candidate | |
| 1583 | 432 | J13417+582 | StM 187 | | 13:41:46.48 | +58:15:18.9 | M3.5 V | Multiple | |
| 1584 | 432 | | Gaia DR3 1658968054798747008 | | 13:41:46.39 | +58:15:18.6 | M4.0 V | Multiple | |
| 1585 | | J13427+332 | Ross 1015 | 3801 | 13:42:43.13 | +33:17:12.9 | M3.5 V | Single | |
| 1586 | | J13430+090 | GJ 3802 | 3802 | 13:43:00.91 | +09:04:21.8 | M3.0 V | Candidate | |
| 1587 | | J13434+111 | TYC 896–760–1 | | 13:43:25.03 | +11:06:42.1 | M0.5 V | Single | |
| 1588 | 433 | J13421–160 | GJ 3800 | 3800 | 13:42:09.28 | -16:00:24.1 | M4.0 V | Multiple | |
| 1589 | 434 | J13444+516 | Ross 492 | 3803 | 13:44:27.00 | +51:41:08.6 | M2.0 V | Multiple | |
| 1590 | 435 | J13445+249 | LP 379–98 A | | 13:44:33.38 | +24:57:03.6 | M1.0 V | Multiple | |
| 1591 | 435 | | LP 379–98 B | | 13:44:33.38 | +24:57:04.5 | M1.0 V | Multiple | |
| 1592 | | J13450+176 | Wolf 497 | 525 | 13:45:05.59 | +17:46:38.2 | M0.0 V | Single | |
| 1593 | | J13455+609 | MCC 699 | | 13:45:31.28 | +60:58:58.3 | M0.5 V | Single | |
| 1594 | | J13457+148 | HD 119850 | 526 | 13:45:45.74 | +14:53:06.2 | M1.5 V | Single | |
| 1595 | | J13458–179 | GJ 3804 | 3804 | 13:45:50.37 | -17:58:14.5 | M3.5 V | Single | |
| 1596 | 436 | J13477+214 | BD+22 2632A | | 13:47:42.49 | +21:27:36.3 | M0.0 V | Multiple | |
| 1597 | 436 | | BD+22 2632B | | 13:47:42.54 | +21:27:35.2 | M3.5 V | Multiple | |
| 1598 | 437 | J13481–137 | LP 738–14 | | 13:48:06.52 | -13:44:39.8 | M4.5 V | Multiple | |
| 1599 | 437 | | LP 738–14 B | | 13:48:02.91 | -13:44:07.2 | T5.5 | Multiple | A.10 |
| 1600 | 438 | | GJ 1179 B | 1179 B | 13:48:01.28 | +23:34:48.4 | DC9 | Multiple | A.9 |
| 1601 | 438 | J13482+236 | GJ 1179 A | 1179 A | 13:48:11.69 | +23:36:50.7 | M5.5 V | Multiple | A.9 |
| 1602 | | J13485+563 | Ross 493 | | 13:48:34.32 | +56:20:09.6 | M1.5 V | Single | |
| 1603 | | J13488+041 | Wolf 1494 | 3808 | 13:48:48.61 | +04:05:59.4 | M4.0 V | Single | |
| 1604 | 439 | J13490+026 | Wolf 1495 A | 3809 A | 13:49:01.16 | +02:47:23.6 | M1.5 V | Multiple | |
| 1605 | 439 | | Wolf 1495 B | 3809 B | 13:49:01.19 | +02:47:23.2 | M1.5 V | Multiple | |
| 1606 | 440 | J13507–216 | GJ 3810 | 3810 | 13:50:43.96 | -21:41:33.0 | M3.0 V | Multiple | |
| 1607 | 440 | J13503–216 | LP 798–41 | | 13:50:23.73 | -21:37:25.9 | M3.5 V | Multiple | |
| 1608 | | J13508+367 | Ross 1019 | 3812 | 13:50:51.18 | +36:44:18.5 | M3.5 V | Single | |
| 1609 | | J13518+127 | RX J1351.8+1247 | | 13:51:53.02 | +12:47:07.0 | M2.0 V | Single | |
| 1610 | 441 | J13526+144 | Wolf 515 | 3813 | 13:52:36.26 | +14:25:15.7 | M2.0 V | Multiple | |
| 1611 | 441 | | Wolf 515 B | | 13:52:36.26 | +14:25:16.9 | M3.5 V | Multiple | |
| 1612 | 442 | J13528+656 | GJ 533.1 | 533.1 | 13:52:48.61 | +65:37:17.7 | M1.0 V | Multiple | |
| 1613 | | J13528+668 | GJ 3815 | 3815 | 13:52:49.25 | +66:48:57.2 | M5.0 V | Single | |
| 1614 | | J13536+776 | LP 21–224 | | 13:53:39.91 | +77:37:07.9 | M4.0 V | Single | |
| 1615 | | J13529+536 | LP 97–259 | | 13:52:55.76 | +56:36:17.0 | M1.0 V | Single | |
| 1616 | 443 | J13534+129 | Ross 835 | 533 B | 13:53:27.37 | +12:56:22.9 | M0.0 V | Multiple | |
| 1617 | 444 | J13537+521 | PM J13537+5210A | | 13:53:45.89 | +52:10:27.3 | M3.5 V | Multiple | |
| 1618 | 444 | | PM J13537+5210B | | 13:53:45.88 | +52:10:28.3 | M2.5 V | Multiple | |
| 1619 | | J13537+788 | GJ 534.2 | 534.2 | 13:53:45.76 | +78:51:08.7 | M0.0 V | Single | |
| 1620 | | J13582+125 | Ross 837 | 3817 | 13:58:13.56 | +12:34:55.4 | M3.0 V | Single | |
| 1621 | | J13582–120 | LP 739–2 | | 13:58:15.80 | -12:02:58.4 | M4.5 V | Single | |
| 1622 | | J13583–132 | LP 739–3 | | 13:58:19.96 | -13:16:26.0 | M4.0 V | Single | |
| 1623 | | J13587–000 | GJ 3818 | 3818 | 13:58:43.20 | -00:04:54.3 | M3.5 V | Single | |
| 1624 | | J13591–198 | GJ 3820 | 3820 | 13:59:09.78 | -19:50:06.6 | M4.0 V | Single | |
| 1625 | | J14010–026 | HD 122303 | 536 | 14:01:02.31 | -02:39:07.9 | M1.0 V | Single | |
| 1626 | 445 | J14019+154 | GJ 536.1 A | 536.1 A | 14:01:58.86 | +15:29:40.7 | M0.0 V | Multiple | |
| 1627 | 445 | | GJ 536.1 B | 536.1 B | 14:01:58.89 | +15:29:39.1 | M0.5 V | Multiple | A.2 |
| 1628 | 446 | J14019+432 | PM J14019+4316A | | 14:01:58.67 | +43:16:41.1 | M2.5 V | Multiple | |
| 1629 | 446 | | PM J14019+4316B | | 14:01:58.69 | +43:16:43.1 | M3.0 V | Multiple | A.2 |
| 1630 | | J14023+136 | GJ 3822 | 3822 | 14:02:19.73 | +13:41:20.4 | M0.5 V | Single | |
| 1631 | | J14024–210 | GJ 3821 | 3821 | 14:02:29.43 | -21:00:42.9 | M3.5 V | Single | |
| 1632 | 447 | J14025+463S | GJ 537 A | 537 A | 14:02:34.03 | +46:20:23.0 | M0.5 V | Multiple | |
| 1633 | 447 | J14025+463N | GJ 537 B | 537 B | 14:02:34.19 | +46:20:26.4 | M0.5 V | Multiple | |
| 1634 | | J14039+242 | LSPM J1403+2440 | | 14:03:54.74 | +24:40:44.2 | M2.5 V | Single | |
| 1635 | 448 | | BD+21 2602 | | 14:04:09.85 | +20:45:32.5 | K4 V | Multiple | A.8 |
| 1636 | 448 | J14041+207 | StKM 1–1119 | | 14:04:09.06 | +20:44:30.9 | M1.0 V | Multiple | A.8 |
| 1637 | 448 | | Gaia DR3 1247168140942467200 | | 14:04:09.06 | +20:44:31.2 | M1.5 V | Multiple | A.8 |
| 1638 | | J14062+693 | NLT 36313 | | 14:06:14.66 | +69:18:38.8 | M3.0 V | Single | |

Table A.1: Complete sample studied in this work^a (cont.).

| Star id. | System id. | Karmn | Name | GJ | α (J2016.0) | δ (J2016.0) | Spectral type | Multiplicity type | In tables |
|----------|------------|-------------|--------------------------|--------|-----------------------|-----------------------|---------------|-------------------|-----------|
| 1639 | | J14082+805 | GJ 540 | 540 | 14:08:14.37 | +80:35:41.5 | M1.0 V | Single | |
| 1640 | | J14083+758 | GJ 3826 | 3826 | 14:08:20.91 | +75:51:13.2 | M0.5 V | Candidate | |
| 1641 | 449 | J14121-005 | GJ 3828 A | 3828 A | 14:12:10.22 | -00:35:00.3 | M2.5 V | Multiple | |
| 1642 | 449 | | GJ 3828 B | 3828 B | 14:12:11.36 | -00:35:12.6 | M6.5 V | Multiple | |
| 1643 | 450 | J14130-120 | GQ Vir | 540.2 | 14:13:04.19 | -12:01:32.9 | M4.5 V | Multiple | A.4 |
| 1644 | 451 | | HD 124498A | | 14:14:21.24 | -15:21:24.8 | K7 V | Multiple | |
| 1645 | 451 | | HD 124498B | | 14:14:21.34 | -15:21:24.4 | M2.0 V | Multiple | A.2 |
| 1646 | 451 | J14142-153 | GJ 3832 | 3832 | 14:14:16.87 | -15:21:15.9 | M3.5 V | Multiple+ | |
| 1647 | | J14144+234 | GJ 3834 | 3834 | 14:14:26.33 | +23:27:26.4 | M3.5 V | Single | |
| 1648 | | J14152+450 | Ross 992 | 3836 | 14:15:15.96 | +45:00:49.7 | M3.0 V | Single | |
| 1649 | | J14153+153 | LP 439-350 | | 14:15:20.63 | +15:23:01.5 | M2.0 V | Single | |
| 1650 | 452 | J14155+046 | GJ 1182 | 1182 | 14:15:31.75 | +04:39:19.1 | M5.0 V | Multiple | A.4 |
| 1651 | 453 | J14157+594 | LP 97-674 A | | 14:15:42.13 | +59:27:29.1 | M2.0 V | Multiple | |
| 1652 | 453 | | LP 97-674 B | | 14:15:41.61 | +59:27:25.9 | M3.0 V | Multiple | |
| 1653 | | J14159+362 | G 165-58 | | 14:15:56.39 | +36:16:42.2 | M3.5 V | Single | |
| 1654 | | J14161+233 | LP 81-30 | | 14:16:11.25 | +23:23:26.5 | M1.0 V | Single | |
| 1655 | | J14170+105 | GJ 3838 | 3838 | 14:17:04.56 | +10:35:34.3 | M1.5 V | Single | |
| 1656 | 454 | J14170+317 | GJ 3839 | 3839 | 14:17:02.14 | +31:42:44.7 | M4.0 V | Multiple | |
| 1657 | 455 | J14171+088 | PM J14171+0851 | | 14:17:07.18 | +08:51:37.1 | M4.5 V | Multiple | |
| 1658 | 456 | J14174+454 | GJ 541.2 | 541.2 | 14:17:24.45 | +45:26:39.8 | M0.0 V | Multiple | |
| 1659 | 456 | J14173+454 | RX J1417.3+4525 | | 14:17:22.17 | +45:25:45.7 | M5.0 V | Multiple+ | |
| 1660 | | J14175+025 | RX J1417.5+0233 | | 14:17:30.18 | +02:33:42.5 | M3.0 V | Candidate | |
| 1661 | | J14177+214 | LP 381-94 | | 14:17:47.76 | +21:25:58.8 | M1.0 V | Candidate | |
| 1662 | | J14179-005 | GJ 3840 | 3840 | 14:17:58.75 | -00:31:33.8 | M2.5 V | Single | |
| 1663 | | J14189+386 | LP 220-78 | | 14:18:58.09 | +38:38:22.5 | M1.0 V | Candidate | |
| 1664 | | J14191-073 | Wolf 534 | 9478 | 14:19:09.81 | -07:18:24.0 | M3.0 V | Single | |
| 1665 | | J14194+029 | LP 560-1 | | 14:19:29.37 | +02:54:34.1 | M5.0 V | Single | |
| 1666 | | J14200+390 | IZ Boo | 3842 | 14:20:04.66 | +39:03:02.5 | M2.5 V | Candidate | |
| 1667 | | J14201-096 | Ross 848 | 545 | 14:20:06.71 | -09:37:26.8 | M3.5 V | Single | |
| 1668 | | J14212-011 | GJ 3843 | 3843 | 14:21:15.31 | -01:07:29.8 | M3.5 V | Single | |
| 1669 | | J14215-079 | PM J14215-0755 | | 14:21:33.96 | -07:55:18.0 | M4.0 V | Single | |
| 1670 | | J14219+376 | LP 270-68 | | 14:21:55.61 | +37:39:45.5 | M1.5 V | Single | |
| 1671 | | J14227+164 | LP 440-13 | | 14:22:43.19 | +16:24:47.2 | M5.0 V | Single | |
| 1672 | | J14231-222 | GJ 3845 | 3845 | 14:23:07.49 | -22:17:16.7 | M4.0 V | Single | |
| 1673 | | J14249+088 | GJ 3846 | 3846 | 14:24:56.58 | +08:53:18.0 | M2.5 V | Single | |
| 1674 | 457 | J14210+275 | GJ 3844 | 3844 | 14:21:03.13 | +27:35:34.5 | M2.5 V | Multiple | |
| 1675 | 458 | | HD 126660 | 549 A | 14:25:11.39 | +51:50:56.3 | F7 V | Multiple+ | A.8 |
| 1676 | 458 | J14251+518 | HD 126660B | 549 B | 14:25:11.17 | +51:49:46.6 | M2.5 V | Multiple | A.8 |
| 1677 | | J14255-118 | LP 740-10 | | 14:25:33.79 | -11:48:51.5 | M4.0 V | Candidate | |
| 1678 | 459 | J14257+236W | GJ 548 A | 548 A | 14:25:44.40 | +23:36:43.6 | M0.0 V | Multiple | |
| 1679 | 459 | J14257+236E | GJ 548 B | 548 B | 14:25:47.58 | +23:36:55.8 | M0.5 V | Multiple | |
| 1680 | | J14259+142 | V358 Boo | | 14:25:55.87 | +14:12:09.6 | M0.0 V | Candidate | |
| 1681 | | J14269+241 | LSPM J1426+2408 | | 14:26:58.63 | +24:08:56.9 | M1.0 V | Single | |
| 1682 | 460 | J14279-003S | GJ 1183 A | 1183 A | 14:27:55.69 | -00:22:30.5 | M4.5 V | Multiple+ | |
| 1683 | 460 | J14279-003N | GJ 1183 B | 1183 B | 14:27:56.01 | -00:22:18.3 | M4.5 V | Multiple | |
| 1684 | | J14280+139 | LP 500-35 | | 14:28:03.75 | +13:56:05.4 | M7.0 V | Single | |
| 1685 | 461 | J14283+053 | LP 560-27 | | 14:28:21.12 | +05:19:00.3 | M3.0 V | Multiple | |
| 1686 | 461 | J14282+053 | LP 560-26 | | 14:28:17.18 | +05:18:44.8 | M3.5 V | Multiple+ | |
| 1687 | | J14294+155 | Ross 130 | 552 | 14:29:28.53 | +15:32:18.3 | M2.0 V | Single | |
| 1688 | | J14299+295 | GJ 3853 | 3853 | 14:29:59.26 | +29:33:54.9 | M4.0 V | Single | |
| 1689 | | J14306+597 | GJ 3855 | 3855 | 14:30:36.08 | +59:43:27.4 | M6.5 V | Single | |
| 1690 | | J14307-086 | HD 127339 | 553 | 14:30:46.35 | -08:38:50.6 | M0.5 V | Single | |
| 1691 | | J14310-122 | Wolf 1478 | 9484 | 14:31:00.72 | -12:17:52.3 | M3.5 V | Single | |
| 1692 | | J14312+754 | LSPM J1431+7526 | | 14:31:12.59 | +75:26:41.7 | M4.0 V | Single | |
| 1693 | | J14320+738 | G 255-55 | | 14:32:01.99 | +73:49:23.3 | M2.0 V | Single | |
| 1694 | | J14321+081 | LP 560-35 | | 14:32:07.99 | +08:11:31.4 | M6.0 V | Single | |
| 1695 | | J14321+160 | GJ 3856 | 3856 | 14:32:11.00 | +16:00:48.2 | M4.0 V | Single | |
| 1696 | | J14322+496 | GJ 3858 | 3858 | 14:32:13.58 | +49:39:04.2 | M3.5 V | Single | |
| 1697 | 462 | J14331+610 | G 224-13A | | 14:33:06.93 | +61:00:43.9 | M2.5 V | Multiple | |
| 1698 | 462 | | G 224-13B | | 14:33:06.80 | +61:00:43.6 | M3.0 V | Multiple | A.2 |
| 1699 | | J14342-125 | HN Lib | 555 | 14:34:16.42 | -12:31:00.9 | M4.0 V | Single | A.11 |
| 1700 | | J14366+143 | StKM 1-1170 | | 14:36:38.98 | +14:21:52.6 | M1.0 V | Single | |
| 1701 | 463 | J14368+583 | GJ 3861 | 3861 | 14:36:54.24 | +58:20:43.6 | M2.5 V | Multiple | A.4 |
| 1702 | 464 | J14371+756 | LSPM J1437+7536N | | 14:37:09.94 | +75:36:54.7 | M2.0 V | Multiple | |
| 1703 | 464 | | LSPM J1437+7536S | | 14:37:13.27 | +75:36:41.5 | M4.0 V | Multiple | |
| 1704 | 465 | J14376+677 | G 239-22 | | 14:37:39.32 | +67:45:34.9 | M1.5 V | Multiple | |
| 1705 | | J14388+422 | GPM 219.718548+42.229288 | | 14:38:51.66 | +42:13:43.9 | M1.5 V | Candidate | |
| 1706 | | J14415+064 | LP 560-66 | | 14:41:32.72 | +06:27:41.2 | M1.5 V | Single | |
| 1707 | 466 | J14423+660 | GJ 9492 | 9492 | 14:42:20.79 | +66:03:20.2 | M2.0 V | Multiple | A.10 |
| 1708 | 466 | | GJ 9492 B | 9492 B | 14:42:21.17 | +66:03:20.1 | LO | Multiple | A.2 A.10 |
| 1709 | | J14438+667 | NLT 38291 | | 14:43:50.67 | +66:44:34.6 | M1.0 V | Single | |
| 1710 | | J14472+570 | RX J1447.2+5701 | | 14:47:13.67 | +57:01:54.4 | M4.0 V | Candidate | |
| 1711 | | J14485+101 | LP 501-17 | | 14:48:32.79 | +10:06:55.7 | M3.5 V | Single | |
| 1712 | | J14501+323 | LP 326-34 | | 14:50:11.14 | +32:18:13.8 | M3.5 V | Single | |
| 1713 | | J14511+311 | LP 326-38 | | 14:51:09.97 | +31:06:37.4 | M4.0 V | Single | |
| 1714 | | J14524+123 | GJ 3871 | 3871 | 14:52:28.47 | +12:23:29.2 | M2.0 V | Single | |
| 1715 | | J14525+001 | Wolf 555 | 3870 | 14:52:32.27 | +00:10:02.8 | M2.0 V | Candidate | |
| 1716 | 467 | J14469+170 | Ross 994 | | 14:46:59.22 | +17:05:07.5 | M1.5 V | Multiple | |
| 1717 | 468 | J14538+235 | Ross 52A | 568 A | 14:53:50.59 | +23:33:22.5 | M3.5 V | Multiple | 5 |
| 1718 | 468 | | Ross 52B | 568 B | 14:53:50.66 | +23:33:22.5 | M4.5 V | Multiple | 5 |
| 1719 | 469 | J14544+161 | CE Boo | 569 A | 14:54:29.55 | +16:06:01.9 | M1.0 V | Multiple | |
| 1720 | 469 | | GJ 569 B | 569 B | 14:54:29.77 | +16:06:05.6 | M8.5 V | Multiple | A.2 |

Table A.1: Complete sample studied in this work^a (cont.).

| Star id. | System id. | Karmn | Name | GJ | α (J2016.0) | δ (J2016.0) | Spectral type | Multiplicity type | In tables |
|----------|------------|-------------|------------------------------|--------|-----------------------|-----------------------|---------------|-------------------|-----------|
| 1721 | | J14544+355 | Ross 1041 | 3873 | 14:54:28.10 | +35:32:43.5 | M3.5 V | Single | |
| 1722 | | J14548+099 | Ross 1028b | 3874 | 14:54:53.15 | +09:56:30.1 | M1.0 V | Single | |
| 1723 | 470 | J14549+411 | GJ 3875 | 3875 | 14:54:54.61 | +41:08:50.5 | M4.5 V | Multiple | A.4 |
| 1724 | | J14557+072 | G 66–42 | | 14:55:47.82 | +07:17:47.7 | M0.5 V | Candidate | |
| 1725 | 471 | J14564+168 | G 136–35 | | 14:56:28.16 | +16:48:29.1 | M1.5 V | Multiple | A.4 |
| 1726 | 472 | | KX Lib | 570 A | 14:57:29.18 | -21:25:23.3 | K4 V | Multiple | A.8 A.10 |
| 1727 | 472 | J14574–214 | HD 131976 | 570 C | 14:57:27.70 | -21:25:07.9 | M1.5 V | Multiple | A.8 A.10 |
| 1728 | 472 | | GJ 570 D | 570 D | 14:57:14.96 | -21:21:47.8 | T8 | Multiple | A.8 A.10 |
| 1729 | 473 | J14575+313 | Ross 53A | | 14:57:31.43 | +31:23:25.9 | M2.0 V | Multiple | |
| 1730 | 473 | | Ross 53B | | 14:57:31.41 | +31:23:26.6 | M0.5 V | Multiple | |
| 1731 | | J14578+566 | GJ 1187 | 1187 | 14:57:54.28 | +56:39:14.1 | M5.5 V | Candidate | |
| 1732 | 474 | J15009+454 | GJ 572 | 572 | 15:00:55.91 | +45:25:39.8 | M0.5 V | Multiple | |
| 1733 | 474 | | BD+45 2247B | | 15:00:55.96 | +45:25:37.9 | M4.5 V | Multiple | |
| 1734 | | J15011+354 | Ross 1042 | 3886 | 15:01:11.98 | +35:27:10.5 | M1.5 V | Single | |
| 1735 | | J15013+055 | GJ 3885 | 3885 | 15:01:20.20 | +05:32:48.5 | M3.0 V | Single | |
| 1736 | | J15018+550 | GJ 3891 | 3891 | 15:05:48.60 | +55:04:45.8 | M3.5 V | Candidate | |
| 1737 | | J15030+704 | LP 41–431 | | 15:03:01.68 | +70:26:14.0 | M3.0 V | Single | |
| 1738 | | J15043+294 | GJ 575.1 | 575.1 | 15:04:22.56 | +29:28:39.9 | M2.5 V | Candidate | |
| 1739 | | J15043+603 | Ross 1051 | 3890 | 15:04:17.09 | +60:23:07.4 | M1.0 V | Single | |
| 1740 | | J15049–211 | GJ 3888 | 3888 | 15:04:57.53 | -21:07:03.9 | M4.5 V | Single | |
| 1741 | | J15060+453 | PM J15060+4521 | | 15:06:03.02 | +45:21:52.8 | M1.5 V | Single | |
| 1742 | | J15073+249 | GJ 579 | 579 | 15:07:22.59 | +24:56:15.8 | M0.0 V | Single | |
| 1743 | 475 | J15011+071 | Ross 1030a | 3884 | 15:01:10.20 | +07:09:46.5 | M3.5 V | Multiple | |
| 1744 | 476 | | HD 135363 | | 15:07:55.68 | +76:14:01.8 | G5 V | Multiple | A.8 |
| 1745 | 476 | J15079+762 | LSPM J1507+7613 | | 15:07:56.64 | +76:14:01.8 | M4.5 V | Multiple | A.8 |
| 1746 | 477 | J15081+623 | LSPM J1508+6221 | | 15:08:11.53 | +62:21:56.4 | M4.0 V | Multiple | |
| 1747 | 477 | | Gaia DR3 1619631553142673664 | | 15:08:11.66 | +62:21:56.7 | M3.5 V | Multiple | |
| 1748 | | J15095+031 | Ross 1047 | 3892 | 15:09:34.95 | +03:10:08.3 | M3.0 V | Single | |
| 1749 | | J15100+193 | GJ 3893 | 3893 | 15:10:04.82 | +19:21:20.2 | M4.0 V | Single | |
| 1750 | | J15118–102 | GJ 3894 | 3894 | 15:11:49.55 | -10:14:22.1 | M4.5 V | Single | |
| 1751 | | J15119+179 | GJ 3895 | 3895 | 15:11:55.49 | +17:57:07.4 | M3.5 V | Single | |
| 1752 | 478 | J15147+645 | LP 67–339 | | 15:14:45.76 | +64:33:50.3 | M3.5 V | Multiple | |
| 1753 | | J15151+333 | LP 272–63 | | 15:15:06.93 | +33:17:57.0 | M2.0 V | Single | |
| 1754 | | J15156+638 | PM J15156+6349 | | 15:15:37.69 | +63:49:50.8 | M1.5 V | Single | |
| 1755 | | J15166+391 | LP 222–65 | | 15:16:40.44 | +39:10:47.4 | M7.0 V | Candidate | |
| 1756 | 479 | J15126+457 | GJ 3898 | 3898 | 15:12:37.60 | +45:43:52.3 | M4.0 V | Multiple | |
| 1757 | 480 | J15188+292 | StKM 1–1229 | | 15:18:49.75 | +29:15:06.4 | M1.0 V | Multiple | |
| 1758 | 480 | | Gaia DR3 1275127175448008448 | | 15:18:49.78 | +29:15:06.7 | M0.0 V | Multiple | A.2 |
| 1759 | 480 | | UCAC4 597–051773 | | 15:18:48.67 | +29:14:05.7 | M3.5 V | Multiple | |
| 1760 | | J15193+678 | GJ 3902 | 3902 | 15:19:17.35 | +67:51:24.0 | M3.0 V | Single | |
| 1761 | | J15194–077 | HO Lib | 581 | 15:19:25.51 | -07:43:21.7 | M3.0 V | Single | A.11 |
| 1762 | | J15197+046 | PM J15197+0439 | | 15:19:45.88 | +04:39:36.0 | M4.0 V | Single | |
| 1763 | | J15210+309 | PM J15210+3057 | | 15:21:00.56 | +30:57:00.9 | M2.5 V | Single | |
| 1764 | | J15214+042 | TYC 344–504–1 | | 15:21:25.39 | +04:14:49.9 | M1.5 V | Single | |
| 1765 | | J15218+209 | OT Ser | 9520 | 15:21:53.03 | +20:58:42.0 | M1.5 V | Single | |
| 1766 | | J15219+185 | LP 442–37 | | 15:21:56.83 | +18:35:47.9 | M1.5 V | Single | |
| 1767 | | J15238+174 | Ross 508 | 585 | 15:23:50.70 | +17:27:37.3 | M4.5 V | Single | A.11 |
| 1768 | 481 | J15191–127 | GJ 3900 | 3900 | 15:19:10.93 | -12:45:09.3 | M4.0 V | Multiple | |
| 1769 | 482 | J15238+561 | StKM 1–1240 | | 15:23:54.01 | +56:09:31.5 | M1.0 V | Multiple | A.4 |
| 1770 | 482 | | PM J15237+5609 | | 15:23:46.47 | +56:09:06.0 | M0.0 V | Multiple | |
| 1771 | | J15238+584 | G 224–65 | | 15:23:51.06 | +58:28:11.2 | M4.0 V | Candidate | |
| 1772 | 483 | J15273+415 | TYC 3055–1525–1 | | 15:27:19.05 | +41:30:09.9 | M1.5 V | Multiple+ | |
| 1773 | 483 | | PM J15273+4130N | | 15:27:19.11 | +41:30:44.2 | M6.5 V | Multiple | |
| 1774 | | J15276+408 | G 179–29 | | 15:27:38.85 | +40:52:02.2 | M1.0 V | Single | |
| 1775 | | J15280+257 | GJ 587.1 | 587.1 | 15:28:01.43 | +25:47:22.9 | M0.0 V | Single | |
| 1776 | 484 | J15290+467 | RX J1529.0+4646 | | 15:29:02.77 | +46:46:23.5 | M4.5 V | Multiple | |
| 1777 | | | RX J1532.6+4653 | | 15:32:37.17 | +46:53:04.6 | M1.0 V | Single | |
| 1778 | | J15305+094 | LP 502–56 | | 15:30:30.13 | +09:26:04.4 | M5.5 V | Single | |
| 1779 | 485 | J15297+428 | GJ 3907 | 3907 | 15:29:44.63 | +42:52:38.9 | M4.5 V | Multiple | |
| 1780 | | J15336+462 | GJ 3911 | 3911 | 15:33:39.33 | +46:15:06.1 | M3.5 V | Single | |
| 1781 | 486 | J15319+288 | GJ 3910 | 3910 | 15:31:53.50 | +28:51:10.2 | M4.5 V | Multiple | A.4 |
| 1782 | 487 | J15339+379 | GJ 588.1 | 588.1 | 15:33:54.82 | +37:54:48.4 | M0.5 V | Multiple | |
| 1783 | 487 | | Gaia DR3 1375767330164975616 | | 15:33:54.89 | +37:54:48.3 | M2.5 V | Multiple | A.2 |
| 1784 | | J15340+513 | LP 135–414 | | 15:34:03.52 | +51:22:06.8 | M4.5 V | Single | |
| 1785 | | J15345+142 | Ross 512 | 1193 | 15:34:29.76 | +14:16:15.5 | M4.0 V | Single | |
| 1786 | | J15349–143 | 2MUCD 11346 | | 15:34:55.92 | -14:18:54.5 | M8.5 V | Single | |
| 1787 | 488 | J15353+177S | Ross 513 | 589 A | 15:35:19.17 | +17:42:44.3 | M2.5 V | Multiple | |
| 1788 | 488 | J15353+177N | Ross 513B | 589 B | 15:35:18.98 | +17:43:01.7 | M4.5 V | Multiple | |
| 1789 | | J15357+221 | GJ 3913 | 3913 | 15:35:45.31 | +22:09:01.6 | M3.5 V | Single | |
| 1790 | | J15368+375 | BK CrB | | 15:36:49.97 | +37:34:48.0 | M0.0 V | Candidate | |
| 1791 | | J15369–141 | Ross 802 | 592 | 15:36:58.13 | -14:08:11.8 | M4.0 V | Single | |
| 1792 | | J15386+371 | G 179–42 | | 15:38:36.68 | +37:07:28.0 | M3.5 V | Single | |
| 1793 | 489 | J15400+434N | GJ 1194 A | 1194 A | 15:40:05.37 | +43:29:34.1 | M3.0 V | Multiple | |
| 1794 | 489 | J15400+434S | GJ 1194 B | 1194 B | 15:40:05.54 | +43:29:30.0 | M3.5 V | Multiple | |
| 1795 | 490 | J15412+759 | UU UMi | 597 | 15:41:20.12 | +75:59:22.5 | M3.0 V | Multiple | A.4 |
| 1796 | 491 | | HD 140232 | | 15:41:54.65 | +18:27:51.4 | A8 V | Multiple | A.7 |
| 1797 | 491 | | Gaia DR3 1197801408884577408 | | 15:41:54.81 | +18:27:51.5 | M3.5 V | Multiple | A.7 |
| 1798 | 491 | J15416+184 | StKM 1–1264 | | 15:41:37.17 | +18:28:09.2 | M1.5 V | Multiple+ | A.7 |
| 1799 | 492 | J15421–194 | GJ 595 | 595 | 15:42:04.27 | -19:28:34.9 | M3.0 V | Multiple | A.4 |
| 1800 | 493 | J15474–108 | GJ 3916 | 3916 | 15:47:24.21 | -10:53:53.2 | M2.0 V | Multiple | A.4 |
| 1801 | | J15476+226 | 1RXS J154741.3+224108 | | 15:47:40.51 | +22:41:16.0 | M4.5 V | Candidate | |
| 1802 | 494 | J15474+451 | LP 177–102 | | 15:47:27.03 | +45:07:54.5 | M4.0 V | Multiple | A.4 A.5 |

Table A.1: Complete sample studied in this work^a (cont.).

| Star id. | System id. | Karmn | Name | GJ | α (J2016.0) | δ (J2016.0) | Spectral type | Multiplicity type | In tables |
|----------|------------|-------------|------------------------------|---------|-----------------------|-----------------------|---------------|-------------------|-------------|
| 1803 | 495 | J15480+043 | RX J1548.0+0421 | | 15:48:02.78 | +04:21:38.4 | M2.5 V | Multiple | |
| 1804 | 495 | | UCAC4 472-052890 | | 15:47:54.89 | +04:18:02.9 | M4.0 V | Multiple+ | |
| 1805 | | J15488+305 | PM J15488+3030 | | 15:48:48.60 | +30:30:38.7 | M3.0 V | Single | |
| 1806 | | J15493+250 | G 168-13 | | 15:49:20.38 | +25:03:48.5 | M2.0 V | Single | |
| 1807 | | J15496+510 | GJ 3920 | 3920 | 15:49:35.62 | +51:03:02.0 | M2.0 V | Single | |
| 1808 | | J15499+796 | LP 23-35 | | 15:49:53.83 | +79:39:53.6 | M5.0 V | Candidate | |
| 1809 | | J15501+009 | Wolf 587 | 3918 | 15:50:11.41 | +00:57:32.0 | M2.5 V | Single | |
| 1810 | | J15512+306 | TYC 2572-633-1 | | 15:51:14.63 | +30:40:42.2 | M1.5 V | Candidate | |
| 1811 | | J15513+295 | GJ 3923 | 3923 | 15:51:21.51 | +29:30:59.2 | M3.5 V | Single | |
| 1812 | 496 | J15496+348 | GJ 3919 | 3919 | 15:49:37.37 | +34:49:07.8 | M4.0 V | Multiple | |
| 1813 | 497 | J15531+347N | Ross 806 | 3925 | 15:53:06.69 | +34:45:05.9 | M2.5 V | Multiple | |
| 1814 | 497 | J15531+347S | GJ 3926 | 3926 | 15:53:06.97 | +34:44:39.5 | M3.5 V | Multiple | |
| 1815 | | J15538+641 | NLTT 41533 | | 15:53:48.31 | +64:09:36.2 | M0.5 V | Single | |
| 1816 | 498 | J15555+352 | GJ 3928 | 3928AB | 15:55:31.51 | +35:12:05.2 | M4.5 V | Multiple | |
| 1817 | 498 | | G 180-11B | | 15:55:31.39 | +35:12:04.7 | M5.0 V | Multiple | |
| 1818 | | J15557+686 | RX J1555.7+6840 | | 15:55:47.10 | +68:40:16.0 | M2.5 V | Single | |
| 1819 | | J15569+376 | RX J1556.9+3738 | | 15:56:58.12 | +37:38:14.3 | M2.5 V | Candidate | |
| 1820 | | J15578+090 | LSPM J1557+0901 | | 15:57:48.42 | +09:01:07.6 | M4.0 V | Single | |
| 1821 | | J15581+494 | V1022 Her | | 15:58:10.41 | +49:27:05.5 | M1.0 V | Candidate | |
| 1822 | | J15583+354 | GJ 3929 | 3929 | 15:58:18.61 | +35:24:29.4 | M3.5 V | Single | A.11 |
| 1823 | | J15587+346 | StM 258 | | 15:58:45.75 | +34:48:53.8 | M3.5 V | Candidate | |
| 1824 | 499 | J15597+440 | RX J1559.7+4403 | | 15:59:47.20 | +44:03:59.6 | M2.0 V | Multiple | |
| 1825 | 499 | | PM J15597+4403B | | 15:59:46.70 | +44:04:01.0 | M8.0 V | Multiple | |
| 1826 | | J15598-082 | GJ 606 | 606 | 15:59:53.60 | -08:15:12.0 | M1.0 V | Single | |
| 1827 | | J16008+403 | GJ 3933 | 3933 | 16:00:50.40 | +40:19:38.7 | M3.0 V | Single | |
| 1828 | | J16017+301 | GJ 607 | 607 | 16:01:43.15 | +30:10:52.9 | M3.0 V | Single | |
| 1829 | 500 | J16018+304 | GJ 3935 | 3935 | 16:01:52.43 | +30:27:37.0 | M2.5 V | Multiple | |
| 1830 | 500 | J16017+304 | GJ 3936 | 3936 | 16:01:44.35 | +30:27:42.9 | M4.5 V | Multiple+ | |
| 1831 | | J16028+205 | GJ 609 | 609 | 16:02:49.85 | +20:35:01.2 | M4.0 V | Single | |
| 1832 | | J16033+175 | PM J16033+1735 | | 16:03:20.60 | +17:35:55.0 | M2.0 V | Candidate | |
| 1833 | | J16043-062 | GJ 3937 | 3937 | 16:04:19.91 | -06:16:59.9 | M4.5 V | Single | |
| 1834 | | J16046+263 | BPM 91242 | | 16:04:36.85 | +26:20:44.6 | M0.5 V | Single | |
| 1835 | 501 | | HD 144579 | 611 A | 16:04:56.01 | +39:09:24.3 | G8 V | Multiple | A.8 |
| 1836 | 501 | J16048+391 | HD 144579B | 611 B | 16:04:50.08 | +39:09:36.6 | M4.0 V | Multiple | A.8 |
| 1837 | | J16054+769 | GJ 3941 | 3941 | 16:05:26.51 | +76:54:58.5 | M2.5 V | Candidate | |
| 1838 | | J16062+290 | LP 329-30 | | 16:06:13.41 | +29:02:01.6 | M2.0 V | Candidate | |
| 1839 | 502 | J16066+083 | GJ 611.3 | 611.3 | 16:06:40.66 | +08:23:19.6 | M0.5 V | Multiple | |
| 1840 | 502 | | Gaia DR3 4451575895400385536 | | 16:06:40.51 | +08:23:20.4 | M3.5 V | Multiple | |
| 1841 | | J16074+059 | GJ 3939 | 3939 | 16:07:27.90 | +05:57:56.0 | M3.5 V | Single | |
| 1842 | | J16082-104 | GJ 1198 | 1198 | 16:08:14.56 | -10:26:35.1 | M4.5 V | Single | |
| 1843 | | J16090+529 | GJ 3942 | 3942 | 16:09:03.50 | +52:56:39.0 | M0.0 V | Single | A.11 |
| 1844 | | J16092+093 | LP 504-59 | | 16:09:15.90 | +09:21:11.0 | M3.0 V | Single | |
| 1845 | | J16102-193 | K2-33 | | 16:10:14.73 | -19:19:09.8 | M3.0 V | Single | A.11 |
| 1846 | 503 | J16120+033 | TYC 371-1053-1 | | 16:12:04.68 | +03:18:19.8 | M2.0 V | Multiple+ | |
| 1847 | 503 | | 1RXS J161204.8+031850 | | 16:12:05.06 | +03:18:52.4 | M3.5 V | Multiple+ | |
| 1848 | | J16126-188 | LP 804-27 | | 16:12:41.82 | -18:52:35.2 | M3.0 V | Single | A.11 |
| 1849 | 504 | | σ CrB A | 9550 A | 16:14:40.51 | +33:51:29.6 | F6 V | Multiple | A.4 A.7 A.8 |
| 1850 | 504 | | σ CrB B | 9550 B | 16:14:40.01 | +33:51:25.8 | G1 V | Multiple | A.7 A.8 |
| 1851 | 504 | J16139+337 | σ CrB C | 9549 | 16:13:55.90 | +33:46:22.7 | M2.5 V | Multiple | A.7 A.8 |
| 1852 | | J16144-028 | LP 624-54 | | 16:14:25.19 | -02:50:54.9 | M5.0 V | Single | |
| 1853 | | J16145+191 | GJ 1200 | 1200 | 16:14:30.36 | +19:06:16.7 | M3.5 V | Single | |
| 1854 | | J16147+048 | GJ 3946 | 3946 | 16:14:43.36 | +04:52:09.7 | M3.5 V | Single | |
| 1855 | | J16155+244 | GJ 3947 | 3947 | 16:15:32.10 | +24:27:50.9 | M1.0 V | Single | |
| 1856 | 505 | J16167+672S | HD 147379 | 617 A | 16:16:41.37 | +67:14:21.2 | M0.0 V | Multiple | A.11 |
| 1857 | 505 | J16167+672N | EW Dra | 617 B | 16:16:43.98 | +67:15:23.9 | M3.0 V | Multiple | |
| 1858 | | J16180+062 | 1RXS J161804.9+061702 | | 16:18:05.01 | +06:17:12.0 | M3.0 V | Candidate | |
| 1859 | 506 | J16170+552 | CR Dra | 9552 | 16:17:05.52 | +55:16:01.9 | M1.5 V | Multiple | |
| 1860 | 507 | J16204-042 | GJ 618.1 A | 618.1 A | 16:20:24.34 | -04:16:02.6 | M0.0 V | Multiple | A.10 |
| 1861 | 507 | | GJ 618.1 B | 618.1 B | 16:20:25.72 | -04:16:32.0 | L2.5 | Multiple | A.10 |
| 1862 | | J16220+228 | V1169 Her | | 16:22:01.12 | +22:50:22.8 | M1.5 V | Candidate | |
| 1863 | | J16247+229 | LSPM J1624+2254 | | 16:24:43.71 | +22:54:19.3 | M1.0 V | Candidate | |
| 1864 | | J16254+543 | GJ 625 | 625 | 16:25:25.41 | +54:18:12.0 | M1.5 V | Single | A.11 |
| 1865 | 508 | J16241+483 | GJ 623 | 623 | 16:24:11.16 | +48:21:03.1 | M2.5 V | Multiple | |
| 1866 | | J16255+323 | LP 330-13 | | 16:25:32.91 | +32:18:34.1 | M2.0 V | Single | |
| 1867 | | J16259+834 | TYC 4647-2406-1 | | 16:25:59.21 | +83:24:23.2 | M1.5 V | Single | |
| 1868 | 509 | J16255+260 | GJ 3953 | 3953 | 16:25:32.12 | +26:01:38.0 | M3.0 V | Multiple | |
| 1869 | 510 | J16268-173 | GJ 3954 | 3954 | 16:26:47.75 | -17:23:40.5 | M4.5 V | Multiple | |
| 1870 | 511 | J16280+155 | GJ 3955 | 3955 | 16:28:02.04 | +15:33:52.1 | M2.5 V | Multiple | |
| 1871 | | J16303-126 | V2306 Oph | 628 | 16:30:17.96 | -12:40:04.3 | M3.5 V | Single | |
| 1872 | | J16313+408 | GJ 3959 | 3959 | 16:31:18.59 | +40:51:56.6 | M5.0 V | Candidate | |
| 1873 | | J16315+175 | GJ 1202 | 1202 | 16:31:34.69 | +17:33:35.9 | M3.5 V | Single | |
| 1874 | | J16327+126 | GJ 1203 | 1203 | 16:32:44.36 | +12:36:43.8 | M3.0 V | Single | |
| 1875 | | J16328+098 | GJ 3960 | 3960 | 16:32:53.09 | +09:50:28.5 | M3.5 V | Candidate | |
| 1876 | | J16342+543 | LP 137-37 | | 16:34:13.28 | +54:23:48.5 | M1.0 V | Single | |
| 1877 | 512 | J16302-146 | GJ 2121 | 2121 | 16:30:12.52 | -14:39:53.0 | M3.0 V | Multiple | |
| 1878 | 513 | | GJ 630.1 B | 630.1 B | 16:34:19.37 | +57:10:28.1 | DQ8 | Multiple | A.9 |
| 1879 | 513 | J16343+571 | CM Dra | 630.1 A | 16:34:18.14 | +57:10:03.3 | M4.5 V | Multiple | A.4 A.5 A.9 |
| 1880 | | J16360+088 | GJ 1204 | 1204 | 16:36:05.09 | +08:48:46.7 | M4.0 V | Single | |
| 1881 | | J16395+505 | G 202-68 | | 16:39:30.81 | +50:33:57.0 | M1.0 V | Single | |
| 1882 | | J16401+007 | GJ 3967 | 3967 | 16:40:06.17 | +00:42:16.3 | M4.0 V | Single | |
| 1883 | | J16403+676 | GJ 3971 | 3971 | 16:40:19.87 | +67:36:10.6 | M5.5 V | Candidate | |
| 1884 | | J16408+363 | Ross 812 | 3968 | 16:40:48.72 | +36:19:02.9 | M2.0 V | Candidate | |

Table A.1: Complete sample studied in this work^a (cont.).

| Star id. | System id. | Karmn | Name | GJ | α (J2016.0) | δ (J2016.0) | Spectral type | Multiplicity type | In tables |
|----------|------------|-------------|------------------------------|---------|-----------------------|-----------------------|---------------|-------------------|-----------|
| 1885 | | J16420+192 | PM J16420+1916 | | 16:42:00.72 | +19:16:11.6 | M2.5 V | Single | |
| 1886 | | J16462+164 | GJ 3972 | 3972 | 16:46:13.35 | +16:28:33.2 | M2.5 V | Single | |
| 1887 | | J16465+345 | LP 276–22 | | 16:46:31.03 | +34:34:49.0 | M6.0 V | Single | |
| 1888 | 514 | J16354+350 | V1200 Her | 3966 | 16:35:27.61 | +35:00:55.3 | M4.0 V | Multiple | |
| 1889 | | J16487–157 | GJ 3973 | 3973 | 16:48:45.95 | -15:44:23.7 | M1.5 V | Single | |
| 1890 | | J16508–048 | GJ 3975 | 3975 | 16:50:52.99 | -04:50:38.8 | M3.5 V | Single | |
| 1891 | | J16509+224 | GJ 3976 | 3976 | 16:50:57.98 | +22:27:12.1 | M4.5 V | Single | |
| 1892 | | J16528+630 | GSC 04194–01561 | | 16:52:49.82 | +63:04:41.2 | M4.5 V | Single | |
| 1893 | | J16529+400 | GJ 3979 | 3979 | 16:52:54.92 | +40:05:04.6 | M3.5 V | Candidate | |
| 1894 | | J16542+119 | Ross 644 | 642 | 16:54:11.44 | +11:54:57.9 | M0.0 V | Single | |
| 1895 | 515 | J16487+106 | LSPM J1648+1038 | | 16:48:46.40 | +10:38:51.1 | M2.5 V | Multiple | |
| 1896 | 516 | J16554–083S | V1054 Oph | 644 B | 16:55:27.89 | -08:20:25.2 | M3.0 V | Multiple | A.4 |
| 1897 | 516 | J16554–083N | Wolf 629 | 643 | 16:55:24.34 | -08:19:35.7 | M3.5 V | Multiple | |
| 1898 | 516 | J16555–083 | GJ 644 C | 644 C | 16:55:34.38 | -08:23:54.7 | M7.0 V | Multiple | |
| 1899 | | J16570–043 | GJ 1207 | 1207 | 16:57:06.25 | -04:21:02.3 | M3.5 V | Single | |
| 1900 | | J16573+124 | GJ 3980 | 3980 | 16:57:23.12 | +13:28:06.6 | M4.0 V | Candidate | |
| 1901 | 517 | J16573+271 | PM J16573+2708 | | 16:57:22.27 | +27:08:31.2 | M2.0 V | Multiple | |
| 1902 | 517 | | PM J16573+2708B | | 16:57:22.34 | +27:08:30.6 | M3.0 V | Multiple | |
| 1903 | | J16574+777 | GJ 3986 | 3986 | 16:57:29.79 | +77:43:06.3 | M2.5 V | Single | |
| 1904 | 518 | J16577+132 | GJ 647 | 647 | 16:57:46.15 | +13:17:31.1 | M0.0 V | Multiple | |
| 1905 | 519 | | V1090 Her | 649.1 A | 16:57:52.95 | +47:22:04.4 | K3 V | Multiple | A.8 A.11 |
| 1906 | 519 | J16578+473 | HD 153557B | 649.1 B | 16:57:53.40 | +47:22:06.7 | M1.5 V | Multiple | A.8 |
| 1907 | 519 | | V1089 Her | 649.1 C | 16:57:42.01 | +47:21:47.9 | K3 V | Multiple | A.8 |
| 1908 | | J16581+257 | Ross 860 | 649 | 16:58:08.71 | +25:44:30.8 | M1.0 V | Single | A.11 |
| 1909 | 520 | J16584+139 | GJ 3981 A | 3981 A | 16:58:24.81 | +13:58:10.9 | M4.0 V | Multiple | |
| 1910 | 520 | | GJ 3981 B | 3981 B | 16:58:24.79 | +13:58:10.8 | M4.5 V | Multiple | |
| 1911 | | J16587+688 | LP 43–338 | | 16:58:42.17 | +68:53:55.8 | M1.5 V | Single | |
| 1912 | 521 | J16591+209 | V1234 Her | | 16:59:09.58 | +20:58:18.3 | M3.5 V | Multiple | |
| 1913 | 521 | | PM J16591+2058B | | 16:59:09.62 | +20:58:17.9 | M4.0 V | Multiple | |
| 1914 | | J17003+253 | GJ 3983 | 3983 | 17:00:20.18 | +25:21:05.1 | M2.5 V | Single | |
| 1915 | | J17006+063 | G 139–4 | | 17:00:38.65 | +06:18:42.0 | M1.0 V | Single | |
| 1916 | | J17010+082 | GJ 3984 | 3984 | 17:01:01.85 | +08:12:23.5 | M3.5 V | Single | |
| 1917 | | J17027–060 | GJ 3987 | 3987 | 17:02:49.45 | -06:04:07.6 | M0.0 V | Single | |
| 1918 | | J17033+514 | GJ 3988 | 3988 | 17:03:24.10 | +51:24:32.6 | M4.5 V | Single | |
| 1919 | 522 | J17038+321 | LP 331–57 A | | 17:03:53.09 | +32:11:47.6 | M2.0 V | Multiple | A.4 |
| 1920 | 522 | | LP 331–57 B | | 17:03:53.14 | +32:11:46.4 | M4.0 V | Multiple | A.2 |
| 1921 | | J17043+169 | GJ 1209 | 1209 | 17:04:22.49 | +16:55:37.5 | M3.0 V | Single | |
| 1922 | 523 | | HD 154363 | 653 | 17:05:02.41 | -05:04:17.7 | K4.5 V | Multiple | A.8 |
| 1923 | 523 | J17052–050 | HD 154363B | 654 | 17:05:12.80 | -05:05:57.4 | M1.5 V | Multiple | A.8 |
| 1924 | 524 | | LP 387–36 | | 17:05:52.54 | +26:05:46.7 | DC7 | Multiple | A.9 |
| 1925 | 524 | J17058+260 | LP 387–37 | | 17:05:52.55 | +26:05:27.4 | M1.5 V | Multiple | A.9 |
| 1926 | | J17071+215 | Ross 863 | 655 | 17:07:06.96 | +21:33:14.1 | M3.0 V | Single | |
| 1927 | | J17082+516 | G 203–44 | | 17:08:12.71 | +51:38:10.6 | M1.0 V | Single | |
| 1928 | 525 | J17076+073 | GJ 1210 | 1210 | 17:07:40.31 | +07:22:00.6 | M5.0 V | Multiple | |
| 1929 | | J17098+119 | GJ 3990 | 3990 | 17:09:52.36 | +11:55:32.8 | M4.0 V | Candidate | |
| 1930 | 526 | J17095+436 | GJ 3991 | 3991 | 17:09:32.03 | +43:40:48.4 | M3.5 V | Multiple | A.4 |
| 1931 | 527 | J17104+279 | StM 336 | | 17:10:25.49 | +27:58:38.6 | M2.5 V | Multiple | |
| 1932 | 527 | | CTI 170958.5+275905 | | 17:10:28.32 | +27:58:08.4 | M5.5 V | Multiple | |
| 1933 | 528 | J17121+456 | HD 155876 | 661 | 17:12:08.21 | +45:39:32.6 | M3.5 V | Multiple | |
| 1934 | 528 | | Gaia DR3 1364668825433435776 | 661 B | 17:12:08.21 | +45:39:33.7 | M3.0 V | Multiple | |
| 1935 | | J17115+384 | Wolf 654 | 3992 | 17:11:35.04 | +38:26:33.2 | M4.0 V | Single | |
| 1936 | 529 | J17118–018 | GJ 660 | 660 | 17:11:51.82 | -01:51:10.5 | M3.0 V | Multiple | |
| 1937 | 529 | | Gaia DR3 4367834134894197888 | 3991 | 17:11:51.82 | -01:51:10.3 | M3.0 V | Multiple | |
| 1938 | | J17146+269 | GJ 3994 | 3994 | 17:14:39.87 | +26:55:44.4 | M2.0 V | Candidate | |
| 1939 | | J17153+049 | GJ 1214 | 1214 | 17:15:19.56 | +04:57:38.1 | M4.5 V | Single | A.11 |
| 1940 | 530 | J17136–084 | V2367 Oph | 1212 | 17:13:40.00 | -08:25:21.4 | M3.5 V | Multiple | |
| 1941 | 531 | J17158+190 | GJ 3997 | 3997 | 17:15:49.95 | +19:00:00.3 | M0.5 V | Multiple | |
| 1942 | 531 | | BD+19 3268B | | 17:15:49.84 | +19:00:00.3 | M4.5 V | Multiple | A.2 |
| 1943 | | J17160+110 | GJ 3998 | 3998 | 17:16:00.49 | +11:03:22.1 | M1.0 V | Single | A.11 |
| 1944 | | J17166+080 | GJ 2128 | 2128 | 17:16:40.68 | +08:03:29.1 | M2.0 V | Single | |
| 1945 | 532 | J17177+116 | GJ 1215 | 1215 | 17:17:43.71 | +11:40:05.3 | M5.0 V | Multiple | |
| 1946 | 533 | J17177–118 | GJ 3999 | 3999 | 17:17:45.28 | -11:48:59.0 | M3.0 V | Multiple | |
| 1947 | 533 | | GJ 4000 | 4000 | 17:17:44.51 | -11:48:31.1 | M3.0 V | Multiple | |
| 1948 | 534 | J17183+181 | GJ 4002 | 4002 | 17:18:22.44 | +18:08:52.4 | M3.0 V | Multiple | |
| 1949 | 535 | J17183–017 | GJ 4001 | 4001 | 17:18:21.82 | -01:46:55.4 | M0.0 V | Multiple | |
| 1950 | 536 | J17199+265 | V647 Her | 669 A | 17:19:53.95 | +26:30:08.7 | M3.5 V | Multiple | |
| 1951 | 536 | J17198+265 | V639 Her | 669 B | 17:19:52.70 | +26:30:08.3 | M4.5 V | Multiple | |
| 1952 | | J17198+417 | GJ 671 | 671 | 17:19:53.12 | +41:42:36.4 | M2.5 V | Single | |
| 1953 | | J17207+492 | GJ 1216 | 1216 | 17:20:47.19 | +49:15:01.4 | M4.0 V | Single | |
| 1954 | | J17219+214 | GJ 4003 | 4003 | 17:21:54.44 | +21:25:51.3 | M4.0 V | Single | |
| 1955 | | J17225+055 | PM J17225+0531 | | 17:22:33.80 | +05:31:15.1 | M2.5 V | Single | |
| 1956 | | J17242–043 | GJ 4005 | 4005 | 17:24:16.69 | -04:21:54.1 | M2.5 V | Single | |
| 1957 | | J17276+144 | GJ 1219 | 1219 | 17:27:38.65 | +14:28:56.4 | M3.5 V | Single | |
| 1958 | | J17285+374 | Wolf 750 | 4009 | 17:28:30.41 | +37:27:04.1 | M3.0 V | Single | |
| 1959 | | J17303+055 | Wolf 751 | 9592 | 17:30:22.76 | +05:32:50.7 | M0.0 V | Single | |
| 1960 | | J17312+820 | GJ 1220 | 1220 | 17:31:14.95 | +82:05:27.8 | M4.0 V | Single | |
| 1961 | | J17316+047 | Wolf 755 | | 17:31:37.97 | +01:47:48.0 | M1.5 V | Single | |
| 1962 | | J17321+504 | GJ 4011 | 4011 | 17:32:07.82 | +50:24:41.7 | M2.5 V | Candidate | |
| 1963 | | J17328+543 | G 226–64 | | 17:32:53.06 | +54:20:19.6 | M2.0 V | Single | |
| 1964 | | J17338+169 | V1274 Her | | 17:33:53.03 | +16:55:11.0 | M5.5 V | Candidate | |
| 1965 | 537 | | RX J1734.0+4447A | | 17:34:05.43 | +44:47:08.9 | M2.0 V | Multiple | |
| 1966 | 537 | J17340+446 | RX J1734.0+4447B | | 17:34:05.47 | +44:47:08.4 | M3.5 V | Multiple | A.2 |

Table A.1: Complete sample studied in this work^a (cont.).

| Star id. | System id. | Karmn | Name | GJ | α (J2016.0) | δ (J2016.0) | Spectral type | Multiplicity type | In tables |
|----------|------------|-------------------------|-------------------------|--------|-----------------------|-----------------------|---------------|-------------------|--------------|
| 1967 | 538 | HD 160269A | | 684 | 17:35:00.16 | +61:52:20.8 | G0 IV/V | Multiple | A.7 A.8 |
| 1968 | 538 | J17355+616 | GJ 685 | 685 | 17:35:35.07 | +61:40:45.4 | M0.5 V | Multiple | A.7 A.8 A.11 |
| 1969 | | J17364+683 | GJ 687 | 687 | 17:36:24.97 | +68:20:00.6 | M3.0 V | Single | A.11 |
| 1970 | | J17376+220 | GJ 4015 | 4015 | 17:37:36.52 | +22:05:45.2 | M4.0 V | Single | |
| 1971 | | J17378+185 | GJ 686 | 686 | 17:37:54.39 | +18:35:45.9 | M1.0 V | Single | A.11 |
| 1972 | 539 | HD 160934B | | 4020 B | 17:38:39.61 | +61:14:16.8 | M4.0 V | Multiple | |
| 1973 | 539 | J17386+612 | GJ 4021 | 4021 | 17:38:40.87 | +61:14:00.0 | M4.0 V | Multiple | A.2 |
| 1974 | | J17388+080 | GJ 4016 | 4016 | 17:38:51.16 | +08:01:31.7 | M2.5 V | Single | |
| 1975 | 540 | J17395+277S | GJ 4018 | 4018 | 17:39:30.73 | +27:45:40.8 | M0.5 V | Multiple | |
| 1976 | 540 | J17395+277N | GJ 4019 | 4019 | 17:39:32.26 | +27:46:33.5 | M3.0 V | Multiple | |
| 1977 | | J17419+407 | G 204–25 | | 17:41:57.04 | +40:44:44.3 | M1.5 V | Single | |
| 1978 | | J17421–088 | Wolf 1471 | 4023 | 17:42:09.85 | -08:49:07.8 | M3.0 V | Single | |
| 1979 | | J17423+574 | 2MASS J17422264+5726521 | | 17:42:22.63 | +57:26:52.0 | M0.0 V | Single | |
| 1980 | | J17425–166 | GJ 690.1 | 690.1 | 17:42:32.15 | -16:38:35.9 | M2.5 V | Single | |
| 1981 | 541 | J17430+057 | GJ 4024 | 4024 | 17:43:01.06 | +05:47:20.5 | M1.0 V | Multiple | |
| 1982 | 542 | J17431+854 | G 259–20 | | 17:43:07.85 | +85:26:25.5 | M2.0 V | Multiple+ | A.10 |
| 1983 | 542 | 2MASS J17430860+8526594 | | | 17:43:07.13 | +85:26:55.2 | L5 | Multiple | A.10 |
| 1984 | | J17432–185 | Ross 133 | 9600 | 17:43:17.37 | -18:31:27.7 | M1.5 V | Candidate | |
| 1985 | | J17439+433 | GJ 694 | 694 | 17:43:55.98 | +43:22:33.3 | M2.5 V | Single | |
| 1986 | | J17460+246 | GJ 4026 | 4026 | 17:46:04.22 | +24:39:13.1 | M4.0 V | Single | |
| 1987 | 543 | J17455+468 | GJ 694.2 | 694.2 | 17:45:33.50 | +46:51:19.8 | M0.0 V | Multiple | |
| 1988 | 544 | HD 161797 | | 695 A | 17:46:27.17 | +27:43:02.2 | G5 IV | Multiple | A.8 |
| 1989 | 544 | GJ 695 B | | 695 B | 17:46:24.69 | +27:42:49.5 | M2.5 V | Multiple | A.8 |
| 1990 | 544 | GJ 695 C | | 695 C | 17:46:24.65 | +27:42:49.8 | M3.5 V | Multiple | A.2 A.8 |
| 1991 | | J17469+228 | StKM 1–1528 | | 17:46:55.96 | +22:48:01.6 | M1.0 V | Single | |
| 1992 | | J17481+159 | PM J17481+1558 | | 17:48:11.19 | +15:58:48.4 | M3.0 V | Single | |
| 1993 | | J17502+237 | GJ 4030 | 4030 | 17:50:14.74 | +23:45:58.1 | M3.5 V | Single | |
| 1994 | | J17515+147 | GJ 4031 | 4031 | 17:51:30.58 | +14:45:32.4 | M3.5 V | Single | |
| 1995 | | J17521+647 | G 227–20 | | 17:52:11.83 | +64:46:02.9 | M0.5 V | Single | |
| 1996 | 545 | J17464+087 | Wolf 1473 | | 17:46:29.28 | -08:42:43.4 | M3.5 V | Multiple | A.4 |
| 1997 | 546 | J17530+169 | GJ 4032 A | 4032 A | 17:53:00.32 | +16:54:59.5 | M3.0 V | Multiple | |
| 1998 | 546 | GJ 4032 B | | 4032 B | 17:53:00.38 | +16:54:59.2 | M4.0 V | Multiple | |
| 1999 | | J17542+073 | GJ 1222 | 1222 | 17:54:16.48 | +07:22:40.2 | M4.0 V | Single | |
| 2000 | | J17547+128 | LSPM J1754+1251 | | 17:54:43.24 | +12:51:18.6 | M2.0 V | Single | |
| 2001 | 547 | J17570+157 | GJ 4038 | 4038 | 17:57:03.33 | +15:46:39.3 | M3.0 V | Multiple | |
| 2002 | 547 | G 183–13B | | | 17:57:03.41 | +15:46:39.1 | M3.0 V | Multiple | |
| 2003 | | J17572+707 | LP 44–162 | | 17:57:15.43 | +70:42:06.4 | M7.5 V | Candidate | |
| 2004 | | J17578+046 | Barnard's star | 699 | 17:57:47.64 | +04:44:21.9 | M3.5 V | Single | |
| 2005 | 548 | J17578+465 | GJ 4040 | 4040 | 17:57:50.94 | +46:35:28.4 | M2.5 V | Multiple | A.10 |
| 2006 | 548 | G 204–39B | | | 17:58:05.45 | +46:33:09.9 | T7 | Multiple | A.10 |
| 2007 | | J17589+807 | LP 24–152 | | 17:58:55.00 | +80:42:53.9 | M3.5 V | Candidate | |
| 2008 | | J18010+508 | Wolf 1403 | | 18:01:05.86 | +50:49:38.9 | M1.5 V | Single | |
| 2009 | | J18012+355 | G 182–34 | | 18:01:16.14 | +35:35:41.4 | M3.5 V | Single | |
| 2010 | | J18022+642 | LP 71–82 | | 18:02:17.09 | +64:15:38.1 | M5.0 V | Single | |
| 2011 | | J18027+375 | GJ 1223 | 1223 | 18:02:46.49 | +37:30:44.7 | M5.0 V | Single | |
| 2012 | | J18031+179 | Wolf 792 | | 18:03:06.02 | +17:54:20.0 | M1.0 V | Candidate | |
| 2013 | | J18037+247 | Ross 820 | | 18:03:47.68 | +25:45:16.7 | M0.0 V | Single | |
| 2014 | 550 | J18042+359 | GJ 4041 | 4041 | 18:04:17.70 | +35:57:21.5 | M0.5 V | Multiple | |
| 2015 | | J18051–030 | HD 165222 | 701 | 18:05:08.19 | -03:01:58.1 | M1.0 V | Single | |
| 2016 | | J18063+728 | NLT 46021 | | 18:06:18.11 | +72:49:20.1 | M0.0 V | Single | |
| 2017 | | J18074+184 | Wolf 806 | | 18:07:27.99 | +18:27:54.1 | M1.0 V | Single | |
| 2018 | | J18075–159 | GJ 1224 | 1224 | 18:07:32.15 | -15:57:52.6 | M4.5 V | Single | |
| 2019 | | J18096+318 | LP 334–11 | | 18:09:40.77 | +31:52:16.0 | M1.0 V | Single | |
| 2020 | | J18103+512 | Wolf 1412 | | 18:10:23.37 | +51:15:55.0 | M2.0 V | Single | |
| 2021 | | J18109+220 | StKM 1–1582 | | 18:10:56.18 | +22:01:31.2 | M0.0 V | Single | |
| 2022 | 549 | J18116+061 | LP 569–163 | | 18:11:36.49 | +06:06:27.9 | M3.0 V | Multiple | |
| 2023 | 549 | LP 569–163 B | | | 18:11:36.51 | +06:06:27.3 | M4.5 V | Multiple | |
| 2024 | | J18131+260 | V1334 Her | 4044 | 18:13:06.83 | +26:01:51.3 | M4.0 V | Single | |
| 2025 | 551 | J18134+054 | LP 569–15 | | 18:13:28.12 | +05:26:54.8 | M1.5 V | Multiple | |
| 2026 | 551 | LP 569–16 | | | 18:13:33.09 | +05:32:08.4 | M4.0 V | Multiple | |
| 2027 | | J18157+189 | HD 348274 | 4046 | 18:15:43.54 | +18:56:12.7 | M0.0 V | Candidate | |
| 2028 | | J18160+139 | GJ 708.2 | 708.2 | 18:16:02.36 | +13:54:40.2 | M0.0 V | Single | |
| 2029 | | J18163+015 | GJ 708.3 | 708.3 | 18:16:17.74 | +01:31:17.1 | M3.0 V | Single | |
| 2030 | | J18165+048 | G 140–51 | | 18:16:31.37 | +04:52:52.3 | M5.0 V | Single | |
| 2031 | | J18165+455 | GJ 709 | 709 | 18:16:31.07 | +45:33:33.7 | M0.5 V | Single | |
| 2032 | | J18174+483 | V401 Dra | | 18:17:25.05 | +48:22:03.1 | M2.0 V | Single | |
| 2033 | 552 | J18180+387E | GJ 4048 | 4048 | 18:18:03.73 | +38:46:16.2 | M3.0 V | Multiple | |
| 2034 | 552 | J18180+387W | GJ 4049 | 4049 | 18:18:02.88 | +38:46:17.4 | M4.0 V | Multiple | |
| 2035 | | J18189+661 | GJ 4053 | 4053 | 18:18:58.38 | +66:11:26.2 | M4.5 V | Single | |
| 2036 | | J18193–057 | GJ 4051 | 4051 | 18:19:21.68 | -05:46:33.5 | M2.0 V | Single | |
| 2037 | | J18195+420 | PM J18195+4201 | | 18:19:34.48 | +42:01:37.4 | M1.5 V | Single | |
| 2038 | 553 | J18209–010 | GJ 1226 A | 1226 A | 18:20:56.62 | -01:03:14.2 | M3.5 V | Multiple | |
| 2039 | 553 | GJ 1226 B | | 1226 B | 18:20:56.63 | -01:03:12.8 | M4.0 V | Multiple | |
| 2040 | | J18221+063 | Ross 136 | 712 | 18:22:05.40 | +06:20:39.4 | M4.0 V | Single | |
| 2041 | | J18224+620 | GJ 1227 | 1227 | 18:22:24.92 | +62:02:42.0 | M4.0 V | Single | |
| 2042 | | J18227+379 | G 205–19 | | 18:22:43.47 | +37:57:41.1 | M1.0 V | Candidate | |
| 2043 | 554 | J18234+281 | Ross 708A | | 18:23:28.24 | +28:10:01.0 | M3.5 V | Multiple | |
| 2044 | 554 | Ross 708B | | | 18:23:28.25 | +28:09:59.7 | M5.5 V | Multiple | |
| 2045 | | J18240+016 | GJ 4056 | 4056 | 18:24:05.35 | +01:41:12.3 | M2.0 V | Single | |
| 2046 | 555 | J18248+282 | Ross 710 | | 18:24:52.32 | +28:17:22.3 | M1.5 V | Multiple | |
| 2047 | | J18250+246 | HD 336196 | 4057 | 18:25:04.75 | +24:37:57.3 | M0.0 V | Single | |
| 2048 | | J18255+383 | GJ 4058 | 4058 | 18:25:31.82 | +38:21:00.8 | M0.0 V | Single | |

Table A.1: Complete sample studied in this work^a (cont.).

| Star id. | System id. | Karmn | Name | GJ | α (J2016.0) | δ (J2016.0) | Spectral type | Multiplicity type | In tables |
|----------|------------|------------------|-------------------------|--------|-----------------------|-----------------------|---------------|-------------------|---------------|
| 2049 | 556 | LSPM J1826+1120S | | | 18:26:24.42 | +11:20:45.1 | DA | Multiple | A.9 |
| 2050 | 556 | J18264+113 | GJ 4059 | 4059 | 18:26:24.58 | +11:20:52.9 | M3.5 V | Multiple | A.9 |
| 2051 | | J18292+638 | TYC 4222-2195-1 | | 18:29:13.36 | +63:51:10.9 | M1.5 V | Candidate | |
| 2052 | | J18296+338 | 2MASS J18294012+3350130 | | 18:29:40.02 | +33:50:13.3 | M3.0 V | Single | |
| 2053 | | J18312+068 | LP 570-92 | | 18:31:16.21 | +06:50:08.2 | M1.0 V | Single | |
| 2054 | | J18319+406 | GJ 4062 | 4062 | 18:31:58.24 | +40:41:17.6 | M3.5 V | Single | |
| 2055 | | J18346+401 | GJ 4063 | 4063 | 18:34:36.73 | +40:07:23.1 | M3.5 V | Single | |
| 2056 | 557 | J18352+243 | G 184-13A | | 18:35:13.42 | +24:18:39.2 | M2.5 V | Multiple | |
| 2057 | 557 | G 184-13B | | | 18:35:13.44 | +24:18:41.7 | M3.5 V | Multiple | |
| 2058 | | J18352+414 | GJ 4064 | 4064 | 18:35:18.38 | +41:29:14.5 | M1.5 V | Single | |
| 2059 | 558 | J18353+457 | GJ 720 A | 720 A | 18:35:19.08 | +45:44:44.4 | M0.5 V | Multiple | A.11 |
| 2060 | 558 | J18354+457 | GJ 720 B | 720 B | 18:35:27.99 | +45:45:46.7 | M2.5 V | Multiple | |
| 2061 | | J18356+329 | LSPM J1835+3259 | | 18:35:37.79 | +32:59:41.2 | M8.5 V | Single | A.11 |
| 2062 | | J18358+800 | GJ 4068 | 4068 | 18:35:52.58 | +80:05:42.9 | M3.5 V | Single | |
| 2063 | | J18362+567 | G 227-39 | | 18:36:12.72 | +56:44:37.8 | M0.0 V | Single | |
| 2064 | | J18363+136 | Ross 149 | 4065 | 18:36:19.43 | +13:36:30.8 | M4.0 V | Single | |
| 2065 | 559 | J18387+047 | LP 570-22 | | 18:38:47.63 | +04:46:01.7 | M0.5 V | Multiple | |
| 2066 | | J18394+690 | RX J1839.4+6903 | | 18:39:25.71 | +69:03:06.8 | M2.0 V | Candidate | |
| 2067 | | J18395+298 | LP 335-12 | | 18:39:33.18 | +29:52:12.9 | M6.5 V | Single | |
| 2068 | | J18395+301 | LP 335-13 | | 18:39:32.00 | +30:09:52.1 | M0.0 V | Single | |
| 2069 | | J18399+334 | GJ 4067 | 4067 | 18:39:59.94 | +33:24:58.9 | M3.5 V | Single | |
| 2070 | 560 | J18400+726 | LP 44-334 | | 18:40:02.20 | +72:40:57.2 | M6.5 V | Multiple | |
| 2071 | 560 | LP 44-334 B | | | 18:40:02.32 | +72:40:56.6 | M6.5 V | Multiple | |
| 2072 | 561 | J18387-144 | GJ 2138 | 2138 | 18:38:44.87 | -14:29:35.1 | M2.5 V | Multiple | |
| 2073 | | J18402-104 | Wolf 1466 | 723 | 18:40:17.68 | -10:28:04.1 | M0.0 V | Single | |
| 2074 | | J18405+595 | G 227-43 | | 18:40:35.77 | +59:30:53.6 | M2.0 V | Single | |
| 2075 | 562 | BD+31 3330 | | | 18:40:54.99 | +31:31:45.7 | K2.5 V | Multiple | A.8 |
| 2076 | 562 | J18409+315 | BD+31 3330B | | 18:40:55.33 | +31:31:37.3 | M1.0 V | Multiple | A.8 |
| 2077 | 562 | BD+31 3330C | | | 18:40:55.31 | +31:31:37.5 | M1.0 V | Multiple | A.8 |
| 2078 | | J18409-133 | Ross 720 | 724 | 18:40:57.20 | -13:22:57.3 | M1.0 V | Single | |
| 2079 | 563 | J18411+247S | GJ 1230 A | 1230 A | 18:41:10.35 | +24:47:15.8 | M4.5 V | Multiple | A.4 |
| 2080 | 563 | J18411+247N | GJ 1230 B | 1230 B | 18:41:10.39 | +24:47:20.5 | M5.0 V | Multiple | |
| 2081 | | J18416+397 | GJ 4069 | 4069 | 18:41:37.04 | +39:42:09.3 | M4.0 V | Single | |
| 2082 | | J18419+318 | Ross 145 | 4070 | 18:41:58.66 | +31:49:49.9 | M3.0 V | Single | |
| 2083 | | J18427+139 | V816 Her | 4071 | 18:42:44.94 | +13:54:22.4 | M4.0 V | Single | |
| 2084 | 564 | J18427+596N | HD 173739 | 725 A | 18:42:43.94 | +59:38:18.1 | M3.0 V | Multiple | |
| 2085 | 564 | J18427+596S | HD 173740 | 725 B | 18:42:43.94 | +59:38:06.5 | M3.5 V | Multiple | |
| 2086 | | J18432+253 | TYC 2112-920-1 | | 18:43:14.51 | +25:22:43.1 | M1.0 V | Single | |
| 2087 | 565 | J18433+406 | V492 Lyr | 4073 | 18:43:21.96 | +40:40:30.8 | M7.5 V | Multiple | |
| 2088 | | J18451+063 | IRXS J184510.6+062016 | | 18:45:10.23 | +06:20:14.7 | M1.0 V | Single | |
| 2089 | | J18453+188 | G 184-24 | | 18:45:22.79 | +18:51:54.3 | M4.0 V | Single | |
| 2090 | | J18480-145 | GJ 4077 | 4077 | 18:48:01.01 | -14:34:55.0 | M2.5 V | Single | |
| 2091 | | J18482+076 | G 141-36 | | 18:48:17.94 | +07:41:25.2 | M5.0 V | Single | |
| 2092 | | J18487+615 | LSPM J1848+6135 | | 18:48:47.07 | +61:35:06.3 | M2.0 V | Single | |
| 2093 | | J18498-238 | V1216 Sgr | 729 | 18:49:50.11 | -23:50:13.6 | M3.5 V | Single | |
| 2094 | | J18499+186 | G 184-31 | | 18:49:54.34 | +18:40:24.2 | M4.5 V | Single | |
| 2095 | | J18500+030 | Ross 142 | 730 | 18:50:00.63 | +03:05:10.7 | M0.5 V | Single | |
| 2096 | | J18507+479 | GJ 4083 | 4083 | 18:50:45.66 | +47:58:17.3 | M3.5 V | Single | |
| 2097 | | J18515+027 | BD+02 3698 | | 18:51:35.59 | +02:46:19.2 | M0.5 V | Single | |
| 2098 | | J18516+244 | GJ 4084 | 4084 | 18:51:40.44 | +24:27:31.7 | M3.0 V | Single | |
| 2099 | | J18518+165 | HD 229793 | 731 | 18:51:50.93 | +16:34:52.1 | M0.0 V | Single | |
| 2100 | | J18519+130 | IRXS J185200.0+130005 | | 18:51:59.66 | +13:00:01.1 | M2.0 V | Candidate | |
| 2101 | | J18534+028 | G 141-46 | | 18:53:25.68 | +02:50:49.4 | M2.5 V | Candidate | |
| 2102 | | J18548+008 | BD+00 4050 | | 18:54:53.14 | +00:51:44.8 | M0.0 V | Single | |
| 2103 | 566 | HD 230017A | | 734 A | 18:54:53.67 | +10:58:42.4 | M0.0 V | Multiple | A.7.7 |
| 2104 | 566 | J18548+109 | HD 230017B | 734 B | 18:54:53.86 | +10:58:45.1 | M3.5 V | Multiple | A.2 A.7.7 |
| 2105 | 566 | PM J18542+1058 | | | 18:54:17.14 | +10:58:11.0 | M4.0 V | Multiple | A.2 A.3 A.7.7 |
| 2106 | 567 | J18554+084 | GJ 735 | 735 | 18:55:27.51 | +08:24:07.9 | M3.0 V | Multiple | A.4 |
| 2107 | 568 | MCC 806A | | 4091A | 18:56:16.00 | +54:31:42.3 | M1.0 V | Multiple | |
| 2108 | 568 | MCC 806B | | | 18:56:15.98 | +54:31:42.4 | M1.0 V | Multiple | |
| 2109 | 568 | J18563+544 | GJ 4091 B | 4091 B | 18:56:18.29 | +54:29:45.5 | M2.0 V | Multiple | A.4 |
| 2110 | | J18564+463 | GJ 4089 | 4089 | 18:56:26.40 | +46:22:58.5 | M4.0 V | Candidate | |
| 2111 | | J18571+075 | GJ 4088 | 4088 | 18:57:10.40 | +07:34:14.7 | M2.0 V | Single | |
| 2112 | 569 | LP 141-14 | | | 18:57:39.78 | +53:30:32.5 | DC | Multiple | A.9 A.11 |
| 2113 | 569 | J18576+535 | G 229-20A | | 18:57:38.42 | +53:31:14.4 | M3.5 V | Multiple | A.9 |
| 2114 | 569 | LP 141-13 | | | 18:57:38.34 | +53:31:12.2 | M3.0 V | Multiple | A.9 |
| 2115 | | J18580+059 | HD 176029 | 740 | 18:57:59.93 | +05:54:09.7 | M0.5 V | Single | A.11 |
| 2116 | | J18596+079 | GJ 4092 | 4092 | 18:59:39.00 | +07:59:11.2 | M0.0 V | Single | |
| 2117 | | J19025+704 | GJ 4093 | 4093 | 19:02:30.83 | +70:25:53.6 | M2.5 V | Single | |
| 2118 | | J19025+754 | LSPM J1902+7525 | | 19:02:32.79 | +75:25:06.6 | M1.5 V | Single | |
| 2119 | | J19032+034 | G 141-57 | | 19:03:13.40 | +03:24:01.4 | M3.0 V | Single | |
| 2120 | 570 | J19032+639 | GJ 4094 | 4094 | 19:03:17.46 | +63:59:35.9 | M3.5 V | Multiple | |
| 2121 | 570 | StKM 1-1676B | | | 19:03:17.96 | +63:59:37.4 | M2.0 V | Multiple | A.2 |
| 2122 | | J19032-135 | GJ 741 | 741 | 19:03:16.10 | -13:34:12.9 | M4.0 V | Single | |
| 2123 | | J19041+211 | IRXS J190405.9+211030 | | 19:04:06.24 | +21:10:32.7 | M2.0 V | Single | |
| 2124 | 571 | J19044+590 | LSPM J1907+5905 | | 19:07:24.98 | +59:05:11.9 | M3.0 V | Multiple | |
| 2125 | 571 | LSPM J1907+5905B | | | 19:07:24.72 | +59:05:14.7 | M6.0 V | Multiple | |
| 2126 | | J19045+240 | TYC 2122-1204-1 | | 19:04:31.24 | +24:01:54.8 | M2.0 V | Single | |
| 2127 | 572 | J19072+208 | HD 349726 | 745 B | 19:07:12.66 | +20:52:31.9 | M2.0 V | Multiple | |
| 2128 | 572 | J19070+208 | Ross 730 | 745 A | 19:07:05.02 | +20:53:11.4 | M2.0 V | Multiple | |
| 2129 | | J19082+265 | GJ 1231 | 1231 | 19:08:15.55 | +26:34:57.6 | M4.5 V | Candidate | |
| 2130 | | J19084+322 | GJ 4098 | 4098 | 19:08:29.67 | +32:16:48.0 | M3.0 V | Single | |

Table A.1: Complete sample studied in this work^a (cont.).

| Star id. | System id. | Karmn | Name | GJ | α (J2016.0) | δ (J2016.0) | Spectral type | Multiplicity type | In tables |
|----------|------------|-------------|------------------------------|---------|-----------------------|-----------------------|---------------|-------------------|-----------|
| 2131 | 573 | J19077+325 | GJ 747 | 747 | 19:07:44.54 | +32:32:59.3 | M3.0 V | Multiple | |
| 2132 | 574 | J19093+382 | GJ 4099 | 4099 | 19:09:19.01 | +39:12:00.7 | M1.0 V | Multiple | |
| 2133 | 574 | J19095+391 | LSPM J1909+3910 | | 19:09:31.54 | +39:10:48.4 | M2.0 V | Multiple | |
| 2134 | | J19093-147 | Ross 727 | 9644 | 19:09:20.08 | -14:45:02.4 | M2.5 V | Single | |
| 2135 | | J19098+176 | GJ 1232 | 1232 | 19:09:50.16 | +17:39:59.6 | M4.5 V | Single | |
| 2136 | 575 | J19106+015 | GJ 4100 | 4100 | 19:10:38.38 | +01:32:07.3 | M1.5 V | Multiple | |
| 2137 | 575 | | GJ 4100 B | 4100 B | 19:10:37.90 | +01:32:18.7 | M4.5 V | Multiple | |
| 2138 | | J19116+050 | TYC 471-1564-1 | | 19:11:47.89 | +05:00:37.4 | M1.0 V | Single | |
| 2139 | | J19124+355 | GJ 4105 | 4105 | 19:12:29.70 | +35:33:50.2 | M2.0 V | Single | |
| 2140 | 576 | J19122+028 | Wolf 1062 | 748 | 19:12:16.50 | +02:53:02.6 | M3.5 V | Multiple | |
| 2141 | 577 | J19146+193N | Ross 733 | 9652 A | 19:14:38.46 | +19:19:10.7 | M3.5 V | Multiple | |
| 2142 | 577 | J19146+193S | Ross 734 | 9652 B | 19:14:38.51 | +19:18:29.9 | M3.5 V | Multiple | |
| 2143 | 578 | J19169+051N | V1428 Aql | 752 A | 19:16:54.64 | +05:09:46.7 | M2.5 V | Multiple | |
| 2144 | 578 | J19169+051S | V1298 Aql | 752 B | 19:16:56.97 | +05:08:39.7 | M8.0 V | Multiple | |
| 2145 | 579 | J19185+580 | LSPM J1918+5803 | | 19:18:30.48 | +58:03:16.6 | M1.0 V | Multiple | |
| 2146 | 579 | | Gaia DR3 214323084400445696 | | 19:18:30.33 | +58:03:18.1 | M8.0 V | Multiple | |
| 2147 | 580 | | GJ 754.1 A | 754.1 A | 19:20:34.86 | -07:40:02.7 | DBQAS | Multiple | A.11 |
| 2148 | 580 | J19205-076 | GJ 754.1 B | 754.1 B | 19:20:33.38 | -07:39:46.6 | M2.5 V | Multiple | A.9 |
| 2149 | 581 | J19206+731S | 2MASS J19204172+7311434 | | 19:20:41.75 | +73:11:42.4 | M4.0 V | Multiple | A.11 |
| 2150 | 581 | J19206+731N | 2MASS J19204172+7311467 | | 19:20:41.76 | +73:11:45.5 | M4.5 V | Multiple | |
| 2151 | | J19216+208 | GJ 1235 | 1235 | 19:21:37.62 | +20:51:40.0 | M4.5 V | Single | |
| 2152 | | J19218+286 | V2078 Cyg | 756 | 19:21:52.48 | +28:40:02.3 | M1.5 V | Single | |
| 2153 | | J19220+070 | GJ 1236 | 1236 | 19:22:01.28 | +07:02:23.2 | M3.0 V | Single | |
| 2154 | | J19228+307 | GSC 02654-01527 | | 19:22:48.64 | +30:45:13.5 | M0.0 V | Candidate | |
| 2155 | | J19234+666 | NLTT 47788 | | 19:23:24.51 | +66:39:54.2 | M1.0 V | Single | |
| 2156 | 582 | J19215+425 | IRXS J192132.1+423041 | | 19:21:32.18 | +42:30:54.8 | M2.0 V | Multiple | |
| 2157 | 583 | J19242+797 | TYC 4592-101-1 | | 19:24:15.66 | +79:43:37.3 | M1.0 V | Multiple | |
| 2158 | 583 | J19237+797 | PM J19237+7944 | | 19:23:46.46 | +79:44:37.6 | M1.5 V | Multiple | |
| 2159 | | J19242+755 | GJ 1238 | 1238 | 19:24:17.89 | +75:33:21.3 | M5.5 V | Single | |
| 2160 | | J19251+283 | Ross 164 | 4109 | 19:25:08.74 | +28:21:19.8 | M3.0 V | Single | |
| 2161 | | J19255+096 | LSPM J1925+0938 | | 19:25:31.00 | +09:38:19.4 | M8.5 V | Candidate | |
| 2162 | | J19260+244 | G 185-23 | | 19:26:01.84 | +24:26:18.7 | M4.5 V | Single | |
| 2163 | | J19268+167 | GJ 4110 | 4110 | 19:26:49.42 | +16:42:58.3 | M3.0 V | Single | |
| 2164 | | J19284+289 | TYC 2137-1575-1 | | 19:28:25.51 | +28:54:09.6 | M0.0 V | Single | |
| 2165 | | J19289+066 | PM J19289+0638 | | 19:28:55.70 | +06:38:24.5 | M1.5 V | Single | |
| 2166 | 584 | J19312+361 | G 125-15 | | 19:31:12.38 | +36:07:28.2 | M4.5 V | Multiple | A.4 |
| 2167 | 584 | | G 125-14 | | 19:31:11.56 | +36:08:12.8 | M4.5 V | Multiple | |
| 2168 | | J19326+005 | GJ 761.2 | 761.2 | 19:32:38.15 | +00:34:39.5 | M0.0 V | Single | |
| 2169 | | J19336+395 | Ross 1063 | 4113 | 19:33:39.75 | +39:31:29.9 | M1.5 V | Candidate | |
| 2170 | | J19346+045 | HD 184489 | 763 | 19:34:40.40 | +04:35:02.0 | M0.0 V | Single | |
| 2171 | | J19349+532 | Wolf 1108 | 4117 | 19:34:55.56 | +53:15:31.3 | M2.5 V | Single | |
| 2172 | 585 | J19351+084S | GJ 4114 | 4114 | 19:35:06.24 | +08:27:37.9 | M0.0 V | Multiple | |
| 2173 | 585 | J19351+084N | GJ 4115 | 4115 | 19:35:06.33 | +08:27:43.4 | M2.5 V | Multiple | A.2 |
| 2174 | | J19358+413 | Ross 1064 | | 19:35:51.00 | +41:19:06.7 | M0.0 V | Candidate | |
| 2175 | | J19395+718 | GJ 4120 | 4120 | 19:39:32.22 | +71:52:12.1 | M0.0 V | Single | |
| 2176 | | J19419+031 | GJ 1242 | 1242 | 19:41:53.93 | +03:09:08.3 | M2.0 V | Candidate | |
| 2177 | 586 | J19354+377 | RX J1935.4+3746 | | 19:35:29.02 | +37:46:06.7 | M3.5 V | Multiple | A.4 |
| 2178 | | J19422-207 | 2MASS J19421282-2045477 | | 19:42:12.81 | -20:45:50.4 | M5.0 V | Single | |
| 2179 | 587 | J19420-210 | LP 869-19 | | 19:42:00.74 | -21:04:09.4 | M3.5 V | Multiple | A.4 |
| 2180 | 588 | J19457+271 | Ross 165A | 766 A | 19:45:45.41 | +27:07:11.7 | M4.0 V | Multiple | |
| 2181 | 588 | | Ross 165B | 766 B | 19:45:45.55 | +27:07:12.8 | M4.0 V | Multiple | |
| 2182 | | J19457+323 | GJ 4122 | 4122 | 19:45:50.25 | +32:23:16.8 | M1.0 V | Single | |
| 2183 | 589 | J19463+320 | HD 331161A | 767 A | 19:46:24.51 | +32:00:55.2 | M0.5 V | Multiple | |
| 2184 | 589 | J19464+320 | HD 331161B | 767 B | 19:46:24.83 | +32:00:51.1 | M2.5 V | Multiple | |
| 2185 | | J19468-019 | PM J19468-0157 | | 19:46:50.63 | -01:57:40.1 | M3.0 V | Candidate | |
| 2186 | | J19470+352 | LSPM J1947+3516 | | 19:47:03.30 | +35:16:55.5 | M2.0 V | Single | |
| 2187 | | J19486+359 | G 125-34 | | 19:48:40.88 | +35:55:12.6 | M3.5 V | Single | |
| 2188 | 590 | J19500+325 | GJ 4124 | 4124 | 19:50:03.10 | +32:35:05.5 | M2.5 V | Multiple | |
| 2189 | 591 | J19502+317 | GJ 4125 | 4125 | 19:50:16.11 | +31:47:05.7 | M2.5 V | Multiple | |
| 2190 | 592 | | HD 187691 | 9671 A | 19:51:01.91 | +10:24:54.4 | F8 V | Multiple | A.8 |
| 2191 | 592 | J19510+104 | GJ 9671 B | 9671 B | 19:51:00.97 | +10:24:38.0 | M3.5 V | Multiple+ | A.8 |
| 2192 | | J19511+464 | GJ 1243 | 1243 | 19:51:09.60 | +46:29:04.5 | M4.0 V | Single | |
| 2193 | | J19512+622 | G 260-35 | | 19:51:11.69 | +62:17:15.7 | M2.0 V | Single | |
| 2194 | | J19535+341 | GJ 4127 | 4127 | 19:53:32.73 | +34:08:32.2 | M1.5 V | Single | |
| 2195 | 593 | J19539+444W | V1581 Cyg | 1245 A | 19:53:55.14 | +44:24:44.4 | M5.5 V | Multiple | |
| 2196 | 593 | J19539+444E | GJ 1245 B | 1245 B | 19:53:55.66 | +44:24:46.5 | M5.5 V | Multiple | A.2 |
| 2197 | | J19540+325 | GJ 4128 | 4128 | 19:54:02.88 | +32:33:55.8 | M2.0 V | Candidate | |
| 2198 | | J19546+202 | TYC 1624-397-1 | | 19:54:37.52 | +20:13:05.5 | M0.0 V | Single | |
| 2199 | | J19558+512 | Wolf 1122 | 9674 | 19:55:53.62 | +51:16:27.7 | M1.0 V | Single | |
| 2200 | 594 | J19565+591 | GJ 9677 A | 9677 A | 19:56:33.06 | +59:09:40.3 | M0.0 V | Multiple+ | |
| 2201 | 594 | J19564+591 | GJ 9677 B | 9677 B | 19:56:23.96 | +59:09:19.7 | M3.5 V | Multiple | |
| 2202 | 595 | | HD 188807 | 773 A | 19:57:19.54 | -12:34:13.0 | K7 V | Multiple | |
| 2203 | 595 | J19573-125 | GJ 773 B | 773 B | 19:57:23.71 | -12:33:58.5 | M5.0 V | Multiple+ | |
| 2204 | | J19582+020 | GJ 4129 | 4129 | 19:58:15.38 | +02:02:02.5 | M2.5 V | Single | |
| 2205 | | J19582+650 | G 260-38 | | 19:58:16.31 | +65:02:25.0 | M3.5 V | Single | |
| 2206 | | J20011+002 | LP 634-16 | | 20:01:06.21 | +00:16:12.0 | M2.0 V | Single | |
| 2207 | 596 | J20005+593 | IRXS J200031.8+592127 | | 20:00:31.98 | +59:21:29.9 | M4.0 V | Multiple | |
| 2208 | 596 | | Gaia DR3 2237179062111268096 | | 20:00:32.02 | +59:21:29.7 | M4.5 V | Multiple | |
| 2209 | 597 | | HD 190360 | 777 A | 20:03:38.25 | +29:53:40.1 | G7 IV/V | Multiple | A.8 A.11 |
| 2210 | 597 | J20034+298 | GJ 777 B | 777 B | 20:03:27.42 | +29:51:51.1 | M4.5 V | Multiple | A.8 |
| 2211 | | J20037+644 | IRXS J200348.4+642542 | | 20:03:47.80 | +64:25:45.3 | M0.0 V | Candidate | |
| 2212 | | J20038+059 | GJ 1248 | 1248 | 20:03:50.47 | +05:59:31.4 | M1.5 V | Single | |

Table A.1: Complete sample studied in this work^a (cont.).

| Star id. | System id. | Karmn | Name | GJ | α (J2016.0) | δ (J2016.0) | Spectral type | Multiplicity type | In tables |
|----------|------------|-------------|------------------------------|---------|-----------------------|-----------------------|---------------|-------------------|--------------|
| 2213 | | J20039–081 | GJ 4132 | 4132 | 20:03:58.37 | -08:07:51.4 | M4.0 V | Single | |
| 2214 | 598 | J20050+544 | V1513 Cyg | 781 | 20:05:00.07 | +54:25:48.8 | M1.0 V | Multiple | A.4 A.9 A.10 |
| 2215 | 598 | | Wolf 1130 B | 781 B | 20:05:20.38 | +54:24:33.9 | T8p | Multiple | A.9 A.10 |
| 2216 | | J20057+529 | Wolf 1131 | 4135 | 20:05:44.59 | +52:58:21.1 | M3.5 V | Single | |
| 2217 | | J20079–015 | GJ 4136 | 4136 | 20:07:57.91 | -01:32:31.5 | M3.0 V | Single | |
| 2218 | | J20082+333 | GJ 1250 | 1250 | 20:08:18.35 | +33:18:19.0 | M4.5 V | Candidate | |
| 2219 | | J20093–012 | PM J20093–0113 | | 20:09:18.20 | -01:13:44.3 | M5.0 V | Single | |
| 2220 | 599 | J20105+065 | LP 574–21 | | 20:10:34.49 | +06:32:10.7 | M4.0 V | Multiple | A.4 |
| 2221 | 599 | | 2MASS J20103539+0634367 | | 20:10:35.44 | +06:34:33.5 | M8.5 V | Multiple | |
| 2222 | 600 | | HD 191785 | 783.2 A | 20:11:05.61 | +16:11:23.2 | K0 V | Multiple | A.8 |
| 2223 | 600 | J20112+161 | GJ 783.2 B | 783.2 B | 20:11:12.80 | +16:11:14.4 | M4.0 V | Multiple | A.8 |
| 2224 | | J20112+379 | LSPM J2011+3757 | | 20:11:12.85 | +37:57:48.1 | M1.5 V | Single | |
| 2225 | 601 | J20129+342 | LP 283–5 | | 20:12:54.72 | +34:16:54.5 | M1.0 V | Multiple | |
| 2226 | 601 | | LP 283–4 | | 20:12:54.41 | +34:16:37.6 | M1.0 V | Multiples+ | |
| 2227 | 602 | | StKM 1–1767a | | 20:13:11.14 | +02:56:20.5 | K5 V | Multiple | A.8 |
| 2228 | 602 | J20132+029 | [R78b] 440 | | 20:13:12.94 | +02:56:02.3 | M1.0 V | Multiple | A.8 |
| 2229 | | J20138+133 | Ross 754 | 9689 | 20:13:52.27 | +13:23:20.0 | M1.0 V | Single | A.11 |
| 2230 | 603 | | V1412 Aql | 784.2 B | 20:13:55.41 | +06:42:35.5 | DC7 | Multiple | A.9 |
| 2231 | 603 | J20139+066 | GJ 784.2 A | 784.2 A | 20:13:58.71 | +06:41:06.8 | M3.5 V | Multiple | A.9 |
| 2232 | | J20151+635 | LP 106–240 | | 20:15:10.64 | +63:31:16.4 | M0.0 V | Single | |
| 2233 | | J20165+351 | G 210–11 | | 20:16:32.04 | +35:10:37.6 | M2.0 V | Single | |
| 2234 | | J20187+158 | GJ 4143 | 4143 | 20:18:44.75 | +15:50:45.3 | M2.5 V | Single | |
| 2235 | 604 | J20195+080 | GJ 4144 | 4144 | 20:19:34.60 | +08:00:27.1 | M3.0 V | Multiple | |
| 2236 | 604 | | Gaia DR3 4250232535851803136 | | 20:19:34.55 | +08:00:26.9 | M3.0 V | Multiple | |
| 2237 | 605 | J20198+229 | LP 395–8 A | | 20:19:49.36 | +22:56:38.1 | M3.0 V | Multiple | A.4 A.10 |
| 2238 | 605 | | LP 395–8 B | | 20:19:49.35 | +22:56:40.0 | M3.5 V | Multiple | A.2 A.10 |
| 2239 | 605 | | Gaia DR3 1829571684884360832 | | 20:19:48.73 | +22:56:44.8 | L2 | Multiple | A.10 |
| 2240 | 606 | J20220+216 | TYC 1643–120–1 | | 20:22:01.62 | +21:47:19.7 | M2.0 V | Multiple | |
| 2241 | 606 | | PM J20220+2147B | | 20:22:01.98 | +21:47:21.8 | M4.5 V | Multiple | |
| 2242 | | J20223+322 | PM J20223+3217 | | 20:22:18.82 | +32:17:15.1 | M3.5 V | Single | |
| 2243 | | J20229+106 | G 143–48 | | 20:22:55.79 | +10:40:44.5 | M3.0 V | Single | |
| 2244 | 607 | J20232+671 | LP 73–196 | | 20:23:18.57 | +67:10:12.9 | M5.0 V | Multiple | |
| 2245 | 607 | | LP 73–196 B | | 20:23:18.43 | +67:10:12.1 | M5.5 V | Multiple | |
| 2246 | | J20260+585 | Wolf 1069 | 1253 | 20:26:05.84 | +58:34:31.4 | M5.0 V | Single | A.11 |
| 2247 | | J20287–114 | LP 755–19 | | 20:28:43.80 | -11:28:32.4 | M1.5 V | Single | |
| 2248 | 608 | J20269+275 | GJ 4146 | 4146 | 20:26:56.29 | +27:31:03.1 | M2.0 V | Multiple | |
| 2249 | 609 | J20298+096 | HU Del | 791.2 B | 20:29:49.04 | +09:41:22.2 | M4.5 V | Multiple | |
| 2250 | | J20305+654 | GJ 793 | 793 | 20:30:33.18 | +65:27:02.9 | M2.5 V | Single | |
| 2251 | 610 | J20301+798 | IRXS J203011.0+795040 | | 20:30:07.75 | +79:50:47.4 | M3.0 V | Multiple | A.4 |
| 2252 | | J20336+617 | GJ 1254 | 1254 | 20:33:41.53 | +61:45:28.2 | M4.0 V | Single | |
| 2253 | 611 | J20314+385 | Ross 188 | 792 | 20:31:25.91 | +38:33:55.8 | M4.0 V | Multiple | |
| 2254 | 612 | J20337+233 | GJ 4148 | 4148 | 20:33:43.10 | +23:22:15.4 | M3.0 V | Multiple | |
| 2255 | 612 | | G 186–29B | | 20:33:43.11 | +23:22:14.5 | M4.0 V | Multiple | |
| 2256 | | J20339+643 | GJ 4150 | 4150 | 20:33:58.81 | +64:19:08.1 | M3.5 V | Single | |
| 2257 | | J20347+033 | GJ 4149 | 4149 | 20:34:43.33 | +03:20:43.6 | M2.5 V | Single | |
| 2258 | | J20349+592 | Wolf 1074 | 4151 | 20:34:54.81 | +59:17:26.0 | M3.5 V | Single | |
| 2259 | | J20367+388 | GJ 4152 | 4152 | 20:36:46.27 | +38:50:30.3 | M3.5 V | Single | |
| 2260 | 613 | J20373+219 | Wolf 1351 | 4153 A | 20:37:20.77 | +21:56:47.8 | M0.5 V | Multiples+ | |
| 2261 | 613 | | GJ 4153 B | 4153 B | 20:37:23.97 | +21:56:21.4 | M4.5 V | Multiple | A.2 |
| 2262 | | J20403+616 | TYC 4246–488–1 | | 20:40:18.59 | +61:41:28.4 | M1.0 V | Single | |
| 2263 | | J20405+154 | GJ 1256 | 1256 | 20:40:35.33 | +15:30:09.3 | M4.5 V | Single | |
| 2264 | 614 | | HD 197076 | 797 A | 20:40:45.28 | +19:56:12.9 | G5 V | Multiple | A.8 |
| 2265 | 614 | J20407+199 | GJ 797 B | 797 B | 20:40:44.65 | +19:54:08.2 | M2.5 V | Multiple | A.8 |
| 2266 | 615 | J20409–101 | GJ 4155 | 4155 | 20:40:56.32 | -10:06:43.1 | M1.5 V | Multiple | A.4 |
| 2267 | 616 | J20451–313 | AU Mic | 803 | 20:45:09.88 | -31:20:33.0 | M0.5 V | Multiple | A.7 A.11 |
| 2268 | 616 | J20418–324 | AT Mic A | | 20:41:51.44 | -32:26:13.3 | M4.5 V | Multiple | A.7 |
| 2269 | 616 | | AT Mic B | | 20:41:51.54 | -32:26:15.1 | M4.5 V | Multiple | A.2 A.7 |
| 2270 | | J20429–189 | Ross 751 | 800 A | 20:42:57.83 | -18:55:19.8 | M1.5 V | Single | |
| 2271 | | J20433+047 | LP 575–35 | | 20:43:24.35 | +04:45:52.9 | M5.0 V | Candidate | |
| 2272 | | J20435+240 | Wolf 1360 | | 20:43:34.69 | +24:07:40.2 | M2.5 V | Single | |
| 2273 | | J20436+642 | G 262–26 | | 20:43:42.13 | +64:16:52.5 | M0.0 V | Single | |
| 2274 | | J20436–001 | GJ 4159 | 4159 | 20:43:41.71 | -00:10:37.5 | M0.0 V | Single | |
| 2275 | 617 | J20433+553 | Wolf 1084 | 802 | 20:43:20.89 | +55:21:20.5 | M5.0 V | Multiple | |
| 2276 | 618 | J20443+197 | HD 352860 | 804 | 20:44:21.98 | +19:44:49.8 | M0.0 V | Multiple | |
| 2277 | 619 | J20445+089S | GJ 4160 | 4160 | 20:44:30.94 | +08:54:12.6 | M1.5 V | Multiple | |
| 2278 | 619 | J20445+089N | GJ 4161 | 4161 | 20:44:30.67 | +08:54:27.1 | M3.5 V | Multiple | A.4 |
| 2279 | | J20450+444 | GJ 806 | 806 | 20:45:04.75 | +44:30:01.0 | M1.5 V | Single | A.11 |
| 2280 | | J20496–003 | Wolf 882 | 4164 | 20:49:39.86 | -00:21:06.7 | M3.5 V | Single | |
| 2281 | 620 | J20488+197 | GJ 4163 | 4163 | 20:48:52.27 | +19:43:01.6 | M4.0 V | Multiple | |
| 2282 | | J20525–169 | LP 816–60 | | 20:52:32.67 | -16:58:28.4 | M4.0 V | Single | |
| 2283 | 621 | J20519+691 | GJ 4170 | 4170 | 20:52:00.55 | +69:10:07.6 | M1.0 V | Multiple | |
| 2284 | | J20533+621 | HD 199305 | 809 | 20:53:19.79 | +62:09:03.4 | M1.0 V | Single | |
| 2285 | | J20535+106 | GJ 4169 | 4169 | 20:53:32.53 | +10:36:55.0 | M4.0 V | Single | |
| 2286 | | J20549+675 | LP 74–35 | | 20:54:54.90 | +67:35:09.8 | M2.0 V | Single | |
| 2287 | 622 | J20532–023 | LP 636–19 | | 20:53:14.87 | -02:21:21.7 | M3.0 V | Multiple | |
| 2288 | 623 | J20556–140N | GJ 810 A | 810 A | 20:55:39.31 | -14:02:15.6 | M4.0 V | Multiple | A.4 |
| 2289 | 623 | J20556–140S | GJ 810 B | 810 B | 20:55:38.68 | -14:04:02.4 | M5.0 V | Multiple | |
| 2290 | | J20567–104 | Wolf 896 | 9711 | 20:56:46.56 | -10:27:12.7 | M2.5 V | Single | |
| 2291 | 624 | | Ross 193B | 812 B | 20:56:48.62 | -04:50:43.1 | DC10 | Multiple | A.9 |
| 2292 | 624 | J20568–048 | FR Aqr | 812 A | 20:56:49.39 | -04:50:52.6 | M4.0 V | Multiple | A.4 A.9 |
| 2293 | | J20574+223 | Wolf 1373 | 813 | 20:57:26.24 | +22:21:42.4 | M2.0 V | Single | |
| 2294 | | J20586+342 | GJ 4173 | 4173 | 20:58:42.31 | +34:16:24.7 | M0.0 V | Single | |

Table A.1: Complete sample studied in this work^a (cont.).

| Star id. | System id. | Karmn | Name | GJ | α (J2016.0) | δ (J2016.0) | Spectral type | Multiplicity type | In tables |
|----------|------------|-------------|------------------------------|---------|-----------------------|-----------------------|---------------|-------------------|-----------|
| 2295 | | J21001+495 | G 212–14 | | 21:00:09.24 | +49:35:20.8 | M2.0 V | Single | |
| 2296 | 625 | J21000+400 | V1396 Cyg | 815 | 21:00:06.23 | +40:04:08.6 | M1.5 V | Multiple | |
| 2297 | 626 | J21012+332 | GJ 4176 | 4176 | 21:01:16.51 | +33:14:30.7 | M3.0 V | Multiple | |
| 2298 | 626 | J21013+332 | GJ 4177 | 4177 | 21:01:21.03 | +33:14:25.9 | M3.5 V | Multiple | |
| 2299 | | J21019–063 | Wolf 906 | 816 | 21:01:58.39 | -06:19:14.5 | M2.5 V | Single | |
| 2300 | | J21027+349 | G 211–9 | | 21:02:46.40 | +34:54:31.2 | M4.5 V | Candidate | |
| 2301 | | J21044+455 | TYC 3588–5589–1 | | 21:04:28.94 | +45:35:42.3 | M2.0 V | Single | |
| 2302 | | J21048–169 | Ross 769 | 817 | 21:04:52.36 | -16:58:04.6 | M1.0 V | Single | |
| 2303 | 627 | J21014+207 | GJ 4175 | 4175 | 21:01:24.40 | +20:43:31.6 | M3.5 V | Multiple | |
| 2304 | 628 | J21055+061 | PM J21055+0609N | | 21:05:32.09 | +06:09:16.2 | M3.0 V | Multiple | |
| 2305 | 628 | | PM J21055+0609S | | 21:05:32.17 | +06:09:11.2 | M5.5 V | Multiple | A.2 |
| 2306 | 629 | J21057+502 | PM J21057+5015E | | 21:05:45.54 | +50:15:44.1 | M3.5 V | Multiple | |
| 2307 | 629 | | PM J21057+5015W | | 21:05:42.60 | +50:15:58.1 | M3.5 V | Multiple | |
| 2308 | | J21059+044 | GJ 4180 | 4180 | 21:05:56.52 | +04:25:38.0 | M2.5 V | Single | |
| 2309 | | J21074+468 | PM J21074+4651 | | 21:07:28.14 | +46:51:55.4 | M2.0 V | Single | |
| 2310 | | J21076–130 | 1RXS J210736.5–130500 | | 21:07:36.86 | -13:04:59.6 | M3.0 V | Candidate | |
| 2311 | 630 | J21087–044S | GJ 9721 | 9721 | 21:08:45.41 | -04:25:36.7 | M1.0 V | Multiple | 7 |
| 2312 | 630 | J21087–044N | DENIS J210844.8–042517 | | 21:08:44.75 | -04:25:18.3 | M3.0 V | Multiple | A.27 |
| 2313 | | J21092–133 | Wolf 918 | 821 | 21:09:18.21 | -13:18:40.9 | M1.0 V | Single | |
| 2314 | 631 | J21100–193 | 1RXS J211004.9–192005 | | 21:10:05.46 | -19:19:59.1 | M2.0 V | Multiple | |
| 2315 | 631 | | UCAC4 354–189365 | | 21:10:04.71 | -19:20:32.0 | M5.0 V | Multiple+ | |
| 2316 | | J21123+359 | LP 285–9 | | 21:12:22.66 | +35:55:24.7 | M1.5 V | Candidate | |
| 2317 | | J21127–073 | PM J21127–0719 | | 21:12:45.71 | -07:19:56.5 | M3.5 V | Single | |
| 2318 | 632 | J21109+294 | Ross 824 | 4182 | 21:10:54.47 | +29:25:18.6 | M1.5 V | Multiple | |
| 2319 | 633 | J21137+087 | LSPM J2113+0846N | | 21:13:44.77 | +08:46:09.1 | M2.0 V | Multiple | |
| 2320 | 633 | | LSPM J2113+0846S | | 21:13:44.56 | +08:46:01.1 | M1.5 V | Multiple | |
| 2321 | | J21138+180 | Ross 772 | | 21:13:53.01 | +18:05:58.8 | M3.0 V | Single | |
| 2322 | | J21145+508 | LSPM J2114+5052 | | 21:14:32.61 | +50:52:31.6 | M2.5 V | Single | |
| 2323 | 634 | | GJ 9728 B | 9728 B | 21:14:47.68 | +38:02:50.6 | G5 V | Multiple | A.8 |
| 2324 | 634 | J21147+380 | GJ 822.1 C | 822.1 C | 21:14:47.09 | +38:01:21.0 | M2.5 V | Multiple | A.8 |
| 2325 | | J21152+257 | GJ 4184 | 4184 | 21:15:12.76 | +25:47:41.2 | M3.0 V | Single | |
| 2326 | 635 | J21160+298E | Ross 776 | 4185 | 21:16:06.06 | +29:51:51.5 | M3.5 V | Multiple | |
| 2327 | 635 | J21160+298W | Ross 826 | 4186 | 21:16:04.10 | +29:51:46.7 | M3.5 V | Multiple | |
| 2328 | | J21164+025 | LSPM J2116+0234 | | 21:16:27.55 | +02:34:50.8 | M3.0 V | Single | A.11 |
| 2329 | 636 | J21173+208N | Ross 773A | 4190 | 21:17:23.09 | +20:53:59.2 | M3.5 V | Multiple | |
| 2330 | 636 | J21173+208S | Ross 773B | 4189 | 21:17:23.00 | +20:54:03.4 | M3.0 V | Multiple | |
| 2331 | | J21173+640 | G 262–38 | | 21:17:22.75 | +64:02:39.1 | M5.0 V | Candidate | |
| 2332 | 637 | J21176–089N | GJ 4187 | 4187 | 21:17:36.07 | -08:54:11.7 | M2.5 V | Multiple | |
| 2333 | 637 | J21176–089S | GJ 4188 | 4188 | 21:17:39.55 | -08:54:49.6 | M3.0 V | Multiple | A.2 |
| 2334 | | J21185+302 | 1RXS J211833.8+301434 | | 21:18:33.83 | +30:14:34.3 | M1.5 V | Candidate | |
| 2335 | | J21221+229 | TYC 2187–512–1 | | 21:22:06.41 | +22:55:55.0 | M1.0 V | Single | A.11 |
| 2336 | | J21243+085 | GJ 4192 | 4192 | 21:24:19.08 | +08:30:03.6 | M3.5 V | Candidate | |
| 2337 | | J21245+400 | LSPM J2124+4003 | | 21:24:33.07 | +40:04:06.7 | M5.5 V | Candidate | |
| 2338 | | J21267+037 | GJ 828.1 | 828.1 | 21:26:42.41 | +03:44:12.9 | M0.0 V | Single | |
| 2339 | | J21272–068 | Wolf 920 | 9740 | 21:27:16.89 | -06:50:45.8 | M0.5 V | Single | |
| 2340 | | J21275+340 | V2160 Cyg | 4196 | 21:27:32.60 | +34:01:25.7 | M1.0 V | Candidate | |
| 2341 | | J21277+072 | Ross 778 | 4195 | 21:27:46.19 | +07:17:45.9 | M1.0 V | Candidate | |
| 2342 | | J21280+179 | LP 457–38 | | 21:28:05.57 | +17:54:02.7 | M1.5 V | Single | |
| 2343 | | J21283–223 | GJ 4197 | 4197 | 21:28:18.04 | -22:18:36.5 | M2.5 V | Single | |
| 2344 | 638 | J21296+176 | Ross 775 | 829 B | 21:29:37.94 | +17:38:41.9 | M3.5 V | Multiple | A.4 |
| 2345 | 639 | J21313–097 | BB Cap | 831 B | 21:31:19.92 | -09:47:27.5 | M4.5 V | Multiple | |
| 2346 | 640 | J21323+245 | GJ 4201 A | 4201 A | 21:32:22.33 | +24:33:41.9 | M3.5 V | Multiple | |
| 2347 | 640 | | GJ 4201 B | 4201 B | 21:32:22.23 | +24:33:41.1 | M4.0 V | Multiple | A.2 |
| 2348 | 641 | J21338+017S | GJ 4203 | 4203 | 21:33:49.11 | +01:46:44.9 | M4.0 V | Multiple | |
| 2349 | 641 | J21338+017N | GJ 4204 | 4204 | 21:33:49.13 | +01:46:50.0 | M4.0 V | Multiple | |
| 2350 | | J21338–068 | Wolf 923 | 4202 | 21:33:49.04 | -06:51:18.4 | M4.0 V | Single | |
| 2351 | | J21348+515 | Wolf 926 | 4205 | 21:34:51.13 | +51:32:18.6 | M3.0 V | Single | |
| 2352 | 642 | J21366+394 | V2168 Cyg | 834 A | 21:36:38.29 | +39:27:18.0 | M0.0 V | Multiple | |
| 2353 | 642 | | GJ 834 B | 834 B | 21:36:38.20 | +39:27:17.8 | M2.5 V | Multiple | A.2 |
| 2354 | | J21369+561 | Ross 215 | | 21:36:58.82 | +56:07:07.2 | M1.5 V | Single | |
| 2355 | 643 | J21374–059 | PM J21374–0555 | | 21:37:29.02 | -05:55:05.7 | M3.0 V | Multiple | |
| 2356 | 643 | | Gaia DR3 2670835278558316160 | | 21:37:29.01 | -05:55:05.5 | M3.5 V | Multiple | |
| 2357 | | J21378+530 | Ross 199 | 4208 | 21:37:50.77 | +53:04:49.9 | M0.0 V | Candidate | |
| 2358 | 644 | J21376+016 | 1RXS J213740.3+013711 | | 21:37:40.28 | +01:37:12.7 | M4.5 V | Multiple | |
| 2359 | 645 | J21380+277 | GJ 835 | 835 | 21:38:00.96 | +27:43:24.4 | M0.0 V | Multiple | |
| 2360 | 645 | | BD+27 4120B | | 21:38:01.04 | +27:43:27.6 | M5.0 V | Multiple | |
| 2361 | | J21402+370 | LP 286–1 | | 21:40:12.27 | +37:03:24.1 | M0.5 V | Single | |
| 2362 | 646 | J21399+276 | GJ 4210 | 4210 | 21:39:54.70 | +27:36:39.8 | M1.5 V | Multiple | |
| 2363 | | J21421–121 | Ross 206 | 9749 | 21:42:07.58 | -12:09:59.3 | M3.0 V | Candidate | |
| 2364 | 647 | J21419+276 | GJ 4212 | 4212 | 21:41:58.03 | +27:41:14.2 | M3.5 V | Multiple | |
| 2365 | 648 | J21441+170S | GJ 4214 | 4214 | 21:44:09.31 | +17:03:35.0 | M4.0 V | Multiple | |
| 2366 | 648 | J21441+170N | GJ 4215 | 4215 | 21:44:08.25 | +17:04:37.3 | M4.5 V | Multiple | |
| 2367 | 649 | J21442+066 | GJ 4213 | 4213 | 21:44:12.64 | +06:38:26.6 | M3.0 V | Multiple | A.4 |
| 2368 | 650 | J21449+442 | G 215–12 | | 21:44:53.78 | +44:16:58.4 | M1.5 V | Multiple | |
| 2369 | 651 | | G 126–32A | | 21:45:04.94 | +19:53:31.8 | M1.0 V | Multiple | A.10 |
| 2370 | 651 | J21450+198 | G 126–32B | | 21:45:04.90 | +19:53:31.7 | M1.5 V | Multiple | A.10 |
| 2371 | 651 | | G 126–32C | | 21:45:05.04 | +19:53:36.9 | L1 | Multiple | A.10 |
| 2372 | | J21450–057 | Wolf 937 | 4216 | 21:45:00.59 | -05:47:20.3 | M3.0 V | Single | |
| 2373 | | J21454–059 | Wolf 939 | 4217 | 21:45:24.74 | -05:54:11.5 | M3.5 V | Single | |
| 2374 | | J21463+382 | LSPM J2146+3813 | | 21:46:22.29 | +38:13:03.1 | M4.0 V | Single | |
| 2375 | | J21466+668 | G 264–12 | | 21:46:41.30 | +66:48:14.0 | M4.0 V | Single | A.11 |
| 2376 | 652 | J21466–001 | Wolf 940 | 1263 | 21:46:41.24 | -00:10:31.9 | M4.0 V | Multiple | A.10 |

Table A.1: Complete sample studied in this work^a (cont.).

| Star id. | System id. | Karmn | Name | GJ | α (J2016.0) | δ (J2016.0) | Spectral type | Multiplicity type | In tables |
|----------|------------|-------------|------------------------------|--------|-----------------------|-----------------------|---------------|-------------------|-----------|
| 2377 | 652 | | Wolf 940 B | 1263 B | 21:46:38.83 | -00:10:38.6 | T8 | Multiple | A.10 |
| 2378 | | J21469+466 | Wolf 944 | 4219 | 21:46:56.68 | +46:38:06.1 | M4.0 V | Single | |
| 2379 | | J21472-047 | PM J21472-0444 | | 21:47:17.73 | -04:44:40.6 | M4.5 V | Single | |
| 2380 | 653 | J21474+627 | TYC 4266-736-1 | 1247 | 21:47:24.39 | +62:45:13.7 | M0.0 V | Multiple | A.11 |
| 2381 | 653 | | LSPM J2147+6246 | | 21:47:25.40 | +62:46:22.4 | M6.0 V | Multiple | |
| 2382 | | J21478+502 | Wolf 945 | 4223 | 21:47:53.64 | +50:14:54.6 | M3.5 V | Single | |
| 2383 | | J21479+058 | Ross 779 | 4220 | 21:47:57.57 | +05:49:16.4 | M1.5 V | Single | |
| 2384 | | J21481+014 | GJ 4221 | 4221 | 21:48:10.46 | +01:26:42.0 | M3.5 V | Single | |
| 2385 | | J21482+279 | GJ 4225 | 4225 | 21:48:15.02 | +27:55:31.0 | M2.0 V | Single | |
| 2386 | | J21512+128 | GJ 4227 | 4227 | 21:51:18.24 | +12:50:33.2 | M4.0 V | Single | |
| 2387 | 654 | J21518+136 | GJ 4228 | 4228 | 21:51:48.53 | +13:36:13.8 | M4.5 V | Multiple | |
| 2388 | 655 | | UCAC4 747-070768 | | 21:51:39.93 | +59:17:34.5 | DAH | Multiple | A.9 |
| 2389 | 655 | J21516+592 | TYC 3980-1081-1 | | 21:51:38.15 | +59:17:40.0 | M4.0 V | Multiple+ | A.2 A.9 |
| 2390 | | J21521+274 | GJ 4232 | 4232 | 21:52:12.12 | +27:24:48.2 | M4.0 V | Single | |
| 2391 | | J21539+417 | GJ 839 | 839 | 21:53:59.55 | +41:46:38.7 | M0.0 V | Single | |
| 2392 | | J21566+197 | Ross 263 | 4240 | 21:56:37.83 | +19:46:06.8 | M3.5 V | Candidate | |
| 2393 | | J21569-019 | GJ 4239 | 4239 | 21:56:56.61 | -01:53:59.5 | M5.0 V | Single | |
| 2394 | | J21574+081 | Wolf 953 | 4241 | 21:57:26.64 | +08:08:15.5 | M1.5 V | Single | |
| 2395 | | J21584+755 | GJ 842.2 | 842.2 | 21:58:25.51 | +75:35:21.0 | M0.5 V | Single | |
| 2396 | | J21585+612 | LSPM J2158+6117 | | 21:58:36.41 | +61:17:07.8 | M6.0 V | Single | |
| 2397 | | J21593+418 | GJ 4246 | 4246 | 21:59:22.08 | +41:51:25.4 | M3.0 V | Single | |
| 2398 | | J22012+283 | V374 Peg | 4247 | 22:01:13.58 | +28:18:25.6 | M4.0 V | Single | |
| 2399 | 656 | J21521+056 | GJ 4231 | 4231 | 21:52:10.52 | +05:37:33.5 | M3.0 V | Multiple | |
| 2400 | 657 | J22012+323 | Wolf 1154 A | | 22:01:14.13 | +32:23:13.9 | M1.5 V | Multiple | A.10 |
| 2401 | 657 | | Wolf 1154 B | | 22:01:14.04 | +32:23:13.2 | M3.5 V | Multiple | A.10 |
| 2402 | 657 | | 2MASS J22011701+3222062 | | 22:01:17.01 | +32:22:06.2 | T2.5 | Multiple | A.10 |
| 2403 | 658 | J22018+164 | Ross 265 | 844 | 22:01:49.49 | +16:28:05.2 | M2.0 V | Multiple | |
| 2404 | | J22020-194 | GJ 843 | 843 | 22:02:01.85 | -19:28:58.0 | M3.5 V | Single | |
| 2405 | | J22021+014 | HD 209290 | 846 | 22:02:09.79 | +01:23:56.4 | M0.5 V | Single | |
| 2406 | | J22033+674 | GJ 4251 | 4251 | 22:03:22.74 | +67:29:55.1 | M3.5 V | Single | |
| 2407 | | J22051+051 | Wolf 983 | 4252 | 22:05:07.30 | +05:08:14.2 | M4.0 V | Single | |
| 2408 | 659 | J22035+036 | IRXS J220330.8+034001 | | 22:03:33.39 | +03:40:21.4 | M4.0 V | Multiple | |
| 2409 | 660 | J22057+656 | GJ 4258 | 4258 | 22:05:44.55 | +65:38:58.9 | M1.5 V | Multiple | |
| 2410 | 660 | | G 264-18B | | 22:05:45.29 | +65:38:53.9 | M4.5 V | Multiple | |
| 2411 | 661 | J22058-119 | Wolf 1548 | 4254 | 22:05:51.00 | -11:54:53.7 | M0.0 V | Multiple+ | A.7 |
| 2412 | 661 | | LP 759-25 | | 22:05:35.44 | -11:04:31.8 | M6.0 V | Multiple | A.2 A.7 |
| 2413 | | J22060+393 | GJ 4256 | 4256 | 22:06:00.76 | +39:17:55.6 | M3.0 V | Single | |
| 2414 | | J22067+034 | Wolf 990 | 4257 | 22:06:46.87 | +03:24:58.7 | M4.0 V | Single | |
| 2415 | | J22088+117 | PM J22088+1144 | | 22:08:50.44 | +11:44:12.4 | M4.5 V | Single | |
| 2416 | | J22095+118 | LP 519-38 | | 22:09:31.86 | +11:52:51.6 | M3.0 V | Single | |
| 2417 | | J22096-046 | Wolf 1329 | 849 | 22:09:41.56 | -04:38:27.0 | M3.5 V | Single | A.11 |
| 2418 | | J22097+410 | GJ 4260 | 4260 | 22:09:43.64 | +01:02:09.5 | M3.5 V | Single | A.11 |
| 2419 | | J22102+587 | UCAC4 744-073158 | | 22:10:15.18 | +58:42:21.9 | M2.0 V | Single | A.11 |
| 2420 | 662 | J22107+079 | Wolf 1003 A | | 22:10:44.98 | +07:54:32.9 | M0.5 V | Multiple | |
| 2421 | 662 | | Wolf 1003 B | | 22:10:44.98 | +07:54:33.8 | M1.0 V | Multiple | |
| 2422 | | J22112+410 | G 214-14 | | 22:11:16.65 | +41:00:58.6 | M0.0 V | Single | |
| 2423 | | J22112-025 | GJ 4262 | 4262 | 22:11:13.95 | -02:32:38.2 | M2.0 V | Single | |
| 2424 | | J22114+409 | IRXS J221124.3+410000 | | 22:11:24.04 | +40:59:59.8 | M5.5 V | Single | |
| 2425 | | J22115+184 | Ross 271 | 851 | 22:11:30.46 | +18:25:37.2 | M2.0 V | Single | |
| 2426 | 663 | J22117-207 | WT 2221 | | 22:11:42.27 | -20:44:19.3 | M3.5 V | Multiple+ | |
| 2427 | 663 | | WT 2220 | | 22:11:41.51 | -20:44:12.0 | M3.0 V | Multiple | |
| 2428 | | J22125+085 | Wolf 1014 | 9773 | 22:12:36.06 | +08:33:00.9 | M3.0 V | Single | |
| 2429 | 664 | | Gaia DR3 2005884249925303168 | | 22:13:00.46 | +55:05:48.3 | D? | Multiple | A.9 |
| 2430 | 664 | J22129+550 | LF 4 +54 152 | | 22:12:56.63 | +55:04:50.8 | M0.0 V | Multiple+ | A.9 |
| 2431 | | J22134-147 | Wolf 1556 | 4263 | 22:13:28.46 | -14:44:58.8 | M3.5 V | Single | |
| 2432 | | J22135+259 | GJ 4264 | 4264 | 22:13:35.90 | +25:58:08.1 | M3.5 V | Single | |
| 2433 | | J22137-176 | GJ 1265 | 1265 | 22:13:43.82 | -17:41:13.6 | M4.5 V | Single | A.11 |
| 2434 | 665 | J22138+052 | Wolf 1019 | 4265 | 22:13:53.53 | +05:16:34.9 | M1.5 V | Multiple | |
| 2435 | | J22154+662 | GJ 4267 | 4267 | 22:15:26.16 | +66:13:31.1 | M3.5 V | Single | |
| 2436 | 666 | J22142+255 | IRXS J221419.3+253411 | | 22:14:17.88 | +25:34:05.6 | M4.5 V | Multiple | |
| 2437 | 667 | | V447 Lac | 4268 | 22:15:54.53 | +54:40:23.5 | K1 V | Multiple | A.8 |
| 2438 | 667 | J22160+546 | GJ 4269 | 4269 | 22:16:02.99 | +54:40:00.5 | M4.0 V | Multiple | A.8 |
| 2439 | | J22163+709 | GJ 1266 | 1266 | 22:16:23.03 | +70:56:39.2 | M2.0 V | Single | |
| 2440 | 668 | J22173-088N | FG Aqr | 852 A | 22:17:18.47 | -08:48:16.9 | M4.0 V | Multiple+ | |
| 2441 | 668 | J22173-088S | Wolf 1561 B | 852 B | 22:17:18.16 | -08:48:23.4 | M5.0 V | Multiple | |
| 2442 | | J22176+565 | PM J22176+5633 | | 22:17:37.21 | +56:33:11.1 | M1.5 V | Candidate | |
| 2443 | | J22202+067 | Wolf 1034 | | 22:20:13.57 | +06:43:36.5 | M2.5 V | Single | |
| 2444 | 669 | J22212+377 | LSPM J2221+3744A | | 22:21:13.22 | +37:44:50.8 | M1.5 V | Multiple | |
| 2445 | 669 | | LSPM J2221+3744B | | 22:21:13.06 | +37:44:50.2 | M2.0 V | Multiple | |
| 2446 | | J22228+280 | GJ 4275 | 4275 | 22:22:51.34 | +28:01:46.4 | M4.0 V | Single | |
| 2447 | | J22231-176 | GJ 4274 | 4274 | 22:23:07.34 | -17:36:37.8 | M4.5 V | Single | |
| 2448 | 670 | J22234+324 | Wolf 1225 A | 856 A | 22:23:29.44 | +32:27:29.9 | M3.0 V | Multiple | |
| 2449 | 670 | | Wolf 1225 B | 856 B | 22:23:29.34 | +32:27:29.5 | M3.5 V | Multiple | A.2 |
| 2450 | | J22249+520 | GJ 1268 | 1268 | 22:24:56.33 | +52:00:25.6 | M4.5 V | Single | |
| 2451 | | J22250+356 | Wolf 1231 | | 22:25:01.66 | +35:40:05.3 | M2.0 V | Single | |
| 2452 | | J22252+594 | GJ 4276 | 4276 | 22:25:17.32 | +59:24:44.9 | M4.0 V | Single | A.11 |
| 2453 | 671 | J22262+030 | Wolf 1201 | 4277 A | 22:26:15.24 | +03:00:11.3 | M3.5 V | Multiple | |
| 2454 | 671 | | GJ 4277 B | 4277 B | 22:26:14.97 | +03:00:00.4 | M6.0 V | Multiple | |
| 2455 | | J22264+583 | PM J22264+5823 | | 22:26:24.73 | +58:23:03.9 | M3.0 V | Single | |
| 2456 | | J22270+068 | GJ 4279 | 4279 | 22:27:03.00 | +06:49:32.1 | M3.5 V | Single | |
| 2457 | 672 | J22279+576 | HD 239960A | 860 A | 22:27:58.11 | +57:41:38.5 | M3.0 V | Multiple | 5 |
| 2458 | 672 | | DO Cep | 860 B | 22:27:57.93 | +57:41:38.8 | M4.0 V | Multiple | 5 A.2 |

Table A.1: Complete sample studied in this work^a (cont.).

| Star id. | System id. | Karmn | Name | GJ | α (J2016.0) | δ (J2016.0) | Spectral type | Multiplicity type | In tables |
|----------|------------|-------------|------------------------------|--------|-----------------------|-----------------------|---------------|-------------------|-----------|
| 2459 | | J22287+189 | GJ 9784 | 9784 | 22:28:46.13 | +18:55:52.1 | M0.0 V | Single | |
| 2460 | | J22289-134 | GJ 4281 | 4281 | 22:28:53.99 | -13:25:36.2 | M6.5 V | Single | |
| 2461 | | J22290+016 | LP 640-74 | | 22:29:05.91 | +01:39:45.0 | M0.5 V | Single | |
| 2462 | | J22298+414 | GJ 1270 | 1270 | 22:29:50.68 | +41:28:55.8 | M4.0 V | Single | |
| 2463 | 673 | J22300+488 | PM J22300+4851A | | 22:30:04.10 | +48:51:33.8 | M4.5 V | Multiple | |
| 2464 | 673 | | PM J22300+4851B | | 22:30:03.87 | +48:51:33.1 | M4.5 V | Multiple | |
| 2465 | | J22330+093 | GJ 863 | 863 | 22:33:02.81 | +09:22:43.0 | M1.0 V | Single | |
| 2466 | 674 | J22333-096 | GJ 4282 A | 4282 A | 22:33:22.77 | -09:36:53.6 | M3.0 V | Multiple | |
| 2467 | 674 | | GJ 4282 B | 4282 B | 22:33:22.87 | -09:36:53.7 | M2.5 V | Multiple | |
| 2468 | | J22347+040 | GJ 4283 | 4283 | 22:34:46.11 | +04:02:39.7 | M2.5 V | Single | |
| 2469 | | J22348-010 | GJ 4284 | 4284 | 22:34:54.85 | -01:04:54.5 | M4.5 V | Single | |
| 2470 | | J22353+746 | G 242-3 | | 22:35:20.75 | +74:41:20.1 | M0.0 V | Candidate | |
| 2471 | | J22373+299 | LP 344-27 | | 22:37:23.33 | +29:59:05.6 | M1.5 V | Single | |
| 2472 | 675 | J22361-008 | HD 214100 | 864 | 22:36:09.75 | -00:50:39.8 | M0.0 V | Multiple | |
| 2473 | 676 | J22374+395 | GJ 4287 | 4287 | 22:37:29.83 | +39:22:45.9 | M0.0 V | Multiple | A.10 |
| 2474 | 676 | | G 216-7B | | 22:37:32.51 | +39:22:33.7 | M9.5 V | Multiple | A.10 |
| 2475 | | J22387+252 | G 127-42 | | 22:38:44.65 | +25:13:30.5 | M3.5 V | Single | |
| 2476 | 677 | J22385-152 | EZ Aqr | 866 C | 22:38:36.17 | -15:17:22.7 | M5.5 V | Multiple | A.4 |
| 2477 | 678 | J22387-206S | FK Aqr | 867 A | 22:38:46.09 | -20:37:17.4 | M1.5 V | Multiple | A.4 |
| 2478 | 678 | J22387-206N | FL Aqr | 867 B | 22:38:45.77 | -20:36:52.9 | M3.5 V | Multiple | A.4 |
| 2479 | | J22406+445 | GJ 4290 | 4290 | 22:40:42.53 | +44:35:47.0 | M3.5 V | Candidate | |
| 2480 | | J22415+188 | GJ 9793 | 9793 | 22:41:35.30 | +18:49:28.9 | M0.0 V | Candidate | |
| 2481 | | J22415+260 | IRXS J224134.7+260210 | | 22:41:35.76 | +26:02:13.8 | M3.5 V | Single | |
| 2482 | | J22426+176 | GJ 1271 | 1271 | 22:42:39.99 | +17:40:17.6 | M2.5 V | Single | |
| 2483 | | J22433+221 | GJ 4292 | 4292 | 22:43:23.65 | +22:08:18.1 | M4.5 V | Candidate | |
| 2484 | | J22437+192 | RX J2243.7+1916 | | 22:43:43.73 | +19:16:52.4 | M3.0 V | Candidate | |
| 2485 | 679 | J22441+405 | TYC 3218-905-1 | | 22:44:06.16 | +40:29:58.1 | M1.0 V | Multiple | |
| 2486 | 679 | J22440+405 | TYC 3218-907-1 | | 22:44:04.51 | +40:29:58.5 | M1.0 V | Multiple | |
| 2487 | 680 | J22457+016 | LP 641-4 | | 22:45:46.48 | +01:41:22.0 | M1.0 V | Multiple | |
| 2488 | 680 | | LP 641-4 B | | 22:45:46.51 | +01:41:19.5 | M6.5 V | Multiple | |
| 2489 | | J22464-066 | GJ 4294 | 4294 | 22:46:27.09 | -06:39:35.0 | M5.0 V | Single | |
| 2490 | | J22468+443 | EV Lac | 873 | 22:46:48.68 | +44:19:55.0 | M3.5 V | Single | |
| 2491 | | J22476+184 | LP 461-11 | | 22:47:39.35 | +18:26:40.4 | M2.5 V | Candidate | |
| 2492 | | J22479+318 | GJ 4297 | 4297 | 22:47:54.67 | +31:52:18.4 | M3.0 V | Single | |
| 2493 | | J22489+183 | PM J22489+1819 | | 22:48:54.56 | +18:19:56.9 | M4.5 V | Candidate | |
| 2494 | | J22503-070 | HD 216133 | 875 | 22:50:19.31 | -07:05:22.7 | M0.5 V | Single | |
| 2495 | | J22506+348 | GJ 1274 | 1274 | 22:50:38.79 | +34:51:26.8 | M1.5 V | Single | |
| 2496 | | J22507+286 | GJ 4300 | 4300 | 22:50:45.77 | +28:36:07.7 | M3.0 V | Single | |
| 2497 | | J22509+499 | IRXS J225056.4+495906 | | 22:50:55.28 | +49:59:13.2 | M4.0 V | Single | |
| 2498 | | J22518+317 | GT Peg | 9799 | 22:51:54.19 | +31:45:14.4 | M3.0 V | Single | |
| 2499 | 681 | | HD 216385 | 9801 A | 22:52:24.64 | +09:50:09.1 | F6 V | Multiple | A.8 |
| 2500 | 681 | J22524+099 | GJ 9801 B | 9801 B | 22:52:30.31 | +09:54:04.9 | M3.0 V | Multiple | A.8 |
| 2501 | | J22526+750 | LP 48-305 | | 22:52:40.21 | +75:04:16.7 | M4.5 V | Single | |
| 2502 | | J22543+609 | Ross 226 | | 22:54:19.95 | +60:59:41.5 | M3.5 V | Single | |
| 2503 | | J22547-054 | GJ 4302 | 4302 | 22:54:47.14 | -05:28:21.1 | M4.0 V | Candidate | |
| 2504 | | J22532-142 | IL Aqr | 876 | 22:53:17.79 | -14:16:00.1 | M4.0 V | Single | |
| 2505 | 682 | | GJ 4305 | 4305 | 22:55:56.09 | +05:45:18.4 | DA8.1 | Multiple | A.9 |
| 2506 | 682 | J22559+057 | GJ 4304 | 4304 | 22:55:57.20 | +05:45:14.0 | M1.0 V | Multiple | A.9 |
| 2507 | | J22559+178 | GJ 4306 | 4306 | 22:55:59.87 | +17:48:38.0 | M1.0 V | Single | |
| 2508 | | J22565+165 | HD 216899 | 880 | 22:56:33.65 | +16:33:07.8 | M1.5 V | Single | |
| 2509 | 683 | J22576+373 | G 189-53A | | 22:57:40.20 | +37:19:17.8 | M3.0 V | Multiple | |
| 2510 | 683 | | G 189-53B | | 22:57:40.10 | +37:19:15.6 | M5.0 V | Multiple | |
| 2511 | | J23028+436 | IRXS J230251.9+433814 | | 23:02:52.29 | +43:38:15.5 | M4.0 V | Candidate | |
| 2512 | | J23036+097 | PM J23036+0942 | | 23:03:37.56 | +09:42:59.0 | M3.5 V | Single | |
| 2513 | | J23045+667 | GJ 1278 | 1278 | 23:04:31.03 | +66:45:50.5 | M0.5 V | Single | |
| 2514 | | J23051+519 | PM J23051+5159 | | 23:05:06.47 | +51:59:11.6 | M3.5 V | Single | |
| 2515 | | J23060+639 | GJ 9809 | 9809 | 23:06:05.27 | +63:55:33.4 | M0.0 V | Single | |
| 2516 | 684 | J23051+452 | LSPM J2305+4517 | | 23:05:09.00 | +45:17:32.9 | M3.5 V | Multiple | |
| 2517 | 684 | | Gaia DR2 1935209944573613568 | | 23:05:09.06 | +45:17:33.1 | M5.0 V | Multiple | |
| 2518 | 685 | J23063+126 | LP 521-79 | | 23:06:24.19 | +12:36:25.6 | M0.5 V | Multiple | A.4 |
| 2519 | 685 | | G 67-47 | | 23:06:25.69 | +12:36:55.9 | M2.5 V | Multiple | |
| 2520 | | J23064-050 | 2MUCD 12171 | | 23:06:30.37 | -05:02:36.7 | M7.5 V | Single | |
| 2521 | | J23065+717 | GJ 4311 | 4311 | 23:06:39.95 | +71:43:32.5 | M2.5 V | Single | |
| 2522 | | J23075+686 | GJ 4312 | 4312 | 23:07:33.27 | +68:40:06.1 | M3.5 V | Single | |
| 2523 | | J23081+033 | GJ 889.1 | 889.1 | 23:08:07.49 | +03:19:48.5 | M0.0 V | Single | |
| 2524 | | J23083-154 | HK Aqr | 890 | 23:08:19.67 | -15:24:36.1 | M0.0 V | Single | |
| 2525 | | J23088+065 | StKM 1-2100 | | 23:08:52.60 | +06:33:39.9 | M0.0 V | Candidate | |
| 2526 | 686 | | LSPM J2309+5506E | | 23:09:59.29 | +55:06:50.2 | DA | Multiple | A.9 |
| 2527 | 686 | J23089+551 | G 233-42 | | 23:09:58.62 | +55:06:48.1 | M5.0 V | Multiple | A.9 |
| 2528 | 687 | J23096-019 | GJ 4314 | 4314 | 23:09:39.64 | -01:58:29.9 | M3.5 V | Multiple | A.4 |
| 2529 | 687 | | G 28-44B | | 23:09:39.68 | -01:58:28.3 | M4.0 V | Multiple | |
| 2530 | | J23107-192 | GJ 1281 | 1281 | 23:10:42.22 | -19:13:57.9 | M2.5 V | Single | |
| 2531 | 688 | J23113+085 | G 28-46 | | 23:11:23.45 | +08:30:56.4 | M3.5 V | Multiple | 5 |
| 2532 | 688 | | G 28-46B | | 23:11:23.47 | +08:30:56.4 | M3.0 V | Multiple | 5 A.3 |
| 2533 | | J23121-141 | GJ 4316 | 4316 | 23:12:11.11 | -14:06:23.2 | M3.0 V | Single | |
| 2534 | 689 | J23166+196 | GJ 893.4 | 893.4 | 23:16:39.52 | +19:37:14.2 | M0.5 V | Multiple | |
| 2535 | 690 | J23142-196N | GJ 2154 A | 2154 A | 23:14:17.13 | -19:38:38.5 | M0.5 V | Multiple | |
| 2536 | 690 | J23142-196S | GJ 2154 B | 2154 B | 23:14:16.97 | -19:38:45.4 | M4.0 V | Multiple | |
| 2537 | 691 | J23174+196 | GJ 4326 | 4326 | 23:17:28.54 | +19:36:45.1 | M3.5 V | Multiple | |
| 2538 | 692 | J23174+382 | GJ 4327 | 4327 | 23:17:24.09 | +38:12:34.8 | M2.5 V | Multiple | A.4 |
| 2539 | 693 | J23175+063 | G 29-19 | 4329 | 23:17:34.73 | +06:23:24.5 | M3.0 V | Multiple | A.7 |
| 2540 | 693 | J23161+067 | G 28-50 | 4319 | 23:16:08.65 | +06:44:32.2 | M3.5 V | Multiple | A.7 |

Table A.1: Complete sample studied in this work^a (cont.).

| Star id. | System id. | Karmn | Name | GJ | α (J2016.0) | δ (J2016.0) | Spectral type | Multiplicity type | In tables |
|----------|------------|-------------|------------------------------|---------|-----------------------|-----------------------|---------------|-------------------|-----------|
| 2541 | | J23182+462 | Ross 244 | 9820 | 23:18:18.44 | +46:17:23.6 | M0.0 V | Single | |
| 2542 | | J23182+795 | LP 12-69 | | 23:18:19.85 | +79:34:45.8 | M3.0 V | Single | |
| 2543 | | J23193+154 | StKM 1-2115 | | 23:19:21.03 | +15:24:13.5 | M1.0 V | Single | |
| 2544 | 694 | V368 Cep | | | 23:19:27.78 | +79:00:13.8 | G9 V | Multiple | A.7 A.8 |
| 2545 | 694 | J23194+790 | HD 220140B | | 23:19:25.64 | +79:00:04.8 | M3.5 V | Multiple | A.7 A.8 |
| 2546 | 694 | J23228+787 | LP 12-90 | | 23:22:54.97 | +78:47:39.6 | M5.0 V | Multiple | A.7 A.8 |
| 2547 | | J23215+568 | LSPM J2321+5651 | | 23:21:32.23 | +56:51:19.7 | M1.0 V | Single | |
| 2548 | | J23216+172 | GJ 4333 | 4333 | 23:21:36.85 | +17:17:03.3 | M4.0 V | Single | |
| 2549 | | J23220+569 | G 217-6 | | 23:22:01.52 | +56:59:21.4 | M3.0 V | Single | |
| 2550 | | J23229+372 | PM J23229+3717 | | 23:22:58.46 | +37:17:13.3 | M2.0 V | Single | |
| 2551 | | J23234+155 | LP 522-65 | | 23:23:24.72 | +15:34:09.2 | M2.0 V | Single | |
| 2552 | | J23245+578 | Ross 302 | 895 | 23:24:30.39 | +57:51:11.0 | M1.0 V | Single | |
| 2553 | | J23249+506 | PM J23549+5036 | | 23:54:56.57 | +50:36:15.0 | M3.0 V | Single | |
| 2554 | | J23252+009 | Wolf 1038 | | 23:25:16.81 | +00:57:44.1 | M1.0 V | Single | |
| 2555 | | J23256+531 | GJ 4334 | 4334 | 23:25:42.10 | +53:08:11.1 | M4.5 V | Candidate | |
| 2556 | | J23262+088 | GJ 2155 | 2155 | 23:26:12.93 | +08:53:41.2 | M0.0 V | Single | |
| 2557 | 695 | J23261+170 | PM J23261+1700 | | 23:26:12.00 | +17:00:06.9 | M4.0 V | Multiple | |
| 2558 | | J23265+121 | GJ 4336 | 4336 | 23:26:33.26 | +12:09:37.9 | M3.0 V | Single | |
| 2559 | 696 | J23262+278 | V595 Peg | | 23:26:17.02 | +27:52:02.8 | M3.0 V | Multiple | |
| 2560 | 697 | J23293+414N | GJ 4337 | 4337 | 23:29:24.06 | +41:28:06.0 | M3.5 V | Multiple | |
| 2561 | 697 | J23293+414S | GJ 4338 | 4338 | 23:29:23.18 | +41:27:51.4 | M4.0 V | Multiple | |
| 2562 | 698 | J23317-027 | AF Psc | 1285 | 23:31:45.03 | -02:44:40.7 | M4.5 V | Multiple | A.7 |
| 2563 | 698 | J23301-026 | 2MASS J23301129-0237227 | | 23:30:11.41 | -02:37:23.9 | M6.0 V | Multiple+ | A.2 A.7 |
| 2564 | 699 | J23308+157 | LP 462-51 | | 23:30:53.52 | +15:47:38.8 | M1.0 V | Multiple | |
| 2565 | 700 | J23318+199E | EQ PegA | 896 | 23:31:52.83 | +19:56:13.2 | M3.5 V | Multiple | A.11 |
| 2566 | 700 | J23318+199W | EQ PegB | | 23:31:53.20 | +19:56:14.3 | M4.5 V | Multiple | A.2 |
| 2567 | | J23323+540 | G 217-12 | | 23:32:20.61 | +54:01:48.5 | M2.0 V | Single | |
| 2568 | 701 | | HD 221503 | 898 | 23:32:49.78 | -16:50:47.8 | K7 V | Multiple | A.7 |
| 2569 | 701 | J23302-203 | GJ 1284 | 1284 | 23:30:13.80 | -20:23:30.7 | M3.0 V | Multiple | A.4 A.7 |
| 2570 | 701 | J23327-167 | GJ 897 | 897 | 23:32:46.98 | -16:45:12.3 | M2.0 V | Multiple | A.2 A.7 |
| 2571 | 701 | | Gaia DR3 2395220664463236992 | 897 B | 23:32:46.98 | -16:45:11.7 | M3.0 V | Multiple | A.7 |
| 2572 | | J23340+001 | Wolf 1039 | 899 | 23:34:02.28 | +00:10:30.9 | M2.5 V | Single | |
| 2573 | | J23350+252 | Ross 298 | 4341 | 23:35:03.91 | +25:15:00.7 | M3.0 V | Single | |
| 2574 | | J23351-023 | GJ 1286 | 1286 | 23:35:11.30 | -02:23:34.1 | M5.5 V | Single | |
| 2575 | | J23354+300 | GJ 4342 | 4342 | 23:35:24.05 | +30:03:40.6 | M3.5 V | Candidate | |
| 2576 | | J23357+419 | GJ 4346 | 4346 | 23:35:45.48 | +41:58:06.3 | M1.0 V | Single | |
| 2577 | | J23364+554 | Ross 303 | 4349 | 23:36:26.53 | +55:29:42.1 | M1.5 V | Single | |
| 2578 | | J23376-128 | LP 763-3 | | 23:37:38.56 | -12:50:33.3 | M5.5 V | Candidate | |
| 2579 | | J23381-162 | GJ 4352 | 4352 | 23:38:07.84 | -16:14:11.4 | M2.0 V | Single | |
| 2580 | | J23386+391 | GJ 4354 | 4354 | 23:38:41.41 | +39:09:17.9 | M3.5 V | Single | |
| 2581 | 702 | J23350+016 | GJ 900 | 900 | 23:35:00.64 | +01:36:19.9 | M0.0 V | Multiple | |
| 2582 | 703 | | GJ 4357 | 4357 | 23:38:56.63 | +21:01:21.1 | DA | Multiple | A.9 |
| 2583 | 703 | J23389+210 | GJ 4356 | 4356 | 23:38:56.00 | +21:01:24.5 | M3.5 V | Multiple+ | A.9 |
| 2584 | 704 | J23401+606 | GJ 4358 A | 4358 A | 23:40:07.91 | +60:41:14.4 | M1.0 V | Multiple | |
| 2585 | 704 | | GJ 4358 B | 4358 B | 23:40:08.17 | +60:41:12.9 | M3.0 V | Multiple | |
| 2586 | 705 | J23414+200 | TYC 1727-1708-1 | | 23:41:28.99 | +20:02:31.0 | M0.5 V | Multiple | |
| 2587 | 705 | | LSPM J2341+2002S | | 23:41:28.97 | +20:02:27.0 | M2.0 V | Multiple | |
| 2588 | | J23419+441 | HH And | 905 | 23:41:55.20 | +44:10:13.4 | M5.0 V | Single | |
| 2589 | | J23423+349 | PM J23423+3458 | | 23:42:22.21 | +34:58:25.5 | M4.0 V | Candidate | |
| 2590 | | J23428+308 | GJ 1288 | 1288 | 23:42:52.33 | +30:49:16.9 | M4.5 V | Single | |
| 2591 | | J23431+365 | GJ 1289 | 1289 | 23:43:07.56 | +36:32:10.7 | M4.0 V | Single | |
| 2592 | 706 | | GJ 905.2 B | 905.2 B | 23:43:50.45 | +32:32:45.8 | DA3.8 | Multiple | A.9 |
| 2593 | 706 | J23438+325 | GJ 905.2 A | 905.2 A | 23:43:52.84 | +32:35:37.8 | M3.0 V | Multiple | A.9 |
| 2594 | | J23438+610 | G 217-18 | | 23:43:51.95 | +61:02:07.5 | M3.0 V | Single | |
| 2595 | | J23443+216 | GJ 1290 | 1290 | 23:44:21.41 | +21:36:06.4 | M3.5 V | Single | |
| 2596 | 707 | J23439+647 | Ross 676 | 4359 | 23:44:00.86 | +64:44:30.4 | M0.5 V | Multiple | A.4 |
| 2597 | 708 | J23455-161 | GJ 4360 A | 4360 A | 23:45:30.82 | -16:10:28.8 | M5.0 V | Multiple | |
| 2598 | 708 | | GJ 4360 B | 4360 B | 23:45:30.81 | -16:10:29.1 | M5.0 V | Multiple | |
| 2599 | | J23462+284 | PM J23462+2826 | | 23:46:14.17 | +28:26:05.0 | M3.5 V | Single | |
| 2600 | | J23480+490 | Ross 249 | 907 | 23:48:04.16 | +49:00:58.4 | M1.0 V | Single | |
| 2601 | 709 | J23489+098 | [R78b] 377 | | 23:48:58.98 | +09:51:53.3 | M1.0 V | Multiple | |
| 2602 | 709 | | [R78b] 377B | | 23:48:59.02 | +09:51:55.2 | M3.5 V | Multiple | |
| 2603 | | J23492+024 | BR Psc | 908 | 23:49:13.58 | +02:23:48.9 | M1.0 V | Single | |
| 2604 | | J23492+100 | GJ 4363 | 4363 | 23:49:15.05 | +10:05:32.7 | M4.0 V | Candidate | |
| 2605 | | J23496+083 | GJ 4364 | 4364 | 23:49:37.78 | +08:21:29.1 | M1.0 V | Single | |
| 2606 | | J23505-095 | GJ 4367 | 4367 | 23:50:32.33 | -09:33:39.5 | M4.0 V | Single | |
| 2607 | 710 | J23506+099 | GJ 4368 | 4368 | 23:50:36.86 | +09:56:57.5 | M3.0 V | Multiple | |
| 2608 | 710 | | GJ 4368 B | 4368 B | 23:50:36.94 | +09:56:57.3 | M4.0 V | Multiple | |
| 2609 | | J23509+384 | GJ 4369 | 4369 | 23:50:53.91 | +38:29:30.1 | M4.0 V | Single | |
| 2610 | 711 | J23517+069 | GJ 4370 | 4370 | 23:51:44.72 | +06:58:11.8 | M3.0 V | Multiple | |
| 2611 | 711 | | G 30-26B | | 23:51:44.86 | +06:58:11.3 | M3.0 V | Multiple | |
| 2612 | | J23523-146 | GJ 4371 | 4371 | 23:52:23.92 | -14:41:28.2 | M4.5 V | Candidate | |
| 2613 | 712 | | StKM 2-1787 | | 23:53:35.58 | +12:06:20.4 | K4 V | Multiple | A.8 |
| 2614 | 712 | J23535+121 | PM J23535+1206S | | 23:53:35.69 | +12:06:14.8 | M2.5 V | Multiple | A.8 |
| 2615 | | J23541+516 | GJ 4373 | 4373 | 23:54:10.95 | +51:41:11.0 | M3.5 V | Single | |
| 2616 | | J23544+081 | GJ 4374 | 4374 | 23:54:26.50 | +08:09:42.6 | M3.0 V | Candidate | |
| 2617 | | J23548+385 | RX J2354.8+3831 | | 23:54:51.28 | +38:31:34.8 | M4.0 V | Single | |
| 2618 | | J23554-039 | GJ 4376 | 4376 | 23:55:26.51 | -03:58:59.8 | M3.5 V | Candidate | |
| 2619 | | J23560+150 | LP 523-78 | | 23:56:00.14 | +15:01:37.9 | M2.5 V | Single | |
| 2620 | 713 | J23556-061 | GJ 912 | 912 | 23:55:39.27 | -06:08:39.4 | M2.5 V | Multiple | A.4 |
| 2621 | 714 | J23569+230 | G 129-45 | | 23:56:54.75 | +23:05:04.2 | M1.5 V | Multiple | |
| 2622 | 714 | | G 129-46 | | 23:56:55.00 | +23:04:58.7 | M2.0 V | Multiple | |

Table A.1: Complete sample studied in this work^a (cont.).

| Star id. | System id. | Karmn | Name | GJ | α (J2016.0) | δ (J2016.0) | Spectral type | Multiplicity type | In tables |
|----------|------------|-------------|-------------|------|-----------------------|-----------------------|---------------|-------------------|-----------|
| 2623 | 715 | J23573–129E | GJ 4378 | 4378 | 23:57:20.81 | -12:58:48.6 | M4.0 V | Multiple | |
| 2624 | 715 | J23573–129W | GJ 4379 | 4379 | 23:57:19.59 | -12:58:40.3 | M3.0 V | Multiple | A.4 |
| 2625 | | J23577+197 | GJ 4380 | 4380 | 23:57:45.32 | +19:46:03.4 | M3.5 V | Single | |
| 2626 | | J23577+233 | GJ 1292 | 1292 | 23:57:45.32 | +23:18:00.1 | M3.5 V | Candidate | |
| 2627 | 716 | J23578+386 | GJ 4381 | 4381 | 23:57:49.68 | +38:37:44.4 | M3.0 V | Multiple | |
| 2628 | 717 | J23582–174 | LP 764–40 A | | 23:58:13.95 | -17:24:34.6 | M2.0 V | Multiple | |
| 2629 | 717 | | LP 764–40 B | | 23:58:13.94 | -17:24:32.5 | M2.0 V | Multiple | |
| 2630 | 718 | J23585+076 | Wolf 1051 | 4383 | 23:58:32.74 | +07:39:25.0 | M3.0 V | Multiple | A.4 |
| 2631 | 719 | J23587+467 | GJ 913 | 913 | 23:58:44.50 | +46:43:44.9 | M0.0 V | Multiple | |
| 2632 | 720 | J23590+208 | G 129–51 | | 23:59:00.74 | +20:51:37.2 | M2.5 V | Multiple | |
| 2633 | 720 | | G 129–51B | | 23:59:00.75 | +20:51:36.7 | M2.0 V | Multiple | |
| 2634 | | J23598+477 | GJ 4385 | 4385 | 23:59:50.89 | +47:45:41.3 | M5.0 V | Single | |

Notes. ^(a) The full version of this table (2634 rows, 132 columns) is available in electronic form at the CDS and on a dedicated GitHub repository (<https://github.com/ccifuentesr/CARMENES-IX>).

Table A.2: Components of multiple system that do not comply with one or more of the criteria for physical association.

| Name | Comp. ^a | α (J2016.0) | δ (J2016.0) | μ ratio | ΔPA | Δd | ρ^b [arcsec] | Cause ^c |
|------------------------------|--------------------|-----------------------|-----------------------|-------------|-------------|------------|----------------------|--------------------|
| PM J00026+3821 B | B | 00:02:40.05 | +38:21:45.3 | 0.214 | 12.254 | 0.031 | 1.415 | 1 |
| G 217–32 B | B | 00:07:43.40 | +60:22:53.8 | 0.196 | 9.161 | 0.0032 | 0.848 | 1 |
| LP 296–56 | B | 01:56:41.74 | +30:28:34.6 | 0.012 | 0.027 | 0.163 | 299.1 | 3 |
| PM J02024+1034 A | B | 02:02:28.18 | +10:34:52.7 | 0.545 | 32.513 | 0.012 | 0.911 | 1 |
| LP 198–637 B | B | 03:20:45.35 | +39:42:59.6 | 0.152 | 8.738 | 0.0051 | 0.795 | 1 |
| PM J03247+4447 B | B | 03:24:42.23 | +44:47:39.7 | 0.191 | 4.590 | 0.0048 | 1.912 | 1 |
| Gaia DR3 3296932486866670720 | B | 04:05:38.89 | +05:44:40.1 | 0.331 | 1.614 | ... | 0.817 | 1, 2 |
| GJ 2033 B | B | 04:16:41.80 | -12:33:19.8 | 0.334 | 11.137 | 0.0069 | 2.990 | 1 |
| HG 7–232 B | B | 04:28:29.01 | +17:41:45.3 | 0.227 | 11.403 | 0.047 | 1.663 | 1 |
| V697 Tau B | B | 04:33:23.87 | +23:59:26.5 | 0.200 | 11.095 | 0.150 | 0.767 | 1 |
| GJ 3305 | BC | 04:37:37.51 | -02:29:29.7 | 0.274 | 14.659 | 0.077 | 0.098 | 1 |
| PM J04393+3331 | BC | 04:39:23.22 | +33:31:48.7 | 0.147 | 7.913 | 0.333 | 0.126 | 1 |
| GJ 9163 B | B | 04:40:29.15 | -09:11:46.8 | 0.441 | 1.954 | 0.0064 | 1.715 | 1 |
| GJ 3322 B | B | 05:01:58.89 | +09:58:55.9 | 0.152 | 8.744 | 0.0015 | 1.398 | 1 |
| HD 32450 B | B | 05:02:28.26 | -21:15:27.5 | 0.247 | 6.461 | 0.0063 | 0.888 | 1 |
| LP 359–186 | BC | 05:03:05.77 | +21:22:33.8 | 0.046 | 0.799 | 0.104 | 0.302 | 1, 2 |
| GJ 3332 | B | 05:06:49.48 | -21:35:04.3 | 0.881 | 58.265 | 0.0018 | 8.489 | 1 |
| BD-21 1074 C | C | 05:06:49.55 | -21:35:04.7 | 0.309 | 8.384 | 0.0029 | 1.105 | 1 |
| GJ 3343 | B | 05:20:41.05 | +58:47:12.0 | 0.021 | 1.037 | 0.104 | 14.11 | 3 |
| PM J05243–1601 B | B | 05:24:19.17 | -16:01:15.6 | 0.964 | 52.141 | 0.0066 | 0.444 | 1 |
| G 102–4 A | C | 05:28:56.61 | +12:31:50.4 | 0.023 | 1.307 | 0.169 | 99.39 | 2 |
| PM J05319–0303W | C | 05:31:57.88 | -03:03:37.6 | 0.254 | 4.659 | 0.034 | 150.0 | 1 |
| 2MASS J05315816–0303397 | D | 05:31:58.17 | -03:03:40.7 | 0.257 | 5.562 | 0.048 | 0.1 | 1 |
| ESO-HA 737 | E | 05:32:05.97 | -03:01:16.8 | 0.209 | 5.090 | 0.046 | 254.2 | 1 |
| PM J06066+4633 B | B | 06:06:37.77 | +46:33:45.2 | 0.198 | 2.085 | 0.00038 | 1.790 | 1 |
| LP 362–121 | B | 06:10:22.52 | +22:34:18.1 | 0.057 | 1.898 | 0.258 | 65.16 | 2 |
| Ross 603 B | B | 06:27:43.74 | +09:23:50.5 | 0.167 | 8.901 | 0.0052 | 1.170 | 1 |
| Gaia DR3 2926756741750933120 | B | 06:39:37.22 | -21:01:31.9 | 0.590 | 11.207 | 0.025 | 0.556 | 1 |
| 2MASS J07293670+3554531 | C | 07:29:36.67 | +35:54:51.3 | 0.171 | 6.262 | 0.0063 | 95.88 | 3 |
| Castor C | Cab | 07:34:37.19 | +31:52:08.6 | 0.220 | 11.459 | 0.034 | ... | 1 |
| FP Cnc B | Cab | 08:08:55.38 | +32:49:01.4 | 0.189 | 10.740 | 0.022 | ... | 1 |
| GJ 1116 B | B | 08:58:14.09 | +19:45:45.3 | 0.236 | 5.329 | 0.011 | 2.175 | 1 |
| GJ 397.1 B | BC | 10:31:30.64 | +57:05:20.4 | 0.166 | 3.931 | ... | 0.284 | 1, 2 |
| PM J10367+1521 B | BC | 10:36:44.92 | +15:21:37.9 | 0.174 | 5.147 | ... | 0.858 | 1, 2 |
| GJ 3616 B | B | 10:44:52.43 | +32:24:40.1 | 0.067 | 2.466 | 0.129 | 1.296 | 1 |
| GJ 3617 | C | 10:44:54.79 | +32:24:23.4 | 0.079 | 4.417 | 0.125 | 35.23 | 1, 2 |
| GJ 3628 | B | 10:50:37.91 | +51:45:01.6 | 0.219 | 12.290 | 0.013 | 178.3 | 3 |
| HD 98712 B | B | 11:21:26.84 | -20:27:11.5 | 0.266 | 5.851 | 0.046 | 3.811 | 1 |
| GJ 426.1 B | B | 11:23:55.75 | +10:31:44.7 | 0.213 | 11.741 | 0.020 | 2.050 | 1 |
| Gaia DR3 3699797155055781760 | B | 12:20:25.60 | +00:35:01.3 | 0.641 | 30.528 | 0.0055 | 0.882 | 1 |
| GJ 490 B | CD | 12:57:38.94 | +35:13:16.9 | 0.106 | 5.090 | 0.117 | 0.171 | 1 |
| PM J13260+2735 B | C | 13:26:02.63 | +27:35:02.5 | 0.201 | 8.729 | 0.0015 | 404.1 | 1 |
| GJ 520 B | B | 13:37:50.77 | +48:08:16.3 | 0.166 | 5.256 | 0.000046 | 1.621 | 1 |
| Gaia DR3 1658968054798747008 | B | 13:41:46.39 | +58:15:18.6 | 0.360 | 13.784 | 0.0078 | 0.762 | 1 |
| GJ 536.1 B | B | 14:01:58.89 | +15:29:39.1 | 0.167 | 7.680 | 0.0020 | 1.621 | 1 |
| PM J14019+4316 B | B | 14:01:58.69 | +43:16:43.1 | 0.151 | 8.700 | 0.00081 | 1.960 | 1 |
| HD 124498 B | C | 14:14:21.34 | -15:21:24.4 | 0.175 | 9.130 | 0.077 | 1.553 | 1 |
| G 224–13 B | B | 14:33:06.80 | +61:00:43.6 | 0.190 | 10.854 | 0.0018 | 0.971 | 1 |
| GJ 9492 B | B | 14:42:21.17 | +66:03:20.1 | 0.221 | 11.795 | 0.0013 | 2.290 | 1 |
| GJ 569 B | BC | 14:54:29.77 | +16:06:05.6 | 0.215 | 7.832 | 0.067 | ... | 1 |
| Gaia DR3 1275127175448008448 | B | 15:18:49.78 | +29:15:06.7 | 0.302 | 8.736 | 0.037 | 0.588 | 1 |
| Gaia DR3 1375767330164975616 | B | 15:33:54.89 | +37:54:48.3 | 0.234 | 13.506 | 0.0022 | 0.834 | 1 |
| LP 331–57 B | B | 17:03:53.14 | +32:11:46.4 | 0.175 | 3.536 | 0.0055 | 1.393 | 1 |
| BD+19 3268 B | B | 17:15:49.84 | +19:00:00.3 | 0.699 | 3.435 | 0.0044 | 1.471 | 1 |
| RX J1734.0+4447 B | B | 17:34:05.47 | +44:47:08.4 | 0.403 | 17.500 | 0.058 | 0.633 | 1 |
| GJ 4021 | C | 17:38:40.87 | +61:14:00.0 | 0.232 | 11.069 | 0.016 | 19.05 | 1 |
| GJ 695 C | D | 17:46:24.65 | +27:42:49.8 | 0.160 | 0.847 | 0.0039 | 0.575 | 1 |
| HD 230017 B | B | 18:54:53.86 | +10:58:45.1 | 0.512 | 6.480 | 0.0041 | 3.792 | 1 |
| PM J18542+1058 | C | 18:54:17.14 | +10:58:11.0 | 0.170 | 2.601 | 0.0078 | 538.9 | 1 |
| StKM 1–1676 B | C | 19:03:17.96 | +63:59:37.4 | 0.824 | 54.189 | ... | 3.578 | 1 |
| GJ 4115 | C | 19:35:06.33 | +08:27:43.4 | 0.462 | 17.584 | 0.062 | 5.635 | 1 |
| GJ 1245 B | C | 19:53:55.66 | +44:24:46.5 | 0.174 | 9.449 | 0.0068 | 5.945 | 1 |
| LP 395–8 B | B | 20:19:49.35 | +22:56:40.0 | 0.184 | 10.601 | 0.000044 | 1.918 | 1 |
| GJ 4153 B | B | 20:37:23.97 | +21:56:21.4 | 0.072 | 0.221 | 0.217 | 51.77 | 2 |

Table A.2: Components of multiple system that do not comply with one or more of the criteria for physical association (cont.).

| Name | Comp. ^a | α (J2016.0) | δ (J2016.0) | μ ratio | ΔPA | Δd | ρ^b [arcsec] | Cause ^c |
|-------------------------|--------------------|-----------------------|-----------------------|-------------|-------------|------------|----------------------|--------------------|
| AT Mic B | C | 20:41:51.54 | -32:26:15.1 | 0.298 | 13.947 | 0.012 | 2.102 | 1 |
| PM J21055+0609S | B | 21:05:32.17 | +06:09:11.2 | 0.175 | 5.680 | 0.000069 | 5.094 | 1 |
| DENIS J210844.8-042517 | C | 21:08:44.75 | -04:25:18.3 | 0.652 | 12.094 | 0.012 | 20.89 | 1 |
| GJ 4188 | C | 21:17:39.55 | -08:54:49.6 | 0.166 | 7.927 | 0.098 | 63.99 | 1 |
| GJ 4201 B | B | 21:32:22.23 | +24:33:41.1 | 0.181 | 9.559 | 0.0029 | 1.548 | 1 |
| GJ 834 B | B | 21:36:38.20 | +39:27:17.8 | 0.181 | 9.172 | 0.0041 | 1.003 | 1 |
| UCAC4 747-070768 | B | 21:51:39.93 | +59:17:34.5 | 0.384 | 20.069 | 0.041 | 14.64 | 1 |
| LP 759-25 | B | 22:05:35.44 | -11:04:31.8 | 0.053 | 3.002 | 0.323 | 3030.6 | 3 |
| Wolf 1225 B | B | 22:23:29.34 | +32:27:29.5 | 0.271 | 12.352 | 0.0040 | 1.252 | 1 |
| DO Cep | B | 22:27:57.93 | +57:41:38.8 | 0.438 | 19.178 | 0.0023 | 2.052 | 1 |
| GJ 4282 B | B | 22:33:22.87 | -09:36:53.7 | 0.172 | 5.466 | 0.0022 | 1.399 | 1 |
| 2MASS J23301129-0237227 | B | 23:30:11.41 | -02:37:23.9 | 0.069 | 3.658 | 0.232 | 1469.1 | 3 |
| EQ Peg B | B | 23:31:53.20 | +19:56:14.3 | 0.152 | 8.006 | 0.0015 | 5.376 | 1 |
| GJ 897 | C | 23:32:46.98 | -16:45:12.3 | 0.938 | 66.572 | ...† | 337.9 | 2 |

Notes. ^(a) Component in system. ^(b) Angular separation of the closest component. ^(c) Cause of the deviation: 1: Presence of a very close companion (either resolved or not). This is also applicable to the primary; 2: Distances and proper motions from a source different than *Gaia* DR3, with larger uncertainties, or missing values; 3: New unresolved binary candidates as described in Sect. 3.3. This is applicable to the primary. ^(†) Castor C: Detached eclipsing double-lined spectroscopic binary (DESB2) with $a \lesssim 0.01$ au ([Torres & Ribas 2002](#)); FP Cnc B: SB2 ([Shkolnik et al. 2010](#)) in a quadruple system; GJ 569 B: Ultra-cool companion resolved ($\rho \lesssim 0.1$ arcsec) with the Keck Adaptive Optics Facility ([Martín et al. 2000](#); [Lane et al. 2001](#)); GJ 897: Parallax from Hipparcos removed because of extremely large relative error.

Table A.3: New stellar multiple systems not reported in the literature.

| Name | Karman | Spectral type ^a | Component ^b | α | δ | ϖ^c [mas] | μ_{total} [mas a ⁻¹] | θ [deg] | ρ [arcsec] |
|------------------------------|------------|----------------------------|------------------------|-------------|-------------|---------------------|--|-------------------|--------------------|
| GJ 3261 | J04056+057 | M3.5 V | A | 04:05:38.94 | +05:44:40.4 | 16.094 ± 0.103 | 47.98 ± 0.15 | | |
| Gaia DR3 3296932486866670720 | | M4.0: V | B | 04:05:38.89 | +05:44:40.1 | | | 251.9 | 0.817 |
| V1221 Tau | | M3.0: V | (C) | 04:05:53.46 | +05:31:24.6 | 15.876 ± 0.026 | 49.85 ± 0.03 | 164.8 | 824.8 |
| RX J0507.2+3731 A | J05072+375 | M5.0 V | A | 05:07:14.33 | +37:30:42.1 | 43.800 ± 4.000 | 102.11 ± 4.90 | | |
| RX J0507.2+3731 B | | M5.0: V | (B) | 05:07:14.37 | +37:30:42.1 | 44.022 ± 0.461 | 96.09 ± 0.82 | 93.2 | 0.476 |
| LP 780-23 | J06401-164 | M2.5 V | A | 06:40:08.72 | -16:27:21.5 | ... | 319.03 ± 11.31 | | |
| LP 780-23 B | | M2.5: V | (B) | 06:40:08.72 | -16:27:21.7 | ... | ... | 187.9 | 0.199 |
| GJ 375.2 | J10004+272 | M0.5 V | A | 10:00:26.69 | +27:16:03.5 | 27.767 ± 0.016 | 118.42 ± 0.02 | | |
| 2MASS J10003572+2717054 | | M6.5 V | B | 10:00:35.70 | +27:17:07.5 | 27.723 ± 0.103 | 118.34 ± 0.13 | 61.9 | 136.0 |
| Gaia DR3 740041664172917376 | | M7.5: V | (C) | 10:00:26.56 | +27:16:05.7 | 26.561 ± 0.349 | 117.20 ± 0.34 | 320.9 | 2.882 |
| HD 230017 A [†] | J18548+109 | M0.0 V | A | 18:54:53.67 | +10:58:42.4 | 53.423 ± 0.108 | 133.27 ± 0.16 | | |
| HD 230017 B | | M3.5 V | B | 18:54:53.86 | +10:58:45.1 | 53.644 ± 0.043 | 89.29 ± 0.06 | 45.1 | 3.792 |
| PM J18542+1058 | | M4.0 V | (C) | 18:54:17.14 | +10:58:11.0 | 53.838 ± 0.024 | 114.61 ± 0.03 | 266.7 | 538.9 |
| G 28-46 | J23113+085 | M3.0 V | A | 23:11:23.45 | +08:30:56.4 | 49.800 ± 3.300 | 458.92 ± 11.31 | | |
| G 28-46 B [†] | | M3.0: V | (B) | 23:11:23.47 | +08:30:56.4 | ... | ... | 77.7 | 0.248 |

Notes. ^(a) A colon (:) indicates an estimated spectral type from photometry. ^(b) The new component found in each system is written in parentheses.

^(†) HD 230017 ABC: Members of the Carina association (Gagné & Faherty 2018); G 28-46 AB: System identified as a close binary during the CARMENES exoplanet search (Ribas et al. 2023). A minimum period of 2225 d was tabulated by Sabotta et al. (2021) from spectroscopic observations.

Table A.4: Spectroscopic binaries, triples, and quadruples in our sample.

| Name | Karmn | Type ^a | P_{orb} [d] | $a \sin i$ [au] | $q = M_B/M_A$ | Reference ^b |
|-----------------------|-------------|-------------------|-----------------------------|-----------------|---------------|----------------------------|
| HD 38A | | SB | ... | ... | ... | Abt70, Str93 |
| 1RXS J000806.3+475659 | J00081+479 | SB2 | <4.4 | 0.04 | ... | Shk10, Fou18 |
| EZ Psc | J00162+198W | SB2 | 3.95652 ± 0.00008 | 0.038623 | 0.35 | Bar18 |
| FF And | J00428+355 | SB2 | ... | ... | ... | Bop77, Giz02 |
| RX J0050.2+0837 | J00502+086 | SB2 | ... | ... | ... | Jef18 |
| GJ 1029 | J01056+284 | SB2 | 95.76 ± 0.18 | 0.1331 | 0.72 | Bar18, Win20 |
| PM J01437–0602 | J01437–060 | SB2 | ... | ... | ... | Fou18 |
| G 173–18 | J01453+465 | SB2 | <157.9 | 0.56 | ... | Giz02, Shk10 |
| BD–21 332 | J01531–210 | SB2 | <2.9 | 0.04 | ... | Shk10 |
| GJ 1041 B | J01592+035W | SB2 | <356.4 | 0.93 | ... | Shk10 |
| GJ 3129 | J02027+135 | SB2 | <27.8 | 0.13 | ... | Jen09, Shk10 |
| GJ 3131 | J02033–212 | SB2 | ... | ... | ... | Jef18 |
| V374 And | J02069+451 | SB2 | 897.0 ± 2.3 | ... | 0.70 | Spe19 |
| GJ 3160 | J02289+120 | SB2 | ... | ... | ... | Jef18 |
| GJ 3235 | J03346–048 | ST3 | ... | ... | ... | Jef18 |
| GJ 3236 | J03372+691 | DESB2 | 0.7712600 ± 0.0000023 | 0.0143 | 0.75 | Irw09, Shk10 |
| GJ 3239 | J03375+178N | SB2 | <33.2 | 0.18 | ... | Shk10, Fou18 |
| GJ 3240 | J03375+178S | SB2 | <0.4 | 0.01 | ... | Shk10 |
| HD 278874 | | SB2 | ... | ... | ... | Mon18 |
| Wolf 227 | J03526+170 | SB2 | ... | ... | ... | Bon13a, Jef18 |
| HD 24916 B | J03574–011 | SB | ... | ... | ... | Zak79 |
| LP 414–117 | J04123+162 | SB2 | 128.114 | ... | 0.60 | Ben08 |
| 1RXS J042441.9–064725 | J04247–067 | ST3 | <1.9 | 0.02 | ... | Shk10 |
| GJ 3282 | J04252+080S | SB2 | ... | ... | ... | Jef18 |
| LP 775–31 | J04352–161 | SB2 | ... | ... | ... | Rei09 |
| TYC 694–1183–1 | J04414+132 | SB | ... | ... | ... | Mer09 |
| LP 415–345 | J04425+204 | SB2 | ... | ... | ... | Sta97 |
| LP 416–43 | J04480+170 | SB | 8.49474 ± 0.00007 | 6.2 | ... | Gri85 |
| 1RXS J044847.6+100302 | J04488+100 | SB2 | ... | ... | ... | Jef18 |
| GJ 3322 A | J05019+099 | SB2 | ... | ... | 0.57 | Del98, Del99b |
| HD 285190 | J05032+213 | SB2 | ... | ... | ... | Jef18, Fou18 |
| Capella | | SB2 | 104.02173 ± 0.00022 | 0.7357 | 0.99 | She85, Tor09 |
| GJ 1080 | J05282+029 | SB | ... | ... | ... | Jen09 |
| HD 35956 | | SB1 | ... | ... | ... | Kat13 |
| Ross 42 | J05322+098 | SB2 | <61.1 | 0.23 | 1.00 | Mar87, Shk10 |
| V371 Ori | J05337+019 | SB1 | $0.60417356 \pm 0.00000025$ | ... | ... | Rein12, Bar21 |
| Ross 45 B | J05342+103S | SB | ... | ... | ... | Rein12 |
| V1402 Ori | J05402+126 | SB2 | <138.9 | 0.52 | ... | Shk10 |
| Wolf 237 | J05466+441 | SB2 | ... | ... | ... | Jef18 |
| Ross 59 | J05532+242 | SB2 | 721 ± 2 | 0.6656 | 0.33 | Bar18 |
| LP 86–173 | J06054+608 | SB1 | $0.30992678 \pm 0.00000048$ | 0.0049 | 0.93 | New16, Win20 |
| TYC 4525–194–1 | J06171+751 | ST3? | ... | ... | ... | Fou18 |
| G 108–4 | J06298–027 | SB2 | <46.9 | 0.16 | ... | Shk10 |
| 1RXS J070005.1–190115 | J07001–190 | SB2 | 6.56025 ± 0.00030 | 0.002797 | ... | Bar21 |
| QY Aur | J07100+385 | SB2 | 10.42673 ± 0.00010 | 0.0687 | 0.85 | TP86, Win20 |
| TYC 4530–1414–1 | J07119+773 | SB1 | ... | ... | ... | Jef18 |
| 1RXS J073138.4+455718 | | SB2? | ... | ... | ... | Fou18 |
| GJ 3447 | J07320+173E | SB | ... | ... | ... | Gaia22a |
| Castor | | SB2 + SB2 | 167570 ± 840 | 83.9052 | 0.79 | Bel97, Cur06, Tor22 |
| Castor C | J07346+318 | DESB2 | 0.8142822 ± 0.0000010 | 0.01809 | 1.00 | Joy26, Giz02, Tor02, Tor22 |
| GJ 282 C | J07361–031 | SB1 | 6591 ± 177 | 6.224 | 0.34 | Bar21 |
| GJ 3461 | J07418+050 | EB?/SB2 | ... | ... | ... | Jef18 |
| 1RXS J075434.3+083213 | J07545+085 | SB1 | ... | ... | ... | Jef18 |
| FP Cnc B | J08089+328 | SB2 | <395.5 | 0.92 | ... | Shk10 |
| CU Cnc | J08316+193S | DESB2 | 2.771468 ± 0.000004 | 0.03624 | 0.92 | Del99a, Del99b, Tor10 |
| LSPM J0835+1408 | J08353+141 | ST3 | ... | ... | ... | Ski18 |
| GJ 319 A | J08427+095 | SB1 | 20.9491 ± 0.0019 | 0.021 | 0.22 | Duq88 |
| GJ 3522 | J08589+084 | SB2 | 7.5555 ± 0.0002 | ... | 0.82 | Rei97b, Del99b |
| GJ 3540 | J09120+279 | SB2 | ... | ... | ... | Jef18 |
| LP 427–16 | J09140+196 | SB1 | ... | ... | ... | Bar21 |
| HD 79210 | J09143+526 | SB1 | ... | ... | ... | Jef18 |
| GJ 9303 | J09362+375 | SB2 | ... | ... | ... | Mal14a |
| LP 728–70 | J09506–138 | SB2 | ... | ... | ... | Jef18 |
| GJ 372 | J09531–036 | SB2 | 47.709 ± 0.053 | 39.06 | 0.76 | Har96, Jef18, Bar18 |
| GJ 373 | J09561+627 | SB? | ... | ... | ... | Rein12 |
| LP 790–2 | J10182–204 | SB2 | 5.922845 ± 0.000061 | 0.048242 | 0.58 | Bar18 |

Table A.4: Spectroscopic binaries, triples, and quadruples in our sample (cont.).

| Name | Karmn | Type ^a | P_{orb} [d] | $a \sin i$ [au] | $q = M_B/M_A$ | Reference ^b |
|-----------------------|-------------|-------------------|------------------------------|-------------------------|---------------|------------------------|
| GJ 3612 | J10354+694 | SB2 | 119.41 ± 0.04 | 0.3464 | 0.51 | Bar18 |
| LP 127–502 | J10368+509 | SB2? | ... | ... | ... | Fou18 |
| GJ 3626 | J10504+331 | SB1 | 2996 ± 31 | 0.2355 | ... | Bar21 |
| GJ 3630 | J10520+005 | ST3/SQ4 | <28.1 | 0.11 | ... | Shk10 |
| LP 491–51 | J11036+136 | SB1 | ... | ... | ... | Jef18 |
| GJ 426.1 A | | SB | ... | ... | ... | Abt76 |
| GJ 455 | J12023+285 | SB2 | ... | ... | ... | Giz02 |
| LP 734–34 | J12104–131 | SB2 | 33.6551 ± 0.0046 | 0.0479 | 0.95 | Win20 |
| GJ 3719 | J12169+311 | SB2 | ... | ... | ... | Fou18 |
| G 148–43 | J12191+318 | SB2 | ... | ... | ... | Jef18 |
| GJ 3731 | J12299–054W | SB2 | ... | ... | ... | Jef18 |
| G 123–45 | J12364+352 | SB1 | 34.7557 ± 0.0041 | 0.0219 | ... | Win20 |
| DP Dra | J12490+661 | ST3 | 54.075 ± 0.006 | ... | 0.95 | Del99b |
| GJ 507 B | J13195+351E | SB1 | ... | ... | ... | Jef18 |
| GQ Vir | J14130–120 | SB2 | ... | ... | ... | Jef18 |
| GJ 1182 | J14155+046 | SB2 | 154.2 ± 0.1 | 0.35835 | 0.66 | Bar18 |
| PM J14171+0851 | J14171+088 | SB2 | ... | ... | ... | Jef18 |
| GJ 3861 | J14368+583 | SB2 | ... | ... | ... | Giz02, Jef18 |
| GJ 3875 | J14549+411 | SB | ... | ... | ... | Ski18 |
| G 136–35 | J14564+168 | SB | ... | ... | ... | Ski18 |
| StKM 1–1240 | J15238+561 | SB2 | ... | ... | ... | Fou18 |
| GJ 3910 | J15319+288 | SB1 | ... | ... | ... | Jen09 |
| UU UMi | J15412+759 | SB2 | 5240 ± 410 | 4.7 | 0.59 | Bar18, Bar21 |
| GJ 595 | J15421–194 | SB1 | ... | ... | ... | Nid02 |
| GJ 3916 | J15474–108 | ST3 | 3028 ± 23 | 3.59 | 1.05 | Bar21 |
| LP 177–102 | J15474+451 | DESB2 | 3.5500184 ± 0.0000018 | 0.036535 | 1.00 | Moc02, Har11, Bir12 |
| σ CrB A | | SB2 | $1.139791423 \pm 0.00000008$ | 0.013106 | 0.96 | Str03, Rag09 |
| CM Dra | J16343+571 | DESB2 | $1.268389985 \pm 0.00000005$ | 0.017502 | 0.93 | Mor09, Tor10, Sch19 |
| V1054 Oph | J16554–083S | ST3 | 2.965522 ± 0.000014 | 0.05 | 0.90 | Joy47, Pet84, Del98 |
| LP 331–57 A | J17038+321 | SB2? | ... | ... | ... | Shk09, Fou18 |
| GJ 3991 | J17095+436 | SB1 | ... | ... | ... | Rei97b, Del99b |
| Wolf 1473 | J17464–087 | SB2 | 83.926 ± 0.032 | 0.27559 | 0.93 | Mal14a, Win20 |
| GJ 1230 A | J18411+247S | SB2 | 5.0688 ± 0.00005 | ... | 0.95 | GR96, Del99b |
| GJ 735 | J18554+084 | SB2 | ... | ... | ... | Mar87, Giz02, Kar04 |
| GJ 4091 B | J18563+544 | SB2 | ... | ... | ... | Fou18 |
| G 125–15 | J19312+361 | SB2 | <0.7 | 0.01 | ... | Shk10 |
| RX J1935.4+3746 | J19354+377 | SB1 | ... | ... | ... | Shk09, Jef18 |
| LP 869–19 | J19420–210 | SB2 | ... | ... | ... | Mal14a |
| V1513 Cyg | J20050+544 | SB1 | $0.49670418 \pm 0.00000005$ | 0.010537 ± 0.000005 | ... | Giz97b, Mac18 |
| LP 574–21 | J20105+065 | SB2 | <40.1 | 0.19 | ... | Shk10 |
| LP 395–8 A | J20198+229 | SB2 | 1.1293392 ± 0.0000067 | 0.01057 | 0.56 | Bar18 |
| IRXS J203011.0+795040 | J20301+798 | SB2 | ... | 190.469 | ... | Jef18 |
| GJ 4155 | J20409–101 | SB | ... | ... | ... | Rei12 |
| GJ 4161 | J20445+089N | SB2 | ... | ... | ... | Jef18 |
| GJ 810 A | J20556–140N | SB2 | 812 ± 51 | 0.841 | 0.83 | Bar18 |
| FR Aqr | J20568–048 | SB2 | ... | ... | ... | Jef18 |
| Ross 775 | J21296+176 | SB2 | 53.221 ± 0.004 | ... | 1.00 | Mar87, Del99b |
| GJ 4213 | J21442+066 | SB1 | ... | ... | ... | Jef18 |
| EZ Aqr | J22385–152 | ST3 | 822.6 ± 0.6 | 1189 | 0.53 | Del99c |
| FK Aqr | J22387–206S | SB2 | 4.08322 ± 0.00004 | 0.039372 | 0.80 | Her65, Del99b |
| FL Aqr | J22387–206N | SB1 | 1.795 ± 0.017 | 0.00353 | 0.60 | Dav14 |
| LP 521–79 | J23063+126 | SB2(3?) | <58.9 | 0.31 | ... | Shk10 |
| GJ 4314 | J23096–019 | SB2 | ... | ... | ... | Jef18 |
| GJ 4327 | J23174+382 | SB2 | ... | ... | ... | Jef18 |
| GJ 1284 | J23302–203 | SB2 | 11.838033 ± 0.000076 | 6.48275 | 0.19 | Giz02, Jef18, Car21 |
| Ross 676 | J23439+647 | SB2 | <3 | 0.04 | ... | Shk10 |
| GJ 912 | J23556–061 | SB1 | 5188 ± 58 | 0.505 | 0.12 | Bar21 |
| GJ 4379 | J23573–129W | SB2 | ... | ... | ... | Giz02, Jef18 |
| Wolf 1051 | J23585+076 | ST3 | 4634 ± 17 | 0.4436 | 0.55 | Bar21 |

Notes. ^(a) A spectroscopic binary (SB) that displays one or two lines in the spectrum is a single- or double-lined spectroscopic binary, respectively, and abbreviated as SB1 or SB2. A spectroscopic triple (ST) showing two or three lines is a double- or triple-lined spectroscopic triple, and abbreviated as ST2 or ST3. Spectroscopic quadruples (SQ) are much more rare, and typically are three- or four-lined systems, denominated SQ3 and SQ4, respectively. In our sample, only one star is classified as SQ4 (GJ 3630, J10520+005). ^(b) While recognising the contributions of contemporary investigations (e.g. Shkolnik et al. 2010, Jeffers et al. 2018, Baroch et al. 2018, 2021, and Winters et al. 2020 are the source of many of the parameters in this table), references are often limited for simplicity to the original sources that first identified the systems. However, exceptions are made for prominent systems such as Castor C or nearby stars with a long history of observations, such as CM Dra and CU Cnc. References – Abt70: Abt (1970); Bar18: Baroch et al. (2018); Bar21: Baroch et al. (2021); Bel97: Belopolsky (1897); Ben08: Bender & Simon (2008); Bir12: Birkby et al. (2012); Bon13a: Bonfils et al. (2013); Bop77: Bopp & Fekel (1977); Cur06: Curtis (1906); Dav14: Davison et al. (2014); Del98: Delfosse et al. (1998); Del99a: Delfosse et al. (1999b); Del99b: Delfosse et al. (1999a); Del99c: Delfosse et al. (1999c); Fou18: Fouqué et al. (2018); Gaia22a: Gaia Collaboration (2022); Giz02: Gizis et al. (2002); Giz97b: Gizis (1997); GR96: Gizis & Reid (1996); Har11: Hartman et al. (2011); Har96: Harlow (1996); Her65: Herbig & Moorhead (1965); Irw09: Irwin et al. (2009); Jef18: Jeffers et al. (2018); Jen09: Jenkins et al. (2009); Joy26: Joy & Sanford (1926); Joy47: Joy (1947); Kar04: Karataş et al. (2004); Kat13: Katoh et al. (2013); Mac02: Mochnacki et al. (2002); Mac18: Mace et al. (2018); Mal14a: Malo et al. (2014a); Mar87: Marcy et al. (1987); Mer09: Mermilliod et al. (2009); Moc02: Mochnacki et al. (2002); Mon18: Montes et al. (2018); Mor09: Morales et al. (2009); New16: Newton et al. (2016); Nid02: Nidever et al. (2002); Pet84: Pettersen et al. (1984); Rag09: Raghavan et al. (2009); Rei09: Reiners & Basri (2009); Rein12: Reiners et al. (2012); Rei97b: Reid & Gizis (1997); Scha19: Schanche et al. (2019); She85: Shen et al. (1985); Shk09: Shkolnik et al. (2009); Shk10: Shkolnik et al. (2010); Shk12: Shkolnik et al. (2012); Ski18: Skinner et al. (2018); Spe19: Sperauskas et al. (2019); Sta97: Stauffer et al. (1997); Ste14: Stebbins (1914); Str03: Strassmeier & Rice (2003); Str93: Strassmeier et al. (1993); TP86: Tomkin & Pettersen (1986); Tor09: Torres et al. (2009); Tor22: Torres et al. (2022); Win20: Winters et al. (2020); Zak79: Zakhozhaj (1979).

Table A.5: Eclipsing binaries in our sample^a.

| | GJ 3236 | Castor C | CU Cnc | LP 177–102 | CM Dra |
|-----------------------------|---------------------------|---------------------------|-------------------------|---------------------------|-------------------------------|
| Karmn | J03372+691 | J07346+318 | J08316+193S | J15474+451 | J16343+571 |
| $M_1 [M_\odot]$ | 0.376 ± 0.017 | 0.5992 ± 0.0047 | 0.4349 ± 0.0012 | 0.2576 ± 0.0085 | 0.23102 ± 0.00089 |
| $M_2 [M_\odot]$ | 0.281 ± 0.015 | 0.5992 ± 0.0047 | 0.39922 ± 0.00089 | 0.2585 ± 0.0080 | 0.21409 ± 0.00083 |
| $R_1 [R_\odot]$ | 0.3828 ± 0.0070 | 0.6191 ± 0.0057 | 0.4323 ± 0.0055 | 0.2895 ± 0.0068 | 0.2534 ± 0.0019 |
| $R_2 [R_\odot]$ | 0.2992 ± 0.0075 | 0.6191 ± 0.0057 | 0.3916 ± 0.0094 | 0.2895 ± 0.0068 | 0.2398 ± 0.0018 |
| $P_{\text{orb}} [\text{d}]$ | 0.7712600 ± 0.0000023 | 0.8142822 ± 0.0000010 | 2.771468 ± 0.000004 | 3.5500184 ± 0.0000018 | $1.268389985 \pm 0.000000005$ |
| $a [\text{au}]$ | 0.01430 | 0.01819 | 0.03624 | 0.03654 | 0.01750 |
| Reference | Irw09, Shk10 | Joy26, Giz02, Tor22 | Del99a, Del99b, Tor10 | Moc02, Har11, Bir12 | Mor09, Tor10, Scha19 |

Notes. ^(a) Bir12: [Birkby et al. \(2012\)](#); Del99a: [Delfosse et al. \(1999b\)](#); Del99b: [Delfosse et al. \(1999a\)](#); Giz02: [Gizis et al. \(2002\)](#); Har11: [Hartman et al. \(2011\)](#); Irw09: [Irwin et al. \(2009\)](#); Joy26: [Joy & Sanford \(1926\)](#); Moc02: [Mochnicki et al. \(2002\)](#); Mor09: [Morales et al. \(2009\)](#); Scha19: [Schanche et al. \(2019\)](#); Shk10: [Shkolnik et al. \(2010\)](#); Tor10: [Torres et al. \(2010\)](#); Tor22: [Torres et al. \(2022\)](#).

Table A.6: Description of the online table.

| Parameter | Units | Column(s) | Description |
|--|-----------------------|-----------|--|
| <i>Identification</i> | | | |
| ID_star, ID_system | ... | 1, 2 | Star and system identifiers ^a |
| Name | ... | 3 | Discovery name or most common name ^b |
| GJ | ... | 4 | Gliese-Jahreiss catalogue number ^c |
| Karmn | ... | 5 | Carmencita star identifier (JHHMMm+DDd) ^d |
| RA_J2016, DE_J2016 | hms, dms | 6, 7 | Right ascension and declination in the epoch J2016.0 |
| SpT, SpTnum, SpT_ref | ... | 8–10 | Spectral type, its numerical format, and the reference ^e |
| <i>Multiplicity</i> | | | |
| Type, Class | ... | 11, 12 | Type of system and multiplicity class ^f |
| Component, System | ... | 13, 14 | Component designation and their resolution ^g |
| SB, SB_ref | ... | 15, 16 | Type of spectroscopic system and reference ^h |
| Discoverer | ... | 17 | Discoverer code ⁱ |
| Group, Group_ref | ... | 18, 19 | Stellar group (SKG, cluster or association) and reference ^j |
| Nplanet, Planet_ref | ... | 20, 21 | Number of confirmed planets and reference |
| Category | ... | 22 | Category 1–3 as described in Sect. 4.1 |
| Remarks | ... | 23 | Comments and remarks on multiplicity |
| WDS_... | ... | 24–32 | Washington double star catalogue data ^k |
| s01, s02 | au | 33, 37 | Physical separation between the components in multiple systems ^l |
| s01_ref | ... | 36 | Reference for the closest component ^m |
| rho01, rho02 | arcsec | 34, 38 | Projected angular separation ($s = \rho d$) |
| theta01, theta02 | deg | 35, 39 | Positional angle ⁿ |
| muratio, deltaPA, deltad | ... | 40–42 | μ ratio, ΔPA , Δd criteria for physical association ^o |
| <i>Stellar parameters</i> | | | |
| M_Msol, eM_Msol | M_{\odot} | 43, 44 | Stellar mass and its error |
| R_Rsol, eR_Rsol | R_{\odot} | 45, 46 | Stellar radius and its error |
| MR_ref | ... | 47 | Reference for mass and radius |
| L_Lsol, eL_Lsol, L_ref | \mathcal{L}_{\odot} | 48–50 | Luminosity, error, and reference |
| MG_mag, eMG_mag | mag | 51, 52 | Absolute magnitude in G and its error |
| Teff_K, eTeff_K, Teff_K_ref | K | 53–55 | Effective temperature and its error |
| logg, elogg | dex | 56, 57 | Surface gravity and its error (reference shared with L_Lsol) |
| Fe_H, Fe_H_ref | ... | 58, 59 | Iron abundance (metallicity) and its error |
| <i>System parameters</i> | | | |
| q | ... | 60 | Mass ratio |
| P01, eP01, P01_ref, P02, eP02 | d, a | 61–65 | Orbital periods, errors and reference |
| Ug_J, eUg_J | J | 66, 67 | Binding energy and its error |
| crit_... | Boolean | 68–75 | Criteria for unresolved companions ^p |
| Candidate | Boolean | 76 | Candidate to unresolved companion ^q |
| <i>Astrometry</i> | | | |
| _id | ... | 77–79 | Catalogue identifiers |
| ra, ra_error | deg | 80, 81 | Barycentric right ascension and its error in the epoch J2016.0 |
| dec, dec_error | deg | 82, 83 | Barycentric declination and its error in the epoch J2016.0 |
| parallax, parallax_error, parallax_ref | mas | 84–86 | Parallax, error and reference |
| pmra, pmra_error, pmdec, pmdec_error, pm_ref | mas a^{-1} | 87–91 | Proper motion in right ascension and declination, errors, and reference |
| rv, rv_error, rv_ref | $km\ s^{-1}$ | 92–94 | Radial velocity, error, and reference |
| ruwe | ... | 95 | Renormalised unit weight error from <i>Gaia</i> DR3 |
| [Statistics DR3] | ... | 96–110 | Additional statistical indicators in <i>Gaia</i> DR3 ^r |
| <i>Photometry</i> | | | |
| NN_mag, eNN_mag, Qf_MM | mag | 111–132 | Photometric magnitudes and quality flags in up to 10 passbands ^s |

Notes. ^(a) ID_star is a unique identifier that sorts the table by right ascension but prioritising that components of the same system (equal ID_system) are together and sorted by decreasing brightness.

^(b) Name of the star, Simbad-searchable, obeying the following priority (n designates a natural number): Proper name, variable in constellation (V* Vn Con; but not suspected variables, SV*), Henry Draper (HD n , with $n \leq 225300$), Gliese-Jahreiss (GJ n , only if $n < 4000$), Bonner Durchmusterung (BD $\pm n$), Luyten (LP $n-n$), Giclas (G $n-n$, only if unique Giclas designation), Luyten (LHS n), other designations in chronological order (Haro, StKM/StM, 1RXS/RXS, HIP, LSPM, PM, NLTT, GSC, TYC, MCC, R78b, I81, 2MUCD), catalog identifier (*Gaia* DR3, 2MASS, UCAC4).

^(c) Gliese-Jahreiss (GJ) designation entry, when available. This includes the first catalogue by [Gliese \(1957\)](#) and its update ([Gliese 1969](#)), the supplement by [Woolley et al. \(1970\)](#), and the succeeding editions ([Gliese & Jahreß 1979](#)).

^(d) “HHMMm \pm DDd” are the truncated equatorial coordinates. For close stars with separations less than 5 arcsec, a position of the star in the system is added as “N”, “S”, “E” or “W”.

^(e) SpTnum = 10.0 for O0.0 V, 20.0 for B0.0 V, 30.0 for A0.0 V, 40.0 for F0.0 V, 50.0 for G0.0 V, 60.0 for K0.0 V, 70.0 for M0.0 V, 70.5 for M0.5 V, 80.0 for L0. The values 0.0 and 999 are reserved for white dwarfs and stars with a luminosity class other than main sequence (V), respectively. Spectral types were rounded when necessary (e.g. M0.0 instead of M0.1, or M4.0 instead of M3.8). ‘This work’ refers to spectral type photometric estimation from absolute magnitudes as [Cifuentes et al. \(2020\)](#).

^(f) ‘Candidate’ and ‘Multiple+’ must be read as ‘new unresolved binary candidate’.

^(g) The system nomenclature follows the scheme in Fig. 11.

^(h) Definitions of SB1, SB2, ST2, ST3, and SQ are shown in Table A.4.

⁽ⁱ⁾ WDS discoverer code or literature reference.

^(j) Abbreviations follow the scheme outlined in Table 8.

^(k) id: WDS identifier (see also column Discoverer); comp: Component designations; obs1, obs2: First and last observation years; pa2: Positional angle in the most recent measurement; sep2: Separation in the most recent measurement; mag1, mag2: Magnitudes of the two components. More details can be found in the WDS website: <http://www.astro.gsu.edu/wds/>.

^(l) In systems of three or more components, s01 denotes the separation between the closest components, i.e., s01 < s02.

^(m) The reference is displayed when the value is not calculated in this work using *Gaia* data. The reference for s02 is *Gaia* in all cases. This also applies to the orbital periods.

⁽ⁿ⁾ Measured eastward from the north in the epoch 2016.0. In the programmatic computation of this parameter caution must be taken regarding the “quadrant ambiguity”, i.e., a 180-deg erroneous difference.

^(o) For triple or higher-order systems, this association refers to the primary component.

^(p) Criteria for physical association (crit_association) and statistical metrics from *Gaia* as described in Table 3 (crit_ruwe, crit_ipd_ruwe, crit_rv, crit_rv_error, crit_ipd_fmp, crit_dupl_source, crit_non_single, crit_DR3_non_single).

Orbital: Orbital model for an astrometric binary; OrbitalTargetedSearch: Orbital model for a priori known systems, with a subset containing suffix ‘Validated’; SB1: Single-lined spectroscopic binary; SB2: Double-lined spectroscopic binary; SB2C: Double-lined spectroscopic binary with circular orbit; AstroSpectroSB1: Combined astrometric and single lined spectroscopic orbital model.

^(q) It refers to unknown unresolved binaries. That is, if an unresolved companion already exists (e.g. an spectroscopic binary), the value is ‘false’ regardless of the *Gaia* metrics (Table 3).

^(r) Statistics from DR3 related to the criteria for unresolved binarity: astrometric_excess_noise, astrometric_excess_noise_sig, phot_bp_rp_excess_factor, phot_bp_n blended_transits, phot_rp_n blended_transits, phot_variable_flag, rv_chisq_pvalue, rv_amplitude_robust, rv_nb_transits, renormalised_gof, astrometric_n_obs_al, astrometric_n_good_obs_al, ipd_gof_harmonic_amplitude, duplicated_source (see Sect. 3.2).

^(s) BP, G, RP: G_{BP} , G , and G_{RP} from *Gaia* DR3 ([Gaia Collaboration et al. 2023b](#)); J, H, Ks: J , H , and Ks from 2MASS ([Skrutskie et al. 2006](#)); W1, W2, W3, W4: W1, W2, W3, and W4 from AllWISE ([Cutri et al. 2014](#)). The photometric uncertainties in the *Gaia* passbands have been calculated by us $\Delta\lambda = | -2.5 / \ln 10 \times \Delta F_\lambda / F_\lambda |$, where F_λ and ΔF_λ are the flux and its error in the λ passband, using the errors in the corresponding fluxes, and the zero points as provided by VizieR.

Table A.7: Multiple systems with components at separations larger than 10^4 au.

| Name | Karmn | Spectral type | Comp. | Discoverer ^a | s [au] | π [mas] | μ_{total} [mas a ⁻¹] | $ U_g^* $ [10 ³³ J] | SKG | SKG Ref. ^b |
|-------------------------------|------------|---------------|---------|-------------------------|-----------------|----------------|---|--------------------------------|--------------|-----------------------|
| GJ 3022 | J00169+200 | M3.5 V | A | CRC 43 | 36.96 | 29.310 ± 0.097 | 239.537 ± 0.209 | | | |
| G 131-47 B | | M3.5 V | B | Sma21 | 60679.5 | 29.139 ± 0.071 | 233.362 ± 0.318 | 4764 ± 727 | | |
| LP 404-54 | | M5.0 V | C | | | 28.873 ± 0.034 | 233.800 ± 0.048 | 1.742 ± 0.211 | | |
| V493 And A | J00341+253 | M0.0 V | A | SKF 220 | 77.91 | 20.101 ± 0.039 | 127.914 ± 0.054 | | AB Dor | Jan17 |
| V493 And B | | K7 V | B | Sma21 | 15617.5 | 19.720 ± 0.037 | 129.463 ± 0.056 | 10445 ± 567 | AB Dor | * |
| UCAC4 578-001365 | | M4.0 V | C | | | 19.672 ± 0.234 | 127.043 ± 0.353 | 20.44 ± 1.29 | AB Dor | * |
| EX Cet | | K0.5 V | A | | | 41.564 ± 0.024 | 197.856 ± 0.032 | | Ple/beta Pic | * |
| LP 648-20 ^c | J01369-067 | M3.5 V | B | CAB 3 | 14678.4 | 41.699 ± 0.045 | 200.547 ± 0.052 | 34.09 ± 5.33 | Ple/beta Pic | Alo15b |
| G 221-21 | J03454+729 | M1.5 V | A | | | 39.088 ± 0.013 | 487.290 ± 0.016 | | | |
| LP 31-200 | | M3.5 V | B | WIS 99 | 14667.0 | 39.146 ± 0.015 | 488.277 ± 0.018 | 14.70 ± 1.08 | | |
| LSPM J0401+5131 | | DC8 | A | | | 39.836 ± 0.077 | 883.245 ± 0.117 | | | |
| Ross 25 | J04011+513 | M3.5 V | B | Sma21 | 12401.7 | 39.816 ± 0.021 | 883.463 ± 0.028 | 23.97 ± 4.90 | | |
| GJ 3261 | J04056+057 | M3.5 V | A | MCT 3 | | 16.094 ± 0.103 | 47.984 ± 0.155 | | beta Pic | Gag18b |
| G3 329693-2486866670720 | | M4.0 V | B | This work | | ... | ... | | beta Pic | * |
| V1221 Tau | | M3.0 V | C | | | 15.876 ± 0.026 | 49.854 ± 0.034 | 10.56 ± 0.62 | beta Pic | Gag18b |
| LP 414-117 | J04123+162 | M4.0 V | Aab | Ben08 | | 28.240 ± 0.091 | 156.844 ± 0.155 | | | |
| LSPM J0499+1622 | | M5.5 V | B | Sma21 | 74092.6 | 28.759 ± 0.051 | 161.152 ± 0.075 | 2.339 ± 0.672 | | |
| TYC 78-257-1 | J04224+036 | K3.0 V | A | | | 26.974 ± 0.022 | 139.559 ± 0.028 | | | |
| RX J0422.4+0337 | | M3.5 V | B | Sma21 | 62796.5 | 27.846 ± 0.026 | 143.007 ± 0.039 | 9.22 ± 0.46 | | |
| HD 27848 ^d | F5 V | AB | OCC 615 | | | 19.959 ± 0.026 | 103.388 ± 0.039 | | | |
| V991 Tau | | K4 V | C | | | 18.356 ± 0.019 | 94.411 ± 0.025 | | | |
| V805 Tau | J04252+172 | M3.5 V | DE | AST 4 | | 51890.1 | 19.313 ± 0.193 | 110.653 ± 0.259 | | |
| LP 415-881 | | M7.0 V | F | | 79117.5 | 21.204 ± 0.061 | 105.698 ± 0.088 | | | |
| LP 415-345 | J04225+204 | M3.0 V | Aab | Sta97 | | 20.476 ± 0.022 | 97.452 ± 0.034 | | | |
| LP 415-3051 | | M3.0 V | B | Sma21 | 34713.1 | 19.426 ± 0.020 | 91.262 ± 0.028 | | | |
| G2 34110548488666601472 | | M6.0 V | C | Sma21 | 83728.3 | 19.484 ± 0.118 | 93.825 ± 0.180 | | | |
| PM J05334+4809 | | M0.0 V | A | | | 30.270 ± 0.018 | 66.932 ± 0.022 | | | |
| PM J05341+4732 A | J05341+475 | M2.5 V | B | EB21 | 75945.4 | 30.050 ± 0.027 | 69.013 ± 0.033 | 6.96 ± 0.52 | | |
| PM J05341+4732 B ^e | | M3.0 V | C | EB21 | 75899.1 | 30.039 ± 0.023 | 61.853 ± 0.028 | 5.20 ± 0.52 | | |
| UPM J0533+4809 | | M3.5 V | D | Sma21 | 4219.5 | 30.229 ± 0.235 | 65.011 ± 0.311 | | | |
| 1RXS J073138.4+4557.8 | | M3.0 V | Aab | Fou18 | | 17.880 ± 0.416 | 93.776 ± 0.481 | | | |
| 1RXS J073101.9+4600.30 | J07310+460 | M4.0 V | B | Cir21 | 23780.3 | 18.141 ± 0.052 | 101.748 ± 0.059 | | | |
| G3 975312928903090560 | | M4.5 V | C | Sma21 | 16738.6 | 18.388 ± 0.034 | 100.736 ± 0.042 | | | |
| V869 Mon | | K3 V | A | | | 71.032 ± 0.024 | 286.810 ± 0.030 | | | |
| HD 61606 B | | K7 V | B | BGH 3 | 815.63 | 70.992 ± 0.025 | 294.206 ± 0.031 | 1090 ± 231 | | UMa |
| GJ 282 C | J07361-031 | M1.0 V | Cab | Pov09 | 6.2 273662.8018 | 70.275 ± 0.131 | 302.347 ± 0.173 | 3.766 ± 0.638 | | Tab17 |
| PM J13255+2738 | | M1.0 V | A | Sma21 | 18493.6 | 21.886 ± 0.070 | 72.891 ± 0.109 | 26.54 ± 2.08 | | |
| PM J13260+2735 A | J13260+275 | M3.0 V | B | | 18343.6 | 22.030 ± 0.057 | 63.569 ± 0.092 | 21.74 ± 2.06 | | |
| PM J13260+2735 B | | M2.5 V | C | KPP 3896 | | | | | | |

Table A.7: Multiple systems with components at separations larger than 10^4 au. (cont.)

| Name | Karmn | Spectral type | Comp. | Discoverer ^a | s [au] | π [mas] | μ_{total} [mas a ⁻¹] | $ U_g^* $ [10 ³³ J] | SKG | SKG Ref. ^b |
|------------------------|-------------|---------------|-------|-------------------------|----------------|-----------------|---|--------------------------------|----------|-----------------------|
| HD 140232 | | A8 V | A | DRS 17 | 126.52 | 18.719 ± 0.041 | 82.169 ± 0.044 | | | |
| G3 1197801408884577408 | J1541.6+184 | M3.5 V | B | TOK 302 | 12869.9 | 18.642 ± 0.113 | 82.285 ± 0.167 | 8053 ± 1482 | | |
| SIKM 1-1264 | | MI1.5 V | C | | | 19.367 ± 0.139 | 91.885 ± 0.173 | 165.8 ± 25.7 | | |
| σ CrB A | | F6 V | Aab | Stu03, Rag09 | 0.01 | 44.057 ± 0.046 | 282.061 ± 0.072 | | | |
| σ CrB B | | G1 V | B | STF 2032 | 163.85 | 44.134 ± 0.018 | 301.273 ± 0.026 | 2567 ± 385 | | |
| σ CrB C | J161.39+337 | M2.5 V | CD | STF 2032 | 11.51435.9663 | 44.267 ± 0.159 | 300.693 ± 0.241 | 12.28 ± 0.88 | | |
| HD 160269 A | | G0 IV/V | AB | BU 962 | 9.02 | 69.283 ± 0.200 | 522.563 ± 0.334 | | | |
| GJ 685 | J17355+616 | M0.5 V | C | LDS 2736 | 10561.5 | 69.892 ± 0.015 | 577.333 ± 0.023 | | | |
| HD 230017 A | | M0.0 V | A | VYS 8 | 70.68 | 53.423 ± 0.108 | 133.273 ± 0.161 | | | |
| HD 230017 B | J18548+109 | M3.5 V | B | This work | 10009.5 | 53.644 ± 0.043 | 89.289 ± 0.063 | 6625 ± 637 | Car | Gag18b |
| PM J18542+1058 | | M4.0 V | C | | | 53.838 ± 0.024 | 114.612 ± 0.034 | 38.59 ± 2.21 | Car | This work |
| AU Mic | J20451-313 | M0.5 V | A | LDS 720 | 45473.4 | 102.943 ± 0.023 | 456.998 ± 0.029 | | | |
| AT Mic A | J20418-224 | M4.5 V | B | LDS 720 | 20.62 | 100.792 ± 0.073 | 484.794 ± 0.094 | | | |
| AT Mic B | | M4.5 V | C | | | 101.972 ± 0.077 | 423.100 ± 0.097 | 14879 ± 1575 | beta Pic | Cab09 |
| Wolf 1548 | J22058-119 | M0.0 V | A | WNO 57 | 59342.7 | 38.616 ± 0.533 | 319.261 ± 1.369 | | | |
| LP 759-25 | | M6.0 V | B | | | 51.070 ± 0.054 | 322.495 ± 0.074 | 2.615 ± 0.227 | beta Pic | Ell14 |
| G 29-19 | J23175+063 | M3.0 V | A | | | 48.918 ± 0.027 | 302.148 ± 0.042 | | | |
| G 28-50 | J23161+067 | M3.5 V | B | Sma21 | 36823.1 | 48.976 ± 0.026 | 304.894 ± 0.037 | 6.48 ± 0.38 | | |
| V368 Cep | | G9 V | A | LDS 2035 | 206.38 | 52.784 ± 0.014 | 215.918 ± 0.022 | | | |
| HD 220140 B | J23194+790 | M3.5 V | B | MKR 1 | 18221.8 | 52.840 ± 0.021 | 218.080 ± 0.036 | 3291 ± 548 | Col | Gag18b |
| LP 12-90 | J23228+787 | M5.0 V | C | | | 52.834 ± 0.030 | 217.441 ± 0.051 | 18.03 ± 2.89 | Col | * |
| AF Psc | J23317-027 | M4.5 V | A | CAB24 | 66833.9 | 28.631 ± 0.035 | 118.451 ± 0.051 | | | |
| 2M J23301.129-0237227 | J23301-026 | M6.0 V | B | | | 21.982 ± 0.070 | 122.009 ± 0.110 | | | |
| HD 221503 | | K7 V | A | | | 68.736 ± 0.027 | 405.450 ± 0.036 | | | |
| GJ 1284 | J23302-203 | M3.0 V | Bab | Giz02, SHY 110 | 6.5206051.1082 | 62.868 ± 0.076 | 375.234 ± 0.092 | | | |
| GJ 897 ^f | J23327-167 | M2.0 V | C | LDS 816 | 21894.8 | 64.8 ± 4.1 | 413.04 ± 3.75 | | | |
| G3 2395220664463236992 | | M3.0 V | D | VOU 28 | ... | ... | ... | | | |

Notes. ^(a) References for discovery – Ben08: Bender & Simon (2008); EB21: El-Badry et al. (2021); Fou18: Fouqué et al. (2018); Giz02: Gizis et al. (2002); Gri85: Griffin et al. (1985); Pow09: Poveda et al. (2009); Rag09: Raghavan et al. (2009); Sma21: Gaia Collaboration et al. (2021b); Sta97: Stauffer et al. (1997); Sri03: Strassmeier & Rice (2003); ^(b) References for first designation – Alo15b: Alonso-Floriano et al. (2015a); Cab09: Caballero (2009); Cab10a: Caballero (2010); Cab10c: Caballero (2014); Gag18b: Gagné & Faherty (2018); Jan17: Janson et al. (2017); Kral4b: Kraus et al. (2014b); Lod19: Lodieu et al. (2019); Ros11: Röser et al. (2011); Tab17: Tabernero et al. (2017). The star symbol (*) means the same SKG assignment as its physical companion, therefore sharing bibliographic reference. The list of abbreviations for the SKG can be found in Sect. 4.5. ^(c) LP 648–20: The ~L0 companion reported by Bergfors et al. (2010) based on lucky imaging at 5.587 arcsec is a background star ($\pi = 1.63$ mas). ^(d) HD 27848: System dissected by Benedict et al. (2021). Bona fide single star according to Brandner et al. (2023). ^(e) PM J05341+4732 B: Absent in the WDS but see Ansdel et al. (2015) ($\rho = 2.33$ arcsec). ^(f) GJ 897: Parallax and proper motions from Hipparcos (van Leeuwen 2007).

Table A.8: Multiple systems containing M dwarfs and FGK primaries.

| Name | Kamrn type | Spectral Component | Discoverer ^a | π [mas] | μ_{total} [mas a ⁻¹] | [Fe/H] [dex] | ρ [arcsec] | θ [deg] |
|------------------------|---------------|-----------------------|-------------------------|-----------------|--|------------------|--------------------|-------------------|
| HD 4967 | K5 V | A | LDS 1082 | 65.090 ± 0.025 | 672.691 ± 0.047 | -0.33 | Hou16 | 17.07 |
| HD 4967 B | M5.5 V | B | | 65.073 ± 0.050 | 680.566 ± 0.095 | ... | | 72.1 |
| EX Cet | K0.5 V | A | CAB 3 | 41.564 ± 0.024 | 197.856 ± 0.032 | -0.06 | Zak22 | 612.08 |
| LP 648-20 | M3.5 V | B | | 41.699 ± 0.045 | 200.547 ± 0.052 | ... | | 258.6 |
| Wolf 109 | K5 V | A | | 27.827 ± 0.021 | 466.135 ± 0.031 | ... | | |
| Wolf 109 B | M2.0 V | B | OSV 1 | 28.922 ± 0.353 | 465.771 ± 0.482 | ... | | 14.4 |
| G3 2517912315149114240 | M5.0 V | C | | ... | ... | | | 16.8 |
| HD 15468 | K4.5 V | AB | RST 2280 | 51.606 ± 0.136 | 646.402 ± 0.166 | -0.31 | Mon18 | 0.18 |
| GJ 100 C | M2.5 V | C | UC 744 | 50.972 ± 0.032 | 649.191 ± 0.038 | 0.14 | Kuz19 | 474.57 |
| HD 16160 | K3 V | AB | GK11 | 138.340 ± 0.318 | 2312.099 ± 0.496 | -0.09 | Tin19 | 1.73 |
| BX Cet | M4.0 V | C | PLQ 32 | 138.437 ± 0.042 | 2312.992 ± 0.057 | -0.24 | Mart21 | 164.25 |
| HD 16895 | F8 V | A | | 89.685 ± 0.164 | 346.403 ± 0.244 | 0.04 | Mon18 | 318.4 |
| GJ 107 B | J02441+492 | M1.5 V | B | STF 296 | 89.374 ± 0.032 | 322.947 ± 0.042 | ... | 20.93 |
| HD 18143 A | K2 IV | A | | 44.432 ± 0.021 | 327.700 ± 0.032 | 0.17 | Ros21 | 305.1 |
| HD 18143 B | K7 V | B | STF 326 | 44.505 ± 0.025 | 327.976 ± 0.042 | 0.14 | Gai14b | 4.78 |
| HD 18143 C | M4.0 V | C | LDS 883 | 44.522 ± 0.023 | 328.058 ± 0.035 | ... | | 221.3 |
| HD 18757 | G1.5 V | A | | 42.459 ± 0.020 | 1000.787 ± 0.023 | -0.23 | Hir21 | 43.79 |
| GJ 3195 | J03047+617 | M3.0 V | B | LDS 9142 | 42.534 ± 0.026 | 1000.094 ± 0.033 | ... | 266.3 |
| V577 Per | K2 V | A | | 27.482 ± 0.031 | 188.424 ± 0.039 | -0.09 | Mon18 | 65.8 |
| HD 21845 B | J03332+462 | M0.0 V | B | ES 560 | 27.481 ± 0.016 | 185.831 ± 0.021 | ... | 9.50 |
| HD 278874 | K2 V | A ^{ab} | | Mon18 | 25.434 ± 0.032 | 36.209 ± 0.044 | ... | 142.3 |
| HD 278874 B | J03397+334 | M3.0 V | B | ES 327 | 25.571 ± 0.041 | 38.831 ± 0.061 | ... | |
| HD 23189 | K2 V | A | KUI 13 | 55.825 ± 0.013 | 279.831 ± 0.016 | -0.43 | Hou16 | 13.20 |
| GJ 153 C | ML1.5 V | BC | KUI 13 | 55.984 ± 0.105 | 288.831 ± 0.215 | ... | | 17.2 |
| HD 275867 | K2 V | A | | 30.985 ± 0.016 | 62.067 ± 0.023 | -0.13 | Mon18 | |
| TYC 2868-639-1 | J03519+397 | M0.0 V | B | GRV 197 | 31.021 ± 0.020 | 64.399 ± 0.026 | ... | 53.92 |
| HD 24916 | K4 V | A | | 65.426 ± 0.023 | 234.331 ± 0.031 | 0.09 | Ros21 | 207.5 |
| HD 24916 B | M2.5 V | Bab | Zak79 / BU 543 | 65.492 ± 0.044 | 251.747 ± 0.057 | 0.01 | Kuz19 | 14.13 |
| ^{o2} Eri B | DA2.9 | A | | 199.691 ± 0.051 | 4018.591 ± 0.061 | | | |
| ^{o2} Eri | K0 V | B | STF 518 | 199.608 ± 0.121 | 4089.836 ± 0.165 | -0.20 | Ros21 | 83.34 |
| ^{o2} Eri C | M4.5 V | C | STF 518 | 199.452 ± 0.069 | 4083.715 ± 0.084 | -0.30 | Mart21 | 78.10 |
| TYC 78-257-1 | ~K3.0 V | A | Sma21 | 26.974 ± 0.022 | 139.559 ± 0.028 | -0.06 | Boc18 | 97.5 |
| RX J0422.4+0337 | J04224+036 | M3.5 V | | 27.846 ± 0.026 | 143.007 ± 0.039 | 0.39 | Ter15a | 1748.61 |
| HD 27848 | F5 V | AB | OCC 615 | 19.939 ± 0.026 | 103.388 ± 0.039 | -0.11 | Bud21 | 43.9 |
| V991 Tau | K4 V | C | | 18.356 ± 0.019 | 94.411 ± 0.025 | 0.19 | Bud21 | 641.17 |
| V805 Tau | M3.5 V | DE | AST 4 | 19.313 ± 0.193 | 110.655 ± 0.259 | ... | | 121.9 |
| LP 415-881 | M7.0 V | F | | 21.204 ± 0.061 | 105.698 ± 0.088 | ... | | 47.1 |
| | | | | | | | | 1677.61 |
| | | | | | | | | 93.4 |

Table A.8: Multiple systems containing M dwarfs and FGK primaries (cont.).

| Name | Karmn | Spectral type | Component | Discoverer ^a | π [mas] | μ_{total} [mas a^{-1}] | [Fe/H] [dex] | [Fe/H] Ref. ^b | ρ [arcsec] | θ [deg] |
|-----------------------|------------|-----------------|-----------|-------------------------|-----------------|---|--------------|--------------------------|-----------------|----------------|
| V583 Aur | J04393+335 | K5 V | A | JNN 263 | 11.128 ± 0.018 | 52.345 ± 0.027 | ... | ... | Ter15a | 207.05 |
| PM J04393+3331 | M4.0 V | BC | | EGN 4 | 7.425 ± 0.848 | 50.282 ± 1.831 | 0.10 | ... | Ros21 | 0.44 |
| HD 31412 | F9.5 V | AB | | LDS 9181 | 27.865 ± 0.027 | 233.457 ± 0.035 | 0.04 | ... | ... | 17.7 |
| HD 31412 B | M2.0 V | C | | | 27.851 ± 0.026 | 233.996 ± 0.034 | ... | ... | ... | 21.66 |
| Capella | G3 III | A _{ab} | | She85 / Tor09 | 76.200 ± 0.460 | 433.472 ± 0.608 | -0.37 | Mas08 | 722.84 | 141.8 |
| Capella H | M2.5 V | B | | FRH | 74.932 ± 0.019 | 437.931 ± 0.026 | ... | ... | 346 | 173.5 |
| Capella L | M4.0 V | C | | ST 3 | 75.184 ± 0.053 | 420.381 ± 0.077 | ... | ... | ... | |
| HD 35956 | G0 V | A _{ab} | | Kat13 | 33.788 ± 0.294 | 231.784 ± 0.417 | 0.28 | Ric20 | 5.83 | 71.4 |
| HD 35956 B | M1.0 V | B | | TOK 94 | 35.405 ± 0.020 | 237.813 ± 0.029 | ... | ... | 99.39 | 134.1 |
| G 102-4 A | M4.0 V | C | | LDS 6186 | 39.500 ± 10.200 | 230.586 ± 11.314 | ... | ... | 99.46 | 134.2 |
| G 102-4 B | M4.0 V | D | | RAO 552 | ... | ... | ... | ... | ... | |
| V538 Aur | K1 V | A | | ENG 22 | 81.499 ± 0.025 | 523.485 ± 0.032 | 0.16 | Ros21 | ... | |
| HD 233153 | M1.0 V | B | | | 81.464 ± 0.023 | 515.975 ± 0.027 | -0.02 | Mart21 | 98.03 | 71.2 |
| HD 43587 | G0 V | AB | | CAT 1 | 51.616 ± 0.124 | 269.293 ± 0.196 | -0.03 | Mon18 | 0.84 | 70.9 |
| GJ 231.1 B | M3.5 V | CD | | PRV 3 | 52.139 ± 0.083 | 261.646 ± 0.107 | 0.06 | Kuz19 | 307.40 | 103.2 |
| HD 263175 | K3 V | A | | LDS 6201 | 38.828 ± 0.022 | 467.065 ± 0.027 | -0.24 | Hir21 | ... | |
| HD 263175 B | M1.0 V | B | | | 38.873 ± 0.017 | 472.874 ± 0.025 | ... | ... | 30.85 | 100.1 |
| HD 50281 | K3.5 V | A | | | 114.355 ± 0.042 | 543.702 ± 0.039 | 0.02 | Ros21 | ... | |
| HD 50281 B | M2.0 V | B | | WNO 17 | 114.291 ± 0.022 | 576.479 ± 0.031 | 0.10 | Ros21 | 58.83 | 180.6 |
| GJ 3415 | K4.5 V | A | | | 39.870 ± 0.023 | 452.029 ± 0.026 | ... | ... | ... | |
| GJ 3416 | M0.5 V | B | | KUI 27 | 39.925 ± 0.021 | 446.754 ± 0.026 | -0.21 | Gai14b | 37.81 | 6.8 |
| V869 Mon | K3 V | A | | | 71.032 ± 0.024 | 286.810 ± 0.030 | 0.03 | Ros21 | ... | |
| HD 61606 B | K7 V | B | | BGH 3 | 70.992 ± 0.025 | 294.206 ± 0.031 | -0.11 | Mon18 | 57.90 | 112.7 |
| GJ 282 C | M1.0 V | Cab | | Pov09 | 70.275 ± 0.131 | 302.347 ± 0.173 | -0.04 | Mart21 | 296.71 | 3894.2 |
| HD 68146 | F6.5 V | A | | LDS 204 | 44.340 ± 0.053 | 257.608 ± 0.057 | 0.04 | Luc18 | 96.93 | 236.2 |
| L 818-40 A | M2.5 V | B | | JOD 4 | 44.520 ± 0.049 | 259.911 ± 0.058 | ... | ... | 97.54 | 236.6 |
| L 818-40 B | M4.0 V | C | | | 44.150 ± 0.203 | 245.493 ± 0.316 | ... | ... | ... | |
| ρ^0 Cnc | K0 IV-V | A | | | 79.448 ± 0.043 | 538.903 ± 0.055 | 0.38 | Ros21 | ... | |
| ρ^0 Cnc B | M4.5 V | B | | LDS 6219 | 79.656 ± 0.047 | 539.752 ± 0.053 | -0.10 | Mart21 | 84.83 | 128.1 |
| V405 Hyi | K2 V | A | | | 36.512 ± 0.022 | 112.027 ± 0.026 | 0.07 | Luc18 | ... | |
| 1RXS J090406.8-155512 | J09040-159 | M2.5 V | B | Sma21 | 36.628 ± 0.021 | 113.771 ± 0.025 | ... | ... | 220.02 | 82.9 |
| BD+22 2086 A | K5 V | A | | | 29.405 ± 0.020 | 218.392 ± 0.025 | ... | ... | ... | |
| BD+22 2086 B | M0.0 V | B | | HDS 1348 | 29.444 ± 0.022 | 223.161 ± 0.024 | -0.10 | Gai14b | 8.30 | 343.4 |
| DX Leo | G9 V | A | | | 55.329 ± 0.021 | 287.217 ± 0.025 | 0.07 | Hir21 | ... | |
| HD 82443 B | M5.5 V | B | | LDS 3903 | 55.292 ± 0.071 | 284.171 ± 0.086 | ... | ... | 65.56 | 64.4 |
| HD 82939 | G5 V | A | | | 25.740 ± 0.023 | 134.640 ± 0.024 | -0.08 | Boc18 | ... | |
| GJ 9303 | M0.0 V | Bab | | Mal14a / SKF 254 | 25.836 ± 0.023 | 134.335 ± 0.025 | -0.06 | Jon20 | 301.52 | 162.3 |
| GJ 397.1 | K5 V | A | | LDS 2314 | 57.010 ± 0.014 | 185.374 ± 0.018 | ... | ... | 141.96 | 225.6 |

Table A.8: Multiple systems containing M dwarfs and FGK primaries (cont.).

| Name | Karmn | Spectral type | Component | Discoverer ^a | π [mas] | μ_{total} [mas a^{-1}] | [Fe/H] [dex] | [Fe/H] Ref. ^b | ρ [arcsec] | θ [deg] |
|------------------------|-------------|-----------------|---------------|-------------------------|----------------------|---|--------------|--------------------------|-----------------|----------------|
| GJ 397.1 B | J10315+570 | M4.5 V | BC | RAO 252 | ... | 161.307 \pm 11.314 | -0.01 | Ter15a | 225.59 | 142.0 |
| LZ UMa | G5 V | A | | | 37.386 \pm 0.070 | 196.647 \pm 0.166 | -0.11 | Mon18 | | |
| GJ 3628 | M3.5 V | B | LDS 3019 | | 37.889 \pm 0.028 | 191.404 \pm 0.033 | 0.04 | Ter15a | 178.25 | 186.2 |
| HD 97584 | J10506+517 | K4 V | A | STF 1516 | 69.136 \pm 0.015 | 418.802 \pm 0.024 | -0.17 | Ston20 | | 102.9 |
| HD 97584 B | J111151+734 | M2.5 V | B | Ab76 | 69.134 \pm 0.018 | 396.508 \pm 0.029 | 0.09 | Gai14b | 67.60 | 327.1 |
| GJ 426.1 A | F1 IV | A _{ab} | | | 42.355 \pm 0.398 | 169.810 \pm 0.990 | ... | | | |
| GJ 426.1 B | F5 V | B | STF 1536 | | 41.496 \pm 0.351 | 185.015 \pm 0.974 | ... | | | |
| LSPM J1123+1037 | J11238+106 | M0.5 V | C | STF 1536 | 41.667 \pm 0.274 | 173.499 \pm 0.303 | ... | | | |
| HD 108421 A | K2 V | A | STF 1643 | | 36.504 \pm 0.027 | 265.137 \pm 0.030 | ... | | | |
| HD 108421 B | K4 V | B | LEP 54 | | 36.511 \pm 0.031 | 256.189 \pm 0.037 | ... | | | |
| CX Com | M4.5 V | C | | | 37.636 \pm 0.283 | 265.949 \pm 0.045 | 0.00 | Raj18a | 221.40 | 260.9 |
| HD 115404 | K2 V | A | | | 91.018 \pm 0.024 | 689.139 \pm 0.042 | -0.11 | Ros21 | | |
| HD 115404 B | M0.5 V | B | BU 800 | | 90.948 \pm 0.023 | 701.233 \pm 0.040 | -0.28 | Jon20 | 7.67 | 104.6 |
| GJ 9453 | K5 V | A | | | 25.386 \pm 0.026 | 439.091 \pm 0.046 | ... | | | |
| GJ 9453 B | M3.5 V | B | LDS 1775 | | 25.492 \pm 0.015 | 437.055 \pm 0.026 | ... | | | |
| BD+21 2602 | K4 V | A | | | 24.815 \pm 0.015 | 127.647 \pm 0.019 | ... | | | |
| SKM 1-119 | M1.0 V | B | J 1128 | | ... | 132.085 \pm 3.759 | -0.20 | Gai14b | 62.66 | 190.2 |
| G3 1247168140942467200 | M1.5 V | C | J 1128 | | ... | ... | ... | | 62.31 | 190.3 |
| HD 126660 | F7 V | A | STT 580 | | 69.069 \pm 0.158 | 464.153 \pm 0.232 | 0.03 | Luc17 | | |
| HD 126660 B | M2.5 V | B | | | 68.812 \pm 0.032 | 469.652 \pm 0.047 | -0.14 | Mart21 | 70.16 | 182.5 |
| KX Lib | K4 V | A | | | 169.884 \pm 0.065 | 2008.680 \pm 0.087 | -0.12 | Mon18 | | |
| HD 131976 | M1.5 V | BC | Mar87 / HN 28 | | 168.770 \pm 21.540 | 1933.943 \pm 26.196 | 0.08 | Mal20 | 306.60 | 25.8 |
| GI 570 D | T8 | D | BUG 4 | | 169.300 \pm 1.700 | 1972.880 \pm 5.620 | 0.09 | Bur13 | 234.00 | 317.0 |
| HD 135363 | G5 V | AB | MET 10 | | 33.711 \pm 0.052 | 208.703 \pm 0.102 | -0.07 | Gu19 | 0.36 | 133.1 |
| LSPM J1507+7613 | M4.5 V | C | LEP 72 | | 33.714 \pm 0.027 | 207.105 \pm 0.058 | ... | | 116.45 | 1.7 |
| HD 144579 | J14574-214 | M1.5 V | | | 169.300 \pm 1.700 | | | | | |
| HD 144579 B | T8 | D | | | | | | | | |
| σ CrB A | K3 V | A | | | 69.641 \pm 0.014 | 573.293 \pm 0.023 | -0.53 | Ros21 | | |
| σ CrB B | F6 V | A _{ab} | Str03 / Rag09 | | 44.057 \pm 0.046 | 282.061 \pm 0.072 | -0.01 | Luc17 | | |
| σ CrB C | G1 V | B | STF 2032 | | 44.134 \pm 0.018 | 301.273 \pm 0.026 | -0.02 | Ros21 | 7.23 | 238.5 |
| V1090 Her | J16048+391 | M4.0 V | B | WNO 47 | 69.637 \pm 0.019 | 564.436 \pm 0.030 | -0.62 | Ter15a | 70.00 | 280.1 |
| HD 153557 B | F6 V | A _{ab} | Str03 / Rag09 | | 44.057 \pm 0.046 | 282.061 \pm 0.072 | -0.01 | Luc17 | | |
| V1089 Her | K3 V | C | STFA 32 | | 55.718 \pm 0.016 | 296.941 \pm 0.028 | -0.03 | Ros21 | 112.38 | 261.6 |
| HD 154363 | K4.5 V | A | | | 55.751 \pm 0.016 | 308.703 \pm 0.031 | 0.01 | Ros21 | | |
| HD 154363 B | M1.5 V | B | LDS 585 | | 55.771 \pm 0.017 | 301.441 \pm 0.033 | -0.43 | Mart21 | 184.42 | 122.7 |
| HD 160269 A | G0 IV/V | AB | BU 962 | | 69.283 \pm 0.200 | 522.563 \pm 0.324 | -0.04 | Tau20 | 0.63 | 300.5 |
| GJ 685 | M0.5 V | C | LDS 2736 | | 69.892 \pm 0.015 | 577.333 \pm 0.023 | -0.03 | Mart21 | 738.16 | 160.3 |
| HD 161797 | G5 IV | AB | TRN 2 | | 119.925 \pm 0.154 | 833.789 \pm 0.217 | 0.32 | Ros21 | 1.78 | 254.8 |

Table A.8: Multiple systems containing M dwarfs and FGK primaries (cont.).

| Name | Karmn | Spectral type | Component | Discoverer ^a | π [mas] | μ_{total} [mas a^{-1}] | [Fe/H] [dex] | [Fe/H] Ref. ^b | ρ [arcsec] | θ [deg] |
|-----------------|------------|---------------|-----------|-------------------------|---------------------|--|-----------------|-----------------------------|--------------------|-------------------|
| GJ 695 B | J17464+277 | M2.5 V | C | STF 2220 | 119.887 \pm 0.206 | 899.446 \pm 0.279 | 35.36 | 248.9 | | |
| GJ 695 C | | M3.5 V | D | AC 7 | 120.398 \pm 0.279 | 719.401 \pm 0.489 | 0.58 | 335.9 | | |
| BD+31 3330 | | K2.5 V | A | HJ 1337 | 41.745 \pm 0.016 | 841.174 \pm 0.024 | -0.31 | Hir21 | | |
| BD+31 3330 B | J18409+315 | M1.0 V | B | | ... | ... | ... | | | |
| BD+31 3330 C | | M1.0 V | C | | ... | ... | ... | | | |
| HD 187691 | J19510+104 | F8 V | A | J 124 | 51.313 \pm 0.090 | 277.688 \pm 0.108 | 0.15 | Hir21 | | |
| GJ 9671 B | | M3.5 V | B | LDS 6339 | 51.373 \pm 0.040 | 288.376 \pm 0.052 | ... | | 21.48 | 220.2 |
| HD 190360 | J20034+298 | G7 IV-V | A | | 62.487 \pm 0.035 | 861.921 \pm 0.045 | 0.23 | Ros21 | | |
| GJ 777 B | | M4.5 V | B | | 62.527 \pm 0.022 | 860.495 \pm 0.030 | | | 178.05 | 232.3 |
| HD 191785 | | K0 V | A | | 48.926 \pm 0.023 | 575.386 \pm 0.025 | -0.04 | Ros21 | | |
| GJ 783.2 B | J20112+161 | M4.0 V | B | GIC 163 | 48.928 \pm 0.032 | 577.775 \pm 0.038 | -0.04 | Kuz19 | 103.84 | 94.8 |
| StKM 1-1767a | J20132+029 | K5 V | A | | 27.359 \pm 0.018 | 108.284 \pm 0.023 | ... | | | |
| [R78b] 440 | | M1.0 V | B | CRI 26 | 27.359 \pm 0.023 | 110.727 \pm 0.029 | 0.36 | Gai14b | 32.50 | 123.9 |
| HD 197076 | J20407+199 | G5 V | A | LDS 1045 | 47.746 \pm 0.020 | 334.027 \pm 0.023 | -0.07 | Ros21 | | |
| GJ 797 B | | M2.5 V | BC | RAO 23 | ... | 339.095 \pm 1.980 | -0.07 | Pas18 | 184.06 | 125.1 |
| GJ 9728 B | J21147+380 | G5 V | AB | AGC 13 | 49.576 \pm 0.463 | 472.404 \pm 1.069 | ... | | | |
| GJ 822.1 C | | M2.5 V | CD | AGC 13 | 49.105 \pm 0.042 | 453.205 \pm 0.059 | -0.08 | Gai14b | 184.45 | 89.9 |
| V447 Lac | J22160+546 | K1 V | A | | 45.591 \pm 0.017 | 223.871 \pm 0.023 | 0.09 | Hir21 | | |
| GJ 4269 | | M4.0 V | B | GIC 177 | 45.625 \pm 0.020 | 221.350 \pm 0.032 | -0.04 | Man15 | 76.90 | 107.4 |
| HD 216385 | J22524+099 | F6 V | A | LDS 6388 | 36.558 \pm 0.108 | 523.347 \pm 0.197 | -0.11 | Ste20 | 249.64 | 19.6 |
| GJ 9801 B | | M3.0 V | BC | RAO 30 | 37.250 \pm 0.760 | 530.182 \pm 11.314 | ... | | 250.25 | 19.6 |
| V368 Cep | J23194+790 | G9 V | A | | 52.784 \pm 0.014 | 215.918 \pm 0.022 | -0.03 | Man15 | | |
| HD 220140 B | J23228+787 | M3.5 V | B | LDS 2035 | 52.840 \pm 0.021 | 218.080 \pm 0.036 | ... | | 10.91 | 214.1 |
| LP 12-90 | | M5.0 V | C | MKR 1 | 52.834 \pm 0.030 | 217.441 \pm 0.051 | ... | | 962.74 | 141.1 |
| StKM 2-1787 | J23535+121 | K4 V | A | | 26.840 \pm 0.020 | 120.688 \pm 0.026 | -0.49 | Mon18 | | |
| PM J23535+1206S | | M2.5 V | B | VYS 11 | 26.792 \pm 0.035 | 119.437 \pm 0.045 | -0.06 | Gai14b | 5.78 | 165.1 |

Notes. ^(a) References for discovery – Kat13: Katoh et al. (2013); Mal14a: Malo et al. (2014a); Mar87: Marcy et al. (1987); Pov09: Poveda et al. (2009); Rag09: Raghavan et al. (2009); Ros21: Rosenthal et al. (2021); She85: Shen et al. (1985); Sma21: Gaia Collaboration et al. (2021b); Str03: Strassmeier & Rice (2003); Tor09: Torres et al. (2009); Zak79: Zakhzhaj (1979). ^(b) References for metallicities – Boc18: Bochanski et al. (2018); Bud21: Buder et al. (2021); Burl13: Birmingham et al. (2013); Gai14b: Gaidos et al. (2014); Gui09: Guillout et al. (2009); Hir21: Hirsch et al. (2021); Hou16: Houdebine et al. (2016); Jon20: Jönsson et al. (2020); Kuz19: Kuznetsov et al. (2019); Luc17: Luck (2017); Luc18: Luck (2018); Man15: Mann et al. (2015); Mal20: Maldonado et al. (2020); Man15: Mann et al. (2015); Mart21: Marfil et al. (2021); Mas08: Massarotti et al. (2008); Mon18: Montes et al. (2018); Pas18: Paszegi et al. (2018); Raj18a: Rajpurohit et al. (2018); Ric20: Rice & Brewer (2020); Ros21: Rosenthal et al. (2021); Sie120: Steinmetz et al. (2020); Ston20: Stöckl et al. (2020); Tautvaišiene et al. (2020); Ter15a: Terrien et al. (2015a); Tin19: Ting et al. (2019); Zak22: Zakhzhaj et al. (2022).

Table A.9: Multiple systems containing M dwarfs and white dwarfs.

| Name | Karmn | Spectral type ^a | Discoverer ^b | π [mas] | μ_{total} [mas a ⁻¹] | ρ^c [arcsec] | θ [deg] |
|---|-------------|----------------------------|-------------------------|-----------------|--|----------------------|-------------------|
| GJ 1015 B | | DBQ5 | | 43.659 ± 0.022 | 324.163 ± 0.025 | | |
| GJ 1015 A | J00413+558 | M4.0 V | GIC 13 | 43.735 ± 0.022 | 332.499 ± 0.024 | 10.854 | 248.4 |
| GJ 3118 | | DA5.6 | | 57.799 ± 0.016 | 301.944 ± 0.018 | | |
| GJ 3117 | J01518+644 | M2.5 V | GIC 27 | 57.825 ± 0.016 | 306.369 ± 0.018 | 13.503 | 0.7 |
| GJ 3151 ^d | J02204+377 | M2.5 V + DA | LDS 3370 | 40.867 ± 0.033 | 349.298 ± 0.050 | 2.0 | 89.0 |
| LSPM J0401+5131 | | DC8 | | 39.836 ± 0.077 | 883.245 ± 0.117 | | |
| Ross 25 | J040111+513 | M3.5 V | Sma21 | 39.816 ± 0.021 | 883.463 ± 0.028 | 494.0 | 173.4 |
| o ⁰² Eri B | | DA2.9 | | 199.691 ± 0.051 | 4018.591 ± 0.061 | | |
| o ⁰² Eri | | K0 V | STF 518 | 199.608 ± 0.121 | 4089.836 ± 0.165 | 83.337 | 282.2 |
| o ⁰² Eri C | J04153-076 | M4.5 V | STF 518 | 199.452 ± 0.069 | 4083.715 ± 0.084 | 78.097 | 277.5 |
| GJ 169.1 B | | DC5 | | 181.273 ± 0.020 | 2361.129 ± 0.028 | | |
| GJ 169.1 A | J04311+589 | M4.0 V | STI 2051 | 181.244 ± 0.050 | 2424.355 ± 0.073 | 10.263 | 238.2 |
| GJ 3431 | | DQ8 | | 41.029 ± 0.036 | 357.871 ± 0.053 | | |
| GJ 3430 | J07102+376 | M4.0 V | GIC 69 | 44.601 ± 0.437 | 350.218 ± 0.608 | 12.472 | 223.1 |
| G 107–70 A | | DA | | 83.484 | 1281.725 ± 3.606 | | |
| G 107–70 B | | DA | GIC 75 | ... | ... | 0.667 | 318.1 |
| GJ 275.2 A ^e | J07307+481 | M4.0 V | WNO 49 | 88.723 ± 0.030 | 1287.988 ± 0.034 | 103.1 | 333.9 |
| GJ 283 A | | DZQA6 | | 109.344 ± 0.018 | 1261.341 ± 0.024 | | |
| GJ 283 B | J07403-174 | M6.0 V | LUY 5693 | 109.254 ± 0.039 | 1270.984 ± 0.052 | 20.338 | 279.5 |
| GJ 401 B | | DQ | | 53.190 ± 0.034 | 1962.558 ± 0.057 | | |
| GJ 401 | J10456-191 | M0.5 V | LDS 4013 | 53.172 ± 0.022 | 1963.772 ± 0.034 | 6.655 | 174.5 |
| GJ 1142 B | | DA3 | | 40.293 ± 0.032 | 446.106 ± 0.042 | | |
| GJ 1142 A | J11081-052 | M3.0 V | LDS 852 | 40.180 ± 0.026 | 443.166 ± 0.034 | 279.0 | 159.3 |
| GJ 1155 B | | DA | | 42.773 ± 0.043 | 711.074 ± 0.064 | | |
| GJ 1155 A | J12168+029 | M3.0 V | LDS 935 | 42.820 ± 0.035 | 700.554 ± 0.054 | 2.126 | 357.9 |
| Wolf 485 | | DA3.5 | | 62.148 ± 0.044 | 1207.505 ± 0.056 | | |
| Ross 476 | J13300-087 | M4.0 V | LDS 448 | 62.281 ± 0.042 | 1210.608 ± 0.059 | 502.4 | 198.7 |
| GJ 1179 B | | DC9 | | 84.311 ± 0.029 | 1490.906 ± 0.041 | | |
| GJ 1179 A | J13482+236 | M5.5 V | LDS 4410 | 84.225 ± 0.027 | 1487.630 ± 0.037 | 188.1 | 49.5 |
| GJ 630.1 B | | DQ8 | LDS 1436 | 67.354 ± 0.021 | 1634.847 ± 0.035 | | |
| CM Dra | J16343+571 | M4.5 V | Mor09, Tor10 | 67.288 ± 0.034 | 1623.346 ± 0.061 | 26.726 | 201.9 |
| LP 387–36 | | DC7 | | 28.841 ± 0.054 | 285.375 ± 0.072 | | |
| LP 387–37 | J17058+260 | M1.5 V | LDS 4721 | 28.746 ± 0.019 | 291.032 ± 0.025 | 19.244 | 179.6 |
| LSPM J1826+1120S | | DA | | 37.055 ± 0.066 | 281.066 ± 0.092 | | |
| GJ 4059 | J18264+113 | M3.5 V | NI 38 | 37.056 ± 0.024 | 276.066 ± 0.033 | 8.196 | 16.8 |
| LP 141–14 | | DC | | 40.393 ± 0.051 | 246.401 ± 0.095 | | |
| G 229–20 A | J18576+535 | M3.5 V | LDS 4802 | 40.348 ± 0.015 | 261.445 ± 0.028 | 43.653 | 343.9 |
| LP 141–13 | | M3.0 V | LDS 4802 | 40.365 ± 0.015 | 245.563 ± 0.027 | 2.290 | 17.0 |
| GJ 754.1 A | | DBQA5 | | 95.176 ± 0.029 | 173.039 ± 0.038 | | |
| GJ 754.1 B | J19205-076 | M2.5 V | LDS 678 | 95.178 ± 0.031 | 191.462 ± 0.037 | 27.168 | 306.2 |
| V1513 Cyg ^f | | sdM1.5 + WD | Giz97b | 60.296 ± 0.027 | 1470.281 ± 0.050 | 0.010537 [au] | |
| Wolf 1130 C | J20050+544 | T8p | MGN1 | 62.9 ± 3.3 | ... | 188.54 | 115.00 |
| V1412 Aql | | DC7 | | 43.574 ± 0.038 | 635.705 ± 0.051 | | |
| GJ 784.2 A | J20139+066 | M3.5 V | GIC 164 | 43.570 ± 0.022 | 634.751 ± 0.029 | 101.5 | 150.9 |
| Ross 193 B | | DC10 | LDS 6420 | 61.760 ± 0.052 | 807.720 ± 0.068 | | |
| FR Aqr | J20568-048 | M4.0 V | Jef18 | 61.824 ± 0.074 | 826.321 ± 0.091 | 15.006 | 129.4 |
| UCAC4 747–070768 | | DAH | | 118.155 ± 0.016 | 88.850 ± 0.026 | | |
| TYC 3980–1081–1 | J21516+592 | M4.0 V | KPP 4252 | 123.057 ± 0.594 | 79.885 ± 1.668 | 14.642 | 291.9 |
| Gaia DR3 2005884249925303168 ^g | | D? | | 18.550 ± 0.079 | 108.971 ± 0.123 | | |
| LF 4 +54 152 | J22129+550 | M0.0 V | Sma21 | 18.385 ± 0.153 | 109.131 ± 0.248 | 66.265 | 209.8 |

Table A.9: Multiple systems containing M dwarfs and white dwarfs (cont.).

| Name | Karmn | Spectral type ^a | Discoverer ^b | π [mas] | μ_{total} [mas a ⁻¹] | ρ^c [arcsec] | θ [deg] |
|------------------|------------|----------------------------|-------------------------|--------------------|--|----------------------|-------------------|
| GJ 4305 | | DA8.1 | | 40.325 ± 0.072 | 439.472 ± 0.074 | | |
| GJ 4304 | J22559+057 | M1.0 V | LDS 5021 | 40.347 ± 0.024 | 446.045 ± 0.029 | 17.168 | 104.6 |
| LSPM J2309+5506E | | DA | | 60.895 ± 0.030 | 410.185 ± 0.039 | | |
| G 233–42 | J23089+551 | M5.0 V | NSN 11 | 60.921 ± 0.027 | 411.267 ± 0.035 | 6.150 | 249.6 |
| GJ 4357 | | DA | | 25.367 ± 0.100 | 325.253 ± 0.126 | | |
| GJ 4356 | J23389+210 | M3.5 V | LDS 5108 | 25.402 ± 0.028 | 328.855 ± 0.036 | 9.495 | 290.7 |
| GJ 905.2 B | | DA3.8 | LDS 1070 | 53.762 ± 0.027 | 224.052 ± 0.039 | 174.7 | 10.0 |
| GJ 905.2 A | J23438+325 | M3.0 V | JOD 26 | ... | 223.766 ± 13.688 | 0.109 | 128.0 |

Notes. ^(a) In Simbad's taxonomy of white dwarfs, 'D' stands for degenerate, followed by an abbreviation of the most significant spectral features: 'A' for a hydrogen-rich atmosphere, 'B' for a helium-rich atmosphere, 'C' for no strong spectral lines, 'Q' for carbon lines, and 'Z' for metal lines.

^(b) References — Mor09: [Morales et al. \(2009\)](#); Tor10: [Torres et al. \(2010\)](#); Jef18: [Jeffers et al. \(2018\)](#); Sma21: [Gaia Collaboration et al. \(2021b\)](#).

^(c) Angular separation ρ and position angle θ measured from the white dwarf. ^(d) GJ 3151: White dwarf in a compact configuration ($s \simeq 49$ au) determined spectroscopically ([Schilbach & Röser 2012](#)) but not resolved by [Gaia](#). ^(e) GJ 275.2 A: it has a closer companion according to [Harrington et al. \(1981\)](#), who determined a 0.94-year period and individual masses of 0.17 and 0.08 M_\odot . They also estimated a mean angular separation of ~ 0.05 arcsec, which is compatible with the application of Third Kepler's law. ^(f) Wolf 1130 is a 0.4967-day binary composed of a subdwarf (sdM1.5; [Gizis 1997](#)) and a white dwarf, likely bound to evolve into a cataclysmic variable ([Mace et al. 2018](#)). ^(g) Gaia DR3 2005884249925303168: Unconfirmed spectroscopically but proposed candidate to WD in agreement with [Jiménez-Esteban et al. \(2018\)](#) based on position in HR diagram.

Table A.10: Multiple systems containing M dwarfs and ultra-cool dwarfs.

| Name | Karmn | Spectral type ^a | Comp. | Discoverer ^b | π [mas] | μ_{total} [mas a ⁻¹] | ρ [arcsec] | θ [deg] |
|------------------------|------------|----------------------------|-------|-------------------------|----------------------|--|--------------------|-------------------|
| GJ 3131 | J02033–212 | M2.5 V | Aab | Jef18 | 46.672 ± 0.041 | 471.895 ± 0.051 | ... | ... |
| GJ 3131 B | | L0: | B | Sma21 | 46.747 ± 0.307 | 450.045 ± 0.474 | 4.008 | 252.0 |
| G 196–3 | J10043+503 | M2.5 V | A | | 45.854 ± 0.019 | 246.664 ± 0.022 | | |
| G 196–3 B | | L3 β | B | REB 1 | 46.195 ± 0.545 | 246.291 ± 0.673 | 16.070 | 209.2 |
| GJ 3657 | J11231+258 | M5.0 V | A | | 61.652 ± 0.064 | 1061.305 ± 0.100 | | |
| 2M J11225550+2550250 | | T6 | B | WIS 183 | 62.9 ± 2.8 | 1062.3 ± 4.6 | 254.985 | 221.300 |
| Wolf 462 | J13007+123 | M1.5 V | AB | BEU 16 | 86.901 ± 0.117 | 629.606 ± 0.227 | 0.525 | 60.0 |
| Ross 458 C | | T8.5p | C | GDM 1 | 85.540 ± 1.530 | 639.451 ± 13.454 | 12.060 | 220.2 |
| LP 738–14 | J13481–137 | M4.5 V | A | | 55.028 ± 0.024 | 858.148 ± 0.037 | | |
| LP 738–14 B | | T5.5 | B | DEA 1 | 59.500 ± 3.600 | 857.920 ± 5.371 | 67.340 | 291.50 |
| GJ 9492 | J14423+660 | M2.0 V | A | | 91.479 ± 0.016 | 301.514 ± 0.028 | | |
| GJ 9492 B | | L0 | B | GKI 4 | 91.357 ± 0.091 | 337.307 ± 0.177 | 2.290 | 93.6 |
| KX Lib | | K4 V | A | | 169.884 ± 0.065 | 2008.680 ± 0.087 | | |
| HD 131976 | J14574–214 | M1.5 V | BC | Mar87, HN 28 | 168.770 ± 21.540 | 1933.943 ± 26.196 | 25.762 | 306.6 |
| GJ 570 D | | T8 | D | BUG 4 | 169.300 ± 1.700 | 1972.880 ± 5.620 | 234.0 | 317.0 |
| GJ 618.1 A | J16204–042 | M0.0 V | A | | 34.076 ± 0.019 | 416.694 ± 0.032 | | |
| GJ 618.1 B | | L2.5 | B | WIL 3 | 33.872 ± 0.759 | 415.281 ± 1.118 | 35.907 | 144.8 |
| G 259–20 | J17431+854 | M2.0 V | A | | 45.255 ± 0.314 | 291.245 ± 0.527 | | |
| 2M J17430860+8526594 | | L5 | B | LUH 12 | 45.139 ± 0.280 | 290.996 ± 0.501 | 29.739 | 358.4 |
| GJ 4040 | J17578+465 | M2.5 V | A | | 71.495 ± 0.015 | 578.336 ± 0.028 | | |
| G 204–39 B | | T7 | B | BDK 9 | 73.750 ± 1.840 | 594.569 ± 21.932 | 197.0 | 130.6 |
| V1513 Cyg | J20050+544 | M1.0 V | A | | 60.296 ± 0.027 | 1470.281 ± 0.050 | | |
| Wolf 1130 B | | T8p | B | MGN 1 | ... | ... | 188.5 | 115.00 |
| LP 395–8 A | J20198+229 | M3.0 V | Aab | Bar18 | 33.897 ± 0.026 | 135.400 ± 0.027 | ... | ... |
| LP 395–8 B | | M3.5: V | B | KPP 4191 | 33.896 ± 0.053 | 137.726 ± 0.057 | 1.918 | 355.5 |
| G3 1829571684884360832 | | L2: | C | This work | 33.938 ± 0.342 | 142.755 ± 0.359 | 11.019 | 307.4 |
| G 126–32 A | | M1.0: V | A | | 27.661 ± 0.127 | 219.436 ± 0.143 | | |
| G 126–32 B | J21450+198 | M1.5 V | B | RAO 466 | 26.818 ± 0.296 | 240.736 ± 0.412 | 0.564 | 253.3 |
| G 126–32 C | | L1 | C | Sma21 | 26.252 ± 0.803 | 232.177 ± 1.024 | 5.317 | 16.4 |
| Wolf 940 | J21466–001 | M4.0 V | A | | 80.738 ± 0.052 | 920.673 ± 0.060 | | |
| Wolf 940 B | | T8 | B | BNG 2 | 79.800 ± 4.500 | 919.0 | 31.640 | 250.5 |
| Wolf 1154 A | J22012+323 | M1.5 V | A | | 32.344 ± 0.024 | 133.621 ± 0.029 | | |
| Wolf 1154 B | | M3.5: V | B | GRV 1283 | 32.418 ± 0.083 | 119.082 ± 0.085 | 1.302 | 235.5 |
| 2M J22011701+3222062 | | T2.5 | C | | 31.400 ± 5.400 | 125.765 ± 2.702 | 80.750 | 147.6 |
| GJ 4287 | J22374+395 | M0.0 V | AB | HDS 3211 | 46.887 ± 0.564 | 365.030 ± 0.836 | 0.261 | 11.0 |
| G 216–7 B | | M9.5 V | C | KIR 5 | 47.644 ± 0.137 | 351.145 ± 0.206 | 33.332 | 111.5 |

Notes. ^(a) When spectroscopic classification is not available, a semicolon (:) denotes an estimated spectral type from absolute magnitude M_G .

^(b) References: Jef18: [Jeffers et al. \(2018\)](#); Mar87: [Marcy et al. \(1987\)](#); Bar18: [Baroch et al. \(2018\)](#); Sma21: [Gaia Collaboration et al. \(2021b\)](#). Other alphanumeric correspond to the WDS discoverer code.

Table A.11: Stars hosting planets in our sample.

| Name | Karmn | Spectral type | System class | Number of planets ^a | Discovery ^b |
|---------------------|-------------|---------------|--------------|--------------------------------|---------------------------|
| GJ 1002 | J00067-075 | M5.5 V | Single | 2 | Sua23 |
| GJ 12 | J00158+135 | M3.0 V | Single | 1 | Kuz24, Dho24 |
| GX And | J00183+440 | M1.0 V | Multiple | 2 | How14, Pin18 |
| TOI-1470 | J00403+612 | M2.0 V | Single | 2 | Gon23b |
| GJ 3053 | J00449-152 | M4.5 V | Single | 2 | Dit17, Men19 |
| GJ 3072 | J01023-104 | M0.0 V | Single | 1 | Fen20 |
| Wolf 46 | J01026+623 | M1.5 V | Multiple | 1 | Per19 |
| LSPM J0106+1913 | J01066+192 | M3.0 V | Single | 2 | Cha22 |
| YZ Cet | J01125-169 | M4.5 V | Single | 2 | Ast17b, Sto20a |
| Ross 19 | J02190+353 | M3.5 V | Single | 1 | Sch21 |
| PM J02489-1432W | J02489-145W | M2.0 V | Multiple | 1 | Kos21 |
| Teegarden's Star | J02530+168 | M7.0 V | Single | 2 | Zec19, Dre24 |
| HD 18143 A | | K2 IV | Multiple | 2 | Fen22 |
| LP 14-53 | J02573+765 | M4.0 V | Single | 1 | Sot21 |
| GJ 3193 | J03018-165S | M3.5 V | Multiple | 2 | Win19b, Win22 |
| CD Cet | J03133+047 | M5.0 V | Single | 1 | Bau20 |
| o ⁰² Eri | | K0 V | Multiple | 1 | Dia18 |
| LP 714-47 | J04167-120 | M0.0 V | Single | 1 | Dre20 |
| PM J04343+4302 | J04343+430 | M2.5 V | Single | 1 | Blu21 |
| HD 29391 | | F0 V | Multiple | 1 | Mac15 |
| HD 285968 | J04429+189 | M2.0 V | Single | 1 | For09 |
| Wolf 1539 | J04520+064 | M3.5 V | Single | 1 | How10 |
| GJ 180 | J04538-177 | M2.0 V | Single | 3 | Tuo14 |
| GJ 3323 | J05019-069 | M4.0 V | Single | 2 | Ast17a |
| GJ 229 | J06105-218 | M0.5 V | Multiple | 2 | Tuo14, Fen20 |
| HD 260655 | J06371+175 | M0.0 V | Single | 2 | Luq22 |
| HD 265866 | J06548+332 | M3.0 V | Single | 1 | Sto20b |
| Luyten's Star | J07274+052 | M3.5 V | Single | 2 | Ast17a, Poz20 |
| GJ 3470 | J07590+153 | M1.5 V | Single | 1 | Bon12 |
| GJ 3473 | J08023+033 | M4.0 V | Multiple | 2 | Kem20 |
| GJ 317 | J08409-234 | M3.5 V | Single | 2 | Joh07 |
| GJ 3512 | J08413+594 | M5.5 V | Single | 2 | Mor19 |
| ρ ⁰¹ Cnc | | K0 IV/V | Multiple | 5 | But97, Mar02, Mc04, Fis08 |
| Ross 623 | J08551+015 | M0.0 V | Single | 1 | Rob13 |
| G 41-13 | J08588+210 | M2.0 V | Single | 1 | Stef20 |
| HD 79211 | J09144+526 | M0.0 V | Multiple | 1 | Gon20 |
| LP 727-31 | J09286-121 | M2.5 V | Single | 1 | Ree22 |
| GJ 357 | J09360-216 | M2.5 V | Single | 3 | Luq19 |
| GJ 378 | J10023+480 | M1.0 V | Single | 1 | Hob19 |
| TYC 4384-1735-1 | J10088+692 | M0.5 V | Single | 1 | Blu20, Clo20a |
| LP 729-54 | J10185-117 | M4.0 V | Multiple | 2 | Now20, Clo20b |
| Ross 446 | J10289+008 | M2.0 V | Single | 1 | Ama21 |
| Lalande 21185 | J11033+359 | M1.5 V | Single | 2 | Dia19, Ros21 |
| HD 97101 | J11110+304E | K7 V | Multiple | 2 | Ded21 |
| K2-18 | J11302+076 | M3.0 V | Single | 1 | FM15, Clo17, Sar18 |
| Ross 1003 | J11417+427 | M4.0 V | Single | 2 | Hag10, Tri18 |
| Ross 905 | J11421+267 | M2.5 V | Single | 1 | Butl04 |
| LP 375-23 | J11423+230 | M0.5 V | Multiple | 1 | Sta19 |
| FI Vir | J11477+008 | M4.0 V | Single | 1 | Bon18a |
| GJ 1151 | J11509+483 | M4.5 V | Single | 1 | Bla23 |
| HD 238090 | J12123+544S | M0.0 V | Multiple | 1 | Sto20b |
| Ross 690 | J12230+640 | M3.0 V | Single | 1 | End22 |
| Wolf 433 | J12388+116 | M3.0 V | Single | 1 | Fen20 |
| Wolf 437 | J12479+097 | M3.5 V | Single | 1 | Tri21 |
| PM J13119+6550 | J13119+658 | M3.0 V | Single | 2 | Dem20 |
| HD 115404 | | K2 V | Multiple | 2 | Fen22 |
| Ross 1020 | J13229+244 | M4.0 V | Single | 1 | Luq18 |
| TOI-1238 | J13255+688 | M0.0 V | Single | 2 | Gon22 |
| Ross 490 | J13299+102 | M0.5 V | Single | 1 | Dam22 |
| HD 122303 | J14010-026 | M1.0 V | Single | 1 | Sua17a |
| HN Lib | J14342-125 | M4.0 V | Single | 1 | Gon23a |
| HO Lib | J15194-077 | M3.0 V | Single | 3 | Bon05, May09, Udr07 |
| Ross 508 | J15238+174 | M4.5 V | Single | 1 | Har22 |
| GJ 3929 | J15583+354 | M3.5 V | Single | 2 | Kem22, Bea22 |

Table A.11: Stars hosting planets in our sample (cont.).

| Name | Karmn | Spectral type | System class | Number of planets ^a | Discovery ^b |
|-------------------------|-------------|---------------|--------------|--------------------------------|-----------------------------|
| GJ 3942 | J16090+529 | M0.0 V | Single | 1 | Per17 |
| K2–33 | J16102–193 | M3.0 V | Single | 1 | Dav16 |
| LP 804–27 | J16126–188 | M3.0 V | Single | 1 | App10 |
| HD 147379 | J16167+672S | M0.0 V | Multiple | 1 | Rei18a |
| GJ 625 | J16254+543 | M1.5 V | Single | 1 | Sua17b |
| V2306 Oph | J16303–126 | M3.5 V | Single | 2 | Wri16 |
| V1090 Her | | K3 V | Multiple | 3 | Fen22 |
| Ross 860 | J16581+257 | M1.0 V | Single | 1 | Joh10 |
| GJ 1214 | J17153+049 | M4.5 V | Single | 1 | Cha09 |
| GJ 3998 | J17160+110 | M1.0 V | Single | 2 | Aff16 |
| GJ 685 | J17355+616 | M0.5 V | Multiple | 1 | Pin19 |
| GJ 687 | J17364+683 | M3.0 V | Single | 2 | Burt14 |
| GJ 686 | J17378+185 | M1.0 V | Single | 1 | Aff19 |
| GJ 720 A | J18353+457 | M0.5 V | Multiple | 1 | Gon21 |
| LSPM J1835+3259 | J18356+329 | M8.5 V | Single | 1 | Ber17 |
| LP 141–14 | | DC | Multiple | 1 | Van20 |
| HD 176029 | J18580+059 | M0.5 V | Single | 1 | Tol21 |
| V1428 Aql | J19169+051N | M2.5 V | Multiple | 1 | Kam18 |
| 2MASS J19204172+7311434 | J19206+731S | M4.0 V | Multiple | 1 | Cad22 |
| HD 190360 | | G7 IV/V | Multiple | 2 | Nae03, Vog05 |
| Ross 754 | J20138+133 | M1.0 V | Single | 1 | Mal21 |
| Wolf 1069 | J20260+585 | M5.0 V | Single | 1 | Kos23 |
| AU Mic | J20451–313 | M0.5 V | Multiple | 2 | Pla20, Mart21 |
| GJ 806 | J20450+444 | M1.5 V | Single | 2 | Pal23 |
| LSPM J2116+0234 | J21164+025 | M3.0 V | Single | 1 | Lal19 |
| TYC 2187–512–1 | J21221+229 | M1.0 V | Single | 1 | Qui22 |
| G 264–12 | J21466+668 | M4.0 V | Single | 2 | Ama21 |
| TYC 4266–736–1 | J21474+627 | M0.0 V | Multiple | 1 | Esp22 |
| Wolf 1329 | J22096–046 | M3.5 V | Single | 2 | Butl06, Mone14 |
| UCAC4 744–073158 | J22102+587 | M2.0 V | Single | 1 | Fuk22 |
| GJ 1265 | J22137–176 | M4.5 V | Single | 1 | Luq18 |
| GJ 4276 | J22252+594 | M4.0 V | Single | 1 | Nag19 |
| IL Aqr | J22532–142 | M4.0 V | Single | 4 | Marc98, Mar01, Riv05, Riv10 |
| 2MUCD 12171 | J23064–050 | M7.5 V | Single | 7 | Gil16, Gil17 |
| EQ Peg A | J23318+199E | M3.5 V | Multiple | 1 | Cur22 |

Notes. ^(a) In the majority of cases these planets are classified as ‘Confirmed’ (to the date of publication of this work) by the NASA Exoplanet Archive. A few controversial detections have been excluded (e.g. Barnard’s star or CN Leo). Numbers in parenthesis denote that at least one planet has been challenged (Ribas et al. 2023). ^(b) References for the discovery – Aff16: Affer et al. (2016); Aff19: Affer et al. (2019); Ama21: Amado et al. (2021); App10: Apps et al. (2010); Ast17a: Astudillo-Defru et al. (2017b); Ast17b: Astudillo-Defru et al. (2017a); Bau20: Bauer et al. (2020); Bea22: Beard et al. (2022); Ber17: Berdyugina et al. (2017); Bla23: Blanco-Pozo et al. (2023); Blu20: Bluhm et al. (2020); Blu21: Bluhm et al. (2021); Bon05: Bonfils et al. (2005); Bon12: Bonfils et al. (2012); Bon18a: Bonfils et al. (2018); Burt14: Burt et al. (2014); But97: Butler et al. (1997); Butl04: Butler et al. (2004); Butl06: Butler et al. (2006); Cad22: Cadieux et al. (2022); Cha09: Charbonneau et al. (2009); Cha22: Chaturvedi et al. (2022); Clo17: Cloutier et al. (2017); Clo20a: Cloutier et al. (2020b); Clo20b: Cloutier et al. (2020a); Cur22: Curiel et al. (2022); Dam22: Damasso et al. (2022); Dav16: David et al. (2016); Ded21: Dedrick et al. (2021); Dem20: Demory et al. (2020); Dho24: Dholakia et al. (2024); Dia18: Díaz et al. (2018); Dia19: Díaz et al. (2019); Dit17: Dittmann et al. (2017); Dre20: Dreizler et al. (2020); Dre24: Dreizler et al. (2024); End22: Endl et al. (2022); Esp22: Espinoza et al. (2022); FM15: Foreman-Mackey et al. (2015); Fen20: Feng et al. (2020); Fen22: Feng et al. (2022); Fis08: Fischer et al. (2008); For09: Forveille et al. (2009); Fuk22: Fukui et al. (2022); Gil16: Gillon et al. (2016); Gil17: Gillon et al. (2017); Gon20: González-Álvarez et al. (2020); Gon21: González-Álvarez et al. (2021); Gon22: González-Álvarez et al. (2022); Gon23a: González-Álvarez et al. (2023a); Gon23b: González-Álvarez et al. (2023b); Hag10: Haghhighipour et al. (2010); Har22: Harakawa et al. (2022); Hob19: Hobson et al. (2019); How10: Howard et al. (2010); How14: Howell et al. (2014); Joh07: Johnson et al. (2007); Joh10: Johnson et al. (2010); Kam18: Kaminski et al. (2018); Kem20: Kemmer et al. (2020); Kem22: Kemmer et al. (2022); Kos21: Kossakowski et al. (2021); Kos23: Kossakowski et al. (2023); Kuz24: Kuzuhara et al. (2024); Lal19: Lalitha et al. (2019); Luq18: Luque et al. (2018); Luq19: Luque et al. (2019); Luq22: Luque et al. (2022); Mac15: Macintosh et al. (2015); Mal21: Maldonado et al. (2021); Mar01: Marcy et al. (2001); Mar02: Marcy et al. (2002); Marc98: Marcy et al. (1998); Mart21: Martioli et al. (2021); May09: Mayor et al. (2009); Mc04: McArthur et al. (2004); Men19: Ment et al. (2019); Mon14: Montet et al. (2014); Mor19: Morales et al. (2019); Nae03: Naef et al. (2003); Nag19: Nagel et al. (2019); Now20: Nowak et al. (2020); Pal23: Palle et al. (2023); Per17: Perger et al. (2017); Per19: Perger et al. (2019); Pin18: Pinamonti et al. (2018); Pin19: Pinamonti et al. (2019); Pla20: Plavchan et al. (2020); Poz20: Pozuelos et al. (2020); Qui22: Quirrenbach et al. (2022); Ree22: Reefe et al. (2022); Rei18a: Reiners et al. (2018a); Riv05: Rivera et al. (2005); Riv10: Rivera et al. (2010); Rob13: Robertson et al. (2013); Ros21: Rosenthal et al. (2021); Sar18: Sarkis et al. (2018); Sch21: Schneider et al. (2021); Sot21: Soto et al. (2021); Sta19: Stassun et al. (2019); Stef20: Stefansson et al. (2020); Sto20a: Stock et al. (2020a); Sto20b: Stock et al. (2020b); Sua17a: Suárez Mascareño et al. (2017a); Sua17b: Suárez Mascareño et al. (2017b); Sua23: Suárez Mascareño et al. (2023); Tol21: Toledo-Padrón et al. (2021); Tri18: Trifonov et al. (2018); Tri21: Trifonov et al. (2021); Tuo14: Tuomi et al. (2014); Udr07: Udry et al. (2007); Van20: Vanderburg et al. (2020); Vog05: Vogt et al. (2005); Win19b: Winters et al. (2019b); Win22: Winters et al. (2022); Wri16: Wright et al. (2016); Zec19: Zechmeister et al. (2019).

Table A.12: Bibliographic references for the abbreviations used in the main table.

| Abbreviation | Reference | Abbreviation | Reference | Abbreviation | Reference |
|--------------|--|--------------|---|--------------|--|
| Abt08 | Abt (2008) | Can93 | Cannon & Pickering (1993) | Fen20 | Feng et al. (2020) |
| Abt70 | Abt (1970) | Car21 | Cardona Guillén et al. (2021) | Fen22 | Feng et al. (2022) |
| Abt76 | Abt & Levy (1976) | Cas07 | Casewell et al. (2007) | Fin18 | Finch et al. (2018) |
| Abt81 | Abt (1981) | Cat06 | Catala et al. (2006) | Fis08 | Fischer et al. (2008) |
| Ada35 | Adams et al. (1935) | Cha09 | Charbonneau et al. (2009) | Fle88 | Fleming et al. (1988) |
| Aff16 | Affer et al. (2016) | Cha22 | Chaturvedi et al. (2022) | FM15 | Foreman-Mackey et al. (2015) |
| Aff19 | Affer et al. (2019) | Che20 | Chen et al. (2020) | For04 | Forveille et al. (2004) |
| Alo15a | Alonso-Floriano et al. (2015b) | Che23 | Chevalier et al. (2023) | For09 | Forveille et al. (2009) |
| Alo15b | Alonso-Floriano et al. (2015a) | Chr38 | Christie & Wilson (1938) | Fou18 | Fouqué et al. (2018) |
| Ama21 | Amado et al. (2021) | Chr78 | Christy (1978) | Fre20 | Freund et al. (2020) |
| Ans15 | Ansdel et al. (2015) | Cif20 | Cifuentes et al. (2020) | Fri13 | Frith et al. (2013) |
| App10 | Apps et al. (2010) | Clo03 | Close et al. (2003) | Fuk22 | Fukui et al. (2022) |
| Are19 | Arentsen et al. (2019) | Clo17 | Cloutier et al. (2017) | Gag15a | Gagné et al. (2015) |
| Ast17a | Astudillo-Defru et al. (2017b) | Clo20a | Cloutier et al. (2020b) | Gag18a | Gagné et al. (2018) |
| Ast17b | Astudillo-Defru et al. (2017a) | Clo20b | Cloutier et al. (2020a) | Gag18b | Gagné & Faherty (2018) |
| Bar14 | Bardalez Gagliuffi et al. (2014) | Cor17a | Cortés-Contreras et al. (2017) | Gai14b | Gaidos et al. (2014) |
| Bar18 | Baroch et al. (2018) | Cor24 | Cortés-Contreras et al. (2024) | Gaia22a | Gaia Collaboration (2022) |
| Bar21 | Baroch et al. (2021) | Cru02 | Cruz & Reid (2002) | Gal22 | Gallenne et al. (2022) |
| Bar70 | Barry (1970) | Cru03 | Cruz et al. (2003) | Geb02 | Geballe et al. (2002) |
| Bau20 | Bauer et al. (2020) | Cru09 | Cruz et al. (2009) | Geb16 | Gebran et al. (2016) |
| Bea22 | Beard et al. (2022) | Cur06 | Curtis (1906) | Gen19 | Gentile Fusillo et al. (2019) |
| Bed20 | Bédard et al. (2020) | Cur22 | Curiel et al. (2022) | Gia11 | Gianninas et al. (2011) |
| Bell17 | Bell et al. (2017) | Cve12 | Cvetković et al. (2012) | Gil16 | Gillon et al. (2016) |
| Bel97 | Belopolsky (1897) | Dae07 | Daemgen et al. (2007) | Gil17 | Gillon et al. (2017) |
| Ben00 | Benedict et al. (2000) | Dam22 | Damasso et al. (2022) | Gil18 | Gilhooley et al. (2018) |
| Ben08 | Bender & Simon (2008) | Dav14 | Davison et al. (2014) | Giz00b | Gizis et al. (2000) |
| Ben21 | Benedict et al. (2021) | Dav15 | Davison et al. (2015) | Giz02 | Gizis et al. (2002) |
| Ber06 | Bertout & Genova (2006) | Dav16 | David et al. (2016) | Giz97a | Gizis & Reid (1997) |
| Ber10 | Bergfors et al. (2010) | Daw05 | Dawson & De Robertis (2005) | Giz97b | Gizis (1997) |
| Ber17 | Berdyugina et al. (2017) | Dea12 | Deacon et al. (2012) | Gli91 | Gliese & Jahreiß (1991) |
| Bes15 | Best et al. (2015) | Dea14 | Deacon et al. (2014) | Gol10 | Goldman et al. (2010) |
| Bes20 | Best et al. (2020) | Ded21 | Dedrick et al. (2021) | Gom15 | Gómez de Castro et al. (2015) |
| Bes91 | Bessell (1991) | Dek18 | Deka-Szymankiewicz et al. (2018) | Gon06 | Gontcharov (2006) |
| Bid85 | Bidelman (1985) | Del10 | Delorme et al. (2010) | Gon20 | González-Álvarez et al. (2020) |
| Bill13 | Biller et al. (2013) | Del98 | Delfosse et al. (1998) | Gon21 | González-Álvarez et al. (2021) |
| Bin16 | Binks & Jeffries (2016) | Del99a | Delfosse et al. (1999a) | Gon22 | González-Álvarez et al. (2022) |
| Bir12 | Birkby et al. (2012) | Del99b | Delfosse et al. (1999b) | Gon23a | González-Álvarez et al. (2023a) |
| Bir20 | Birkby et al. (2020) | Del99c | Delfosse et al. (1999c) | Gon23b | González-Álvarez et al. (2023b) |
| Bla23 | Blanco-Pozo et al. (2023) | Dem20 | Demory et al. (2020) | Gon24 | González Hernández et al. (2024) |
| Blu20 | Bluhm et al. (2020) | Des12 | Deshpande et al. (2012) | GR96 | Gizis & Reid (1996) |
| Blu21 | Bluhm et al. (2021) | Dho24 | Dholakia et al. (2024) | Gra01 | Gray et al. (2001) |
| Boc05 | Bochanski et al. (2005) | Dia18 | Díaz et al. (2018) | Gra03 | Gray et al. (2003) |
| Boc18 | Bochanski et al. (2018) | Dia19 | Díaz et al. (2019) | Gra06 | Gray et al. (2006) |
| Bon05 | Bonfils et al. (2005) | Die14 | Dieterich et al. (2014) | Gre84 | Greenstein (1984) |
| Bon12 | Bonfils et al. (2012) | Dit14 | Dittmann et al. (2014) | Gre90 | Greenstein & Liebert (1990) |
| Bon13a | Bonfils et al. (2013) | Dit17 | Dittmann et al. (2017) | Grif85 | Griffin et al. (1985) |
| Bon18a | Bonfils et al. (2018) | DR2 | Gaia Collaboration et al. (2018) | Gui09 | Guillout et al. (2009) |
| Bop77 | Bopp & Fekel (1977) | DR3 | Gaia Collaboration et al. (2023b) | Hag10 | Haghjipour et al. (2010) |
| Bow15a | Bowler et al. (2015) | Dre19 | Dressing et al. (2019) | Hal18 | Halbwachs et al. (2018) |
| Bud19 | Buder et al. (2019) | Dre20 | Dreizler et al. (2020) | Har11 | Hartman et al. (2011) |
| Bud21 | Buder et al. (2021) | Dre24 | Dreizler et al. (2024) | Har12 | Hartkopf et al. (2012) |
| Bur00 | Burgasser et al. (2000) | Dup12 | Dupuy & Liu (2012) | Har22 | Harakawa et al. (2022) |
| Bur11 | Burningham et al. (2011) | Dup17 | Dupuy & Liu (2017) | Har70 | Harlan & Taylor (1970) |
| Bur13 | Burningham et al. (2013) | Dup19 | Dupuy et al. (2019) | Har81 | Harrington et al. (1981) |
| Bur15a | Burgasser et al. (2015) | Dup94 | Dupuis et al. (1994) | Har96 | Harlow (1996) |
| Bur15b | Burgasser et al. (2015) | Duq88 | Duquennoy & Mayor (1988) | Haw96 | Hawley et al. (1996) |
| Burt14 | Burt et al. (2014) | Duq91 | Duquennoy & Mayor (1991) | Hen02 | Henry et al. (2002) |
| But97 | Butler et al. (1997) | Edw76 | Edwards (1976) | Hen18 | Henry et al. (2018) |
| Butl04 | Butler et al. (2004) | Eli14 | Elliott et al. (2014) | Her03 | Herschel (1803) |
| Butl06 | Butler et al. (2006) | End22 | Endl et al. (2022) | Her14 | Herczeg & Hillenbrand (2014) |
| Cab07 | Caballero (2007) | Esp22 | Espinoza et al. (2022) | Her65 | Herbig & Moorhead (1965) |
| Cab09 | Caballero (2009) | Eva67 | Evans (1967) | Hir21 | Hirsch et al. (2021) |
| Cab10a | Caballero (2010) | Fab02 | Fabricius et al. (2002) | Hob19 | Hobson et al. (2019) |
| Cab10b | Caballero et al. (2010) | Fah10 | Faherty et al. (2010) | Hog00 | Hög et al. (2000) |
| Cad22 | Cadieux et al. (2022) | Fah12 | Faherty et al. (2012) | Hoj19 | Hojjatpanah et al. (2019) |

Table A.12: Bibliographic references for the abbreviations used in the main table (cont.).

| Abbreviation | Reference | Abbreviation | Reference | Abbreviation | Reference |
|--------------|-------------------------------|--------------|---------------------------|--------------|----------------------------------|
| Hou16 | Houdebine et al. (2016) | Luc17 | Luck (2017) | Pha06a | Phan-Bao & Bessell (2006) |
| Hou88 | Houk & Smith-Moore (1988) | Luc18 | Luck (2018) | Pha06b | Phan-Bao et al. (2006) |
| Hou99 | Houk & Swift (1999) | Luh12 | Luhman et al. (2012) | Pin18 | Pinamonti et al. (2018) |
| How10 | Howard et al. (2010) | Luq18 | Luque et al. (2018) | Pin19 | Pinamonti et al. (2019) |
| How14 | Howell et al. (2014) | Luq19 | Luque et al. (2019) | Pla20 | Plavchan et al. (2020) |
| Hub22 | Hubbard-James et al. (2022) | Luq22 | Luque et al. (2022) | Pou04 | Pourbaix et al. (2004) |
| Ire08 | Ireland et al. (2008) | Mac13 | Mace et al. (2013) | Poz20 | Pozuelos et al. (2020) |
| Irw09 | Irwin et al. (2009) | Mac15 | Macintosh et al. (2015) | Pre02 | Preibisch et al. (2002) |
| Jah08 | Jahreiß et al. (2008) | Mac18 | Mace et al. (2018) | Put97 | Putney (1997) |
| Jam08 | Jameson et al. (2008) | Mah21 | Mahadevan et al. (2021) | Qui22 | Quirrenbach et al. (2022) |
| Jan12 | Janson et al. (2012) | Mal06 | Malkov et al. (2006) | Rag09 | Raghavan et al. (2009) |
| Jan14a | Janson et al. (2014b) | Mal12 | Malkov et al. (2012) | Raj18a | Rajpurohit et al. (2018) |
| Jan17 | Janson et al. (2017) | Mal13 | Malo et al. (2013) | Reb98 | Rebolo et al. (1998) |
| Jef18 | Jeffers et al. (2018) | Mal14a | Malo et al. (2014a) | Ree22 | Reefe et al. (2022) |
| Jen09 | Jenkins et al. (2009) | Mal14b | Malo et al. (2014b) | Rei02a | Reid & Cruz (2002) |
| Jim18 | Jiménez-Esteban et al. (2018) | Mal20 | Maldonado et al. (2020) | Rei03 | Reid et al. (2003) |
| Jod13 | Jódar et al. (2013) | Mal21 | Maldonado et al. (2021) | Rei04 | Reid et al. (2004) |
| Joh07 | Johnson et al. (2007) | Mal24 | Mallorquí et al. (2024) | Rei05 | Reid & Gizis (2005) |
| Joh10 | Johnson et al. (2010) | Man14 | Mann et al. (2014) | Rei07 | Reid et al. (2007) |
| Jon20 | Jónsson et al. (2020) | Man15 | Mann et al. (2015) | Rei09 | Reiners & Basri (2009) |
| Joy26 | Joy & Sanford (1926) | Mar01 | Marcy et al. (2001) | Rei18a | Reiners et al. (2018a) |
| Joy49 | Joy & Wilson (1949) | Mar02 | Marcy et al. (2002) | Rei18b | Reiners et al. (2018b) |
| Joy74 | Joy & Abt (1974) | Mar07 | Martinache et al. (2007) | Rei95 | Reid et al. (1995) |
| Kam18 | Kaminski et al. (2018) | Mar87 | Marcy et al. (1987) | Rei97b | Reid & Gizis (1997) |
| Kar04 | Karatas et al. (2004) | Marc98 | Marcy et al. (1998) | Rein12 | Reiners et al. (2012) |
| Kat13 | Katoh et al. (2013) | Marf21 | Marfil et al. (2021) | Ria06 | Riaz et al. (2006) |
| Kee89 | Keenan & McNeil (1989) | Mart21 | Martioli et al. (2021) | Rib23 | Ribas et al. (2023) |
| Kem20 | Kemmer et al. (2020) | Mas08 | Massarotti et al. (2008) | Ric20 | Rice & Brewer (2020) |
| Kem22 | Kemmer et al. (2022) | May09 | Mayor et al. (2009) | Rie17 | Riedel et al. (2017) |
| Ker19 | Kervella et al. (2019) | Maz01 | Mazeh et al. (2001) | Riv05 | Rivera et al. (2005) |
| Khr10 | Khrutskaya et al. (2010) | Mc04 | McArthur et al. (2004) | Riv10 | Rivera et al. (2010) |
| Kir11 | Kirkpatrick et al. (2011) | McC02 | McCaughrean et al. (2002) | Riv12 | Riviere-Marichalar et al. (2012) |
| Kir12 | Kirkpatrick et al. (2012) | Men19 | Ment et al. (2019) | Rob12 | Roberts et al. (2012) |
| Kir19 | Kirkpatrick et al. (2019) | Mer09 | Mermilliod et al. (2009) | Rob13 | Robertson et al. (2013) |
| Kir24 | Kirkpatrick et al. (2024) | Mir20 | Miret-Roig et al. (2020) | Rod74 | Rodgers & Eggen (1974) |
| Kir91 | Kirkpatrick et al. (1991) | Mis15 | Mishenina et al. (2015) | Roj12 | Rojas-Ayala et al. (2012) |
| Kir94 | Kirkpatrick et al. (1994) | Moc02 | Mochnacki et al. (2002) | Ros11 | Röser et al. (2011) |
| Kiy20 | Kiyaeva et al. (2020) | Mon01 | Montes et al. (2001) | Ros21 | Rosenthal et al. (2021) |
| Klu20 | Klutsch et al. (2020) | Mon03 | Monet et al. (2003) | Sab21 | Sabotta et al. (2021) |
| Koe10 | Koen et al. (2010) | Mon14 | Montet et al. (2014) | Sal22 | Salama et al. (2022) |
| Kop16 | Kopytova et al. (2016) | Mon18 | Montes et al. (2018) | Sam17 | Samus et al. (2017) |
| Kos21 | Kossakowski et al. (2021) | Mor09 | Morales et al. (2009) | Sar18 | Sarkis et al. (2018) |
| Kos23 | Kossakowski et al. (2023) | Mor10 | Morales et al. (2010) | Sch05 | Scholz et al. (2005) |
| Kou19 | Kounkel et al. (2019) | Mor19 | Morales et al. (2019) | Sch07 | Schmidt et al. (2007) |
| Kra14a | Kraus et al. (2014a) | Mor65 | Morgan & Hiltner (1965) | Sch12 | Schlieder et al. (2012) |
| Kra14b | Kraus et al. (2014b) | Mut10 | Muterspaugh et al. (2010) | Sch19 | Schneider et al. (2019) |
| Kra17 | Kraus et al. (2017) | MWDD | Montreal WD Database | Sch21 | Schneider et al. (2021) |
| Kuz19 | Kuznetsov et al. (2019) | Nae03 | Naeff et al. (2003) | Scha19 | Schanche et al. (2019) |
| Kuz24 | Kuzuhara et al. (2024) | Nag19 | Nagel et al. (2019) | Schw19 | Schweitzer et al. (2019) |
| Laf07 | Lafrenière et al. (2007) | Nap20 | Napiwotzki et al. (2020) | She85 | Shen et al. (1985) |
| Lal19 | Lalitha et al. (2019) | Nes95 | Nesterov et al. (1995) | Shk09 | Shkolnik et al. (2009) |
| Law06 | Law et al. (2006) | New14 | Newton et al. (2014) | Shk10 | Shkolnik et al. (2010) |
| Law08 | Law et al. (2008) | New16 | Newton et al. (2016) | Shk12 | Shkolnik et al. (2012) |
| Lee84 | Lee (1984) | Nid02 | Nidever et al. (2002) | Shk17 | Shkolnik et al. (2017) |
| Lep02 | Lépine et al. (2002) | Now20 | Nowak et al. (2020) | Sim11 | Simon & Schaefer (2011) |
| Lep03 | Lépine et al. (2003) | Osw88 | Oswalt et al. (1988) | Sio09 | Sion et al. (2009) |
| Lep05 | Lépine & Shara (2005) | Pal20 | Palle et al. (2020) | Sio90 | Sion et al. (1990) |
| Lep09 | Lépine et al. (2009) | Pal23 | Palle et al. (2023) | Ski18 | Skinner et al. (2018) |
| Lep13 | Lépine et al. (2013) | Pas18 | Passegger et al. (2018) | Smi14 | Smith et al. (2014) |
| Lim13 | Limoges et al. (2013) | Pau06 | Paulson & Yelda (2006) | Sot21 | Soto et al. (2021) |
| Lim15 | Limoges et al. (2015) | Pec13 | Pecaut & Mamajek (2013) | Sou18 | Soubiran et al. (2018) |
| Lod05 | Lodieu et al. (2005) | Per17 | Perger et al. (2017) | Soub08 | Soubiran et al. (2008) |
| Lod19 | Lodieu et al. (2019) | Per19 | Perger et al. (2019) | Spe16 | Sperauskas et al. (2016) |
| Lop06 | López-Santiago et al. (2006) | Pes97 | Pesch & Bidelman (1997) | Spe19 | Sperauskas et al. (2019) |
| Lot98 | Loth & Bidelman (1998) | Pet84 | Pettersen et al. (1984) | Spi21 | Spina et al. (2021) |
| Sta19 | Stassun et al. (2019) | Tok18 | Tokovinin (2018) | War15 | Ward-Duong et al. (2015) |

Table A.12: Bibliographic references for the abbreviations used in the main table (cont.).

| Abbreviation | Reference | Abbreviation | Reference | Abbreviation | Reference |
|--------------|---|--------------|--|--------------|---|
| Sta97 | Stauffer et al. (1997) | Tok22 | Tokovinin (2022) | Wei16 | Weinberger et al. (2016) |
| Ste86a | Stephenson (1986b) | Tok97 | Tokovinin (1997) | Wes11 | West et al. (2011) |
| Ste86b | Stephenson (1986a) | Tol21 | Toledo-Padrón et al. (2021) | Wes93 | Wesemael et al. (1993) |
| Stef20 | Stefansson et al. (2020) | Tor02 | Torres & Ribas (2002) | Whi01 | White & Ghez (2001) |
| Ste20 | Steinmetz et al. (2020) | Tor06 | Torres et al. (2006) | Whi07 | White et al. (2007) |
| Sto20a | Stock et al. (2020a) | Tor09 | Torres et al. (2009) | Wil53 | Wilson (1953) |
| Sto20b | Stock et al. (2020b) | Tor10 | Torres et al. (2010) | Win17 | Winters et al. (2017) |
| Ston20 | Stonkutė et al. (2020) | Tor22 | Torres et al. (2022) | Win19b | Winters et al. (2019b) |
| Str03 | Strassmeier & Rice (2003) | TP86 | Tomkin & Pettersen (1986) | Win20 | Winters et al. (2020) |
| Str93 | Strassmeier et al. (1993) | Tre20 | Tremblay et al. (2020) | Win22 | Winters et al. (2022) |
| Str94 | Strassmeier (1994) | Tri18 | Trifonov et al. (2018) | Wri16 | Wright et al. (2016) |
| Sua17a | Suárez Mascareño et al. (2017a) | Tri21 | Trifonov et al. (2021) | Xua24 | Xuan et al. (2024) |
| Sua17b | Suárez Mascareño et al. (2017b) | Tuo14 | Tuomi et al. (2014) | Yi14 | Yi et al. (2014) |
| Sua23 | Suárez Mascareño et al. (2023) | Udr07 | Udry et al. (2007) | Zac10 | Zacharias et al. (2010) |
| Tab17 | Tabernero et al. (2017) | van07 | van Leeuwen (2007) | Zac12 | Zacharias et al. (2012) |
| Tam06 | Tamazian et al. (2006) | van09 | van Belle & von Braun (2009) | Zak22 | Zakhozhay et al. (2022) |
| Tam08 | Tamazian et al. (2008) | Van20 | Vanderburg et al. (2020) | Zak79 | Zakhozhaj (1979) |
| Tau20 | Tautvaisiene et al. (2020) | van95 | van Altena et al. (1995) | Zap04 | Zapatero Osorio et al. (2004) |
| Ter15a | Terrien et al. (2015a) | Vog02 | Vogt et al. (2002) | Zbo98 | Zboril & Byrne (1998) |
| Ter15b | Terrien et al. (2015b) | Vog05 | Vogt et al. (2005) | Zec19 | Zechmeister et al. (2019) |
| Tin19 | Ting et al. (2019) | Vri20 | Vrijmoet et al. (2020) | Zon20 | Zong et al. (2020) |
| Tok08 | Tokovinin (2008) | Wan22 | Wang et al. (2022) | | |